Angewandte Chemie
Eine Zeitschrift der Gesellschaft Deutscher Chemiker

Supporting Information

Bioinspired Design Provides High-Strength Benzoxazine Structural Adhesives

*Cody J. Higginson, Katerina G. Malollari, Yunqi Xu, Andrew V. Kelleghan, Nicole G. Ricapito, and Phillip B. Messersmith**

anie_201906008_sm_miscellaneous_information.pdf

Author Contributions

C.H. Conceptualization: Lead; Data curation: Lead; Formal analysis: Lead; Investigation: Lead; Methodology: Lead; Project administration: Supporting; Visualization: Equal; Writing—Original Draft: Lead; Writing—Review & Editing: Lead
K.M. Data curation: Supporting; Formal analysis: Supporting; Investigation: Supporting; Methodology: Supporting; Software: Supporting; Visualization: Supporting; Writing—Original Draft: Supporting; Writing—Review & Editing: Supporting
Y.X. Data curation: Supporting; Investigation: Supporting; Writing—Review & Editing: Supporting
A.K. Formal analysis: Supporting; Investigation: Supporting; Writing—Review & Editing: Supporting
N.R. Conceptualization: Supporting; Project administration: Supporting; Supervision: Supporting; Writing—Review & Editing: Supporting
P.M. Conceptualization: Supporting; Funding acquisition: Lead; Investigation: Supporting; Methodology: Supporting; Project administration: Lead; Resources: Lead; Supervision: Lead; Writing—Review & Editing: Supporting.

Supporting Information

Table of Contents

1. Materials and Instrumentation
- 1.1 Chemicals and Supplies 2
- 1.2 Analyses and Equipment 2

2. Synthetic Procedures 3

3. Model Compound Stability Studies 31

4. Pressure Sensitive Adhesive Behavior of Main-Chain Polybenzoxazine 3b 33

5. Lap Shear Adhesion Testing
- 5.1 Substrate and lap joint preparation 35
- 5.2 Influence of silane adhesion promoters on **B-a**, **1e**, and **2e** adhesion 39
- 5.3 Adhesive strength of blends of **2e** with **3a** and **3b** 40
- 5.4 Adhesive strength of blends of **B-a** and **2e** with MX-551 and MX-154 42

6. Thermal Stability of TBS Ethers in TBS-Protected Precursor S11 44

7. Mechanical Characterization
- 7.1 Sample preparation by compression molding 45
- 7.2 Flexural testing (3-point bending) 52
- 7.3 Nanoindentation measurements 52

8. XPS Analysis of Failed Adhesive Lap Joints 55

9. Thermal Gravimetric Analysis of Thermosets B-a, 1e, and 2e 63

10. Monomer curing behavior assessed by differential scanning calorimetry 66

11. References 77

12. NMR and FTIR Spectra of Compounds 78

1. Materials and Instrumentation

1.1 Chemicals and Supplies

Chemicals were purchased from commercial sources and used as received, unless otherwise stated. Chemical syntheses were carried out under inert atmospheres of nitrogen or argon, unless otherwise indicated. Aniline (Sigma Aldrich) was purified by short-path vacuum distillation prior to use and stored at -20 °C, protected from light under a blanket of argon. Commercial benzoxazine monomer **B-a** (XU 35610) was generously donated by Huntsman Advanced Materials (The Woodlands, Texas, USA), and used as received for all experiments and characterization. Kane Ace toughened epoxy additives MX-551 and MX-154 were kindly donated by Kaneka, Inc. (Pasadena, Texas, USA) and used as received. Thin layer chromatography (TLC) was performed on aluminum-backed silica gel 60 plates containing F_{254} fluorescent contrast agent, and compounds were visualized under UV lamp, and by iodine, potassium permanganate, or ninhydrin staining. Ferric chloride stain was applied for catechol-containing compounds. Dry solvents were obtained by prolonged storage over activated 4 Å molecular sieves under dry nitrogen or argon gas. Ultrapure water was purified on a Millipore Synergy-R apparatus. Flash chromatography was performed on hand-packed silica gel 60 columns, eluting under positive pressure of air or nitrogen. Aluminum 6061 substrates were cut at the UC Berkeley Cory Hall Machine shop from 0.160 cm thick, 10.16 cm x 121.92 cm (0.063" thick, 4"x48") sheet stock purchased from McMaster-Carr (USA). PDMS molds used for compression molding of samples for mechanical characterization were hand-cut from layered clear silicone X-treme tape® (MOCAP). Glass spheres (0.0015" diameter) for bond line control in adhesion studies were purchased from Rock West Composites.

1.2 Analyses and Equipment

^{1}H and ^{13}C NMR spectra were obtained at the UC Berkeley College of Chemistry NMR Facility on a Brüker AVB-400 spectrometer in deuterated solvents (Cambridge Isotope Laboratories, Inc. and Sigma-Aldrich), and spectra were calibrated to the signals of residual protium in the NMR solvent as an internal reference ($CHCl_3$ at 7.26 ppm ^{1}H NMR and 77.16 ppm ^{13}C NMR; CH_3OH at 3.31 ppm ^{1}H-NMR and 49.0 ppm ^{13}C NMR; DMSO at 2.50 ppm ^{1}H NMR and 39.52 ppm ^{13}C NMR; acetone at 2.05 ppm ^{1}H NMR and 29.84 ppm ^{13}C NMR). Peak multiplicities were abbreviated as follows: s = singlet, d = doublet, t = triplet, q = quartet, quint = quintet, m = multiplet, br s = broad singlet. Spectra were processed in MestReNova 11.0 (Mestrelab Research). Digital images of samples were collected with the built-in camera of an iPhone 6s. Fourier Transform Infrared (FTIR) Spectra were collected on a Bruker Vertex 80 Time-resolved FTIR spectrometer equipped with a diamond attenuated total reflectance (ATR) window. Spectra were acquired at a resolution of 4 cm^{-1} for 32 scans. X-ray Photoelectron Spectroscopy (XPS) analyses were performed on a Phi Electronics 5600/5800 instrument equipped with a monochromatic Al Kα X-ray source operating at 350 W. The spectra were calibrated to a C1s peak at 284.5 eV and evaluated with MultiPak and Origin software. Bath ultrasonication was performed in an Emerson Bransonic CPX2800 ultrasonic bath with 40 kHz transducers. Lap shear adhesion testing was carried out using a procedure described in ASTM D1002-10 on an Instron universal materials tester equipped with a 5 kN load cell with a rate of shear of 0.5% per minute. The bonded overlap area was measured with digital calipers prior to testing. Adhesion strength was determined by the maximum load divided by the bonded overlap area, and failure mode was assessed visually. Differential scanning calorimetry (DSC) measurements were performed on a Mettler Toledo DSC 1 STARe System with liquid nitrogen cooling with heating/cooling rates of 10 °C/minute, unless

otherwise indicated. Temperature ranges were within -50 to 300 °C, with typical curing programs consisting of two cycles of heating and cooling from -20 °C to 295 °C. Gel permeation chromatography was performed at the Lawrence Berkeley National Lab Catalysis Facility in Berkeley, CA on a Malvern Viscotek GPC system with tetrahydrofuran mobile phase (flow rate 1 mL/min), calibrating with narrow dispersity polystyrene standards. Thermogravimetric analyses (TGA) were conducted using a TA Instruments TGA Q5000 and decomposition trace was collected under a flow rate of 25 mL/min N_2 gas or air with a temperature ramp rate of 10 °C/min. Compression molding was carried out on a Grizzly Industrial 10-ton benchtop shop press with heated plates (model H6231Z). Flexural testing by 3-point bending was carried out in accordance to ASTM D790 using an Instron A620-325 (Norwood MA) at the crosshead speed of 0.01 mm/min. Nanoindentation measurements were performed using a Triboindenter TI 950 (Hysitron, Minneapolis) with a 150nm Berkovich tip. The tip area function was established from a polycarbonate standard. Scanning electron microscopy (SEM) images were obtained using a FEI Strata 235 dual beam Focused Ion Beam (FIB). The images were taken at beam voltages of 5 and 10 kV at a working distance of ~10 mm relative to the sample surface. All samples were sputter-coated with ~20 A of Au-Pd before imaging to inhibit charging. Scanning helium ion microscopy (SHIM) images were obtained using a Zeiss ORION NanoFab. The images were taken at a beam current of 0.66-0.76 pA and at a working distance of ~9 mm relative to the sample surface. The flood gun to prevent charging was used when needed. Spin coating was performed on a Chemat Technology spin-coater model KW-4A. UV-Vis spectra were collected on a Shimadzu UV-2600 model spectrometer.

2. Synthetic Procedures

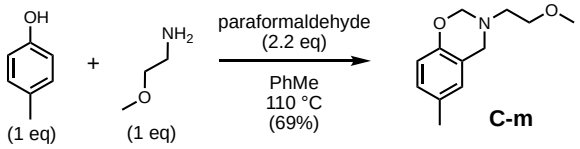

3-(2-methoxyethyl)-6-methyl-3,4-dihydro-2*H*-benzo[*e*][1,3]oxazine, **C-m**: 2-methoxy-ethylamine (806 µL, 9.34 mmols, 1 eq), *p*-cresol (1.01 g, 9.34 mmols, 1 eq), and paraformaldehyde (617 mg, 20.6 mmols formaldehyde, 2.2 eq) were combined in a round bottom flask in toluene (3.5 mL), and the suspension was heated at 110 °C for 5 hours. The reaction was cooled to room temperature and diluted with diethyl ether (50 mL). The solution was washed with 3N NaOH (aq) (4 x 25 mL) and deionized water (3 x 25 mL), and then dried over anhydrous sodium sulfate. The resulting solution was filtered through a 2 cm plug of silica gel and condensed under reduced pressure on a rotary evaporator to produce a colorless viscous residue (1.342 g, 69% yield). R_f 0.45 (30% EtOAc/hexanes), bronze-colored stain with ninhydrin. ^{1}H NMR (400 MHz, $CDCl_3$) δ 6.91 (dd, *J* = 8.2, 1.5 Hz, 1H), 6.76 (d, *J* = 1.5 Hz, 1H), 6.68 (d, *J* = 8.3 Hz, 1H), 4.87 (s, 2H), 4.02 (s, 2H), 3.55 (t, *J* = 5.3 Hz, 2H), 3.39 (s, 3H), 2.97 (t, *J* = 5.3 Hz, 2H), 2.24 (s, 3H). ^{13}C NMR (101 MHz, $CDCl_3$) δ 151.94, 129.83, 128.36, 127.94, 119.74, 116.23, 82.82, 70.94, 59.06, 51.07, 50.62, 20.66.

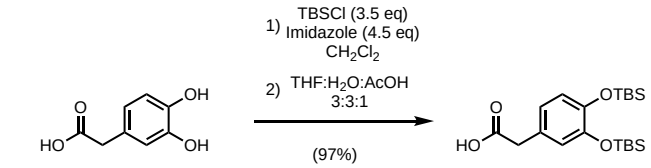

3,4-dihydroxyphenylacetic acid **S1**

2-(3,4-bis((*tert*-butyldimethylsilyl)oxy)phenyl)acetic acid, S1: Precursor **S1** was prepared by adapting conditions previously described by Malik and colleagues for the synthesis of TBS-protected gallic acid.[1] 3,4-dihydroxyphenylacetic acid (10.0 g, 59.5 mmols, 1 eq) and *tert*-butyldimethylsilyl chloride (31.4 g, 208 mmols, 3.5 eq) were suspended in dry CH_2Cl_2 (210 mL) in a dry round bottom flask containing a stir bar. The suspension was cooled in an ice bath under argon, and imidazole (18.2 g, 268 mmols, 4.5 eq) was added under argon flow over 1.5 minutes while stirring. The suspension was stirred for 16 hours, allowing the mixture to reach room temperature, and the resulting imidazole hydrochloride precipitate was removed by filtration. The filtrate was condensed under reduced pressure, and the residue was taken up in diethyl ether (200 mL). The organic solution was washed with water (80 mL), saturated aqueous ammonium chloride (3 x 80 mL), and brine (80 mL), dried over anhydrous sodium sulfate, filtered, and condensed under reduced pressure to provide a viscous liquid crude. The resulting crude contains a mixture of the desired free acid **S1**, and the undesired TBS-protected acid **S1'**. While separable by chromatography, it is preferable to hydrolyze **S1'** by treatment with acetic acid. The combined crude is dissolved in tetrahydrofuran (120 mL), and 1:3 glacial acetic acid:deionized water (160 mL) was added in one portion. The biphasic mixture was stirred vigorously at room temperature under argon for 4 hours, and then poured into ice-chilled deionized water (400 mL). The solution was extracted with ethyl acetate (3 x 100 mL), and the combined organic phases were washed with water (3 x 100 mL) and brine (100 mL), dried over anhydrous sodium sulfate, filtered, and condensed under reduced pressure. The pale-brown oil was dried under high vacuum for an extended period to provide a tan solid (23.02 g, 97% yield). R_f 0.56 (50% EtOAc/hexanes). ^{1}H NMR (400 MHz, $CDCl_3$) δ 6.79 (d, *J* = 2.1 Hz, 1H), 6.77 (d, *J* = 8.2 Hz, 1H), 6.71 (dd, *J* = 8.2, 2.2 Hz, 1H), 3.51 (s, 2H), 0.99 (two overlapping s, 18H), 0.19 (app d from two overlapping singlets, app *J* = 1.3 Hz, 12H). ^{13}C NMR (101 MHz, $CDCl_3$) δ 178.42, 146.90, 146.33, 126.30, 122.42, 122.36, 121.06, 40.57, 26.07 (x2), 18.57 (x2), -3.97, -3.99.

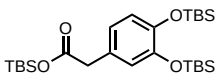

S1'

***tert*-butyldimethylsilyl 2-(3,4-bis((*tert*-butyldimethylsilyl)oxy)phenyl) acetate, S4':** R_f 0.9 (50% EtOAc/hexanes). ^{1}H NMR (400 MHz, $CDCl_3$) δ 6.76 (d, *J* = 8.0 Hz, 1H), 6.73 (d, *J* = 2.1 Hz, 1H), 6.70 (dd, *J* = 8.0, 2.2 Hz, 1H), 3.47 (s, 2H), 0.98 (app d, *J* = 3.0 Hz, 18H), 0.84 (s, 9H), 0.22 (s, 6H), 0.18 (app d, *J* = 1.4 Hz, 12H). ^{13}C NMR (101 MHz, $CDCl_3$) δ 172.25, 146.74, 145.93, 127.89, 122.47, 122.32, 121.13, 42.86, 26.11, 26.08, 25.59, 18.61, 18.55, 17.72, -3.98, -4.78

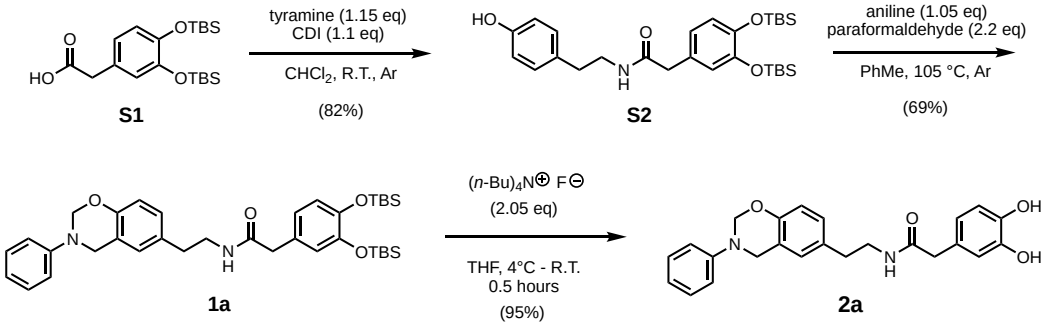

Scheme S2. Synthetic route to deprotected benzoxazine monomer **2a**.

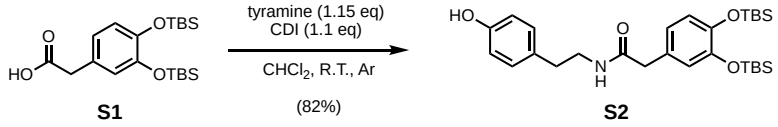

2-(3,4-bis((*tert*-butyldimethylsilyl)oxy)phenyl)-*N*-(4-hydroxyphenethyl)acetamide, **S2:** Acid **S1** (500 mg, 1.26 mmols, 1 eq) was dissolved in dichloromethane (6.4 mL) in a round bottom flask containing a magnetic stir bar and placed under argon. Carbonyl diimidazole (CDI, 225 mg, 1.39 mmols, 1.1 eq) was added portion-wise over 5 minutes, and stirring was continued at room temperature for 20 minutes, at which time tyramine (199 mg, 1.45 mmols, 1.15 eq) was added. The mixture was stirred at room temperature for 1 hour more, and then the solvent was removed under reduced pressure. The residue was taken up in diethyl ether (40 mL), and the solution was washed with saturated aqueous ammonium chloride solution (3 x 20 mL), saturated aqueous sodium bicarbonate solution (2 x 20 mL), and brine (2 x 20 mL), dried over anhydrous sodium sulfate, filtered, and condensed under reduced pressure. The resulting crude was further purified by column chromatography on silica gel, eluting with a gradient from hexanes through 40% ethyl acetate/hexanes. Fractions containing product, as determined by TLC, were condensed under reduced pressure to provide a white solid (533 mg, 82% yield). R_f 0.53 (50% EtOAc/hexane). ^{1}H NMR (400 MHz, $CDCl_3$) δ 7.92 (bs, 1H), 6.93 – 6.85 (m, 2H), 6.82 – 6.74 (m, 3H), 6.69 (d, *J* = 2.2 Hz, 1H), 6.60 (dd, *J* = 8.1, 2.2 Hz, 1H), 5.66 (t, *J* = 5.8 Hz, 1H), 3.46 – 3.39 (m, 4H), 2.62 (t, *J* = 7.1 Hz, 2H), 1.00 (s, 9H), 0.98 (s, 9H), 0.21 (s, 6H), 0.18 (s, 6H). ^{13}C NMR (101 MHz, $CDCl_3$) δ 172.34, 155.47, 147.24, 146.48, 129.66, 129.43, 127.35, 122.63, 122.43, 121.50, 115.73, 43.06, 41.32, 34.75, 25.99, 25.97, 18.51, -4.00.

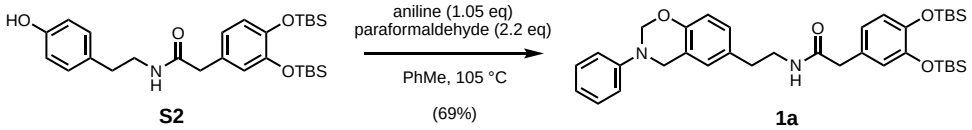

2-(3,4-bis((*tert*-butyldimethylsilyl)oxy)phenyl)-*N*-(2-(3-phenyl-3,4-dihydro-2*H*-benzo[*e*][1,3]-oxazin-6-yl)ethyl)acetamide, **1a:** Phenol **S2** (663 mg, 1.29 mmols, 1 eq), paraformaldehyde (87.0 mg, 2.83 mmols, 2.2 eq of formaldehyde), and aniline (126 mg, 1.35 mmols, 1.05 eq) were combined in toluene (4 mL) in a round bottom flask topped with a reflux condenser under argon and heated at 105 °C for 16 hours. The reaction was cooled to room temperature, loaded directly onto a column of silica gel equilibrated with 1% triethylamine/hexanes, and eluted with a gradient from hexanes through 20% ethyl

acetate/hexanes. Fractions containing product were condensed under reduced pressure to provide an off-white solid after further drying under high vacuum (565 mg, 69% yield). R_f 0.31 (30% EtOAc/hexane). ^{1}H NMR (400 MHz, $CDCl_3$) δ 7.29 – 7.21 (m, 2H), 7.14 – 7.06 (m, 2H), 6.96 – 6.88 (m, 1H), 6.79 (d, *J* = 8.1 Hz, 1H), 6.78 (dd, *J* = 8.3, 2.0 Hz, 1H), 6.74 – 6.67 (m, 3H), 6.62 (dd, *J* = 8.1, 2.2 Hz, 1H), 5.50 (t, *J* = 5.9 Hz, 1H), 5.33 (s, 2H), 4.57 (s, 2H), 3.42 (s, 2H), 3.39 (q, *J* = 7.1 Hz, 2H), 2.60 (t, *J* = 7.0 Hz, 2H), 1.01 (s, 9H), 0.99 (s, 9H), 0.21 (s, 6H), 0.19 (s, 6H). ^{13}C NMR (101 MHz, $CDCl_3$) δ 171.32, 153.02, 148.43, 147.21, 146.32, 131.00, 129.32, 128.14, 127.87, 126.81, 122.51, 122.37, 121.45, 121.41, 120.98, 118.25, 117.05, 79.40, 50.49, 43.26, 40.99, 34.96, 25.99, 25.99, 18.51, 18.51, -3.98, -4.00.

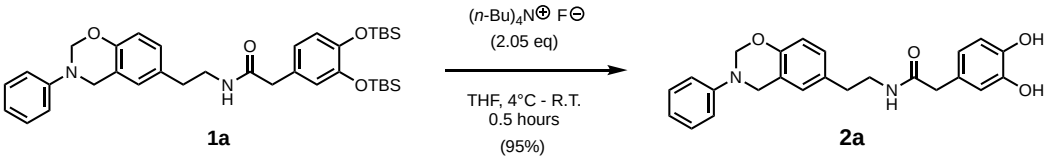

2-(3,4-dihydroxyphenyl)-*N*-(2-(3-phenyl-3,4-dihydro-2*H*-benzo[*e*][1,3]oxazin-6-yl)ethyl)-acetamide, **2a:** Protected benzoxazine **1a** (711 mg, 1.12 mmols, 1 eq) was dissolved in tetrahydrofuran (5.6 mL) in a round bottom flask containing a magnetic stir bar and chilled on an ice bath under argon. A solution of tetrabutylammonium fluoride (TBAF, Sigma, 1M in THF, 2.30 mL, 2.30 mmols, 2.05 eq) was added dropwise by syringe over 3 minutes while stirring to produce an immediate development of a yellow color. Stirring was continued for 30 minutes, at which time pH 7 0.1 M aqueous sodium phosphate buffer (20 mL) was injected to quench the reaction. The mixture was transferred to a separatory funnel and extracted with ethyl acetate (2 x 25 mL). The combined organic layers were washed with pH 7 0.1 M sodium phosphate buffer (30 mL), 1:1 sodium phosphate buffer:brine (30 mL), and brine (30 mL) before drying over anhydrous sodium sulfate, filtering, and condensing under reduced pressure. The residue was further purified by column chromatography on silica gel packed in dichloromethane, eluting with a gradient from dichloromethane through 50% acetone/dichloromethane. Fractions containing product were condensed under reduced pressure to provide a pale-yellow foaming solid (434 mg, 96% yield). R_f 0.48 (30% acetone/hexane). ^{1}H NMR (400 MHz, $CDCl_3$) δ 7.29 – 7.20 (m, 2H), 7.12 – 7.03 (m, 2H), 6.95 – 6.86 (m, 1H), 6.76 (d, *J* = 8.1 Hz, 1H), 6.72 (dd, *J* = 8.4, 2.0 Hz, 1H), 6.70 – 6.61 (m, 3H), 6.47 (dd, *J* = 8.0, 2.1 Hz, 1H), 5.81 (t, *J* = 5.9 Hz, 1H), 5.29 (s, 2H), 4.51 (s, 2H), 3.42 – 3.29 (m, 4H), 2.56 (t, *J* = 6.8 Hz, 2H). ^{13}C NMR (101 MHz, $CDCl_3$) δ 173.31, 153.07, 148.34, 144.94, 144.15, 130.63, 129.41, 128.21, 126.91, 126.14, 121.58, 121.41, 121.12, 118.29, 117.17, 116.23, 115.80, 79.50, 50.43, 43.04, 41.23, 34.60. ATR-FTIR (solid): 3241 (broad strong; O–H stretch), 3029 (m; C-H stretching), 1633 (s; secondary amide C=O stretch), 1598 (m), 1494 (s; asymmetrically tri-substituted aryl C=C bend), 1224 (s; aryl C-O stretch), 943 (m, oxazine related mode), 754 (s; monosubstituted aryl C-H bending), 693 (s; monosubstituted aryl C-H bending).

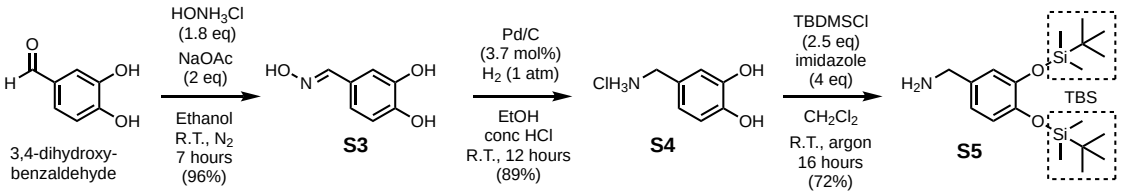

Scheme S1. Synthesis of precursor **S5** from the metabolite 3,4-dihydroxybenzaldehyde.

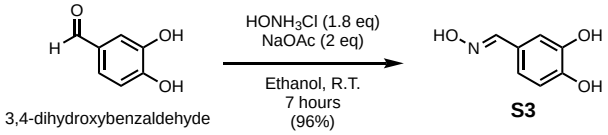

(*E*)-3,4-dihydroxybenzaldehyde oxime, S3: 3,4-dihydroxybenzaldehyde (10.0 g, 72.4 mmols, 1 eq) was suspended in reagent ethanol (290 mL) at room temperature, and the mixture was deoxygenated by bubbling nitrogen for 10 minutes while stirring. Hydroxylamine hydrochloride (9.06 g, 130 mmols, 1.8 eq) and sodium acetate (11.9 g, 145 mmols, 2 eq) were added, and nitrogen bubbling was continued for 6 minutes more. The pale tan suspension was then stirred vigorously at room temperature for 7 hours, and volatiles were then removed under reduced pressure. The residue was taken up in deionized water (150 mL) and extracted with ethyl acetate (3 x 50 mL). The organic phase was washed with brine (2 x 50 mL), dried over anhydrous sodium sulfate, filtered, and condensed under reduced pressure to provide a tan-colored solid (10.61 g, 96% yield). R_f 0.45 (10% MeOH/CH_2Cl_2+0.5% acetic acid). ^{1}H NMR (400 MHz, DMSO-d_6) δ 10.79 (bs, 1H), 9.18 (bs, 2H), 7.92 (s, 1H), 7.05 (d, *J* = 2.0 Hz, 1H), 6.81 (dd, *J* = 8.1, 2.0 Hz, 1H), 6.73 (d, *J* = 8.1 Hz, 1H). ^{13}C NMR (101 MHz, DMSO) δ 148.22, 147.02, 145.55, 124.54, 119.35, 115.61, 112.65.

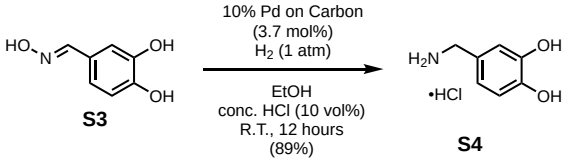

3,4-dihydroxybenzylamine hydrochloride, S4: Oxime **S3** (1.00 g, 6.53 mmols, 1 eq) and 10% palladium on activated carbon (257 mg, 0.242 mmols, 3.7 mol%) were suspended in ethanol (26 mL) and concentrated hydrochloric acid (3 mL). The reaction vessel was evacuated under high vacuum and back-filled with hydrogen gas three times while stirring. The resulting suspension was stirred at room temperature for 12 hours, and then passed through a 3 cm plug of Celite filter aid, washing the filter cake with ethanol (30 mL). The filtrate was condensed to an ivory sticky mass. The residue was triturated in ethyl acetate (50 mL) to yield a white solid which was collected by vacuum filtration, washing with ethyl acetate (50 mL), and then dried under high vacuum (1.026 g, 89% yield). Note: when the above protocol was applied at a scale of 50.79 mmols of **S1**, a yield of 57% was obtained. R_f 0.00 (10% MeOH/CH_2Cl_2 + 0.1% AcOH) ^{1}H NMR (400 MHz, DMSO-d_6) δ 9.04 (bs, 2H), 8.09 (bs, 3H), 6.84 (d, *J* = 2.0 Hz, 1H), 6.75 (d, *J* = 8.0 Hz, 1H), 6.71 (dd, *J* = 8.1, 2.1 Hz, 1H), 3.81 (app q, *J* = 5.7 Hz, 2H). ^{13}C NMR (101 MHz, DMSO) δ 145.69, 145.26, 124.71, 120.26, 116.82, 115.69, 42.07.

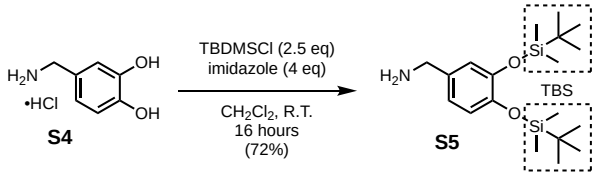

(3,4-bis((*tert*-butyldimethylsilyl)oxy)phenyl)methanamine, S5: 3,4-dihydroxybenzylamine hydrochloride, **S4** (5.10 g, 29.0 mmols, 1 eq), *tert*-butyldimethylsilyl chloride (10.9 g, 72.6 mmols, 2.5 eq), and imidazole (7.91 g, 116, mmols, 4 eq) were combined in a round-bottom flask with a stir bar, and dry dichloromethane (115 mL) was added. The reaction mixture (suspension) was stirred overnight under argon at room temperature, and a large amount of white precipitate was present, which was removed by vacuum filtration, and the filtrate was condensed under reduced pressure. The crude was partitioned between diethyl ether (150 mL) and aqueous saturated ammonium chloride solution (150 mL). The aqueous phase was extracted twice more with diethyl ether (2x70 mL), and the combined organic phases were washed with water (100 mL), saturated aqueous sodium bicarbonate solution (100 mL), and brine (100 mL). The organic layer was dried over anhydrous sodium sulfate, filtered, and condensed in vacuum to provide a pale-yellow viscous liquid which was purified further by column chromatography on silica gel, eluting with a gradient from dichloromethane through 10% methanol/dichloromethane (7.69 g, 72% yield). R_f 0.49 (10% MeOH/CH_2Cl_2), stained with ninhydrin. ^{1}H NMR (400 MHz, $CDCl_3$) δ 6.78 (d, *J* = 8.2 Hz, 1H), 6.76 (d, *J* = 2.2 Hz, 1H), 6.73 (dd, *J* = 8.0, 2.2 Hz, 1H), 3.72 (s, 2H), 1.53 (s, 2H), 0.99 (s, 9H), 0.98 (s, 9H), 0.19 (s, 6H), 0.18 (s, 6H). ^{13}C NMR (101 MHz, $CDCl_3$) δ 146.83, 145.75, 136.77, 121.09, 120.16, 119.98, 46.13, 26.08, 18.57, 18.54, -3.95, -3.97.

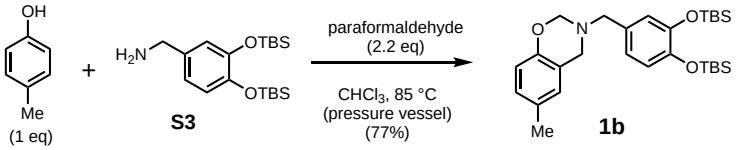

3-(3,4-bis((*tert*-butyldimethylsilyl)oxy)benzyl)-6-methyl-3,4-dihydro-2*H*-benzo[*e*][1,3]-oxazine, 1b: Amine **S3** (566 mg, 1.54 mmols, 1.03 eq) and paraformaldehyde (101 mg, 3.29 mmols of formaldehyde, 2.2 eq) were combined in chloroform (7.5 mL) in a 15 mL capacity pressure vessel with teflon screw cap containing a magnetic stir bar. After stirring at room temperature for 10 minutes, *p*-cresol (162 mg, 1.50 mmols, 1 eq) was added, and the mixture was purged under argon and sealed. The mixture was heated at 85 °C in a pre-warmed oil bath for 16 hours, then cooled to room temperature. The crude reaction mixture was diluted with diethyl ether (50 mL) and transferred to a separatory funnel. The organic solution was washed with 3N aqueous NaOH solution (3 x 40 mL), deionized water (2 x 40 mL), saturated brine (2 x 40 mL), and then dried over anhydrous sodium sulfate. The solids were removed by vacuum filtration, and the filtrate was condensed. The crude was further purified by column chromatography on silica gel, eluting with a gradient from hexanes through 3% EtOAc/hexanes, to provide a white solid after drying under vacuum (575 mg, 77% yield). R_f 0.74 (10% EtOAc/hexanes). ^{1}H NMR (400 MHz, $CDCl_3$) δ 6.95 (dd, *J* = 7.9, 2.0 Hz, 1H), 6.84 (d, *J* = 1.4 Hz, 1H), 6.81 – 6.74 (m, 3H), 6.72 (d, *J* = 8.3 Hz, 1H), 4.84 (s, 2H), 3.92 (s, 2H), 3.79 (s, 2H), 2.26 (s, 3H), 1.00 (overlapping singlets as apparent d, *J* = 1.1 Hz, 18H), 0.21 (overlapping singlets as apparent d, *J* = 2.6 Hz, 12H).^{13}C NMR

(101 MHz, $CDCl_3$) δ 152.06, 146.78, 146.24, 131.41, 129.85, 128.34, 128.13, 122.12, 122.05, 120.99, 119.87, 116.22, 82.17, 55.12, 49.56, 26.11, 20.73, 18.60, -3.94.

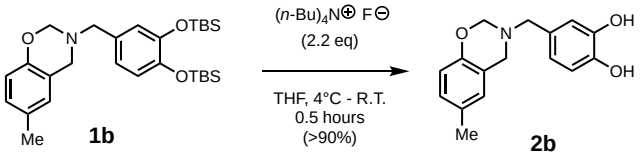

4-((6-methyl-2*H*-benzo[*e*][1,3]oxazin-3(4*H*)-yl)methyl)benzene-1,2-diol, 2b: TBS-protected benzoxazine monomer **1b** (400 mg, 0.800 mmols, 1 eq) was dissolved in tetrahydrofuran (8.2 mL) in a round-bottom flask containing a magnetic stir bar. The vessel was purged with argon, and the solution stirred at 4 °C while tetrabutylammonium fluoride, TBAF (Sigma, 1M in THF, 1.7 mL, 1.7 mmols, 2.1 eq) was added dropwise over 5 minutes. The reaction mixture turned from a clear colorless solution to a pale green color over the next 15 minutes. After stirring for 30 minutes, EtOAc was injected (5 mL), followed by 0.1 M pH 7 sodium phosphate buffer (5 mL). The green color disappeared, yielding a pale-yellow organic phase, and a colorless aqueous phase. The organic layer was separated and washed again with phosphate buffer (5 mL), and brine (5 mL), and dried over anhydrous sodium sulfate. Solids were removed by filtration, and the filtrate was condensed under reduced pressure and dried in high vacuum provide a yellow foaming solid. (200 mg, 92% yield). R_f 0.11 (10% MeOH/CH_2Cl_2). A fraction of the product (75 mg) was submitted to column chromatography on silica gel, eluting with a gradient from CH_2Cl_2 through 30% acetone/CH_2Cl_2 to provide a pale-yellow foaming solid for spectroscopic analysis. (^{1}H NMR (400 MHz, Acetone-d_6) δ 7.90 (bs, 2H), 6.90 (dd, *J* = 8.4, 2.1 Hz, 1H), 6.87 (d, *J* = 2.0 Hz, 1H), 6.78 (d, *J* = 8.0 Hz, 1H), 6.74 (d, *J* = 2.1 Hz, 1H), 6.68 – 6.60 (m, 3H), 4.79 (s, 2H), 3.86 (s, 2H), 3.73 (s, 2H), 2.19 (s, 3H). ^{13}C NMR (101 MHz, $CDCl_3$) δ 151.55, 144.10, 143.86, 130.31, 130.00, 128.55, 128.11, 122.08, 119.32, 116.70, 116.27, 115.44, 81.38, 55.06, 49.69, 20.72.. ATR-FTIR (solid): 3306 (broad strong; O–H stretch), 2922 (m), 2856 (w; alkyl C–H stretch), 1603 (m), 1499 (s; asymmetrically tri-substituted aryl C=C bend), 1213 (s; aryl ether C-O-C asymmetric stretch), 934 (m, oxazine related mode), 813 (s; trisubstituted aromatic C-H bending).

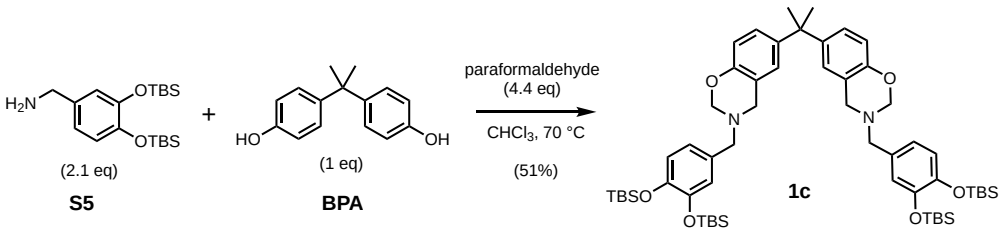

6,6'-(propane-2,2-diyl)bis(3-(3,4-bis((*tert*-butyldimethylsilyl)oxy)benzyl)-3,4-dihydro-2*H*-benzo[*e*][1,3]oxazine), **1c:** Amine **S5** (320 mg, 0.870 mmols, 2.05 eq), bisphenol-A (BPA, 97.0 mg, 0.430 mmols, 1 eq), and paraformaldehyde (56.0 mg, 1.90 mmols, 4.4 eq of formaldehyde) were combined in chloroform (4.3 mL) in a round bottom flask topped with a reflux condenser and heated under argon with stirring for 23 hours, at which time the reaction was cooled to room temperature and diluted with diethyl ether (40 mL). The organic phase was washed with 3M NaOH aqueous solution (3 x 15 mL), deionized water (2 x 15 mL), and brine (1 x 25 mL), dried over

anhydrous sodium sulfate, filtered and condensed under reduced pressure. The crude was further purified by column chromatography on silica gel, eluting with a gradient from hexanes, through 5% ethyl acetate in hexanes. The fractions containing product were condensed under reduced pressure to provide a white foam solid (222 mg, 51% yield). R_f 0.42 (10% EtOAc/hexanes). ^{1}H NMR (400 MHz, $CDCl_3$) δ 6.97 (dd, *J* = 8.5, 2.4 Hz, 1H), 6.85 – 6.83 (m, 1H), 6.82 (d, *J* = 2.4 Hz, 1H), 6.80 – 6.78 (m, 2H), 6.71 (d, *J* = 8.6 Hz, 1H), 4.82 (s, 2H), 3.92 (s, 2H), 3.79 (s, 2H), 1.60 (s, 3H), 0.99 (s, 9H), 0.99 (s, 9H), 0.20 (s, 6H), 0.20 (s, 6H). ^{13}C NMR (101 MHz, $CDCl_3$) δ 152.07, 146.75, 146.23, 143.10, 131.39, 126.40, 125.59, 122.13, 122.09, 121.02, 119.34, 115.93, 82.07, 55.21, 49.92, 41.84, 31.23, 26.11, 26.10, 18.59, -3.90, -3.94.

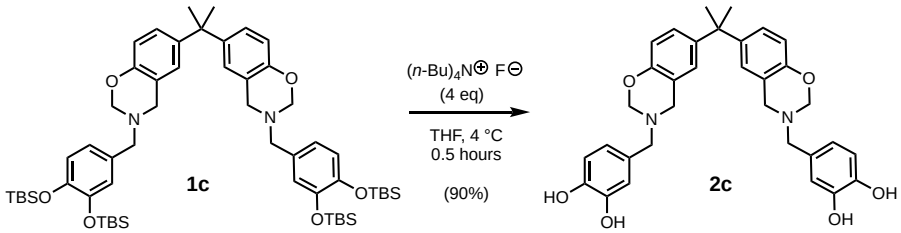

4,4'-((propane-2,2-diylbis(2*H*-benzo[*e*][1,3]oxazine-6,3(4*H*)-diyl))bis(methylene))bis-(benzene-1,2-diol), **2c**: Bis-benzoxazine **1c** (693 mg, 0.685 mmols, 1 eq) was dissolved in tetrahydrofuran (13.5 mL) and the vessel was purged with argon. The solution was stirred at 4 °C while tetrabutylammonium fluoride, TBAF (1M in THF, 2.74 mL, 2.74 mmols, 4 eq) was added dropwise over 3 minutes. The reaction mixture turned from a clear colorless solution to a pale-yellow color within 2 minutes. After stirring for 30 minutes, EtOAc was injected (30 mL), followed by pH 7 0.1 M aqueous sodium phosphate buffer (30 mL). The organic layer was separated and washed again with phosphate buffer (30 mL), and brine (30 mL), and dried over anhydrous sodium sulfate. Solids were removed by filtration, and the filtrate was condensed under reduced pressure to provide a sticky yellow residue, which was dissolved in minimal methanol and diluted with dichloromethane to produce a yellow solid. Solids were collected by vacuum filtration, washed with chilled dichloromethane and hexane, and dried under reduced pressure to provide a yellow foaming solid (363 mg, 95% yield). R_f 0.35 (streak, stains grey-black with $FeCl_3$) (10% methanol/dichloromethane). ^{1}H NMR (400 MHz, Methanol-d_4) δ 6.93 (dd, *J* = 8.6, 2.4 Hz, 2H), 6.82 (d, *J* = 2.4 Hz, 2H), 6.79 (d, *J* = 2.0 Hz, 2H), 6.70 (d, *J* = 8.0 Hz, 2H), 6.63 (d, *J* = 8.5 Hz, 2H), 6.60 (dd, *J* = 8.1, 1.9 Hz, 2H), 4.72 (s, 4H), 3.85 (s, 4H), 3.68 (s, 4H), 1.56 (s, 6H). ^{13}C NMR (101 MHz, MeOD) δ 153.02, 146.27, 145.78, 144.53, 130.44, 127.27, 126.69, 121.88, 120.31, 117.42, 116.59, 116.09, 82.31, 56.02, 54.78, 50.93, 42.68, 31.49. ATR-FTIR (solid): 3200 (broad strong; O–H stretch), 3036 (m), 2963 (w; alkyl C–H stretch), 1606 (m), 1496 (s; asymmetrically tri-substituted aryl C=C bend), 1442 (m, methyl group C-H bending), 1226 (s; aryl ether C-O-C asymmetric stretch), 933 (m, oxazine related mode), 818 (s; trisubstituted aryl C-H bending).

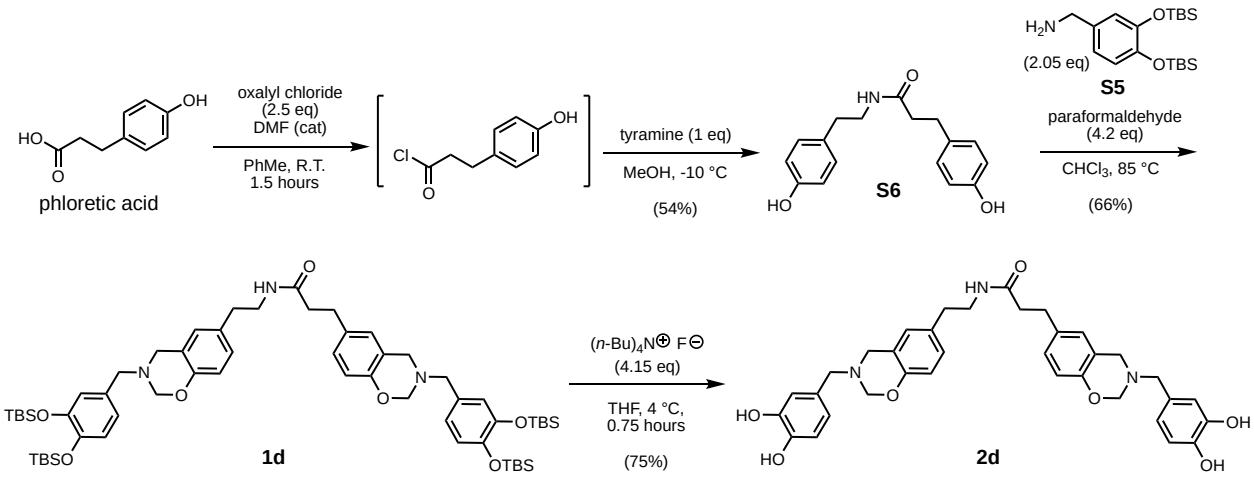

Scheme S3. Synthetic route to prepare **2d** from metabolite-derived precursors.

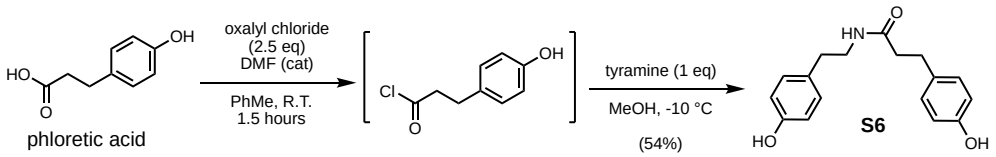

***N*-(4-hydroxyphenethyl)-3-(4-hydroxyphenyl)propenamide**, **S6:** Phloretic acid (1 g, 6.02 mmols, 1.1 eq) was suspended in dry dichloromethane (13 mL) containing dry N,N-Dimethylformamide (50 µL). Oxalyl chloride (1.29 mL, 15.0 mmols, 2.75 eq) was added dropwise over 1 minute while stirring vigorously at room temperature. Stirring was continued for 5 hours, and the mixture was then condensed under reduced pressure to provide a sticky residue, which was taken up again in dry dichloromethane (5 mL). In a separate flask, tyramine (748 mg, 5.46 mmols, 1 eq) was dissolved in methanol (27 mL) containing potassium carbonate (1.50 g, 27.3 mmols, 5 eq) and chilled to -10 °C in a NaCl/ice bath. The solution of crude acid chloride was added dropwise over 10 minutes to the chilled and vigorously-stirring tyramine solution, and stirring was continued for 16 hours, allowing the cooling bath to warm to room temperature. The reaction was quenched by the addition of deionized water (50 mL) and 1N aqueous HCl (25 mL) to form a precipitate, which was collected by vacuum filtration and dried under reduced pressure to provide an off-white solid which was used without further purification (835 mg, 53.6% yield). R_f 0.44 (10% methanol/dichloromethane). ^{1}H NMR (400 MHz, DMSO-d_6) δ 9.18 (s, 1H), 9.16 (s, 1H), 7.84 (t, J = 5.7 Hz, 1H), 7.02 – 6.90 (m, 4H), 6.70 – 6.62 (m, 4H), 3.17 (q, J = 6.9 Hz, 2H), 2.68 (t, J = 7.8 Hz, 2H), 2.54 (t, J = 7.5 Hz, 2H), 2.28 (t, J = 7.8 Hz, 2H). ^{13}C NMR (101 MHz, DMSO) δ 171.38, 155.63, 155.46, 131.45, 129.59, 129.51, 129.09, 115.11, 115.05, 40.60, 37.59, 34.48, 30.42.

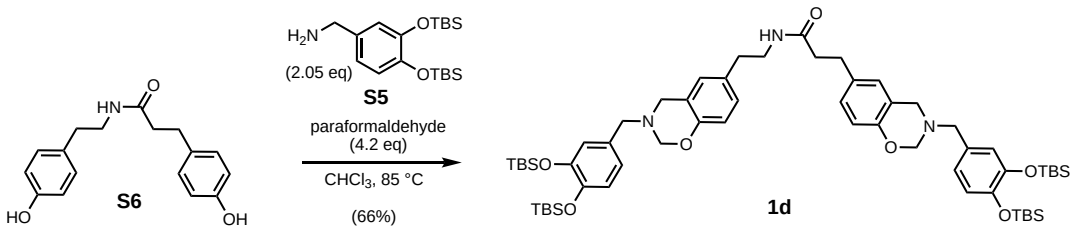

3-(3-(3,4-bis((*tert*-butyldimethylsilyl)oxy)benzyl)-3,4-dihydro-2*H*-benzo[*e*][1,3]oxazin-6-yl)-*N*-(2-(3-(3,4-bis((*tert*-butyldimethylsilyl)oxy)benzyl)-3,4-dihydro-2*H*-benzo[*e*][1,3]oxazin-6-yl)-ethyl)propenamide, **1d:** Bisphenol **S6** (156 mg, 0.546 mmols, 1 eq), amine **S5** (412 mg, 1.12 mmols, 2.05 eq), paraformaldehyde (69.0 mg, 2.29 mmols, 4.2 eq of formaldehyde), and chloroform (2.8 mL) were combined in a 4 mL scintillation vial containing a magnetic stir bar and sealed under argon. The heterogeneous reaction mixture was heated at 85 °C in an oil bath while stirring for 22 hours, and then cooled to room temperature. The resulting crude was loaded directly onto a packed column of silica gel, rinsing with minimal acetone, and eluted with a gradient from hexanes through 35% acetone/hexanes. Fractions containing product, as determined by TLC, were pooled and condensed under reduced pressure to provide an off-white foam solid (387 mg, 66% yield). R_f 0.59 (10% methanol/dichloromethane). ^{1}H NMR (400 MHz, $CDCl_3$) δ 6.95 (dd, *J* = 8.3, 2.2 Hz, 1H), 6.89 – 6.83 (m, 3H), 6.82 – 6.72 (m, 7H), 6.69 (d, *J* = 2.1 Hz, 1H), 5.58 (t, *J* = 5.8 Hz, 1H), 4.81 (app d, app *J* = 4.8 Hz, 4H), 3.92 (app d, app *J* = 2.3 Hz, 4H), 3.77 (app d, app *J* = 5.7 Hz, 4H), 3.44 (q, *J* = 6.6 Hz, 2H), 2.86 (t, *J* = 7.6 Hz, 2H), 2.65 (t, *J* = 6.9 Hz, 2H), 2.40 (t, *J* = 7.6 Hz, 2H), 1.01 (app d, app *J* = 2.1 Hz, 36H), 0.23 – 0.21 (m, 24H). ^{13}C NMR (101 MHz, $CDCl_3$) δ 172.13, 152.89, 152.67, 146.73, 146.22, 146.19, 132.89, 131.16, 131.12, 130.82, 127.94, 127.79, 127.56, 127.50, 122.04, 122.02, 121.93, 121.90, 120.90, 120.28, 120.08, 116.52, 116.48, 81.95, 55.08, 55.05, 49.63, 40.87, 38.82, 35.09, 31.06, 26.04, 18.51, -3.99.

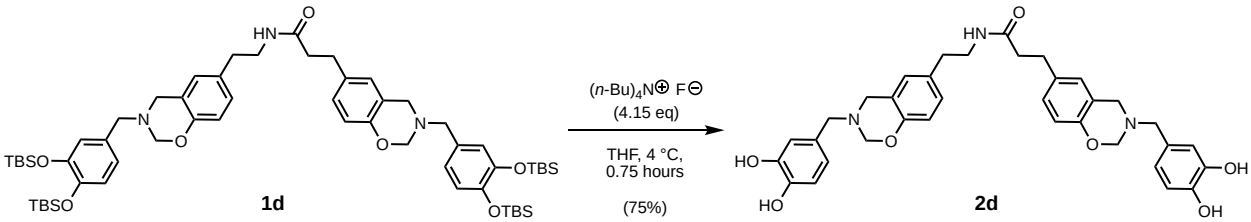

3-(3-(3,4-dihydroxybenzyl)-3,4-dihydro-2*H*-benzo[*e*][1,3]oxazin-6-yl)-*N*-(2-(3-(3,4-dihydroxy-benzyl)-3,4-dihydro-2*H*-benzo[*e*][1,3]oxazin-6-yl)ethyl)propenamide, **2d:** Protected bis-benzoxazine **1d** (741 mg, 0.693 mmols, 1 eq) was dissolved in tetrahydrofuran (4 mL) in a round bottom flask containing a magnetic stir bar and was chilled in an ice bath under argon, and tetrabutylammonium fluoride solution (Sigma, 1M in THF , 2.88 mL, 2.88 mmols, 4.15 eq) was added drop-wise over 2 minutes while stirring. The reaction was allowed to continue for 1 hour and then was quenched by injection of pH 7 0.1 M aqueous sodium phosphate buffer (15 mL). The solution was extracted with ethyl acetate (3 x 15 mL), and the combined organic phases were washed with sodium phosphate buffer (15 mL), deionized water (2 x 15 mL), and brine (2 x 15 mL), dried over anhydrous sodium sulfate, filtered, and condensed under reduced pressure to provide a yellow solid residue. The crude product was taken up in acetone (5 mL) and methanol (0.5 mL) and dropped into a stirring, ice-chilled solution of 85 vol% diethyl ether in hexanes to produce a pale-yellow sticky solid, which was collected by vacuum filtration, washed with excess

diethyl ether, and dried under high vacuum (317 mg, 75% yield). R_f 0.43 (top of streak, stains grey-black with $FeCl_3$) (10% methanol/dichloromethane). ^{1}H NMR (400 MHz, DMSO-d_6) δ 8.87 (bs, 4H), 7.87 (br t, *J* = 5.6 Hz, 1H), 6.91 (dd, *J* = 8.3, 2.2 Hz, 1H), 6.87 (dd, *J* = 8.3, 1.6 Hz, 1H), 6.78 (d, *J* = 2.2 Hz, 1H), 6.77 (d, *J* = 2.0 Hz, 1H), 6.76 – 6.69 (m, 2H), 6.71 – 6.61 (m, 5H), 6.55 – 6.46 (m, 2H), 4.75 (app d, app *J* = 2.8 Hz, 4H), 3.82 (app d, app *J* = 4.6 Hz, 4H), 3.62 (app d, app *J* = 3.1 Hz, 4H), 3.19 (q, *J* = 6.8 Hz, 2H), 2.68 (t, *J* = 7.7 Hz, 2H), 2.54 (t, *J* = 7.5 Hz, 2H), 2.29 (t, *J* = 7.7 Hz, 2H). ^{13}C NMR (101 MHz, MeOD) δ 175.20, 153.72, 153.62, 146.24, 145.75, 134.21, 132.60, 130.43, 129.04, 128.90, 128.65, 128.63, 121.87, 121.85, 120.99, 120.95, 117.42, 117.40, 117.18, 117.14, 116.14, 116.12, 82.48, 55.96, 49.64, 42.09, 39.15, 35.83, 32.23. ATR-FTIR (solid): 3201 (broad strong; O–H stretch), 2858 (w; alkyl C–H stretch), 1638 (s; secondary amide C=O stretch), 1602 (m), 1498 (s; asymmetrically tri-substituted aryl C=C bend), 1229 (s; aryl ether C-O-C asymmetric stretch), 933 (m, oxazine related mode), 817 (m, trisubstituted aryl C-H bend).

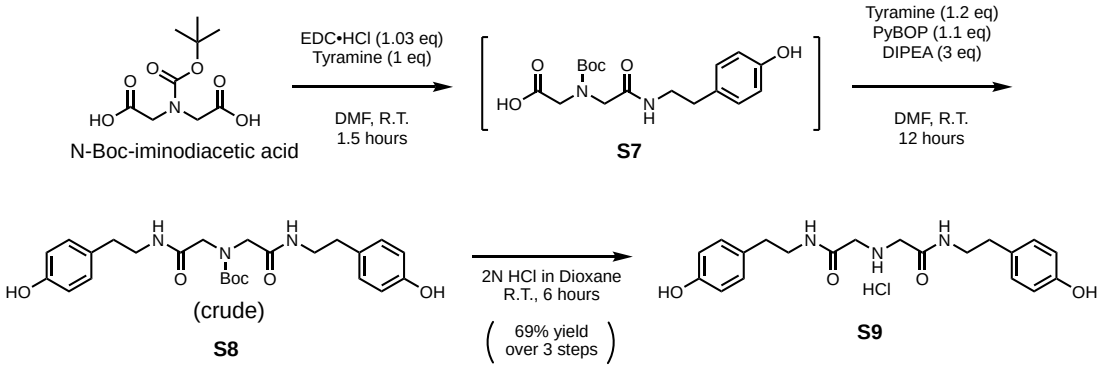

Scheme S4. Synthesis of tyramine-derived amino-bisphenol precursor **S9**.

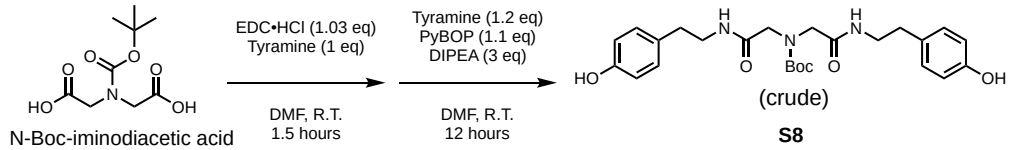

***tert*-butyl bis(2-((4-hydroxyphenethyl)amino)-2-oxoethyl)carbamate**, **S8:** N-Boc-iminodiacetic acid (Boc-IDA, 10.0 g, 42.9 mmols, 1 eq) was dissolved in dry N,N-dimethylformamide (DMF, 60 mL) in a round bottom flask containing a magnetic stir bar and EDC•HCl solid (8.47 g, 44.2 mmols, 1.03 eq) was added at room temperature while stirring. The resulting suspension was stirred vigorously under argon for 30 minutes, at which time a homogeneous solution was formed and TLC indicated consumption of Boc-IDA. Tyramine solid (5.88 g, 42.9 mmols, 1 eq) was added over 2 minutes while stirring in a cool water bath (18 °C) then stirring was continued at room temperature for 1 hour, at which time additional tyramine (6.47 g, 47.2 mmols, 1.1 eq), and diisopropylethylamine (DIPEA, 22.6 mL, 130 mmols, 3.03 eq) were added. The flask was topped with a pressure-equalizing liquid addition funnel containing a solution of (benzotriazole-1-yloxy)tripyrrolidinophosphonium hexafluorophosphate (PyBOP, 23.0 g, 44.2 mmols, 1.03 eq) in DMF (50 mL), and the solution was added drop-wise over 30 minutes while stirring under argon. The resulting solution was allowed to stir overnight at room temperature, and

was then poured into 0.1 N aqueous HCl (300 mL) and extracted with ethyl acetate (3 x 120 mL). The organic extracts were washed with saturated aqueous ammonium chloride (200 mL), and the wash was back-extracted once with ethyl acetate (100 mL). The combined organic phases were then washed with saturated aqueous sodium bicarbonate solution (100 mL), saturated aqueous ammonium chloride (100 mL), deionized water (2 x 100 mL), and brine (100 mL), dried over anhydrous sodium sulfate, filtered, and condensed under reduced pressure to provide a sticky tan-colored foam solid crude, which was analyzed by ^{1}H-NMR in CD_3OD and carried on to the next step without further purification (22.14 g crude, approximately 71.6% yield determined by ^{1}H-NMR). Attempts to purify by column chromatography were hampered by the presence of tri(pyrrolidin-1-yl)phosphine oxide, derived from PyBOP. R_f 0.26 (10% methanol/ dichloromethane + 0.5% acetic acid). ^{1}H NMR (400 MHz, Methanol-d_4) δ 7.07 (d, J = 8.2 Hz, 2H), 7.06 (d, J = 8.2 Hz, 2H), 6.73 (d, J = 8.3 Hz, 2H), 6.72 (d, J = 8.4 Hz, 2H), 3.90 (s, 1H), 3.85 (s, 1H), 3.44 – 3.38 (m, 4H), 2.78 – 2.71 (m, 4HH), 1.42 (s, 9H).

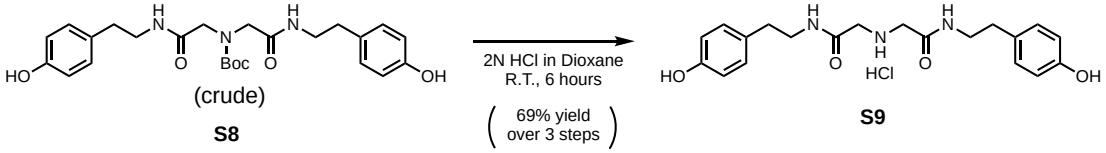

2,2'-azanediylbis(*N*-(4-hydroxyphenethyl)acetamide) hydrochloride, **S9:** Crude **S8** was dissolved in 1,4-dioxane (60 mL) with the aid of mild heating and stirring. 4 N HCl in dioxane (wet, 60 mL) was added to the homogeneous tan solution in one portion, and the mixture was stirred vigorously under argon at room temperature for 6 hours, at which point TLC analysis indicated that the starting material was consumed. The reaction mixture was condensed under reduced pressure to provide a tan solid residue which was dissolved in methanol (30 mL) with aid of heating. The solution was dropped into rapidly stirring ethyl acetate (400 mL) to form an off-white precipitate. Vigorous stirring was continued for 2 hours, and the solids were collected by vacuum filtration, rinsing with ethyl acetate (30 mL) and dried under reduced pressure to provide an ivory-colored solid (12.03 g, 69% yield from boc-iminodiacetic acid over 3 steps). R_f 0.21 (streak, 10% methanol/dichloromethane). ^{1}H NMR (400 MHz, Methanol-d_4) δ 7.04 (d, J = 8.5 Hz, 4H), 6.72 (d, J = 8.5 Hz, 4H), 3.77 (s, 4H), 3.42 (t, J = 7.3 Hz, 4H), 2.72 (t, J = 7.3 Hz, 4H). ^{13}C NMR (101 MHz, MeOD) δ 166.07, 156.96, 130.85, 130.72, 116.27, 48.85, 42.34, 35.48. ATR-FTIR (solid): 3332 (m; secondary N-H stretch), 3262 (broad; O–H stretch), 2944 (broad strong; amine salt N-H stretch), 1663 (s; secondary amide C=O stretch), 1514 (s; asymmetrically tri-substituted aryl C=C bend), 1228 (s; aryl C-O asymmetric stretch), 828 (s; *p*-disubstituted aryl C-H bending).

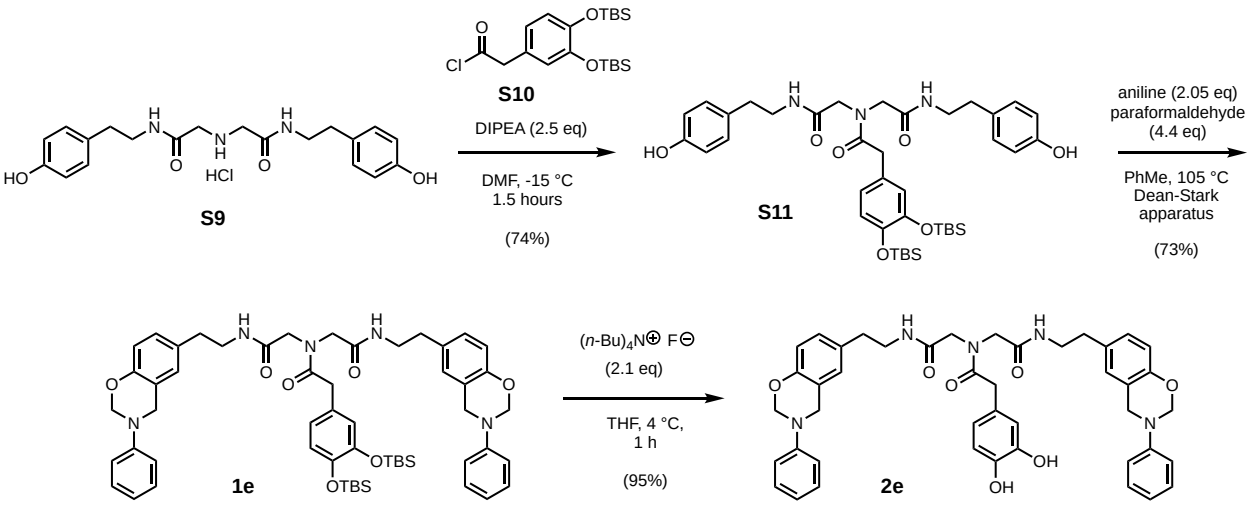

Scheme S5. Synthetic route to mono-catechol-bis-benzoxazine **2e**.

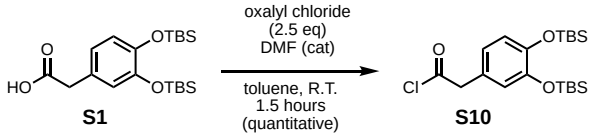

2-(3,4-bis((*tert*-butyldimethylsilyl)oxy)phenyl)acetyl chloride, **S10:** Carboxylic acid **S4** (4.00 g, 10.1 mmols, 1 eq) was dissolved in dry toluene (23.2 mL) containing 10 µL of dry N,N-dimethylformamide in an oven-dried round bottom flask containing a magnetic stir bar. The solution was stirred at room temperature in a water bath, and oxalyl chloride (2.16 mL, 25.2 mmols, 2.5 eq) was added drop-wise over one minute while stirring under argon atmosphere. Bubbling was observed, and stirring was continued at room temperature for 1.5 hours, at which time the reaction was condensed under reduced pressure to provide a yellow oil which was used immediately without further purification (4.19 g, quantitative). ^{1}H NMR (400 MHz, Chloroform-*d*) δ 6.81 (d, *J* = 8.1 Hz, 1H), 6.75 (d, *J* = 2.2 Hz, 1H), 6.70 (dd, *J* = 8.1, 2.3 Hz, 1H), 4.00 (s, 2H), 1.00 (s, 9H) 0.99 (s, 9H), 0.21 (s, 12H). ^{13}C NMR (101 MHz, $CDCl_3$) δ 172.16, 147.25, 147.13, 124.19, 122.70, 122.60, 121.38, 52.57, 26.05, 18.59, 18.58, -3.96, -3.97.

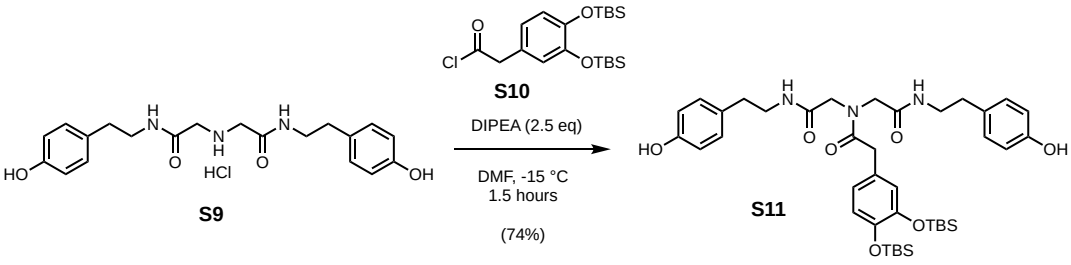

2-(3,4-bis((*tert*-butyldimethylsilyl)oxy)phenyl)-*N*,*N*-bis(2-((4-hydroxyphenethyl)amino)-2-oxoethyl)acetamide, **S11:** Amine **S9** (3.74 g, 9.16 mmols, 1 eq) was dissolved in dry N,N-dimethylformamide (46 mL) in a round bottom flask containing magnetic stir bar under argon at

room temperature and diisopropylethylamine (DIPEA, 3.99 mL, 22.9 mmols, 2.5 eq) was added by syringe. The solution was chilled in a NaCl/ice bath to -15 °C, and a solution of acyl chloride **S10** (4.18 g, 10.1 mmols, 1.1 eq) in chloroform (1 mL) was added dropwise over 12 minutes while stirring. Stirring was continued for 1.5 hours, and the reaction was then quenched by addition of deionized water (150 mL) and ethyl acetate (50 mL). The layers were separated, and the aqueous phase was extracted with ethyl acetate (2 x 50 mL). The combined organic layers were washed with deionized water (50 mL), saturated aqueous ammonium chloride (2 x 50 mL), and brine (2 x 50 mL). The combined aqueous layers were back-extracted with ethyl acetate (2 x 30 mL), and the combined organic phase was dried over anhydrous sodium sulfate, filtered, and condensed under reduced pressure to provide a tan foam solid. The residue was dissolved in minimal dichloromethane and purified by column chromatography on silica gel, eluting with a gradient from dichloromethane through 5% methanol/dichloromethane. Fractions containing product were condensed under reduced pressure to provide a white solid (5.08 g, 74% yield). R_f 0.40 (10% methanol/dichloromethane). ^{1}H NMR (400 MHz, Methanol-d_4) δ 7.05 (d, J = 8.4 Hz, 2H), 7.03 (d, J = 8.3 Hz, 2H), 6.78 (d, J = 8.2 Hz, 1H), 6.75 (d, J = 2.2 Hz, 1H), 6.71 (d, J = 8.4 Hz, 2H), 6.70 (d, J = 8.4 Hz, 2H), 6.63 (dd, J = 8.2, 2.2 Hz, 1H), 4.06 (s, 2H), 3.93 (s, 2H), 3.43 (s, 2H), 3.38 (q, J = 6.7 Hz, 4H), 2.71 (t, J = 7.3 Hz, 4H), 0.98 (s, 18H), 0.20 (s, 6H), 0.17 (s, 6H). ^{13}C NMR (101 MHz, MeOD) δ 174.90, 171.40, 170.98, 156.95, 156.88, 148.12, 147.12, 131.19, 130.94, 130.79, 128.53, 123.30, 122.76, 122.21, 116.24, 116.22, 54.64, 53.79, 42.46, 42.16, 40.34, 35.63, 35.36, 26.54, 26.48, 19.33, 19.29, -3.73, -3.84. ATR-FTIR (solid): 3267 (broad strong; O–H stretch), 3090 (m), 2857 (w; alkyl C–H stretch), 1635 (s; secondary amide C=O stretch), 1512 (s; asymmetrically tri-substituted aryl C=C bend), 1463 (m; methylene group C-H bending), 1219 (s; aryl C-O stretch), 906 (m; Si-CH_3/*t*-Bu rocking), 838 (s; aryl C-H bending).

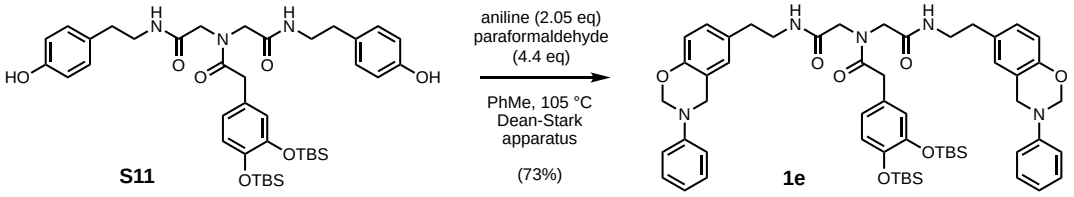

2-(3,4-bis((*tert*-butyldimethylsilyl)oxy)phenyl)-*N*,*N*-bis(2-oxo-2-((2-(3-phenyl-3,4-dihydro-2*H*-benzo[*e*][1,3]oxazin-6-yl)ethyl)amino)ethyl)acetamide, **1e:** Bisphenol **S11** (12.9 g, 17.2 mmols, 1 eq), paraformaldehyde (2.33 g, 75.5 mmols, 4.4 eq of formaldehyde), aniline (3.25 g, 34.8 mmols, 2.03 eq), and toluene (43 mL) were added to a round bottom flask with a magnetic stir bar, and the flask was topped with a Dean-Stark apparatus filled with toluene and placed under argon. The mixture was stirred in a pre-warmed oil bath at 105 °C for 17 hours to produce an amber-colored reaction mixture and visible water condensate in the Dean-Stark trap. The mixture was cooled to room temperature, condensed under reduced pressure, and purified by column chromatography on silica gel packed in dichloromethane, eluting with a gradient from dichloromethane through 20% acetone/dichloromethane. Fractions containing product were concentrated under reduced pressure to provide a white foam solid (12.46 g, 73.7% yield). R_f 0.48, streak (20% acetone/dichloromethane). ^{1}H NMR (400 MHz, Chloroform-*d*) δ 9.05 (t, J = 5.5 Hz, 1H), 7.27 – 7.17 (m, 4H), 7.11 – 7.04 (m, 4H), 6.97 – 6.83 (m, 6H), 6.78 – 6.65 (m, 4H), 6.58 (dd, J = 8.2, 2.2 Hz, 1H), 6.15 (t, J = 5.8 Hz, 1H), 5.31 (s, 2H), 5.28 (s, 2H), 4.59 (s, 2H), 4.56 (s, 2H), 3.85 (s, 2H), 3.62 (s, 2H), 3.46 (q, J = 6.5, 6.0 Hz, 2H), 3.40 (q, J = 6.8 Hz, 2H), 3.38 (s, 2H), 2.75 (t, J = 7.4 Hz, 2H), 2.68 (t, J = 7.1 Hz, 2H), 0.96 – 0.96 (s, 18H), 0.17 (s, 6H), 0.16 (s, 6H). ^{13}C

NMR (101 MHz, $CDCl_3$) δ 172.55, 169.45, 168.56, 153.09, 152.88, 148.43, 148.40, 146.99, 146.12, 131.27, 130.88, 129.36, 129.33, 128.29, 128.26, 127.17, 127.03, 126.58, 121.86, 121.63, 121.44, 121.42, 121.13, 121.09, 120.76, 118.20, 118.17, 117.10, 116.90, 79.37, 79.34, 54.91, 53.91, 50.54, 41.19, 40.94, 39.71, 34.59, 34.49, 26.03, 26.01, 18.49 (2), -3.96, -4.00. ATR-FTIR (solid): 2856 (w; alkyl C–H stretch), 1645 (s; secondary amide C=O stretch), 1496 (s; asymmetrically tri-substituted aryl C=C bend), 1461 (m; methylene group C-H bending), 1226 (s; aryl C-O-C stretching), 945 (m, oxazine related mode), 905 (m; Si-CH_3/*t*-Bu rocking), 837 (s; trisubstituted aryl C-H bending), 755 (s; monosubstituted aryl C-H bend), 692 (s; monosubstituted aryl C-H bend).

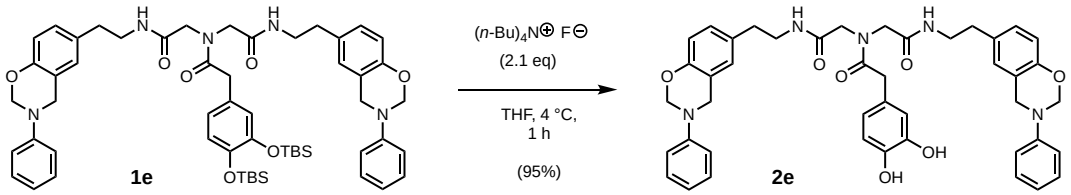

1e **2e**

2-(3,4-dihydroxyphenyl)-*N*,*N*-bis(2-oxo-2-((2-(3-phenyl-3,4-dihydro-2*H*-benzo[*e*][1,3]oxazin-6-yl)ethyl)amino)ethyl)acetamide, **2e:** Protected benzoxazine **1e** (12.5 g, 12.7 mmols, 1 eq) was dissolved in tetrahydrofuran (36.7 mL) with stirring and chilled in an ice/water bath under argon. Tetrabutylammonium fluoride solution (Sigma, 1M in THF, 26.5 mL, 26.5 mmols, 2.1 eq) was added drop-wise by syringe over 6 minutes to produce a yellow-green solution and stirring was continued for 1 hour, at which time the reaction was quenched by addition of ethyl acetate (60 mL) and pH 7 0.1 M aqueous sodium phosphate buffer (60 mL). The reaction becomes yellow upon quenching. The layers were separated, and the aqueous phase was extracted once more with ethyl acetate (60 mL). The combined organic phases were washed with pH 7 0.1 M aqueous sodium phosphate buffer (2 x 60 mL) and brine (2 x 60 mL), dried over anhydrous sodium sulfate, filtered, and condensed under reduced pressure to a sticky pale-yellow crude. The residue was dissolved in dichloromethane (12 mL) and was added to rapidly stirring hexanes (200 mL) to produce an ivory-colored precipitate, which was collected by vacuum filtration. The precipitate was dissolved in 1:2:2 methanol/dichloromethane/acetone (25 mL) and dropped into rapidly stirring ice-chilled diethyl ether (200 mL) to produce a fluffy off-white precipitate. The mixture was kept cold for 2 hours, after which the precipitate was collected by vacuum filtration, washing with additional ice-chilled diethyl ether, and drying under high vacuum to provide an off-white solid powder (9.071 g, 95% yield). R_f 0.22, streak, staining grey-black with ferric chloride (40% acetone/dichloromethane). ^{1}H NMR (400 MHz, DMSO-d_6) δ 8.88 (t, *J* = 5.6 Hz, 1H), 8.82 (s, 1H), 8.76 (s, 1H), 8.34 (t, *J* = 5.6 Hz, 1H), 7.22 (t, *J* = 7.2 Hz, 4H), 7.10 (t, *J* = 7.3 Hz, 4H), 6.99 – 6.90 (m, 4H), 6.84 (t, *J* = 7.2 Hz, 2H), 6.68 – 6.58 (m, 4H), 6.41 (dd, *J* = 8.0, 2.1 Hz, 1H), 5.40 (s, 2H), 5.37 (s, 2H), 4.61 (s, 2H), 4.58 (s, 2H), 4.03 (s, 2H), 3.88 (s, 2H), 3.33 (s, 2H), 3.34 – 3.19 (m, 4H), 2.62 (t, *J* = 7.4 Hz, 2H), 2.61 (t, *J* = 7.4 Hz, 2H). ^{13}C NMR (101 MHz, DMSO) δ 171.77, 169.10, 168.84, 152.34, 147.86, 147.83, 145.07, 143.97, 131.24, 131.17, 129.10, 127.88, 127.22, 127.17, 125.65, 121.04, 120.99, 120.41, 120.39, 119.87, 117.29, 116.55, 116.12, 116.09, 115.31, 78.50, 52.95, 51.69, 48.97, 40.53, 40.48, 38.69, 34.27, 34.20. ATR-FTIR (solid): 3300 (broad strong; O–H stretch), 1641 (s; secondary amide C=O stretch), 1498 (s; asymmetrically tri-substituted aryl C=C bend), 1227 (s; aryl ether C-O-C asymmetric stretch), 946 (m, oxazine related mode), 752 (s; monosubstituted aryl C-H bend), 693 (s; monosubstituted aryl C-H bend).

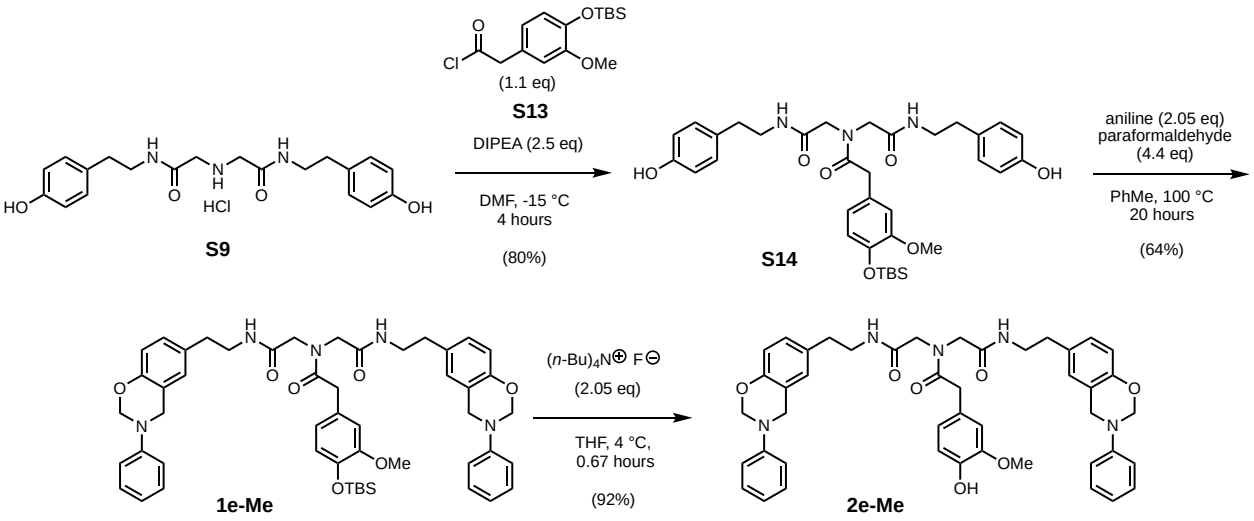

Scheme S6. Synthesis of **1e** and **2e** derivatives **1e-Me** and **2e-Me**.

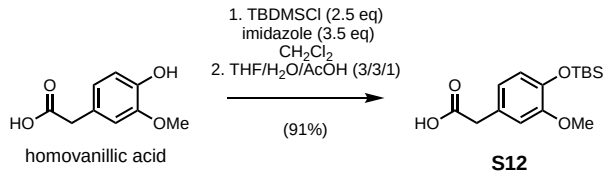

2-(4-((*tert*-butyldimethylsilyl)oxy)-3-methoxyphenyl)acetic acid, **S12:** Homovanillic acid (700 mg, 4.17 mmols, 1 eq), *tert*-butyldimethylsilyl chloride (1.57 g, 10.4 mmols, 2.5 eq), and imidazole (993 mg, 14.6 mmols, 3.5 eq) were combined in a round bottom flask containing a magnetic stir bar and placed under argon. Dichloromethane (16 mL) was added by syringe with vigorous stirring on a water bath, and the suspension was stirred at room temperature for 16 hours. The suspension was filtered to remove precipitated imidazole hydrochloride, and the filtrate was condensed under reduced pressure. The residue was dissolved in diethyl ether (50 mL) and washed with 0.5 M aqueous citric acid (25 mL), saturated sodium chloride (2 x 25 mL), and brine (25 mL), dried over anhydrous sodium sulfate, filtered, and condensed to a colorless oil. The crude was diluted with tetrahydrofuran (10 mL), and water (10 mL) and glacial acetic acid (3.35 mL) were added while stirring vigorously. Stirring was continued at room temperature for 4 hours, at which time the reaction mixture was poured into ice-chilled deionized water (50 mL) and extracted with ethyl acetate (3 x 25 mL). The organic phases were washed with brine (3 x 25 mL), dried over anhydrous sodium sulfate, filtered, and condensed under reduced pressure to provide a white solid (1.122 g, 91% yield). R_f 0.39 (30% EtOAc/hexanes). ^{1}H NMR (400 MHz, Chloroform-*d*) δ 10.27 (s, 1H), 6.79 (d, *J* = 8.1 Hz, 1H), 6.78 (d, *J* = 2.1 Hz, 1H), 6.73 (dd, *J* = 8.0, 2.1 Hz, 1H), 3.79 (s, 3H), 3.57 (s, 2H), 0.99 (s, 9H), 0.15 (s, 6H). ^{13}C NMR (101 MHz, $CDCl_3$) δ 178.26, 151.01, 144.49, 126.61, 121.82, 120.97, 113.40, 55.62, 40.91, 25.85, 25.75, 18.58, -4.47.

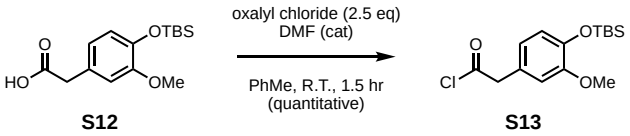

2-(4-((tert-butyldimethylsilyl)oxy)-3-methoxyphenyl)acetyl chloride, **S13:** Carboxylic acid **S12** (632 mg, 2.13 mmols, 1 eq) was dissolved in dry toluene (5 mL) containing dry N,N-dimethylformamide (5 µL) at room temperature and stirred under argon atmosphere. Oxalyl chloride (457 µL, 5.32 mmols, 2.5 eq) was added by syringe over 1.5 minutes while stirring, and the resulting yellow solution was stirred at room temperature for 1.5 hours before removing volatile contents under reduced pressure. The yellow oil was used without further purification (670 mg, quantitative yield). ^{1}H NMR (400 MHz, Chloroform-*d*) δ 6.82 (d, *J* = 7.8 Hz, 1H), 6.75 – 6.70 (m, 2H), 4.06 (s, 2H), 3.81 (s, 3H), 0.99 (s, 9H), 0.16 (s, 6H). ^{13}C NMR (101 MHz, $CDCl_3$) δ 172.27, 151.30, 145.22, 124.52, 122.23, 121.24, 113.40, 55.67, 52.92, 25.83, 18.58, -4.48.

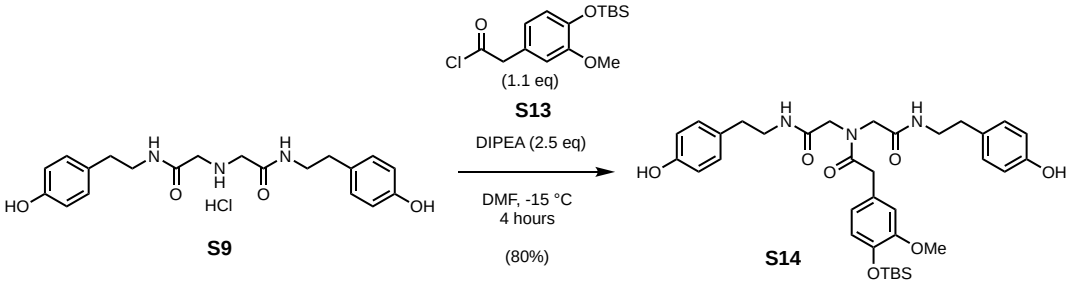

2-(4-((tert-butyldimethylsilyl)oxy)-3-methoxyphenyl)-N,N-bis(2-((4-hydroxyphenethyl)-amino)-2-oxoethyl)acetamide, **S14:** Amine **S9** (778 mg, 1.91 mmols, 1 eq) and diisopropylethylamine (832 µL, 4.78 mmols, 2.5 eq) were combined in N,N-dimethylformamide (9.5 mL) and stirred at -15 °C on a sodium chloride/ice bath. A solution of crude **S13** (670 mg, 2.10 mmols, 1.1 eq) in chloroform (1 mL) was added dropwise over 5 minutes while stirring under an argon atmosphere; white vapors were observed during this step. The mixture was allowed to reach room temperature and then stirred for 14 hours, at which time the mixture was poured into 0.1 M aqueous HCl (50 mL), and saturated aqueous sodium chloride solution (25 mL) was added. The aqueous mixture was extracted with ethyl acetate (5x20 mL) and the combined organic phases were washed with brine (3 x 25 mL), dried over anhydrous sodium sulfate, filtered, and condensed under reduced pressure. The residue was purified by silica gel column chromatography, eluting with a gradient from dichloromethane through 7% methanol in dichloromethane to provide an off-white foam solid (996 mg, 80% yield). R_f 0.52 (10% MeOH/CH_2Cl_2). ^{1}H NMR (400 MHz, Methanol-d_4) δ 7.06 – 7.00 (m, 4H), 6.79 (d, *J* = 2.0 Hz, 1H), 6.75 (d, *J* = 8.0 Hz, 1H), 6.73 – 6.68 (m, 4H), 6.62 (dd, *J* = 8.1, 2.1 Hz, 1H), 4.07 (s, 2H), 3.93 (s, 2H), 3.78 (s, 3H), 3.50 (s, 2H), 3.37 (t, *J* = 7.4 Hz, 2H) 3.34 (t *J* = 7.4 Hz, 2H), 2.69 (q, *J* = 7.8 Hz, 4H), 0.98 (s, 9H), 0.12 (s, 6H). ^{13}C NMR (101 MHz, MeOD) δ 175.01, 171.38, 170.87, 156.91, 156.87, 152.28, 145.18, 131.17, 130.95, 130.78, 128.84, 122.37, 121.79, 116.22, 114.14, 55.92, 54.60, 53.62, 42.44, 42.13, 40.73, 35.60, 35.24, 26.21, 19.27, -4.43.

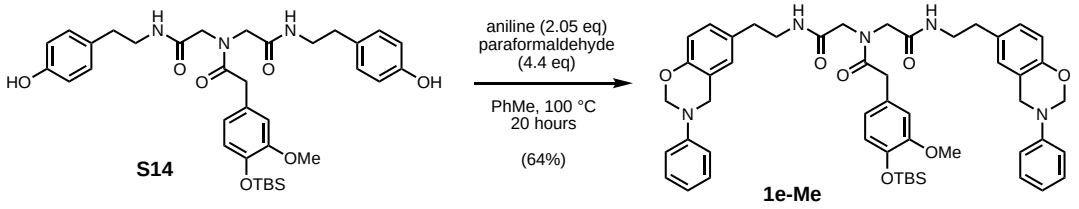

2-(4-((tert-butyldimethylsilyl)oxy)-3-methoxyphenyl)-N,N-bis(2-oxo-2-((2-(3-phenyl-3,4-dihydro-2H-benzo[e][1,3]oxazin-6-yl)ethyl)amino)ethyl)acetamide, **1e-Me:** Bisphenol **S14** (650 mg, 1.00 mmols, 1 eq), aniline (191 mg, 2.05 mmols, 2.05 eq), and 97% paraformaldehyde (136 mg, 4.40 mmols, 4.4 eq) were combined in toluene (3 mL) and placed under a reflux condenser and argon atmosphere before heating at 100 °C for 20 hours. Volatiles were removed under reduced pressure before purifying by silica gel column chromatography, eluting with a gradient from dichloromethane through 35% acetone/dichloromethane to provide a pale-yellow foam solid (570 mg, 64% yield). R_f 0.33 (5% MeOH/CH_2Cl_2). ^{1}H NMR (400 MHz, Chloroform-*d*) δ 8.94 (t, *J* = 5.5 Hz, 1H), 7.29 – 7.19 (m, 4H), 7.13 – 7.03 (m, 4H), 6.98 – 6.83 (m, 6H), 6.78 – 6.68 (m, 4H), 6.60 (dd, *J* = 8.1, 2.1 Hz, 1H), 5.82 (t, *J* = 5.8 Hz, 1H), 5.34 (s, 2H), 5.29 (s, 2H), 4.62 (s, 2H), 4.57 (s, 2H), 3.90 (s, 2H), 3.76 (s, 3H), 3.63 (s, 2H), 3.53 – 3.38 (m, 6H), 2.74 (t, *J* = 7.2 Hz, 2H), 2.70 (t, *J* = 7.2 Hz, 2H), 0.97 (s, 9H), 0.12 (s, 6H). ^{13}C NMR (101 MHz, $CDCl_3$) δ 172.46, 169.45, 168.55, 152.84, 152.73, 150.90, 148.20, 148.17, 144.06, 131.10, 130.85, 129.19, 129.17, 128.09, 128.02, 127.03, 126.96, 126.86, 121.21, 121.10, 120.89, 120.77, 120.65, 117.96, 117.91, 116.82, 116.71, 112.90, 79.18, 55.39, 54.67, 53.51, 50.19, 41.09, 40.82, 39.77, 34.40, 34.31, 25.66, 18.34, -4.65. ATR-FTIR (solid): 2855 (w; alkyl C–H stretch), 1644 (s; secondary amide C=O stretch), 1496 (s; asymmetrically tri-substituted aryl C=C bend), 1227 (s; aryl ether C-O-C asymmetric stretch), 944 (m, oxazine related mode), 898 (m; Si-CH_3/*t*-Bu rocking), 755 (s; monosubstituted aryl C-H bend), 693 (s; monosubstituted aryl C-H bend).

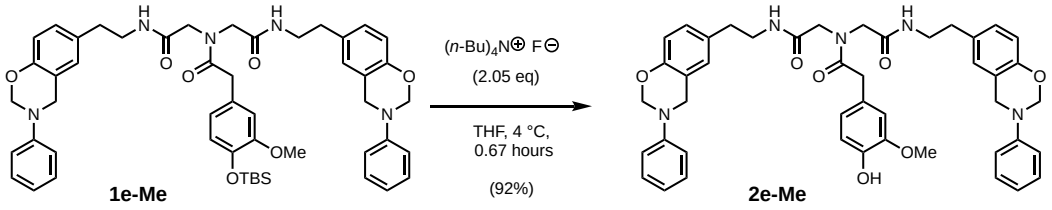

2-(4-hydroxy-3-methoxyphenyl)-N,N-bis(2-oxo-2-((2-(3-phenyl-3,4-dihydro-2H-benzo[e][1,3]-oxazin-6-yl)ethyl)amino)ethyl)acetamide, **2e-Me:** Protected monomer **1e-Me** (335 mg, 0.379 mmols, 1 eq) was dissolved in tetrahydrofuran (1.5 mL) and placed under argon atmosphere. While stirring at 4 °C, a 1M solution of tetrabutylammonium fluoride in tetrahydrofuran (Sigma, 0.398 mL, 0.398 mmols, 1.05 eq) was added, and the resulting solution was stirred for 40 minutes before quenching by addition of pH 7 0.1M sodium phosphate buffer (10 mL) by syringe. The mixture was extracted with ethyl acetate (2x10 mL), and the organic phases were washed with 1:1 0.1M sodium phosphate buffer and saturated aqueous ammonium chloride solution (20 mL), and saturated aqueous sodium chloride solution (15 mL). The organic phase was dried over sodium sulfate, filtered, and condensed under reduced pressure. The crude was further purified by silica gel column chromatography, eluting with a gradient from

dichloromethane through 10% methanol/dichloromethane to provide a pale-yellow solid foam (262 mg, 92% yield). R_f 0.50 (10% MeOH/CH_2Cl_2). ^{1}H NMR (400 MHz, Chloroform-*d*) δ 8.99 (t, *J* = 5.5 Hz, 1H), 7.24 – 7.19 (m, 4H), 7.12 – 7.01 (m, 4H), 6.96 – 6.83 (m, 6H), 6.80 (d, *J* = 8.0 Hz, 1H), 6.73 (d, *J* = 8.4 Hz, 1H), 6.72 – 6.68 (m, 2H), 6.61 (dd, *J* = 8.1, 2.0 Hz, 1H), 6.29 (t, *J* = 5.8 Hz, 1H), 6.14 (s, 1H), 5.31 (s, 2H), 5.28 (s, 2H), 4.58 (s, 2H), 4.55 (s, 2H), 3.88 (s, 2H), 3.79 (s, 3H), 3.62 (s, 2H), 3.48 – 3.34 (m, 6H), 2.76 – 2.65 (m, 4H). ^{13}C NMR (101 MHz, $CDCl_3$) δ 172.69, 169.47, 168.65, 153.06, 152.87, 148.35, 146.91, 144.94, 131.21, 130.84, 129.35, 129.32, 128.23, 128.19, 127.13, 127.01, 125.35, 121.71, 121.43, 121.39, 121.08, 120.81, 118.15, 118.11, 117.06, 116.87, 114.71, 111.76, 79.37, 79.33, 55.96, 54.81, 53.76, 50.44, 41.17, 40.94, 40.00, 34.56, 34.38. ATR-FTIR (solid): 3253 (broad strong; O–H stretch), 1642 (s; secondary amide C=O stretch), 1495 (s; asymmetrically tri-substituted aryl C=C bend), 1225 (s; aryl ether C-O-C asymmetric stretch), 944 (m, oxazine related mode), 755 (s; monosubstituted aryl C-H bend), 693 (s; monosubstituted aryl C-H bend).

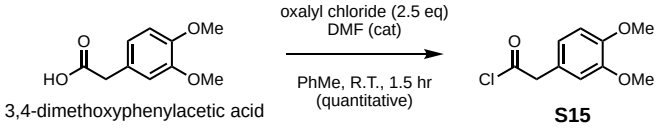

2-(3,4-dimethoxyphenyl)acetyl chloride, **S15**: 3,4-dimethoxyphenylacetic acid (417 mg, 2.13 mmols, 1 eq) was suspended in dry toluene (5 mL) containing dry N,N-dimethylformamide (10 µL). The mixture was placed under argon atmosphere and oxalyl chloride (459 µL, 5.32 mmols, 2.5 eq) was added drop-wise by syringe over 1.5 minutes. The mixture was stirred for 1.5 hours, followed by removal of volatile materials under reduced pressure to yield a yellow liquid which was used immediately without further purification (457 mg, quantitative yield). ^{1}H NMR (400 MHz, Chloroform-*d*) δ 6.86 (d, *J* = 8.2 Hz, 1H), 6.82 (dd, *J* = 8.2, 1.9 Hz, 1H), 6.76 (d, *J* = 1.9 Hz, 1H), 4.08 (s, 2H), 3.88 (s, 3H), 3.88 (s, 3H). ^{13}C NMR (101 MHz, $CDCl_3$) δ 172.33, 149.31, 149.08, 123.67, 122.10, 112.51, 111.44, 56.07, 56.03, 52.83.

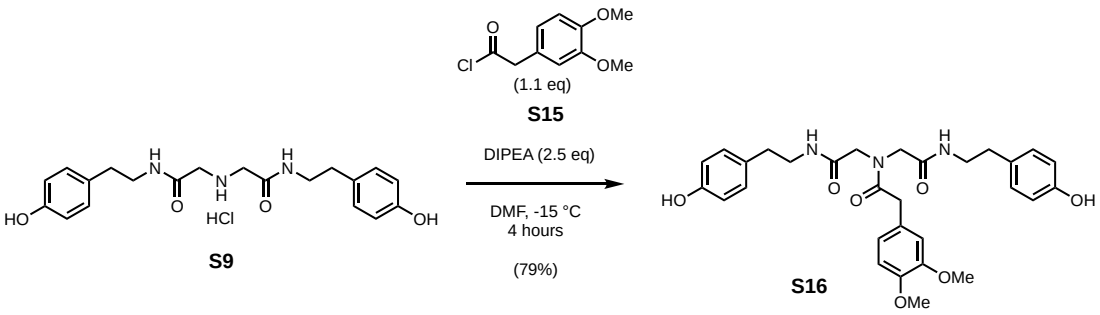

2-(3,4-dimethoxyphenyl)-N,N-bis(2-((4-hydroxyphenethyl)amino)-2-oxoethyl)acetamide, **S16:** Amine **S9** (778 mg, 1.91 mmols, 1 eq) was dissolved in N,N-dimethylformamide (9.5 mL) and diisopropylethylamine (832 µL, 4.78 mmols, 2.5 eq) was added at room temperature. The solution was stirred and chilled on a sodium chloride/ice bath (-15 °C) under argon, and a solution

of **S15** (457 mg, 0.213 mmols, 1.1 eq) in chloroform (1 mL) was added dropwise over 5 minutes; white vapors were observed during this addition (HCl formation). The mixture was allowed to reach room temperature and then stirred for 14 hours, at which time the mixture was poured into 0.1 M aqueous HCl (50 mL), and saturated aqueous sodium chloride solution (25 mL) was added. The aqueous mixture was extracted with ethyl acetate (5x20 mL) and the combined organic phases were washed with brine (3x25 mL), dried over anhydrous sodium sulfate, filtered, and condensed under reduced pressure. The residue was purified by silica gel column chromatography, eluting with a gradient from dichloromethane through 10% methanol in dichloromethane to provide an off-white foam solid (837 mg, 79% yield). R_f 0.39 (10% MeOH/CH_2Cl_2). ^{1}H NMR (400 MHz, Methanol-d_4) δ 7.08 – 6.97 (m, 4H), 6.84 (d, J = 8.2 Hz, 1H), 6.79 (d, J = 2.0 Hz, 1H), 6.73 – 6.66 (m, 5H), 4.07 (s, 2H), 3.92 (s, 2H), 3.80 (s, 3H), 3.76 (s, 3H), 3.50 (s, 2H), 3.40 – 3.25 (m, 4H), 2.69 (t, 7.3 Hz, 2H), 2.66 (t, 7.3 Hz, 2H). ^{13}C NMR (101 MHz, MeOD) δ 175.01, 171.38, 170.89, 156.93, 156.87, 150.43, 149.46, 131.19, 130.97, 130.79, 130.75, 128.03, 122.54, 116.22, 113.87, 113.01, 56.38, 54.57, 53.59, 42.44, 42.12, 40.65, 35.59, 35.22.

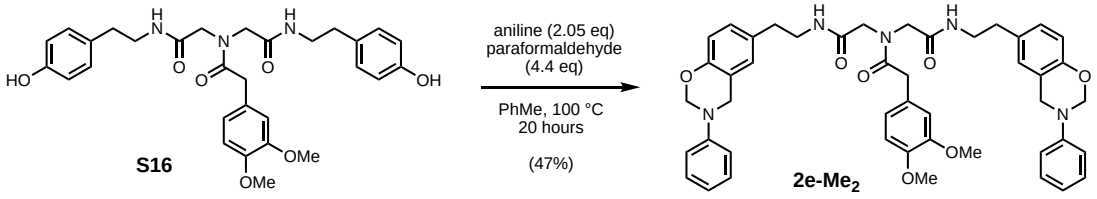

2-(3,4-dimethoxyphenyl)-N,N-bis(2-oxo-2-((2-(3-phenyl-3,4-dihydro-2H-benzo[e][1,3]-oxazin-6-yl)ethyl)amino)ethyl)acetamide, **2e-Me$_2$:** Bisphenol **S16** (550 mg, 1.00 mmols, 1 eq), aniline (191 mg, 2.05 mmols, 2.05 eq), 97% paraformaldehyde (136 mg, 4.40 mmols, 4.4 eq) were combined in toluene (3 mL) and ethanol (0.5 mL), placed under an argon atmosphere, and heated at 100 °C under a reflux condenser for 20 hours before cooling to room temperature, condensing under reduced pressure and purifying by silica gel column chromatography, eluting with a gradient from dichloromethane containing 0.4% triethylamine through 1% MeOH/CH_2Cl_2 with 0.4% triethylamine. A white foam solid was collected (366.5 mg, 47% yield). R_f 0.31 (4% MeOH/CH_2Cl_2 + 0.2% triethylamine). ^{1}H NMR (400 MHz, Chloroform-d) δ 9.09 (t, J = 5.5 Hz, 1H), 7.25 – 7.19 (m, 4H), 7.12 – 7.03 (m, 4H), 6.99 – 6.81 (m, 6H), 6.78 – 6.65 (m, 5H), 6.64 (t, J = 5.7 Hz, 1H), 5.30 (s, 2H), 5.27 (s, 2H), 4.57 (s, 2H), 4.55 (s, 2H), 3.90 (s, 2H), 3.82 (s, 3H), 3.78 (s, 3H), 3.66 (s, 2H), 3.46 (s, 2H), 3.43 – 3.36 (m, 4H), 2.73 (t, J = 7.5 Hz, 2H), 2.68 (t, J = 7.2 Hz, 2H). ^{13}C NMR (101 MHz, $CDCl_3$) δ 172.37, 169.36, 168.46, 152.85, 152.71, 148.90, 148.16, 148.01, 131.07, 130.78, 129.18, 129.16, 128.05, 128.00, 126.99, 126.84, 126.11, 121.20, 121.06, 120.89, 120.65, 117.91, 116.83, 116.69, 112.15, 111.19, 79.17, 55.78, 55.74, 54.68, 53.54, 50.19, 41.05, 40.79, 39.70, 34.40, 34.26. ATR-FTIR (solid): 1644 (s; secondary amide C=O stretch), 1495 (s; asymmetrically tri-substituted aryl C=C bend), 1225 (s; aryl ether C-O-C asymmetric stretch), 943 (m, oxazine related mode), 755 (s; monosubstituted aryl C-H bend), 693 (s; monosubstituted aryl C-H bend).

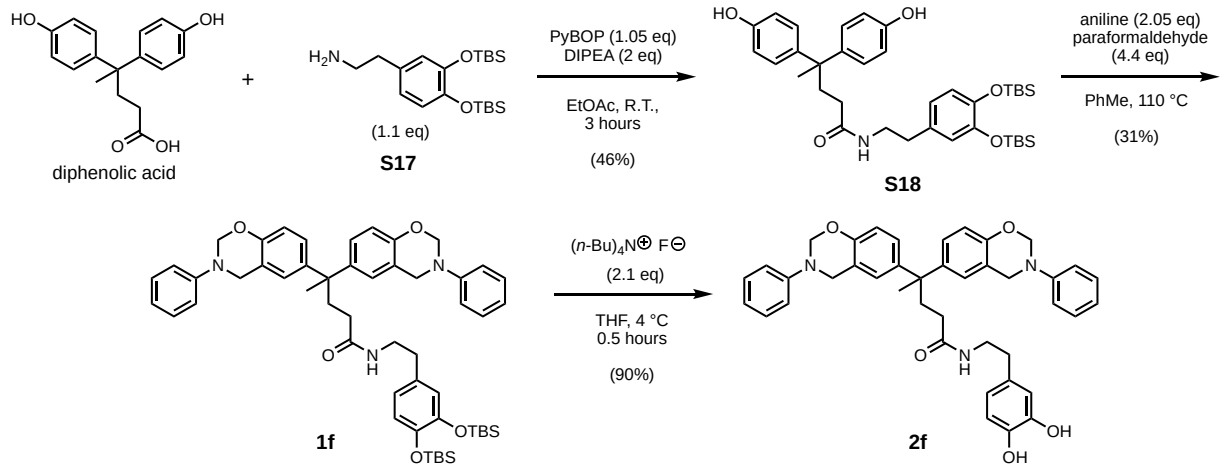

Scheme S7. Synthesis of monomer **2f** from protected dopamine **S17** and diphenolic acid.

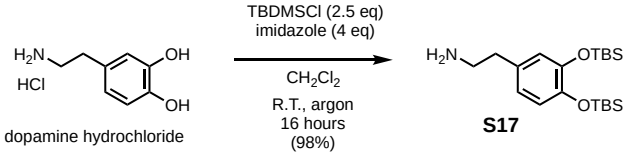

2-(3,4-bis((*tert*-butyldimethylsilyl)oxy)phenyl)ethan-1-amine, **S17:** Precursor **S17** was prepared by adapting a previously reported protocol, with minor changes.[2] Briefly, dopamine hydrochloride (2.50 g, 13.2 mmols, 1 eq), *tert*-butyldimethylsilyl chloride (4.97 g, 33.0mmols, 2.5 eq), and imidazole (3.59 g, 52.7 mmols, 4 eq) were suspended in dry dichloromethane (30 mL) under argon atmosphere at room temperature in a round bottom flask containing a magnetic stir bar. The mixture was stirred vigorously for 16 hours, at which point the resulting suspension was filtered and the filtrate was condensed under reduced pressure. The resulting crude was taken up in diethyl ether (50 mL) and washed with saturated aqueous sodium bicarbonate solution (2 x 25 mL), deionized water (25 mL), and brine (25 mL), dried over sodium sulfate, filtered, and condensed under reduced pressure to a very pale-yellow viscous oil, which was used without further purification (4.939 g, 98% yield). Spectral data were consistent with previous reports. R_f 0.58, streak (10% MeOH in dichloromethane). ^{1}H NMR (400 MHz, Chloroform-*d*) δ 6.78 (d, *J* = 8.0 Hz, 1H), 6.70 (d, *J* = 2.1 Hz, 1H), 6.67 (dd, *J* = 8.0, 2.2 Hz, 1H), 2.95 (t, *J* = 6.9 Hz, 2H), 2.68 (t, *J* = 6.9 Hz, 2H), 1.98 (bs, 2H), 1.02 (s, 9H), 1.02 (s, 9H), 0.22 (s, 6H), 0.22 (s, 6H). ^{13}C NMR (101 MHz, $CDCl_3$) δ 146.74, 145.32, 132.80, 121.79, 121.04, 43.68, 39.27, 26.07, 18.57, 18.55, -3.94, -3.97.

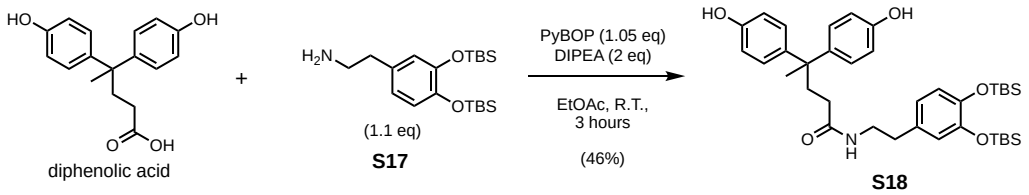

N-(3,4-bis((tert-butyldimethylsilyl)oxy)phenethyl)-4,4-bis(4-hydroxyphenyl)pentanamide, **S18:** Diphenolic acid (2.73 g, 9.55 mmols, 1 eq), amine **S17** (4.19 g, 11.0mmols, 1.15 eq), and diisopropylethylamine (3.32 mL, 19.1 mmols, 2 eq) were combined in dry ethyl acetate (47 mL) to produce a sticky off-white suspension. PyBOP (5.22 g, 10.0 mmols, 1.05 eq) was added, and the suspension was stirred vigorously at room temperature for 3 hours; the reaction becomes a homogeneous yellow solution after 1-1.5 hours. The reaction mixture was condensed under reduced pressure, and the residue was taken up in ethanol (20 mL) and heated to 70 °C in a water. Bath. Deionized water (100 mL) was added to produce an oily layer and a slightly cloudy aqueous phase. The layers were separated, and the oil layer was dissolved in dichloromethane (70 mL) and washed with 1M aqueous citric acid solution (30 mL), deionized water (30 mL), and brine (30 mL), dried over anhydrous sodium sulfate, filtered, and condensed under reduced pressure. The crude was dissolved in dichloromethane (10 mL) and benzene (50 mL) and heated to 70 °C, followed by cooling to produce a solid, which was collected by vacuum filtration. The solid was recrystallized a second time from warm 10% methanol in toluene to provide a white solid that was collected by vacuum filtration and dried under reduced pressure (2.876 g, 46% yield). R_f 0.37 (5% MeOH in dichloromethane). ^{1}H NMR (400 MHz, Methanol-d_4) δ 7.04 – 6.92 (m, 4H), 6.76 (d, J = 8.1 Hz, 1H), 6.72 – 6.62 (m, 6H), 3.28 (t, J = 7.2 Hz, 2H), 2.62 (t, J = 7.3 Hz, 2H), 2.37 – 2.23 (m, 2H), 2.09 – 1.77 (m, 2H), 1.52 (s, 3H), 0.98 (s, 9H), 0.98 (s, 9H), 0.17 (s, 6H), 0.17 (s, 6H). ^{13}C NMR (101 MHz, MeOD) δ 176.38, 156.16, 147.78, 146.45, 141.47, 133.94, 129.31, 122.93, 122.88, 122.14, 115.66, 45.55, 42.07, 38.97, 35.65, 33.27, 28.47, 26.54, 26.52, 19.32, -3.73, -3.79.

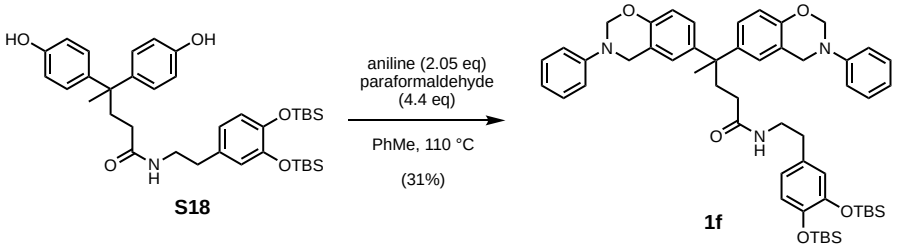

N-(3,4-bis((tert-butyldimethylsilyl)oxy)phenethyl)-4,4-bis(3-phenyl-3,4-dihydro-2H-benzo[e]-[1,3]oxazin-6-yl)pentanamide, **1112**: **1111** (500 mg, 0.769 mmols, 1 eq), aniline (147 mg, 1.58 mmols, 2.05 eq), and 97% paraformaldehyde (101 mg, 3.38 mmols, 4.4 eq) were combined in toluene (5 mL) under argon atmosphere and heated at 110 °C for 16 hours, followed by cooling to room temperature and diluting with toluene (20 mL). The solution was washed with saturated aqueous sodium bicarbonate solution (3x15 mL), and saturated aqueous sodium chloride solution (2x20 mL), dried over anhydrous sodium sulfate, filtered, and condensed under reduced pressure. The residue was purified by silica gel column chromatography, eluting with a gradient from dichloromethane through 2% acetone/dichloromethane to provide an off-white solid (211

mg, 31% yield). R_f 0.34 (2% acetone/CH_2Cl_2). ^{1}H NMR (400 MHz, Chloroform-*d*) δ 7.33 – 7.26 (m, 4H), 7.17 – 7.07 (m, 4H), 6.99 – 6.91 (m, 4H), 6.89 (d, *J* = 2.3 Hz, 2H), 6.81 (d, *J* = 8.1 Hz, 1H), 6.75 (d, *J* = 8.6 Hz, 2H), 6.69 (d, *J* = 2.2 Hz, 1H), 6.64 (dd, *J* = 8.1, 2.2 Hz, 1H), 5.41 (t, *J* = 5.8 Hz, 1H), 5.35 (s, 4H), 4.60 (s, 4H), 3.41 (q, *J* = 6.8 Hz, 2H), 2.66 (t, *J* = 7.0 Hz, 2H), 2.46 – 2.35 (m, 2H), 1.96 – 1.88 (m, 2H), 1.55 (s, 3H), 1.05 (s, 9H), 1.04 (s, 9H), 0.25 (s, 6H), 0.24 (s, 6H). ^{13}C NMR (101 MHz, $CDCl_3$) δ 172.92, 152.34, 148.37, 146.72, 145.44, 141.38, 131.90, 129.27, 126.89, 125.23, 121.56, 121.53, 121.14, 121.03, 120.26, 117.88, 116.51, 79.01, 50.61, 44.64, 40.77, 37.15, 34.94, 32.33, 27.84, 25.99, 18.45, -3.99, -4.03.

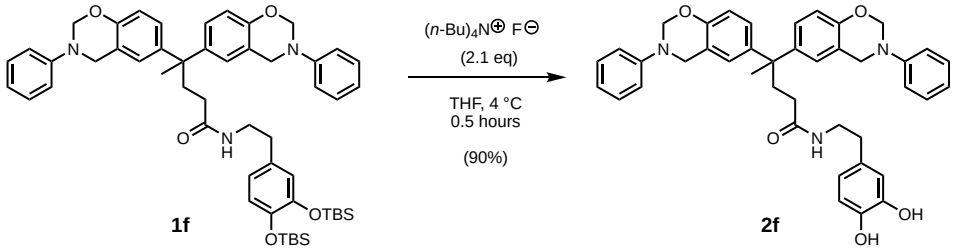

N-(3,4-dihydroxyphenethyl)-4,4-bis(3-phenyl-3,4-dihydro-2H-benzo[e][1,3]oxazin-6-yl)pentanamide, **1113**: **1112** (418 mg, 0.473 mmols, 1 eq) was dissolved in tetrahydrofuran (4 mL) and stirred at 4 °C under argon. Tetrabutylammonium fluoride solution (Sigma, 1 M in THF, 1.04 mL, 1.04 mmols, 2.2 eq) was added drop-wise over 2 minutes, the mixture was stirred for 30 minutes, and then the reaction was quenched by addition of pH 7 0.1 M sodium phosphate buffer (30 mL) and ethyl acetate (25 mL). The organic layer was washed with addition sodium phosphate buffer (2x25 mL), saturated aqueous sodium chloride solution (2x25mL), dried over anhydrous sodium sulfate, filtered, and condensed under reduced pressure. The crude was taken up in minimal dichloromethane and precipitated by addition of hexanes. The pale-yellow solid was collected by vacuum filtration (283 mg, 91% yield). R_f 0.00 (2% acetone/CH_2Cl_2). ^{1}H NMR (400 MHz, Chloroform-*d*) δ 7.30 – 7.20 (m, 4H), 7.08 (app d, *J* = 8.0 Hz, 4H), 6.92 (t, *J* = 7.3 Hz, 2H), 6.85 (dd, *J* = 8.6, 2.3 Hz, 2H), 6.85 – 6.78 (m, 3H), 6.74 – 6.66 (m, 3H), 6.50 (dd, *J* = 8.2, 2.0 Hz, 1H), 5.59 (t, *J* = 5.9 Hz, 1H), 5.29 (s, 4H), 4.53 (s, 4H), 3.28 (q, *J* = 6.8 Hz, 2H), 2.54 (t, *J* = 7.1 Hz, 2H), 2.41 – 2.21 (m, 2H), 2.02 – 1.77 (m, 2H), 1.46 (s, 3H). ^{13}C NMR (101 MHz, $CDCl_3$) δ 174.63, 152.36, 148.32, 144.46, 143.23, 141.21, 130.51, 129.34, 126.90, 125.27, 121.24, 120.48, 120.38, 117.91, 116.59, 115.68, 115.40, 79.07, 50.56, 44.70, 41.09, 37.30, 34.75, 32.50, 27.72. ATR-FTIR (solid): 3280 (broad; O–H stretch), 3026 (m), 1639 (m; secondary amide C=O stretch), 1598 (s), 1493 (s; asymmetrically tri-substituted aryl C=C bend), 1230 (s; aryl ether C-O-C asymmetric stretch), 942 (m, oxazine related mode), 754 (s; monosubstituted aryl C-H bend), 727 (s; 1,2,4-trisubstituted aryl C-H bending), 693 (s; monosubstituted aryl C-H bend).

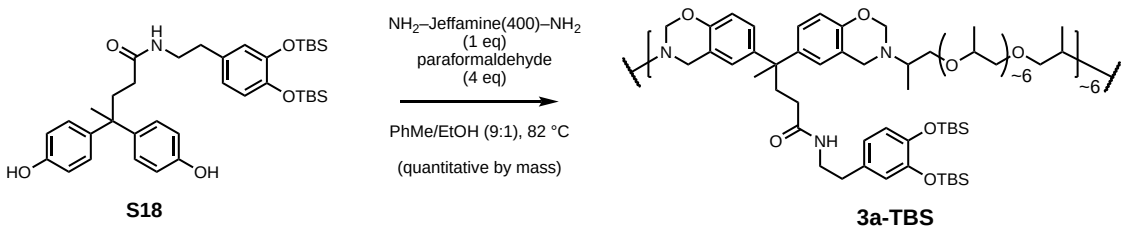

TBS-protected Jeffamine$_{400}$ main-chain benzoxazine, **3a-TBS:** Bisphenol **S18** (351 mg, 0.541 mmols, 1 eq), Jeffamine-400 diamine (216 mg, 0.541 mmols, 1 eq), and 97% paraformaldehyde (67.0 mg, 2.20 mmols, 4.1 eq of formaldehyde) were combined in a 9:1 toluene:ethanol mixture (3 mL), and heated at 82 °C under argon atmosphere for 13 hours. The reaction was then cooled to room temperature and condensed under reduced pressure to provide a tacky yellow residue (611 mg, quantitative yield by mass). Crude ^{1}H-NMR analysis reveals a degree of ring-closure of ~85 mol%.[3] This was calculated by comparing the integration of the peak at ~4.92 ppm to that of the *tert*-butyldimethylsilyl methyl peak at ~0.21 ppm. Molecular weight was determined by gel permeation chromatography in tetrahydrofuran at a flow rate of 1 mL/minute, calibrating with linear low-dispersity polystyrene standards. M_w = 6,157 g/mol, M_n = 2,139 g/mol (Đ = 2.9). The dispersity value greater than 2 indicates that this material likely exhibits some degree of branching due to side reactions occurring in the Mannich condensation employed to prepare these materials. ^{1}H NMR (400 MHz, Chloroform-*d*) δ 7.07 – 6.69 (m, 5H), 6.66 – 6.55 (m, 4H), 5.35 (broad s, 1H), 4.92 (broad s, ~4H), 4.00 (broad s, ~4H), 3.64 – 3.29 (broad m, 22H), 3.11 (broad q, *J* = 5.6, 5.1 Hz, 2H), 2.64 (broad t, *J* = 7.0 Hz, 2H), 1.87 (broad s, 2H), 1.49 (broad s, 3H), 1.17 – 1.07 (broad m, 21H), 0.97 (apparent d, *J* = 1.7 Hz, 18H), 0.18 (s, 6H), 0.17 (s, 6H).

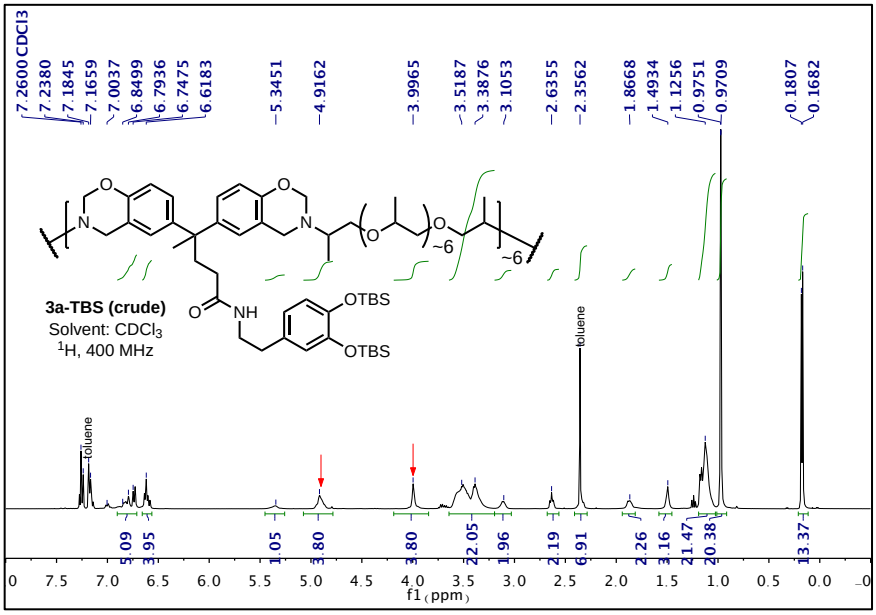

Figure S1. ^{1}H-NMR spectrum of crude **3a-TBS** collected in deuterated chloroform. This sample contains residual toluene. Key benzoxazine resonances are observed at ~4.92 and ~4.00 ppm (red arrows), and TBS protecting groups are intact (~0.97 and ~0.17 ppm).

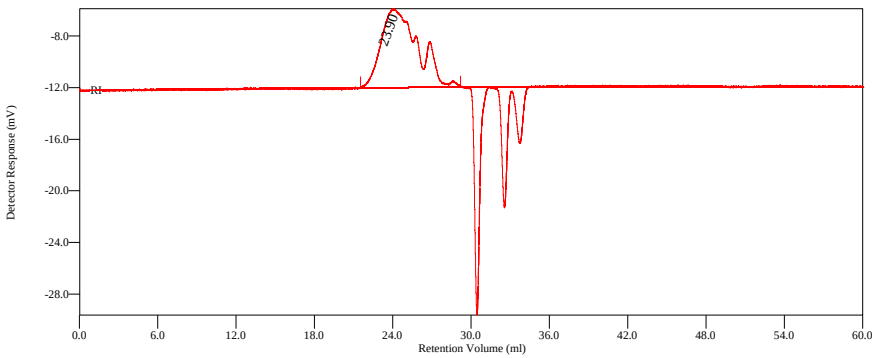

Figure S2. Gel permeation chromatography (GPC) chromatogram of **3a-TBS** in tetrahydrofuran at a flow rate of 1 mL/minute.

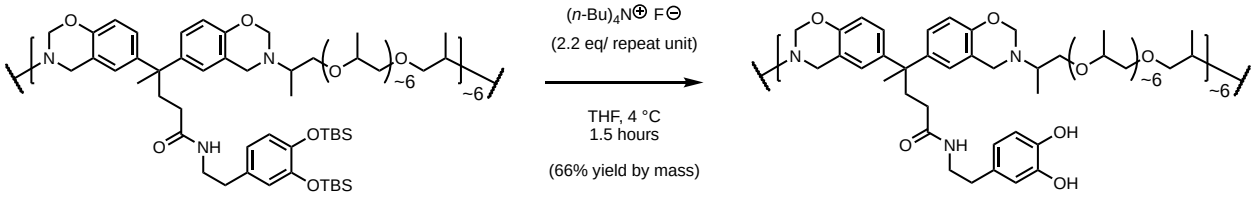

3a-TBS **3a**

Jeffamine$_{400}$ main-chain benzoxazine, **3a:** **3a-TBS** (561 mg, 0.511 mmols of repeating unit = 0.511 mmols of protected catechol) was dissolved in tetrahydrofuran (5 mL) and placed under argon atmosphere at 4 °C. Tetrabutylammonium fluoride solution (Sigma, 1M in THF, 1.12 mL, 1.12 mmols, 2.2 eq per repeating unit) was added dropwise over 2 minutes. The mixture was stirred for 1.5 hours, and then quenched by addition of 0.1 M pH 7 sodium phosphate buffer (10 mL) and dichloromethane (10 mL). The layers were separated, and the organic phase was washed once more with 0.1 M pH 7 sodium phosphate buffer (10 mL). Brine was added to the organic phase (10 mL) to produce a yellow sticky precipitate and a yellow organic solution. The organic solution was separated and dried over anhydrous sodium sulfate, filtered, and condensed under reduced pressure. The crude was taken up in minimal dichloromethane (1 mL) precipitated in hexanes (75 mL) to yield a pale-yellow solid (284 mg, 66% yield by mass). Crude ^{1}H-NMR analysis reveals a degree of ring-closure of ~55 mol%.[3] This was calculated by comparing the integration of the peak at ~4.86 ppm to that of the methyl peak at ~1.44 ppm. Gel permeation chromatography was not performed due to the adhesive nature of the catechol side-chains. ^{1}H NMR (400 MHz, Chloroform-*d*) δ 7.07 – 6.69 (m, 5H), 6.66 – 6.55 (m, 4H), 5.35 (broad s, 1H), 4.92 (broad s, ~4H), 4.00 (broad s, ~4H), 3.64 – 3.29 (broad m, 22H), 3.11 (broad q, *J* = 5.6, 5.1 Hz, 2H), 2.64 (broad t, *J* = 7.0 Hz, 2H), 1.87 (broad s, 2H), 1.49 (broad s, 3H), 1.17 – 1.07 (broad m, 21H), 0.97 (apparent d, *J* = 1.7 Hz, 18H), 0.18 (s, 6H), 0.17 (s, 6H). ATR-FTIR (solid): 3258 (broad strong; O–H stretch), 2869 (s; aliphatic C-H stretch), 1640 (s; secondary amide), 1498 (s; asymmetrically tri-substituted aryl C=C bend), 1232 (s; aryl ether C-O-C asymmetric stretch), 1091 (s; aliphatic ether C-O stretch), 925 (m; oxazine related mode), 821 (m; trisubstituted aryl C-H bend).

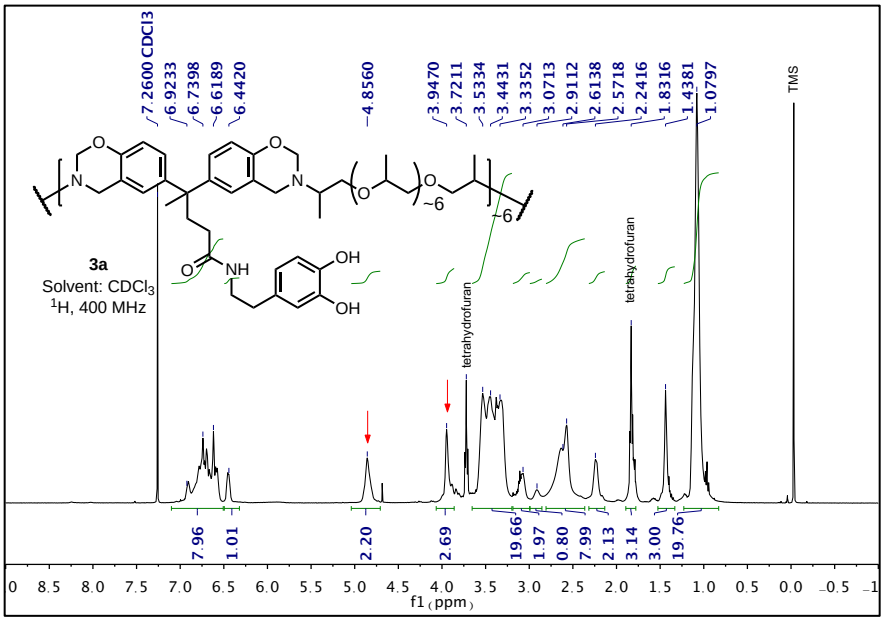

Figure S3. ^{1}H-NMR spectrum of **3a** collected in deuterated chloroform. Distinctive benzoxazine ring resonances are indicated by red arrows.

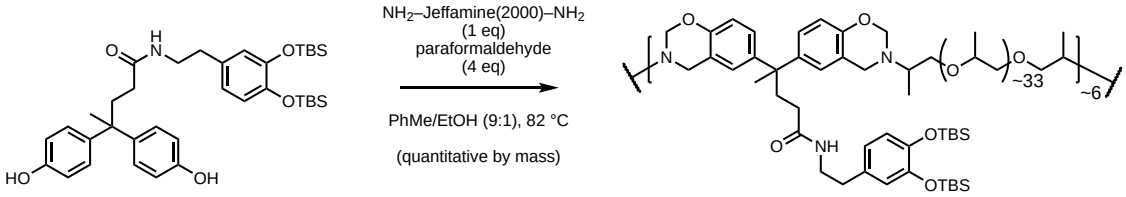

S18 **3b-TBS**

TBS-protected Jeffamine-2000 main-chain benzoxazine, **3b-TBS**: Bisphenol **S18** (803 mg, 1.24 mmols, 1 eq), Jeffamine-2000 diamine (2.47 g, 1.24 mmols, 1 eq), and 97% paraformaldehyde (153 mg, 4.94 mmols, 4 eq of formaldehyde) were combined in a 9:1 toluene:ethanol mixture (2.5 mL), and heated at 82 °C under argon atmosphere for 13 hours. The reaction was then cooled to room temperature and condensed under reduced pressure to provide a very sticky pale-yellow to orange residue (3.34 g, quantitative yield by mass). Crude ^{1}H-NMR analysis reveals a degree of ring-closure of ~89 mol%.[3] This was calculated by comparing the integration of the peak at ~4.91 ppm to that of the diphenolic acid-derived methyl peak at ~1.49 ppm. Molecular weight was determined by gel permeation chromatography in tetrahydrofuran at a flow rate of 1 mL/minute, calibrating with linear low-dispersity polystyrene standards. M_w = 22,424 g/mol, M_n = 3,944 g/mol (Đ = 5.6). The large dispersity value indicates that this material likely exhibits some degree of branching due to side reactions occurring in the Mannich condensation employed to prepare these materials. ^{1}H NMR (400 MHz, Chloroform-*d*) δ 6.87 – 6.68 (broad m, 5H), 6.66 – 6.55 (broad m, 4H), 5.32 (broad s, 1H), 4.97 – 4.80 (m, ~4H), 3.99 broad (s, ~4H), 3.77 – 3.63 (m, 3H), 3.61 – 3.28 (broad m, 126H), 3.21 – 3.06 (m, 3H), 2.63 (broad t, *J* = 7.0 Hz, 2H), 2.40 – 2.24 (m, 2H), 1.96 – 1.73 (m, ~8H), 1.49 (broad s, 3H), 1.20 – 1.05 (broad m, 126H), 0.97 (apparent d, *J* = 1.6 Hz, 18H), 0.17 (s, 6H), 0.16 (s, 6H).

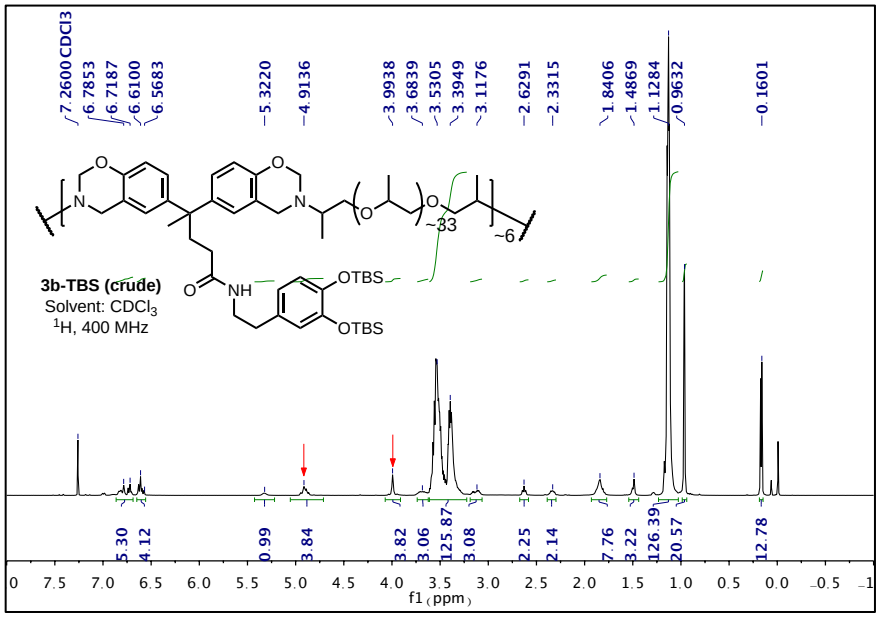

Figure S4. [1]H-NMR spectrum of crude **3b-TBS** collected in deuterated chloroform. Key benzoxazine resonances are observed at ~4.91 and ~3.99 ppm (red arrows), and TBS protecting groups are intact (~0.96 and ~0.16 ppm).

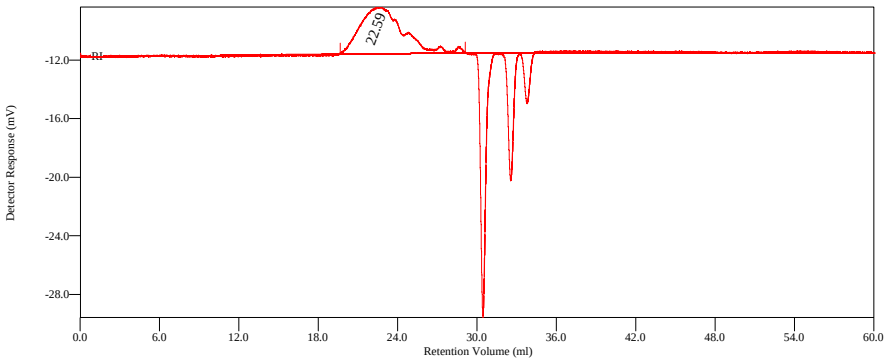

Figure S5. Gel permeation chromatography (GPC) chromatogram of **3b-TBS** in tetrahydrofuran at a flow rate of 1 mL/minute.

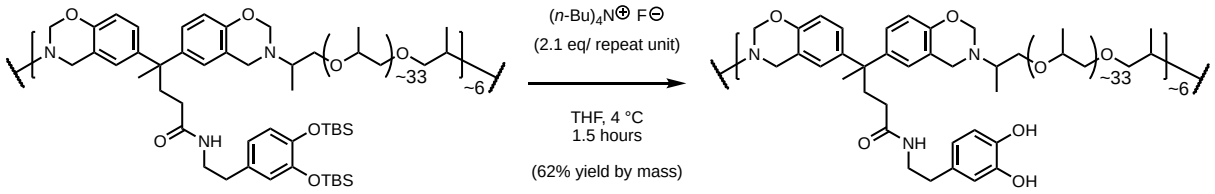

3b-TBS **3b**

Jeffamine$_{2000}$ main-chain benzoxazine, **3b: 3b-TBS** (3.50 grams, ~1.30 mmols of repeating unit = ~1.30 mmols of protected catechol) was dissolved in tetrahydrofuran (14 mL) and placed under argon atmosphere at 4 °C. Tetrabutylammonium fluoride solution (Sigma, 1M in THF, 2.76 mL, 2.76 mmols, 2.1 eq per repeating unit) was added dropwise over 2 minutes. The mixture was stirred for 1.5 hours, and then quenched by addition of 0.1 M pH 7 sodium phosphate buffer (15 mL) and dichloromethane (15 mL). The layers were separated, and the organic phase was washed once more with 0.1 M pH 7 sodium phosphate buffer (10 mL), and brine (10 mL), dried over anhydrous sodium sulfate, filtered, and condensed under reduced pressure. The crude was taken up in minimal tetrahydrofuran (6 mL), and the viscous solution was added to stirring ice-chilled diethyl ether (120 mL) to produce a dense oil layer. Stirring was stopped, and the oil layer was allowed to settle for 1 hour. The supernatant was decanted, and the residue was dried under high vacuum to provide an amber-colored, tacky transparent rubber (2.03 g, 62% yield by mass). Crude ^{1}H-NMR analysis reveals a degree of ring-closure of ~61 mol%.[3] This was calculated by comparing the integration of the peak at ~4.91 ppm to that of the diphenolic acid-derived methyl peak at ~1.48 ppm. Gel permeation chromatography was not performed due to the adhesive nature of the abundant catechol side-chains. ATR-FTIR (elastic semisolid): 3199 (broad; O–H stretch), 1648 (s; secondary amide), 1500 (s; asymmetrically tri-substituted aryl C=C bend), 1236 (s; aryl ether C-O-C asymmetric stretch), 1096 (s; aliphatic ether C-O stretch), 926 (m; benzoxazine related aryl C-H bending mode), 824 (w; trisubstituted aryl C-H bend). ^{1}H NMR (400 MHz, Chloroform-*d*) δ 7.02 – 6.39 (broad m, 9H), 5.36 (broad s, 1H), 5.05 – 4.76 (m, ~3H), 3.99 (broad s, ~3H), 3.80 – 3.61 (m, 3H), 3.60 – 3.29 (broad m, 96H), 3.19 – 3.05 (m, 2H), 2.61 (broad t, *J* = 7.3 Hz, 2H), 2.35 – 2.24 (m, 2H), 1.95 – 1.75 (m, 2H), 1.48 (broad s, 3H), 1.16 – 1.09 (m, 97H).

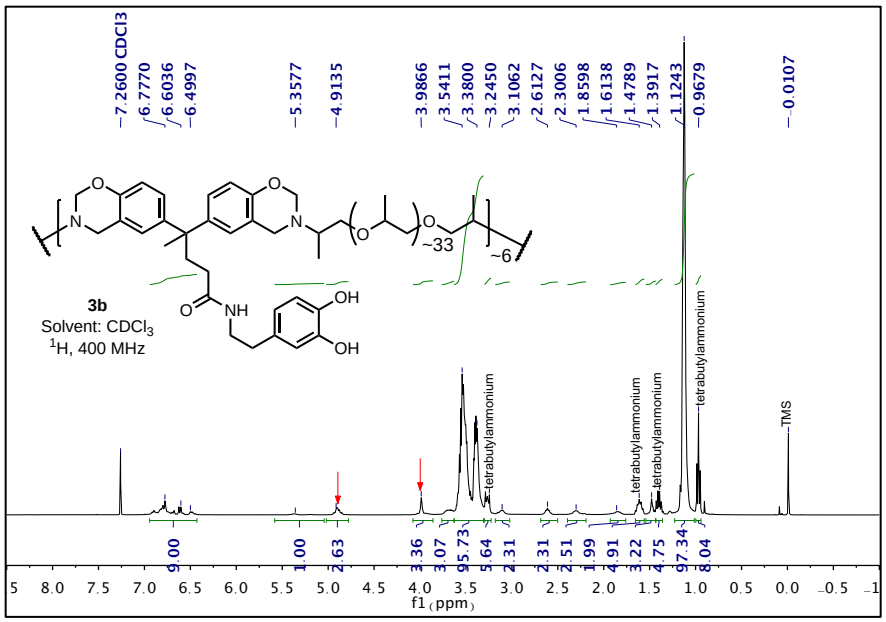

Figure S6. [1]H-NMR spectrum of crude **3b** collected in deuterated chloroform. This sample contains residual tetrabutylammonium (labeled). Key benzoxazine resonances are observed at ~4.92 and ~4.00 ppm (red arrows).

3. Model Compound Stability Studies

The silyl ether protecting group strategy was informed by model compound stability studies with monomer **C-m** (**Figure S7A**). Monomer stability was assessed by [1]H-NMR and TLC, comparing to pure **C-m** starting material (**Figure S7B**). Model reactions were carried out as follows:

Catalytic hydrogenation (feasibility of benzyl ethers): **C-m** (106 mg, 0.512 mmols, 1 eq) was dissolved in 1,4-dioxane (1 mL) at room temperature and 10 weight percent palladium on carbon (54 mg, 0.051 mmols Pd, 10 mol%) was added. The flask was evacuated and purged with hydrogen gas (~1 atm, balloon), and stirred vigorously for 6.5 hours at room temperature. The reaction mixture was passed through a pad of diatomaceous earth, washing with excess 1,4-dioxane, and the filtrate was condensed under reduced pressure to provide 105 mg of a pale-yellow residue. The crude was dissolved in $CDCl_3$ for [1]H-NMR analysis (**Figure S7C**), which revealed quantitative degradation of the benzoxazine, evidenced by the disappearance of the characteristic singlet at 4.87 ppm.

Tetrabutylammonium fluoride treatment (feasibility of silyl ethers): **C-m** (103 mg, 0.498 mmols, 1 eq) was dissolved in tetrahydrofuran (0.5 mL) at room temperature. A solution of tetrabutylammonium fluoride (Sigma, 1M in THF, 0.5 mL, 0.5 mmols, ~1 eq) was added while stirring, and the reaction color changed to light yellow during addition. After 2 hours, the reaction mixture was diluted with diethyl ether (40 mL) and washed with 3M aqueous sodium hydroxide solution (2 x 15 mL), deionized water (2 x 15 mL), and brine (15 mL), dried over anhydrous sodium sulfate, filtered, and condensed under reduced pressure to provide a pale-yellow liquid (71

mg, 69% recovery). The residue was taken up in $CDCl_3$ for ^{1}H-NMR analysis (**Figure S7D**). The presence of a characteristic singlet at 4.86 ppm indicated that the benzoxazine ring was intact.

Incubation with pyrocatechol: **C-m** (101 mg, 0.488 mmols, 1 eq) was dissolved in tetrahydrofuran (1 mL) at room temperature and pyrocatechol (53.7 mg, 0.488 mmols, 1 eq) was added. The solution was stirred at room temperature for 24 hours, at which point TLC analysis indicated no reaction had occurred. The solution was diluted with diethyl ether (10 mL), and washed with 3M aqueous sodium hydroxide solution (2 x 10 mL), deionized water (10 mL), and brine (10 mL), dried over anhydrous sodium sulfate, filtered, and condensed under reduced pressure to provide a pale-yellow liquid (82 mg, 81% recovery). ^{1}H-NMR analysis in $CDCl_3$ revealed that the benzoxazine ring was intact, indicated by a characteristic singlet at 4.86 ppm (**Figure S7E**).

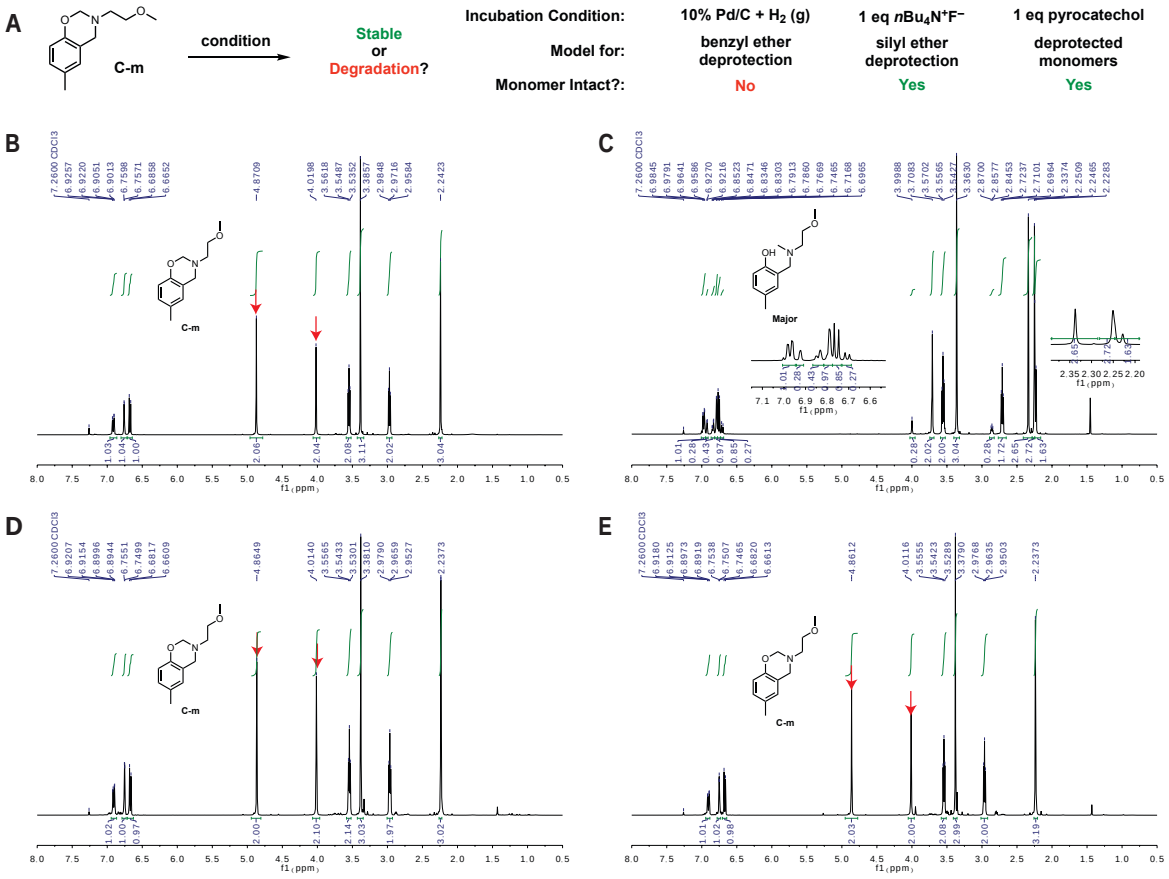

Figure S7. Stability studies conducted with model monomer **C-m** (A) Conditions screened and stability summary. (B) ^{1}H-NMR of **C-m** starting material in $CDCl_3$ (400 MHz). (C) ^{1}H-NMR of crude product in $CDCl_3$ (400 MHz) after catalytic hydrogenation. The structure for the proposed major product is shown. (D) ^{1}H-NMR of organic crude product in $CDCl_3$ (400 MHz) after 2-hour incubation with stoichiometric tetrabutylammonium fluoride. (E) ^{1}H-NMR of organic crude product in $CDCl_3$ (400 MHz) after 24-hour incubation with pyrocatechol.

4. Pressure Sensitive Adhesive Behavior of Main-Chain Polybenzoxazine 3b

Pressure sensitive adhesives (PSAs) are ubiquitous in modern society, encountered almost every day around us in the form of tapes, sticky notes, and labels on consumable product packaging. These materials consist of polymeric materials with low glass transition temperature that bear functional groups capable of adhesive and cohesive interactions to achieve tackiness, adhesion, and resistance to shear (cohesion). During the course of our preparation and characterization of catechol-modified main-chain benzoxazine **3b** as a potential toughener for **2e**, we observed that this material has several characteristics of a rubber PSA: low glass transition temperature, tackiness, and resistance to shear. To probe this behavior further, 10 wt% solutions of **3b** in 15 vol% methanol in tetrahydrofuran were prepared, and solvent cast onto strips of polyethylene terephthalate (PET) film (**Figure S8**). The density of material cast in the dried film was approximately 4.1 mg cm^{-2}. After drying under high vacuum, these strips were nearly colorless in appearance.

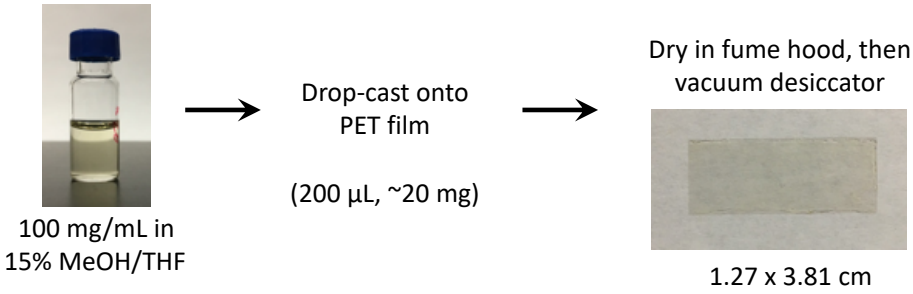

Figure S8. Formation of PSA tapes of **3b** on PET films.

The film tapes were qualitatively found to stick readily to a variety of surfaces, including stainless steel, polycarbonate, aluminum 6061, Kapton, high density polyethylene, and glass. We also found that taped pairs of high-density polyethylene (HDPE) or glass substrates resisted moderate shear, determined by their ability to support 200 grams of weight for extended periods of time. Control experiments performed with silyl ether protected **3b-TBS** revealed that cohesion was severely diminished in this material, as these materials were unable to resist shear of a 200-gram weight for any period of time. In stark contrast, two glass substrates adhered with a **3b** PSA film tape (4.8 cm^2 with 4.1 mg cm^{-2} **3b**) have resisted shearing under a 200 g load for >210 days. HDPE samples secured with a 2.5 cm^2 **3b** PSA held a 200 g weight for 16 hours with minimal changes (**Figure S9**). Increasing the load to 1 kg caused the tape to slip from the HDPE after 20 minutes (primarily adhesive failure, assessed visually).

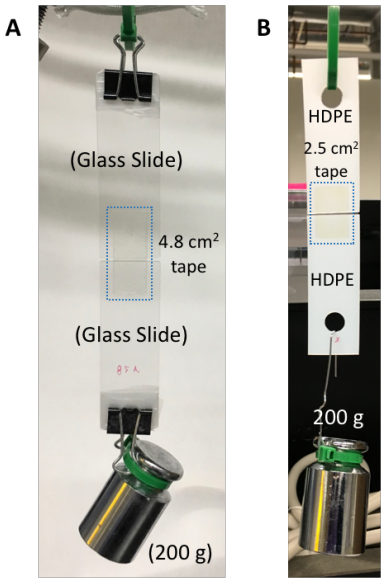

Figure S9. PSA films of **3b** holding together glass slides or HDPE strips under shear load of 200 g weight. (A) Sample on Glass is pictured at 3 days and has remained unchanged (for >210 days). (B) Sample on HDPE is pictured after 16 hours. The nearly colorless transparent tapes are framed by blue dotted boxes as a visual aid.

Inspired by the ability of mussels to bind to surfaces underwater, **3b** PSA films were applied to glass slides that were submerged underwater (DI water, 100 mL). This experiment consisted of taking a **3b** tape into deionized water and pressing it to the surfaces of two adjacent glass slides. We observed that the PSA adhered to the glass slides, and the adhesive joint remained intact after submersion in water for 24 hours more at room temperature (**Figure S10**). However, the tape became opaque, and had noticeably lower tackiness than pristine tapes after peeling from the wet surface.

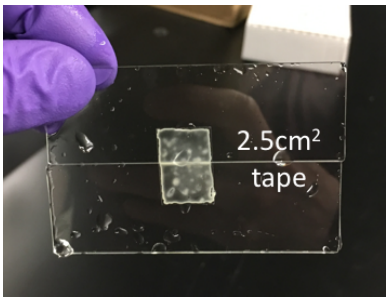

Figure S10. PSA films of **3b** applied to glass slides that were submerged in deionized water. The adhesive joint was still intact after 24 hours of incubation at room temperature. The tape starts to appear opaque after one hour of submersion.

5. Lap Shear Adhesion Testing

The adhesive strength of benzoxazine monomers was assessed by single lap shear testing according to ASTM standard D1002-10 on rectangular aluminum 6061 (Al 6061) substrates (0.16 cm thick x 1 cm width x 10 cm length) and 304 stainless steel substrates (0.09 cm thick x 1 cm width x 10 cm length).[4]

5.1 Substrate and lap joint preparation

Degreased substrates: Aluminum substrates were prepared for adhesive bonding by solvent degreasing. This was performed by wiping substrates with a fresh Kim wipe soaked in acetone, followed by wiping with a second Kim wipe soaked with ethyl acetate. Substrates were air-dried in a fume hood. Just prior to solvent casting of benzoxazine monomer solutions, a 1 cm x 1 cm area at the end of the substrate was isolated with vinyl electrical tape (see **Figure S11A**).

Roughened substrates: For roughened Al 6061 substrates, a previously described etching protocol was employed.[5] Briefly, degreased samples were placed upright in Pyrex test tubes (15 x 150 mm), and 4 mL of 0.1 N aqueous NaOH was added to the tube. Samples were sonicated in an Emerson Bransonic CPX2800 ultrasonic bath with 40 kHz transducers at 100% power for 30 minutes. Samples were fully submerged in fresh deionized water and sonicated for 10 minutes, and this washing step was repeated once more. Substrates were dried in a glassware oven at 120 °C for 1 hour, followed by cooling to room temperature. Just prior to solvent casting of benzoxazine monomer solutions, a 1 cm x 1 cm area at the end of the substrate was isolated with vinyl electrical tape.

304 stainless steel substrates were roughened by manual sanding along the length of both faces with 3M cloth-backed 80 grit aluminum oxide sandpaper. Samples were wiped clean with a paper towel and degreased by bath sonication in 10 vol% Simple Green aqueous solution for 1 hour, followed by sonication in ultrapure water (15 minutes) and acetone (15 minutes). Substrates were dried under a stream of nitrogen. Just prior to solvent casting of benzoxazine monomer solutions, a 1 cm x 1 cm area at the end of the substrate was isolated with vinyl electrical tape (see **Figure S11A**).

Lap joint preparation: Solutions of benzoxazine monomers were prepared at 100 mM in 15 vol% methanol in tetrahydrofuran containing 0.5-1 wt/vol% of suspended glass beads (0.0015”) for bond line control. Solutions (100 µL) were drop-cast onto the 1 cm x 1 cm region at the end of a clean Al 6061 adherend, and the solvent was evaporated at room temperature in a fume hood (10 minutes), followed by drying in a high vacuum desiccator for at least 2 hours (**Figure S11A**, left). Vinyl masking tape was removed to provide Al 6061 adherends with benzoxazine films at one end. Pairs of substrates were overlapped in an antiparallel arrangement, clamped with two small binder clips, and transferred to a pre-heated air oven at 100-120 °C (**Figure S11A**, right). Samples were heated at 100-120 °C for 1 hour, and then the oven temperature was increased to 200-205 °C over 1 hour. Samples were maintained at 200-205 °C for 4 hours, followed by slowly cooling to room temperature over several hours. For samples bonded with mixtures containing main-chain derivatives **3a** or **3b**, the maximum curing temperature was maintained at 195 °C.

Accelerated aqueous aging of bonded samples: For accelerated aging in aqueous conditions, roughened Al 6061 lap joints bonded with **B-a**, **1e**, and **2e** were submerged in deionized water (0.5 L per sample) and incubated at 63 °C for 14 days. Excess polybenzoxazine adhesive was carefully removed with a razor prior to incubation. Samples were blotted dry with paper towels followed by shear testing at room temperature at a rate of 0.5% strain per minute.

Lap shear adhesive testing: Excess polybenzoxazine adhesive was carefully removed from the edges of the bonded area with a razor. Shims were applied to lap joint ends to facilitate mechanical tester grip alignment (**Figure S11B**). Dimensions of the bonded area were measured with calipers, and samples were loaded at 0.5% strain per minute in shear until failure. Adhesive strength (Pa) was determined by the peak load (N) divided by the overlap area (m^2). The apparent failure mode was determined by visual inspection of the failed lap joints.

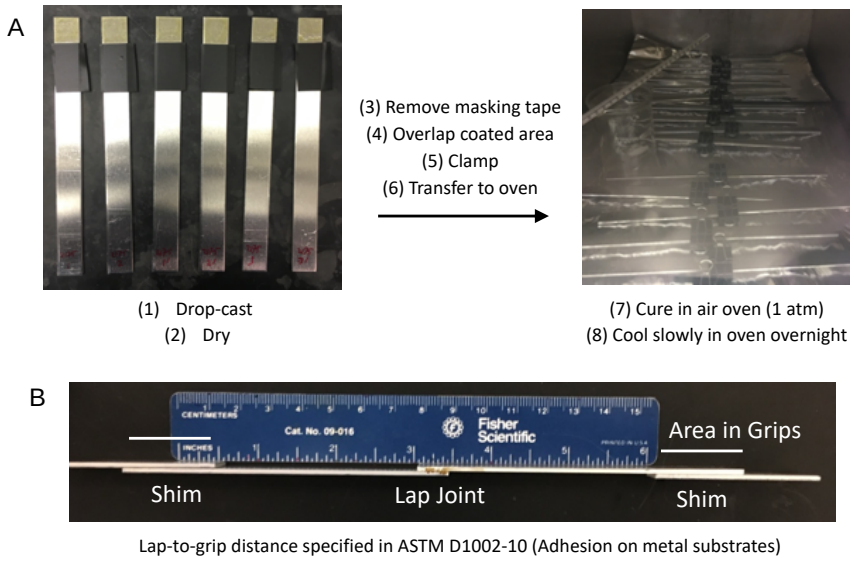

Figure S11. Graphical representation of adhesion lap joint preparation on Al 6061. Shims were used facilitate mechanical tester grip alignment.

Photographs of representative failed lap joints are presented in **Figures S12-S14**. Adhesive failure is assigned when failure occurs at the polybenzoxazine-adherend interface. Cohesive failure is assinged when failure occurs in the polybenzoxazine bulk. Mixed failure is assigned when areas of both adhesive and cohesive failure are observed in the failed lap joints.

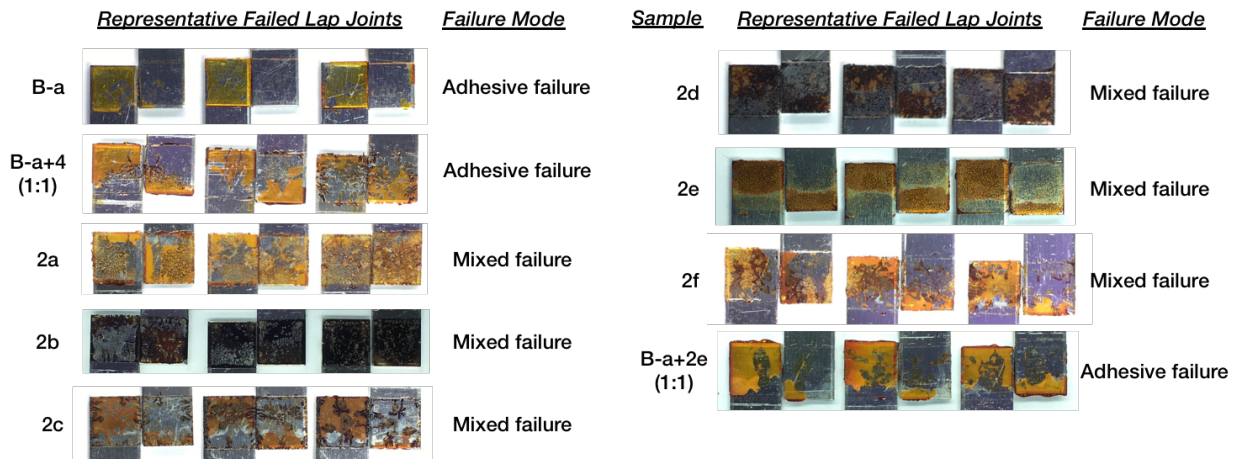

Figure S12. Representative failed lap joints after shear testing of cured monomers presented in Figure 3B of the main text.

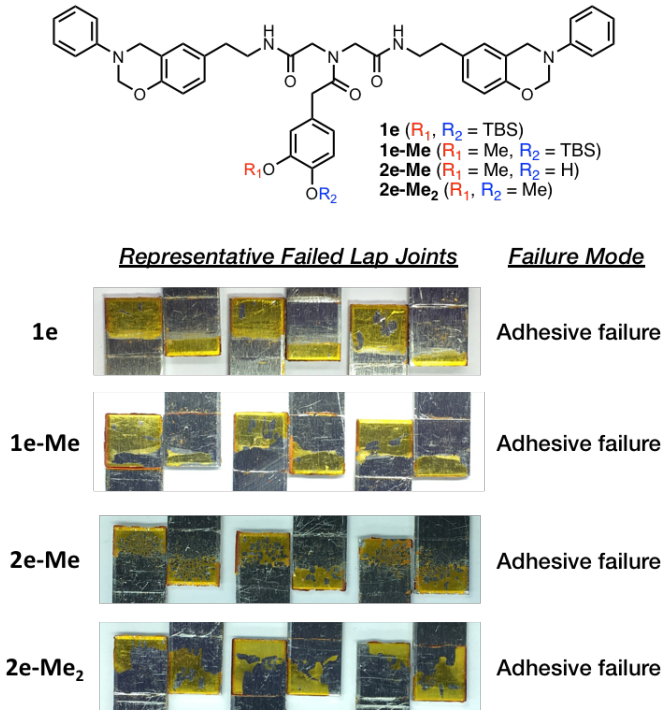

Figure S13. Representative failed lap joints after shear testing of cured monomers presented in Figure 3C of the main text.

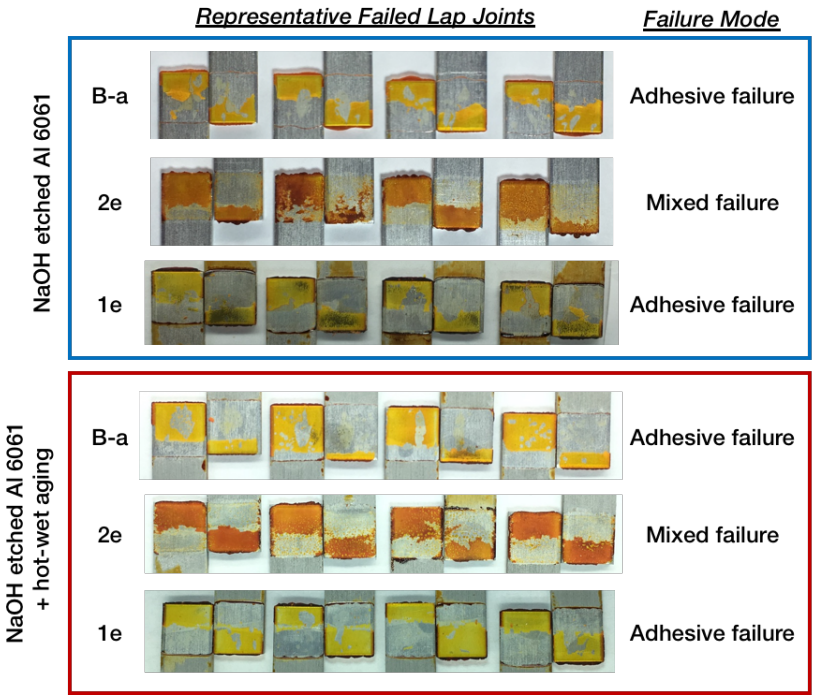

Figure S14. Representative failed lap joints after shear testing of cured monomers presented in Figure 3D of the main text.

Lap-shear testing on sanded 304 stainless steel provided shear strengths comparable to those obtained on NaOH-etched Al 6061 (**Figure S15**). The adhesion strength of cured **2e** and **1e** are statistically comparable (p=0.3), which is consistent with silyl ether deprotection or migration occuring near the metal surface during curing. Lewis acidic sites on the surface of metallic substrates are likely to facilitate deprotection of silyl ethers.[6] The shear strength for cured **B-a** was significantly lower (p<0.0001 for pair-wise comparison to both cured **2e** and **1e**.

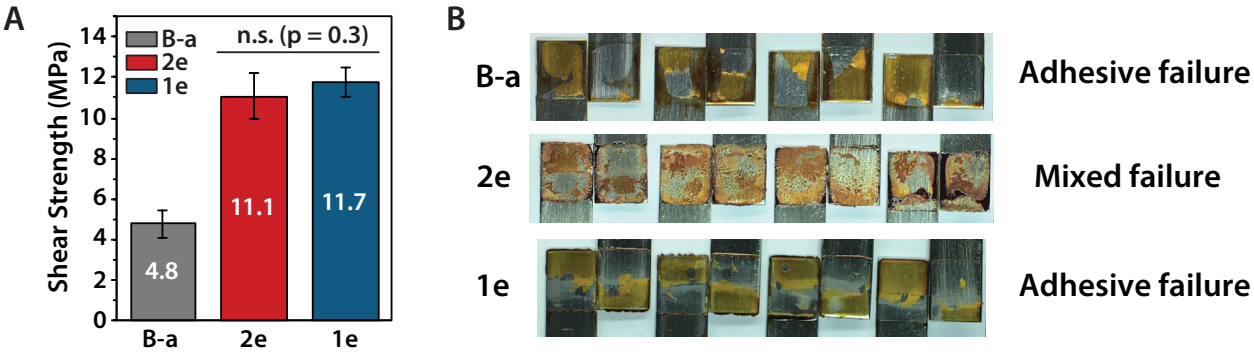

Figure S15. Lap shear testing of cured **B-a**, **2e**, and **1e** on sanded stainless steel 304 substrates. (A) Shear strength of cured thermosets on stainless steel. Error bars represent standard deviation of shear strength for a minimum of five lap joints. (B) Representative failed lap joints after shear testing of cured monomers.

*5.2 Influence of silane adhesion promoters on **B-a**, **1e**, and **2e** adhesion*

The effect of nucleophilic and electrophilic adhesion promoter (i.e. primer layer) on **B-a**, **1e**, and **2e** adhesive strength was investigated by modifying freshly-etched aluminum substrates with (3-aminopropyl)triethoxysilane (APTES) or (3-glycidoxypropyl) triethoxysilane (GPS) to form an interphase layer presenting nucleophilic primary amines or electrophilic epoxides respectively. Modification was performed by dipping NaOH-etched adherends into a solution of either APTES (1 wt% in 90% EtOH/H_2O) or GPS (1 wt% in 90% EtOH/H_2O adjusted to pH ~4.5 with glacial acetic acid) for 90 seconds, followed by blowing dry with nitrogen and baking for 1 hour in air at 100 °C, followed by cooling in a high vacuum desiccator. Benzoxazine solutions were prepared and solution cast, and samples were cured and submitted to adhesion testing as described in section 5.1. Benzoxazine solutions were solvent cast and lap joint curing was started within 2 hours and 4 hours of silane treatment, respectively.

The adhesion strength of **B-a** increased substantially to 13.9 ± 0.6 MPa, while the bond strengths of **2e** and **1e** were relatively unaffected at 9.4 ± 1.6 and 9.2 ± 0.6 MPa, respectively after APTES treatment. GPS modification provided the highest bond strength for **B-a** at 15.2 ± 0.4 MPa. The bond strength of **2e** was enhanced to 12.1 ± 1.3 MPa, but the bond strength for **1e** fell dramatically to 1.8 ± 0.4 MPa (**Figure S16**). Adhesive failure modes were observed for cured **B-a** and **1e**, while a mixed failure mode was observed for **2e** (**Figure S17**).

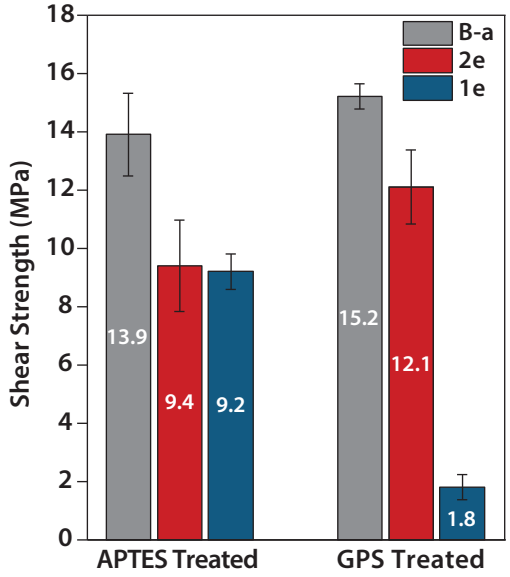

Figure S16. Lap-shear adhesive strength of cured **B-a**, **2e**, and **1e** on NaOH-etched aluminum 6061 treated with APTES and GPS. At least four lap joints per monomer per condition were tested. Error bars represent standard deviation of the adhesive strength.

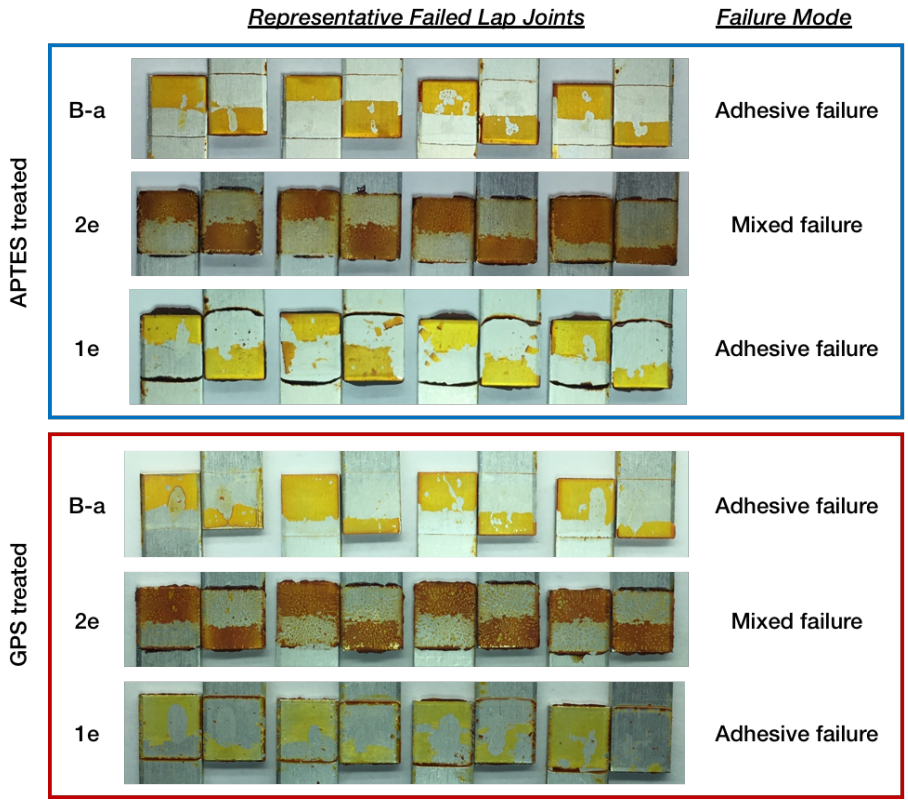

Figure S17. Representative failed lap joints after shear testing of cured monomers on NaOH-etched Al 6061 substrates pre-treated with either (3-aminopropyl)triethoxysilane (APTES) or (3-glycidoxypropyl)triethoxysilane (GPS).

*5.3 Adhesive strength of blends of **2e** with **3a** and **3b***

Main-chain polybenzoxazines **3a** and **3b** were applied as potential performance modifiers for **2e**. Stock solutions of mixtures of **2e** and either **3a** or **3b** were prepared, combining **2e** with either **3a** or **3b** to provide the desired mass ratio of **2e** to main-chain component. The sample was dissolved with sonication in sufficient volume of 15% methanol in tetrahydrofuran (containing glass spheres as described in section 5.1) to bring the concentration of **2e** to 100 mM. For samples bonded with **3a** or **3b** alone, main-chain polybenzoxazines were dissolved at 10 wt%. Stock solutions were solvent cast onto roughened (NaOH-etched) Al 6061 adherends and dried at 60 °C for 12 hours. The appearance of samples before curing was assessed (**Figure S18-S19**), and lap joints were assembled and cured as described in section 5.1.

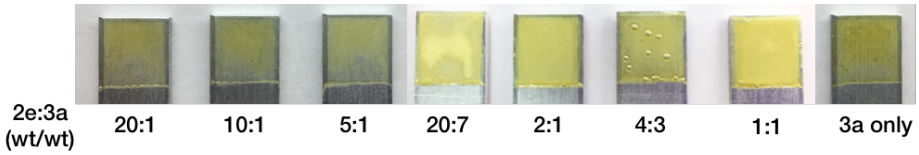

Figure S18. Appearance of solvent-cast films of blends of **2e** and main-chain **3a** before curing.

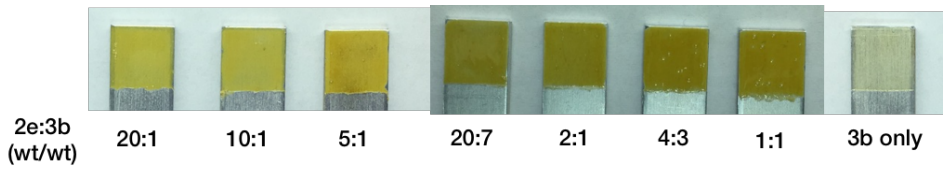

Figure S19. Appearance of solvent-cast films of blends of **2e** and main-chain **3b** before curing.

Lap shear adhesion testing was performed with a shear rate of 0.5% strain per minute and adhesive strength was calculated from the maximum load divided by the bonded area, measured with calipers prior to testing (**Figure S20**). Failed lap joints were inspected visually to assess the apparent failure mode (**Figures S21**-**S22**).

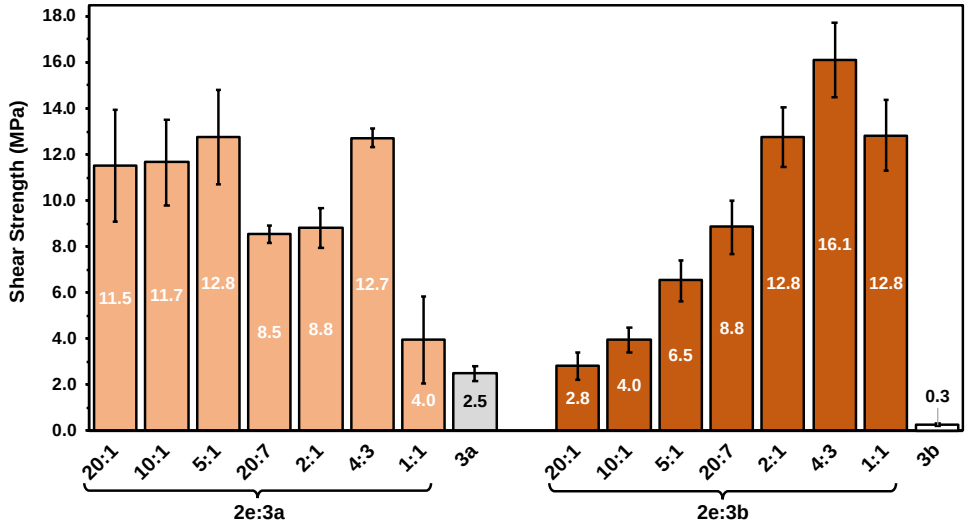

Figure S20. Lap-shear adhesive strength of cured blends of monomer **2e** with main-chain polybenzoxazines **3a** and **3b**. Error bars represent standard deviations in adhesive strength. At least three lap joints were tested for each formulation.

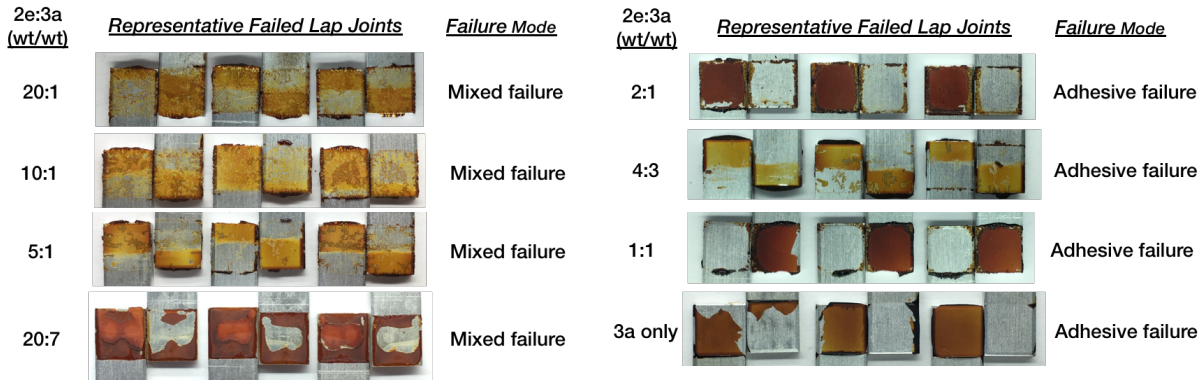

Figure S21. Representative failed lap joints of cured blends of monomer **2e** and main-chain **3a**.

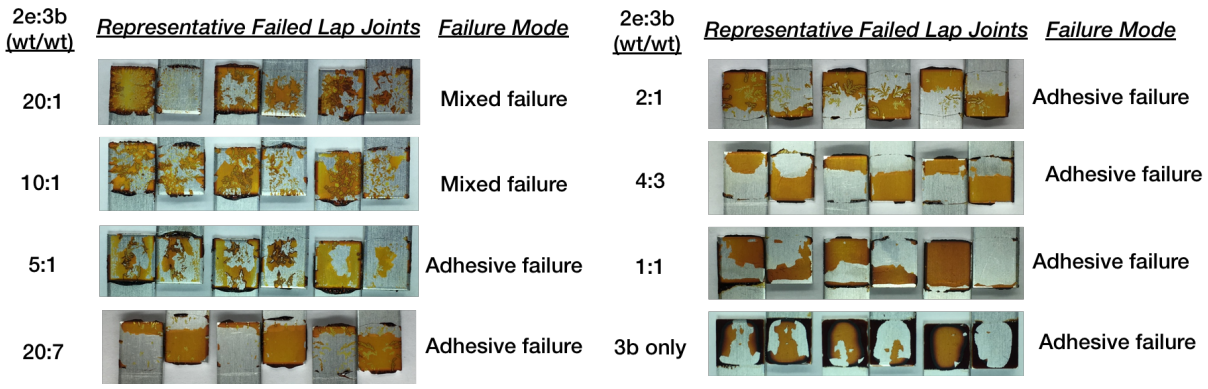

Figure S22. Representative failed lap joints of cured blends of monomer **2e** and main-chain **3b**.

*5.4 Adhesive strength of blends of **B-a** and **2e** with MX-551 and MX-154*

While main-chain benzoxazines **3a** and **3b** provided some enhancement in adhesive strength, relatively large amounts of main-chain component were required to achieve improved adhesive strengths and uniform bond lines. We next turned to commercial Kane Ace® core-shell (C-S) rubber tougheners from Kaneka Aerospace. These additives are provided as stable dispersions of ~100 µm diameter core-shell rubber particles in reactive liquid epoxy resins. Two products were applied: MX-154 and MX-551. MX-154 is supplied as a 40 wt% dispersion of styrene-butadiene rubber (SBR) core particles with BPA-based epoxy-modified shell in a BPA-based liquid epoxy resin. MX-551 is supplied as a 25 wt% dispersion of SBR core particles with cycloaliphatic epoxy-modified shell in liquid cycloaliphatic epoxy resin.

Sample and lap joint preparation and adhesion testing:
Kane Ace tougheners MX-154 and MX-551 were diluted with 15 vol% methanol in THF and combined with either **B-a** or **2e** to provide a 20:1 mass ratio of benzoxazine to C-S rubber particle content. Since MX-154 and MX-551 are provided at different weight percent content of core-shell particles, the formulations differ in the final amount of epoxy in the final mixture. The amounts of each component present in the formulations were calculated for comparison (**Table S1**). The composition was calculated in a manner exemplified below for benzoxazine+MX-551 blends:

Calculation S1. Example calculation of composition of 20:1 benzoxazine:MX-551 formulation.

(1) 100 mg BOA/20 = 5 mg C-S toughener
(2) 5 mg/0.25 = 20 mg MX-551 resin → 20mg resin – 5 mg toughener = 15 mg epoxy content
(3) 100 + 5 + 15 mg = 120 mg total
(4) 100/120*100 = 83.3 wt% BOA, 15/120*100 = 12.5 wt% epoxy, remainder = 4.2 wt% C-S.

Table S1. Composition of benzoxazine and commercial toughener formulations

Formulation	Wt% Benzoxazine	Wt% Epoxy	Wt% C-S Toughener
20:1 benzoxazine: MX-551	83.3	12.5	4.2
20:1 benzoxazine: MX-154	89	6.7	4.3

Blended samples were solution cast as described in sections 5.1 and 5.3 onto NaOH-etched Al 6061 substrates, followed by drying at 60 °C for 12 hours. The resulting films were inspected prior to curing (**Figure S23**). The dried samples were overlapped in pairs, clamped with 2 small binder clips, and then cured in an oven. The curing program was modified slightly compared to previous samples and consisted of a temperature ramp from 130 °C to 195 °C over 1.5 hours, followed by curing at 195 °C for 5 hours and cooling slowly to room temperature over 10 hours. Excess resin was trimmed from the sides of the joint prior to testing in tension at a strain rate of 0.5% strain/min. Adhesion strengths were determined by the peak load divided by the overlap areas (measured prior to testing with calipers). The apparent failure mode was assessed visually, and photographs were collected (**Figure S24**).

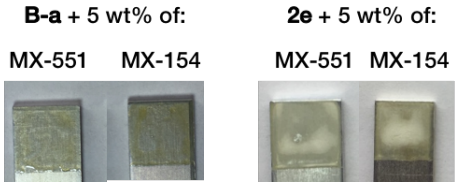

Figure S23. Appearance of solvent-cast films before curing of blends of **2e** and **B-a** with core-shell rubber toughened epoxy additives Kane Ace® MX-551 and MX-154 at a 20:1 weight ratio.

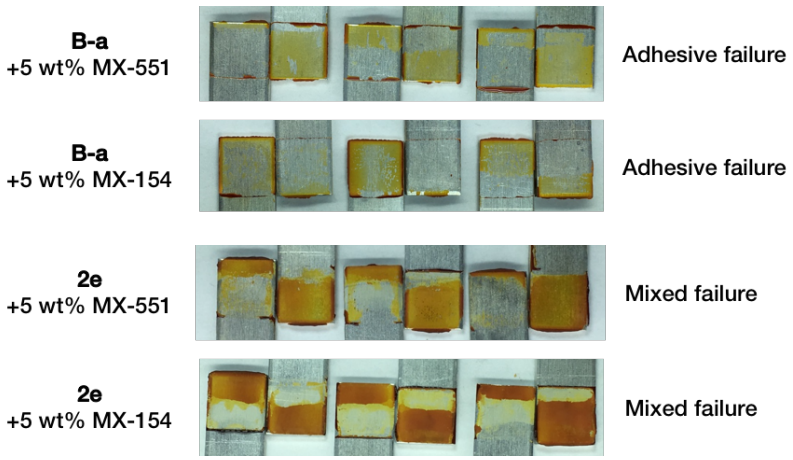

Figure S24. Representative failed lap joints of cured blends of monomer **2e** or **B-a** with core-shell rubber toughened epoxy additives Kane Ace® MX-551 and MX-154 (Kaneka Aerospace).

6. Thermal Stability of TBS Ethers in TBS-Protected Precursor S11

Bisphenol **S11** was employed to test the thermal stability of silyl ethers on aluminum 6061 and glass during a high temperature curing program. **S11** was employed instead of a benzoxazine monomer to maintain solubility of (by)products after incubation under curing conditions. Equal amounts of a 100 mM solution of **S11** in acetone were drop-cast either into a 20 mL glass scintillation vial or onto a 1 cm^2 square of aluminum 6061 and the solvent was evaporated under a stream of nitrogen. The samples were then placed in an air oven at 100 °C for 1 hour, followed by a 1-hour temperature ramp to 205 °C. The oven was kept at 205 °C for 3 hours, then cooled to room temperature (**Figure S25A**). A notable darkening of both samples was observed after heating, likely due to oxidation. The bulk of the samples were dissolved in 550 µL of deuterated methanol (**Figure S25B**), and TLC analysis was performed, staining with ferric chloride solution (**Figure S25C**). The sample treated on aluminum exhibited a darker color, and more intense ferric chloride staining on TLC (**Figure S25B**, right, and **Figure S25C,** grey streaks in right lane). ^{1}H-NMR analysis of the samples revealed clear changes in the aromatic region and in the peaks corresponding to the silyl ether protecting groups (**Figure S25D** and **D25E**, respectively).

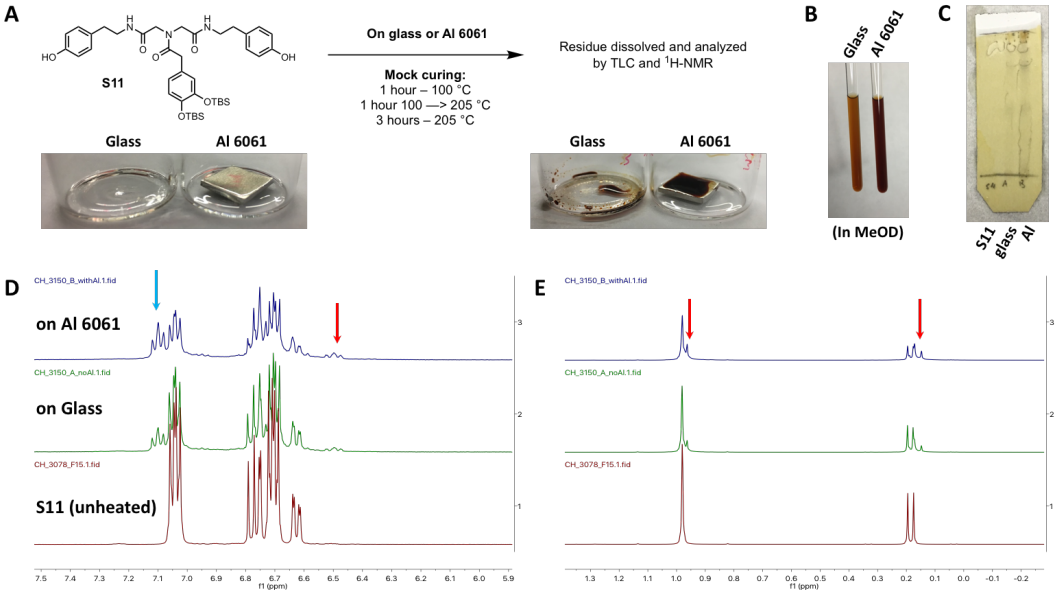

Figure S25. Investigation of stability of silyl ethers during curing protocol. (A) Drop casting of **S11** onto glass or aluminum 6061 followed by heat treatment. (B) Residue dissolved in deuterated methanol. (C) TLC analysis of dissolved residue, staining with ferric chloride. (D and E) ^{1}H-NMR analysis reveals changes in aromatic protons and in silyl ether protons.

The changes observed in the aromatic region are consistent with transfer of silyl ethers from the protected catechol fragment to the pendant phenols (blue arrow, **Figure S25D**). New upfield resonances for more shielded aromatic protons appear, consistent with the unmasking of one or both catechol hydroxyl groups. The extent to which silyl ether transfer occurs is greater in the sample heated in the presence of aluminum. It is important to note that this experiment is only sensitive to samples that were readily dissolved in deuterated methanol, and strongly adsorbed compounds (such as fully deprotected catechol species) may be underrepresented in the ^{1}H-NMR spectra and TLC analysis.

7. Mechanical Characterization

7.1 Sample preparation by compression molding

Compression molding was applied due to the coincidence of melting and curing for monomer **2e**. Flexural specimens from **2e** prepared by curing at atmospheric pressure contained a large number of voids and were not suitable for mechanical testing (**Figure S26**).

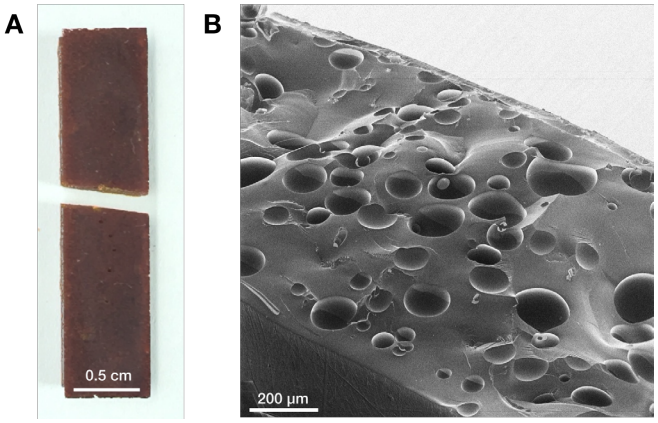

Figure S26. Appearance of rectangular sample of **2e** cured at atmospheric pressure in a silicone mold in air (205 °C or 4 hours). (A) Specimen fractured during demolding. (B) Scanning helium-ion micrograph of cross section of the specimen from panel A showing evidence of voids.

For compression molding, single-use rectangular PDMS molds were cut and formed by hand from self-amalgamating silicone (PDMS) tapes (X-treme tape®, MOCAP). The mold was cut to the approximate sample dimensions of 0.5 cm x 4 cm, with 0.9 mm thickness. **Figure S27** shows a schematic representation of the mold assembly. For **B-a** and **1e**, the molds were filled with solid monomers (150-200 mg each sample) on a hot press at 160 °C to provide liquid melts. Once the molds were filled, the molds were covered with a PDMS sheet, heated to 205 °C over the course of 6 minutes, and pressed between steel plates at 550 psi. Steel shims were applied to prevent over-pressing. Temperature and pressure were maintained for 2 hours, and then the samples were cooled over 15 minutes to room temperature. Samples were cut free from the PDMS molds with a razor, and the edges of samples were sanded (sandpaper, 80 grit aluminum oxide on fabric) to provide rectangular substrates suitable for mechanical testing.

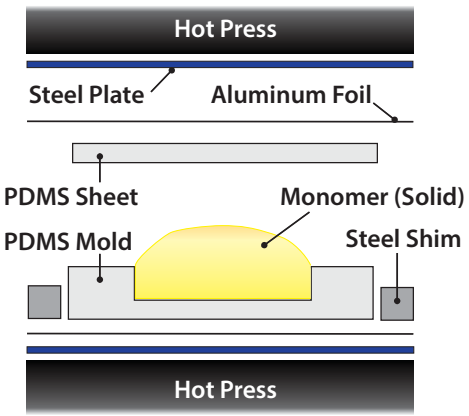

Figure S27. Exploded schematic of mold assembly used for compression molding of polybenzoxazine samples (not drawn to scale).

Resin **2e** was processed with slight modification due to the coincidence of melting and curing for this monomer. Silicone molds were filled with solid **2e**, covered with a PDMS sheet, and sandwiched between steel plates. The assembly was placed on a preheated hot press at 205 °C and immediately pressed to 550 psi. Pressure and temperature were maintained for 2 hours, and then the samples were cooled to room temperature over 15 minutes. Samples were cut free from the PDMS molds and the edges were sanded to provide rectangular specimens. Scanning electron microscopy of a razor-fractured specimen revealed no voids, indicating the samples are suitable for mechanical testing (**Figure S28**).

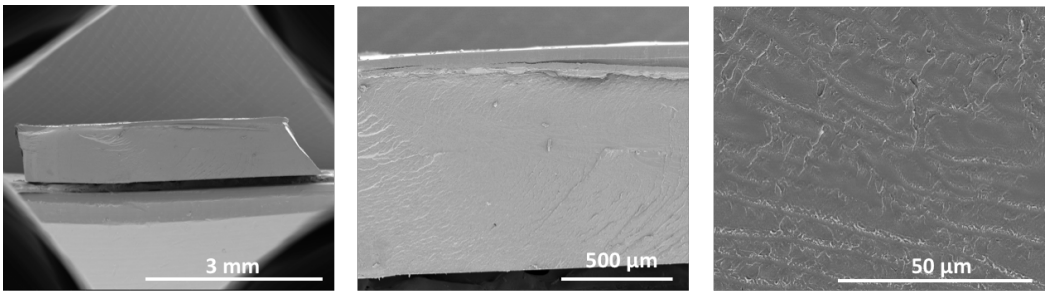

Figure S28. Scanning electron micrograph of a cross-section of cured compression-molded **2e** showing an absence of voids.

To compare the absorbance spectra of cured **B-a** and **2e**, thin films were prepared on glass by spin-coating solutions of **B-a** (300 mM in 15 vol% methanol/THF) and **2e** (67 mM in 15 vol% methanol/THF). 100 µL of **B-a** solution was added in one portion to a ~2.5 x 2.5 cm glass slide (~1 mm thick) spinning at 3000 rpm. The rotation speed was increased to 10000 rpm for 20 seconds. The process was repeated with a second slide, and the coatings were allowed to dry in a fume hood for 20 minutes. The two slides were stacked with the coated faces touching one another to create a sandwich, and were cured in an air oven at 180 °C for 1 hour, and then the temperature was ramped to 205 °C for 4.5 hours. A sandwich configuration was used to minimize dewetting of **B-a** prior to curing, which was observed when curing on the surface of a single glass slide. A film of **2e** was prepared by spin-coating 200 µL of **2e** solution as for **B-a** on a single glass slide, and the film was cured in an air oven as described above. Absorbance spectra from 300-800 nm were collected on a Shimazu UV-2600 spectrometer at room temperature, blanking with clean glass slides mounted on a thin film holder (two stacked slides for **B-a** and one slide for **2e**). The thicknesses of the films were measured using Digimax calipers to the nearest 0.01 mm. The thickness was measured in 3 to 5 locations on the sample, and values were averaged. The thickness of the **B-a** film was 0.05 mm, and **2e** was 0.012 mm. Spectra were normalized by dividing the absorbance value by the film thickness. Normalized spectra are shown in **Figure S29**.

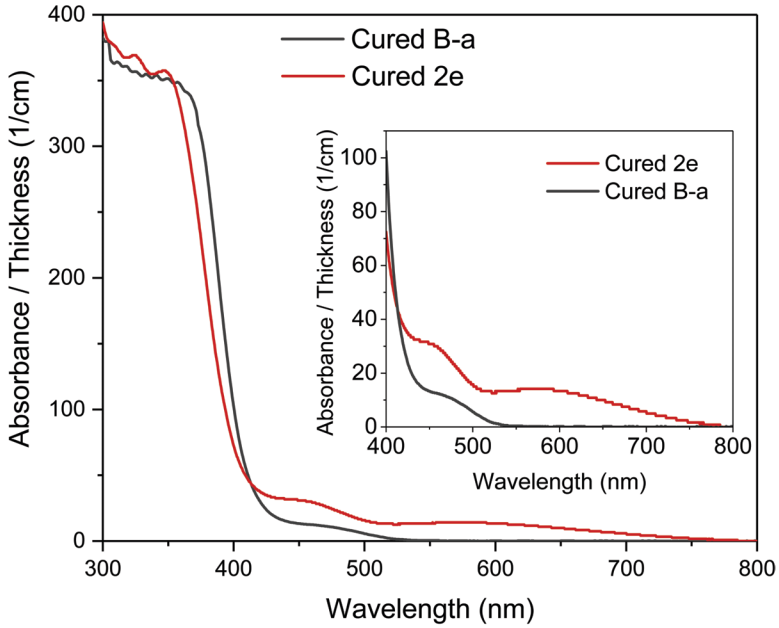

Figure S29. Absorbance spectrum of thin films of cured **B-a** and **2e** on glass. Absorbance values were divided by the film thickness to normalize the spectra. Inset is a zoom of the spectrum from 400-800 nm.

Attenuated total reflectance Fourier transform infrared analysis was performed on monomers **B-a**, **2e**, and **1e** and the corresponding thermosets obtained after compression molding. Spectra are presented in **Figures S30**-**S32**.

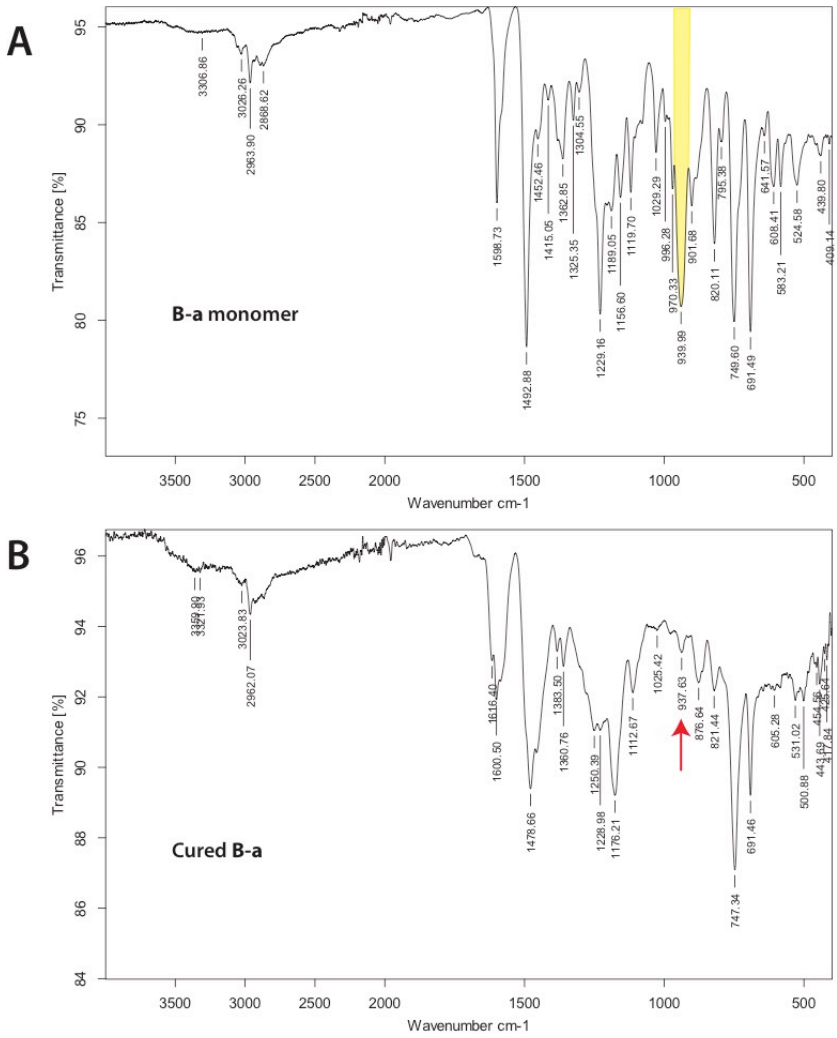

Figure S30. FTIR analysis of **B-a** monomer and **B-a** cured by compression molding. (A) Oxazine-related mode is highlighted in yellow. (B) Oxazine-related mode has disappeared after curing, with the previous location marked by a red arrow.

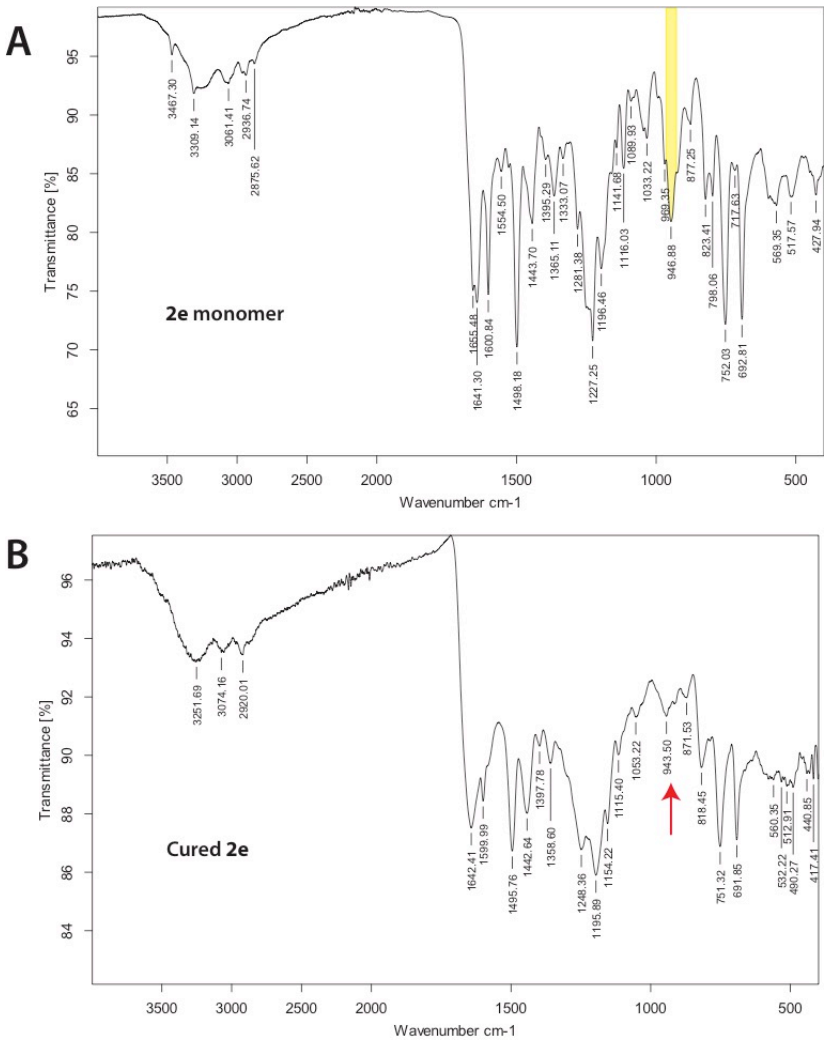

Figure S31. FTIR analysis of **2e** monomer and **2e** cured by compression molding. (A) Oxazine-related mode is highlighted in yellow. (B) Oxazine-related mode has disappeared after curing, with the previous location marked by a red arrow.

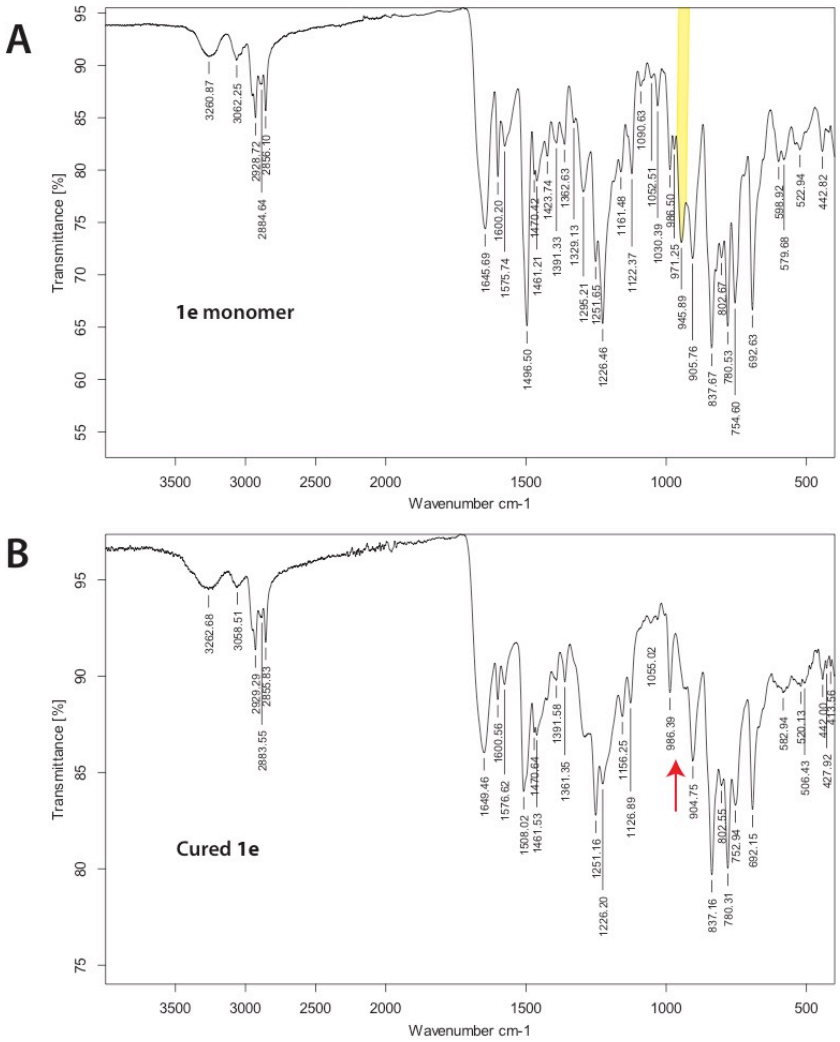

Figure S32. FTIR analysis of **1e** monomer and **1e** cured by compression molding. (A) Oxazine-related mode is highlighted in yellow. (B) Oxazine-related mode has disappeared after curing, with the previous location marked by a red arrow.

Compression molded specimens were analyzed by differential scanning calorimetry, revealing broad glass transitions at 147 °C, 183 °C, and 149 °C for **B-a**, **2e**, and **1e**, respectively. (**Figures S33-S35**). The glass transition temperature of compression-molded **2e** was lower than for samples cured in differential scanning calorimetry at atmospheric pressure under nitrogen with a temperature ramp up to 295 °C (208 °C).

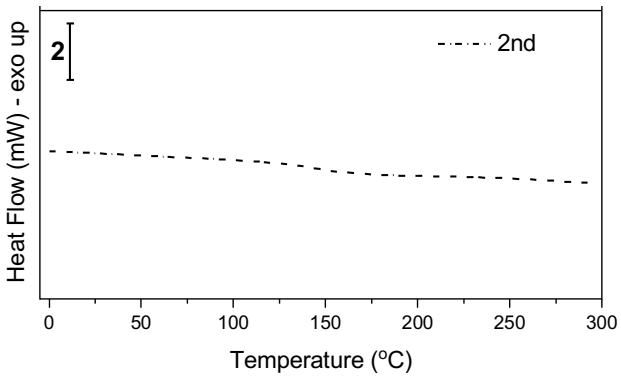

Figure S33. B-a – compression molded and cured. T_g centered at 147 °C.

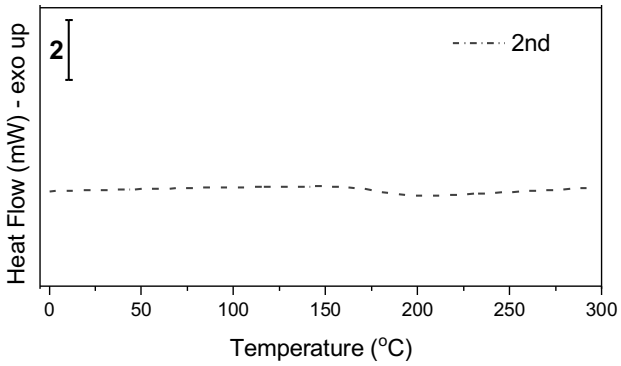

Figure S34. 2e – compression molded and cured. T_g centered at 183 °C.

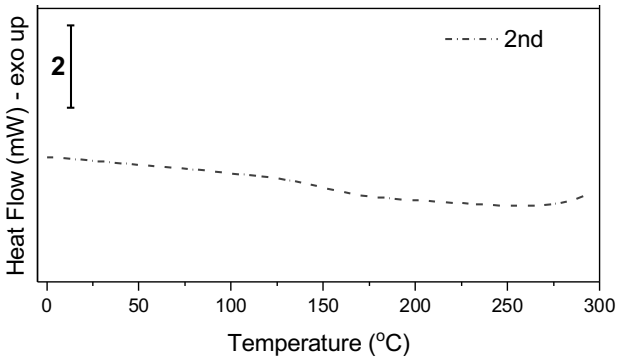

Figure S35. 1e – compression molded and cured. Broad glass transition (T_g) centered at 149 °C.

7.2 Flexural testing (3-point bending)

The flexural properties of the samples were measured in accordance to ASTM D790 using an Instron A620-325 (Norwood MA) at the crosshead speed of 0.01 mm/min. Rectangular specimens (n=8 for **B-a** and **2e**, and n=6 for **1e**) with approximate dimensions of 25 mm (length) x 6 mm (width) x 1 mm (thickness) were tested at room temperature in the three-point bending mode with a fixed support span of 20 mm. The dimensions of each sample were measured with calipers prior to testing. The flexural modulus (elastic, Pa) was determined from the following formula[6]:

$$E_f = \frac{L^3 m}{4bd^3}$$

Where *L* is the support span in the 3-point bending setup, *m* is the slope of the initial linear portion of the load-displacement curve, *b* is the width (breadth) of the specimen, and *d* is the depth (thickness) of the specimen.

The flexural strength (Pa) was calculated from the following formula[7]:

$$\sigma = \frac{3FL}{2bd^2}$$

where *F* is the maximum axial load (at the point of fracture), *L* is the support span in the 3-point bending setup, *b* is the width (breadth) of the specimen, *d* is the depth (thickness) of the specimen.

7.3 Nanoindentation measurements

Indentations were performed using a Triboindenter TI 950 (Hysitron, Minneapolis) with a 150 nm Berkovich tip. The tip area function was established from a polycarbonate standard. All load displacement curves were analyzed using the method described by Oliver and Pharr (50% of the unloading curve was used for the analysis). All indentations were carried out in the open loop feedback mode under loading rate control. The loading and unloading rates were 200 µN/sec and the peak load was approximately 5000 µN. Once at peak, the load was held fixed for a period of 5 seconds.

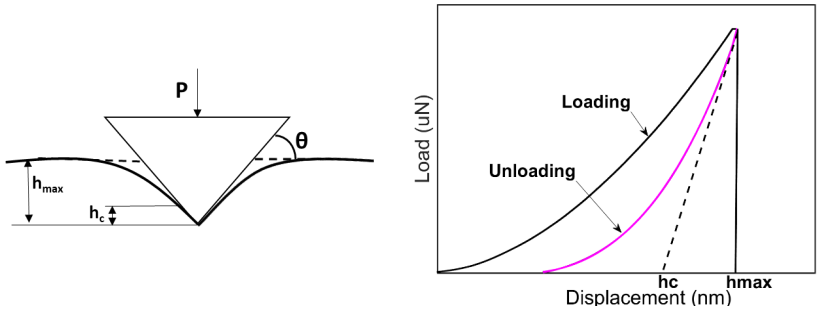

Figure S36. Schematic indentation process (left) and a representative load (P) versus depth (h) response due to a trapezoidal load function.

The indentation test records the load-displacement curve as the indenter is pressed into a softer matter by continuously measuring the load as a function of the indenter displacement.[8] **Figure S36** shows a schematic of the indentation process and a typical load (P) versus depth (h) response due to a trapezoidal load function. The slope of the load-displacement curve, upon unloading, represents the contact stiffness, S, evaluated at the maximum indentation depth, h_{max}.[9]

$$S = (\frac{\partial P}{\partial h})_{h_{max}}$$

The stiffness is used to calculate the reduced Young's modulus E_r using the relationship

$$E_r = \frac{\sqrt{\pi}}{2}\frac{S}{\sqrt{A_c}},$$

where A_c, is the contact area established at h_{max}.[9] A_c is a polynomial function of the contact depth h_c, with coefficients determined from a material of known elastic properties.[9] Here, the coefficients of A_c were obtained from indentations performed on standard polycarbonate and quartz samples.

The reduced elastic modulus, which is nominally independent of the penetration depth, can be expressed as a function of the elastic properties of the indenter and the sample as

$$\frac{1}{E_r} = \frac{(1 - {v_i}^2)}{E_i} + \frac{(1 - {v_s}^2)}{E_s},$$

where *E* and *v* with subscripts *s* and *i* represent the elastic moduli and Poisson's ratio of the sample and the indenter, respectively.[10]

The elastic modulus of cured **B-a**, **1e**, and **2e** were measured by nanoindentation and were found to be in close agreement with the moduli measured by flexural testing with bulk samples. Nanoindentation was also applied to determine the influence of curing pressure on the elastic modulus of cured benzoxazines. Samples of thermoset **B-a** and **1e** were prepared by curing in an open silicone mold with dimensions of 0.5 cm x 2.54 cm x 0.16 cm in an air oven. The curing program consisted of 120 °C for 1 hour with intermittent application of vacuum to remove bubbles, and the temperature was increased to 200-205 °C over 1 hour. The temperature was maintained for 5 hours, followed by cooling slowly to room temperature.

Indentations were performed as described above. Representative load (N)-displacement (nm) curves for cured monomers are shown in **Figure S37**. The elastic moduli for compression molded **B-a**, **1e**, and **2e**, and **1e** and **B-a** cured at atmospheric pressure were calculated as described above. The elastic moduli measured on compression molded samples by nanoindentation were in close agreement to those measured by bulk flexural testing. Furthermore, the moduli for **B-a** and **1e** samples cured at atmospheric pressure were comparable to those measured after compression molding, suggesting that compression molding does not dramatically influence the thermoset mechanical properties (**Figure S38**).

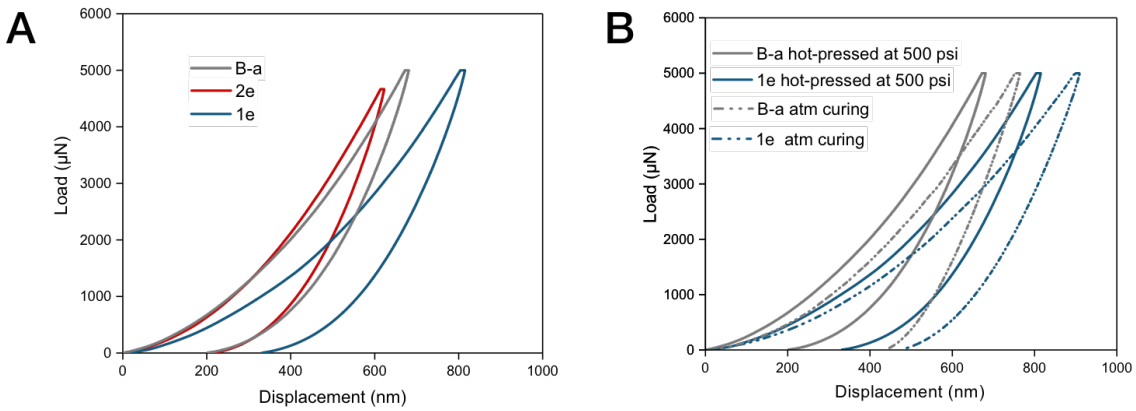

Figure S37. Representative nanoindentation load-displacement curves for thermoset **B-a**, **1e**, and **2e**. (A) Analysis of samples prepared by compression molding at 205 °C. (B) Comparison of data obtained for **B-a** and **1e** when cured by compression molding or at atmospheric pressure (5 hours at 205 °C oven in air).

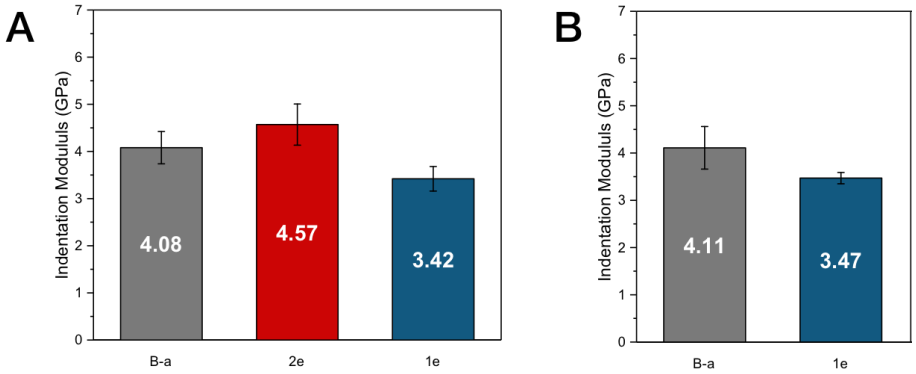

Figure S38. Elastic moduli determined by nanoindentation on cured specimens. (A) Modulus of specimens cured by compression molding at 205 °C for 2 hours at 500-550 psi in air. (B) Modulus of specimens cured at 205 °C at atmospheric pressure (air) for 5 hours.

8. XPS Analysis of Failed Adhesive Lap Joints

X-ray photoelectron spectroscopic analysis of failed lap joints and unpolymerized **B-a** and **2e** monomers was carried out to verify curing (monitoring disappearance of the benzoxazine ring), and to qualitatively assess the status of the catechol in cured **2e**. Failed lap joints coated with **B-a** or **2e** on NaOH-etched Al 6061 (see **Figure S14**) were used to represent cured materials, while monomers were mounted as solid powders on double-sided conductive carbon tape on silicon wafer. High-resolution C1s and O1s spectra and survey scans were collected using a monochromatic Al Kα X-ray source operating at 350 W. The spectra were calibrated to a C1s peak at 284.5 eV. High-resolution C1s and O1s spectra were deconvoluted in Origin software (**Figures S39**-**S42**). Survey spectra for uncured monomers and cured resins are shown in **Figures S43**-**S48**.

Supplemental Results and Discussion:
Deconvolution of the C1s spectrum of uncured **B-a** revealed a peak centered at 287.1 eV that was assigned to the methylene carbon between the nitrogen and oxygen heteroatoms of the oxazine ring (**Figure S39A**). Additional peaks centered at 286.0 and 284.7 eV were assigned to non-oxazine carbon atoms bonded to heteroatoms and aliphatic and aromatic carbons, respectively. Qualitatively, the relative areas for these peaks are in close agreement with the composition of **B-a**. In the high-resolution C1s spectrum for cured **B-a**, the peak assigned to the oxazine carbon disappeared completely, indicating successful ring-opening polymerization (**Figure S39B**). The high-resolution O1s spectrum was fit by a single gaussian curve centered at 532.9 eV, interpreted as the oxazine chemical environment based on the known structure of **B-a** (**Figure S39C**). In cured **B-a**, a small peak assigned to oxidized phenols was observed at 531.2 eV, in addition to another major component assigned to phenolic oxygen at 532.3 eV (**Figure S39D**). A peak designated as silicone contamination from the air oven used in curing lap joints was also present and was assigned based on the sample composition in the survey spectrum of cured **B-a** (**Figure S43**).

Deconvolution of the C1s spectrum of monomer **2e** revealed alkyl/aryl carbon components at 284.6 eV, while carbons bonded to a single electronegative heteroatom were observed at 285.9 eV. A small peak assigned to the oxazine carbon, bonded to two electronegative heteroatoms, was present at 287.3 eV. Lastly, carbonyl carbons were present, consistent with the amide bonds in **2e**, at 288.5 eV (**Figure S40A**). The C1s spectrum of cured **2e** consisted of three main chemical environments: alkyl/aryl carbons at 284.7 eV, carbons bonded to a single electronegative heteroatom at 285.9, and carbonyl carbons at 288.1 eV (**Figure S40B**). The high-resolution O1s spectrum of uncured **2e** was deconvoluted using three peaks, centered at 531.7 eV, 532.4 eV, and 533.3 eV, qualitatively assigned to carbonyl oxygen, oxazine oxygen, and oxygen single-bonded to carbon (**Figure S40C**). The same region in cured **2e** was better fit by only two peaks, assigned as oxygen single-bonded to carbon (533.1 eV), and carbonyl oxygen (531.8 eV). The relative area of carbonyl oxygen is significantly higher than expected based on theory, which was interpreted as partial oxidation of catechols to form *ortho*-quinones (**Figure S40D**). We interpret the dark brown color of cured **2e**, and the broadened carbonyl stretch in FTIR spectra (**Figure S34**, peak centered at 1642 cm^{-1}) as additional data suggestive of quinone formation. Low-resolution survey spectra of monomer **2e** and thermoset **2e** are shown in **Figures S45**-**S46**.

Deconvolution of the C1s spectrum of monomer **1e** revealed alkyl/aryl carbon components at 284.1 eV, while carbons bonded to a single electronegative heteroatom were observed at 285.4 eV. A small peak assigned to the oxazine carbon, bonded to two electronegative heteroatoms, was present at 287.3 eV. Carbonyl carbons were present, consistent with the amide bonds in **1e**, at 290.5 eV (**Figure S41A**). The C1s spectrum of cured **1e** collected from the top of a failed lap joint exhibited three main chemical environments: alkyl/aryl carbons at 284.8 eV, carbons bonded to a single electronegative heteroatom at 286.9, and carbonyl carbons at 289.4 eV (**Figure S41B**). The high-resolution O1s spectrum of uncured **1e** was deconvoluted using three peaks, centered at 531.9 eV, 532.5 eV, and 533.1 eV, qualitatively assigned to carbonyl oxygen, oxazine oxygen, and oxygen single-bonded to carbon (**Figure S41C**). The same region in cured **1e** was fit by two peaks, assigned as oxygen single-bonded to carbon (532.8 eV), and carbonyl oxygen (531.9 eV). The relative area of carbonyl oxygen is significantly higher than expected based on theory, which was interpreted as partial oxidation of catechols formed by deprotection near the substrate surface (**Figure S41D**). Low-resolution survey spectra of monomer **1e** and thermoset **1e** are shown in **Figures S47**-**S48**.

The survey spectrum of **1e** at the surface of a failed lap joint exhibited higher relative oxygen content and lower relative carbon content than expected based on theory. This is consistent with the hypothesis that the metal surface facilitates deprotection and migration of the carbon-rich TBS protecting group, as indicated by model studies with precursor **S11** (see **Figure S25**). The surface of cured **1e** was subsequently scraped with a clean razor to remove material originating from the interface region of the failed lap joint, and XPS analysis was repeated on the underlying cured **1e** surface (**Figure S48**). Survey analysis revealed a decreased relative oxygen content, increased carbon content, and slightly increased silicon content consistent with a greater amount of TBS groups present towards the middle of the sample depth. Deconvolution of the C1s spectrum of the scraped region of cured **1e** presented alkyl/aryl carbon components at 284.1 eV, and carbons bonded to a single electronegative heteroatom were observed at 285.5 eV. A peak similar to that observed for intact oxazine at 287.4 eV was observed, which was assigned to the O-CH_2-N bond present in previously reported phenoxy-type ring-opened benzoxazines.[11] While the presence of uncured **1e** is a possibility, given the disappearance of the oxazine-associated resonance in FTIR spectra for flexural testing samples of **1e** cured at 205 °C for only 2 hours, we consider uncured **1e** unlikely in a sample cured for 4 hours at 205 °C (**Figure S32**). Furthermore, differential scanning thermograms of the same flexural testing samples revealed no residual exotherm associated with benzoxazine ring opening (**Figure S35**). Carbonyl carbons were present, consistent with the amide bonds in **1e**, at 290.5 eV (**Figure S41A**). Along with model studies with **S11**, XPS results reveal that **1e** is prone to deprotection at the metallic surface during curing, likely contributing to the strong lap shear adhesion performance of cured **1e**.

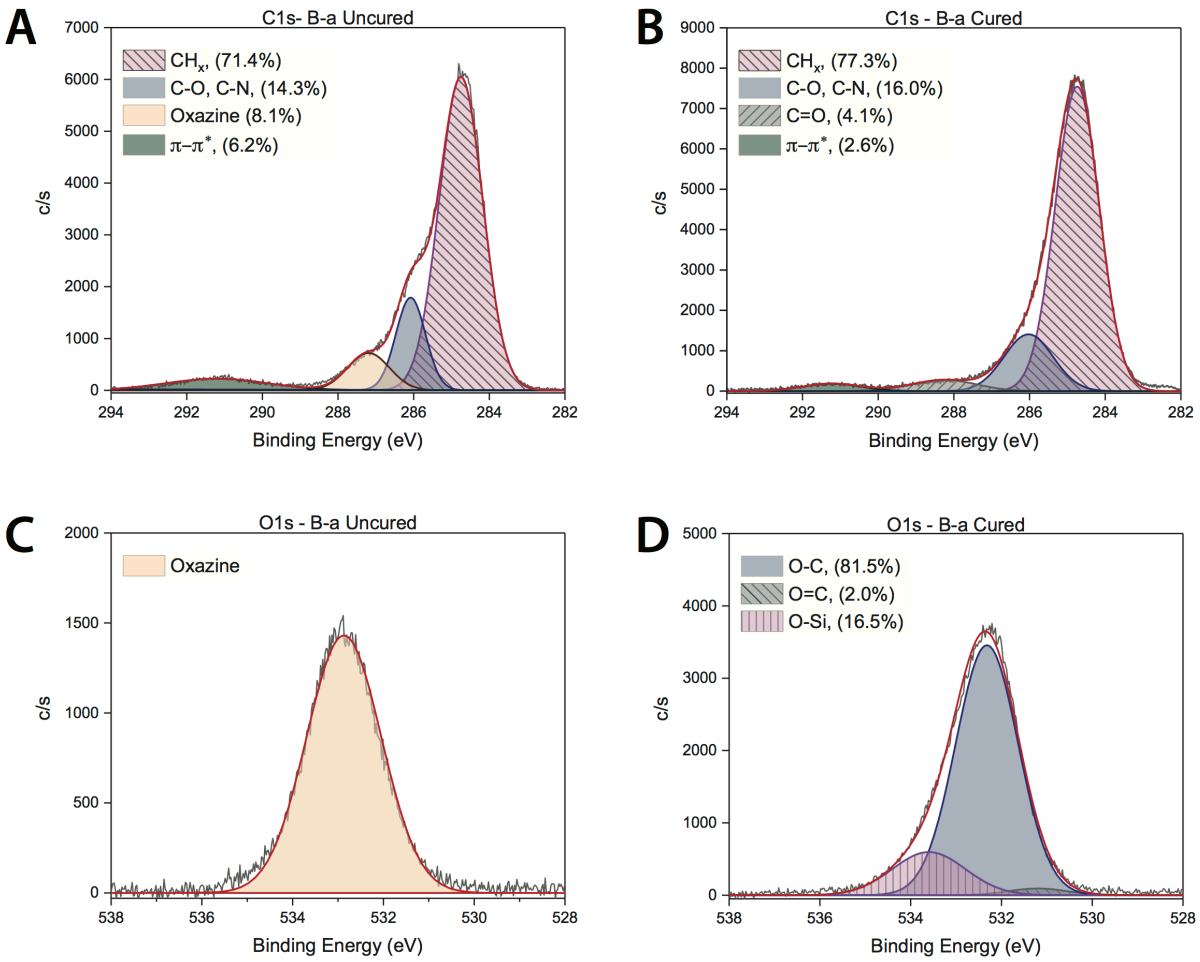

Figure S39. High-resolution X-ray photoelectron spectroscopy analysis of cured **B-a** on a failed lap joint, and uncured monomer as received from Huntsman, mounted on double-sided carbon tape. Cured material contains some silicon contamination. (A) Deconvoluted C1s spectrum for uncured **B-a**. (B) Deconvoluted C1s spectrum for cured **B-a**. (C) Deconvoluted O1s spectrum for uncured **2e**. (D) Deconvoluted O1s spectrum for cured **B-a**. Silicon contaminant is present.

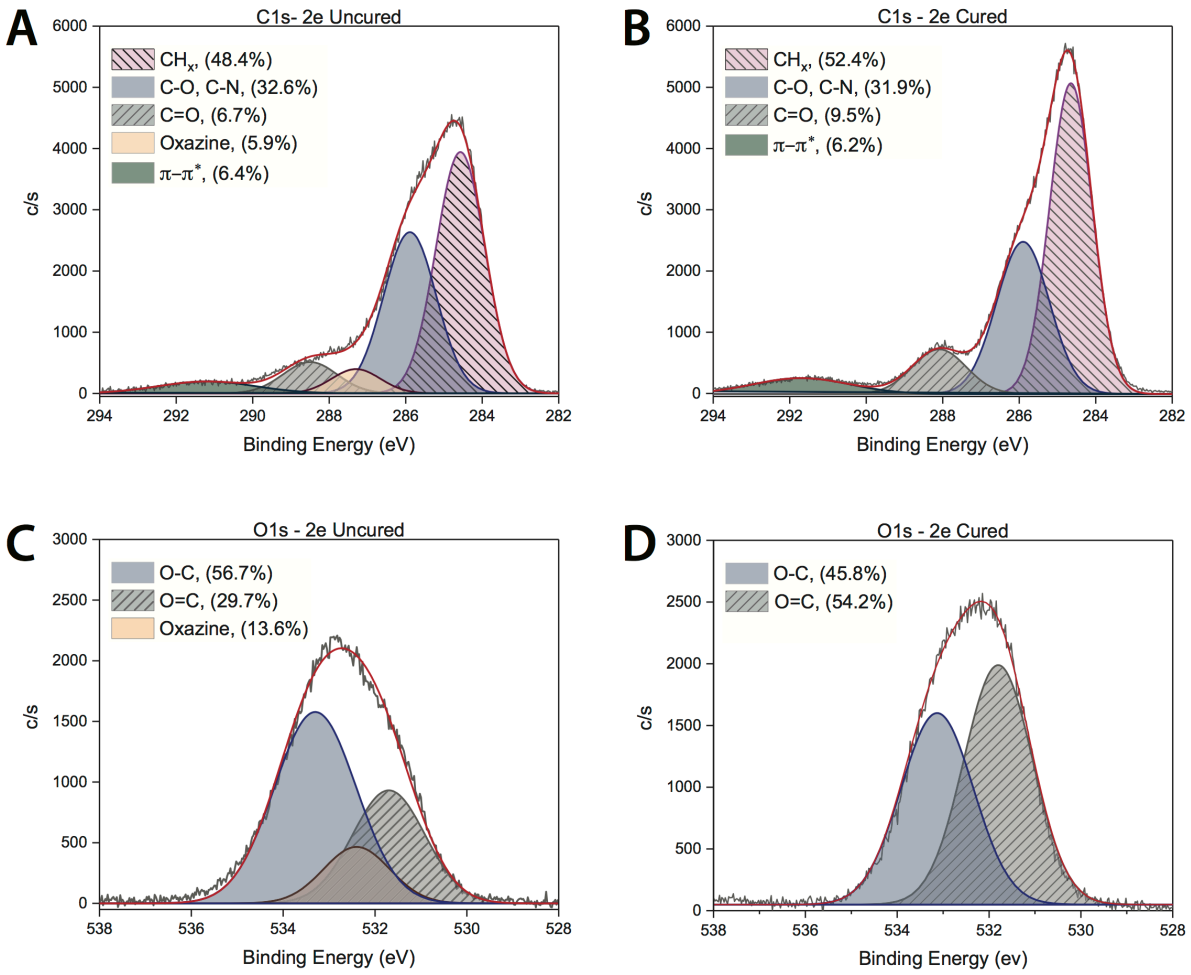

Figure S40. High-resolution X-ray photoelectron spectroscopy analysis of cured **2e** on a failed lap joint, and uncured monomer mounted on double-sided carbon tape. (A) Deconvoluted C1s spectrum for uncured **2e**. (B) Deconvoluted C1s spectrum for cured **2e**. (C) Deconvoluted O1s spectrum for uncured **2e**. (D) Deconvoluted O1s spectrum for cured **2e**.

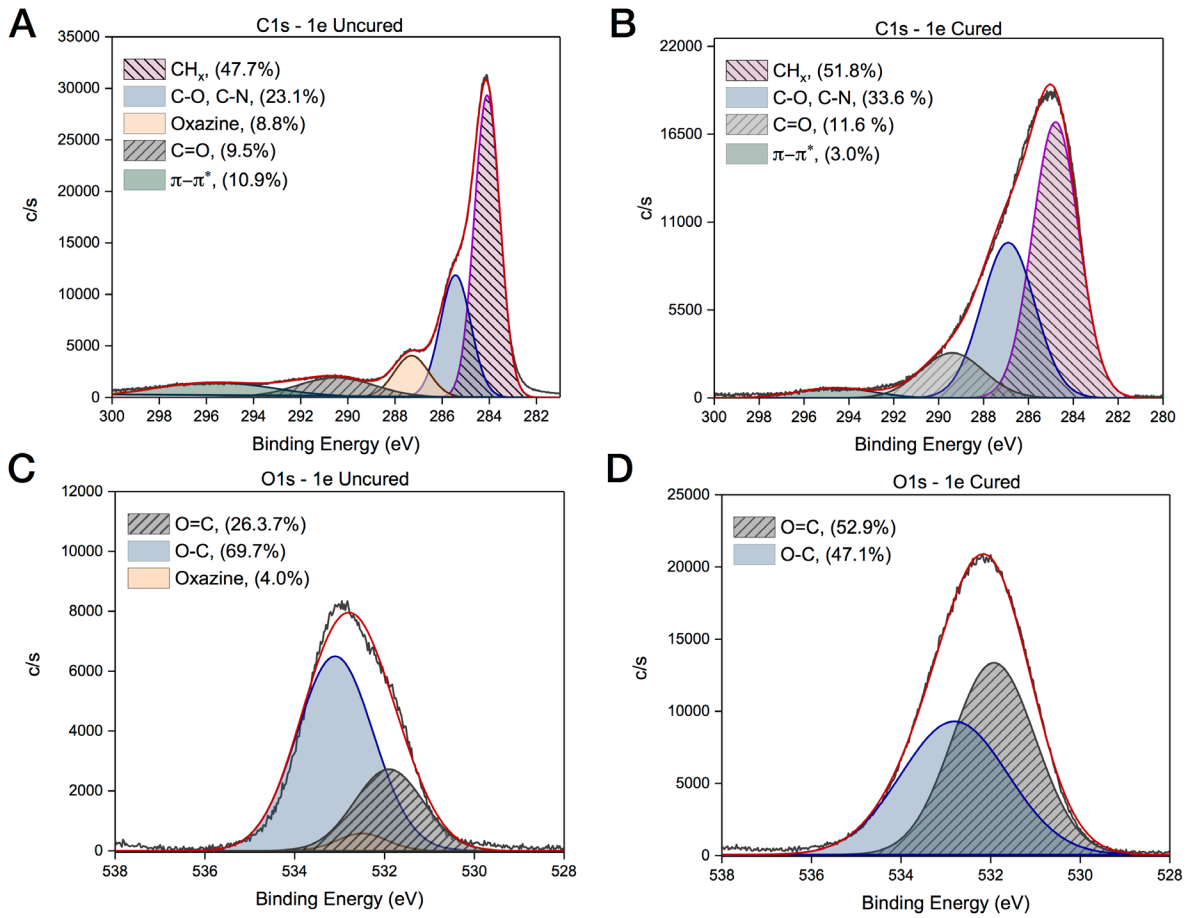

Figure S41. High-resolution X-ray photoelectron spectroscopy analysis of cured **1e** on the surface of a failed lap joint, and uncured monomer mounted on double-sided carbon tape. (A) Deconvoluted C1s spectrum for uncured **1e**. (B) Deconvoluted C1s spectrum for cured **1e**. (C) Deconvoluted O1s spectrum for uncured **1e**. (D) Deconvoluted O1s spectrum for cured **1e**.

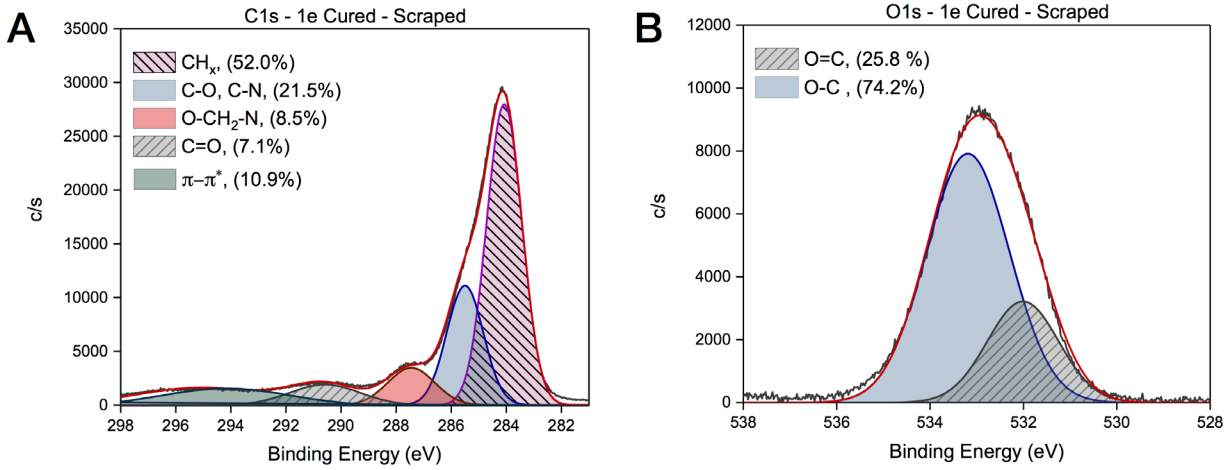

Figure S42. High-resolution X-ray photoelectron spectroscopy analysis of cured **1e** on the surface of a failed lap joint after scraping away some of the sample with a razor. (A) Deconvoluted C1s spectrum of scraped cured **1e** sample. (B) Deconvoluted O1s spectrum of scraped cured **1e** sample.

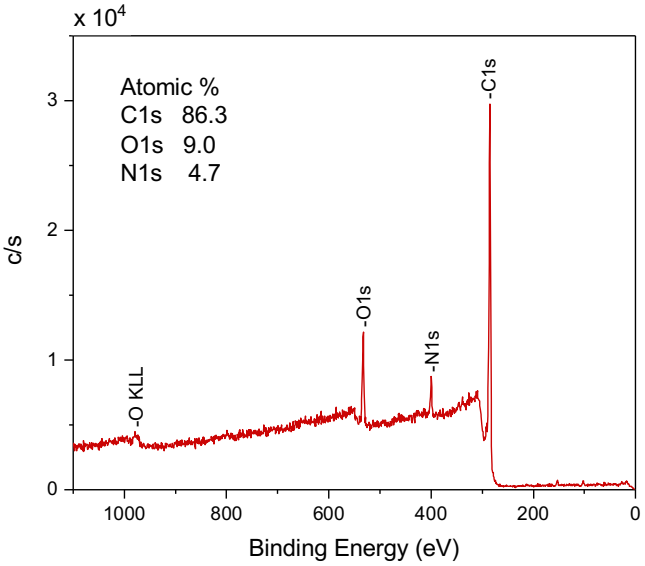

Figure S43. Low resolution XPS survey spectrum of uncured **B-a** on double-sided carbon tape.

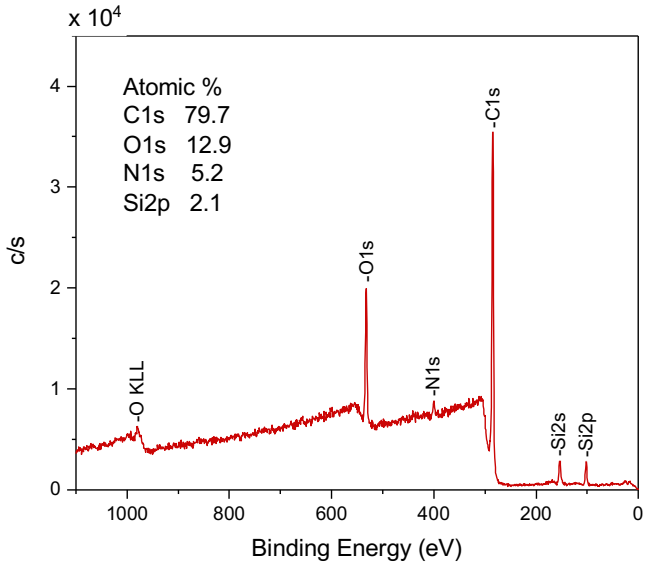

Figure S44. Low resolution XPS survey spectrum of cured **B-a** on Al 6061. Silicon contaminant is present.

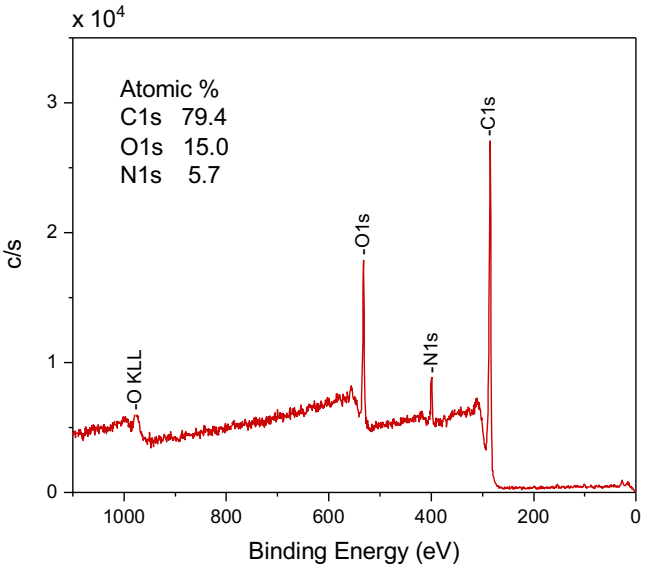

Figure S45. Low resolution XPS survey spectrum of uncured **2e** on double-sided carbon tape.

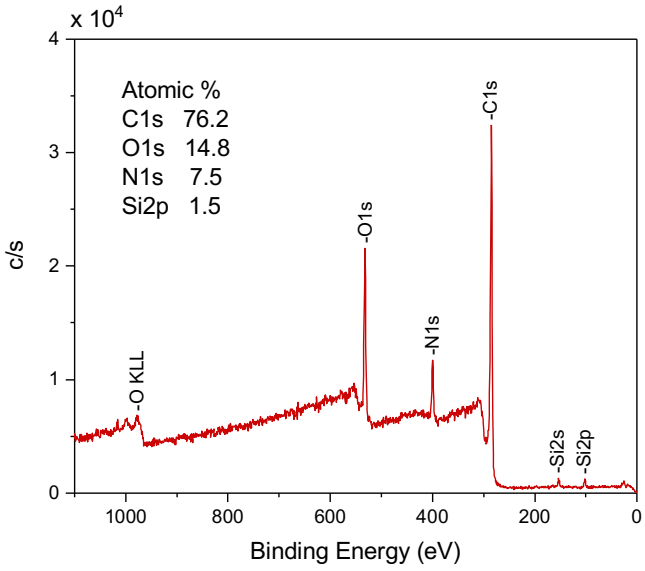

Figure S46. Low resolution XPS survey spectrum of cured **2e** on Al 6061. Minor silicon contaminant is present.

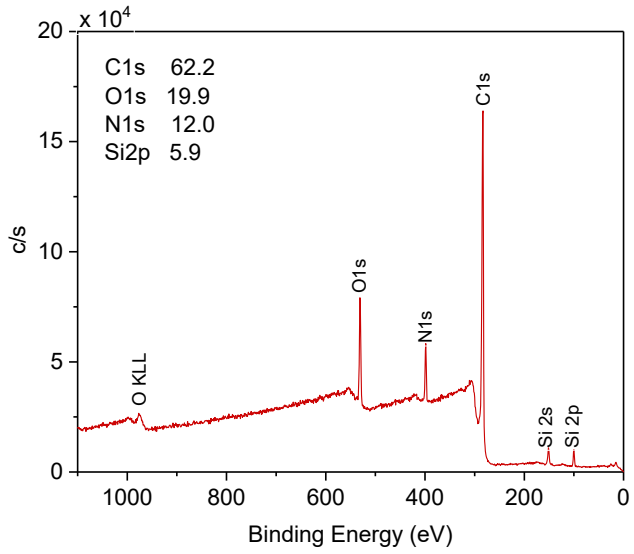

Figure S47. Low resolution XPS survey spectrum of uncured **1e** on double-sided carbon tape.

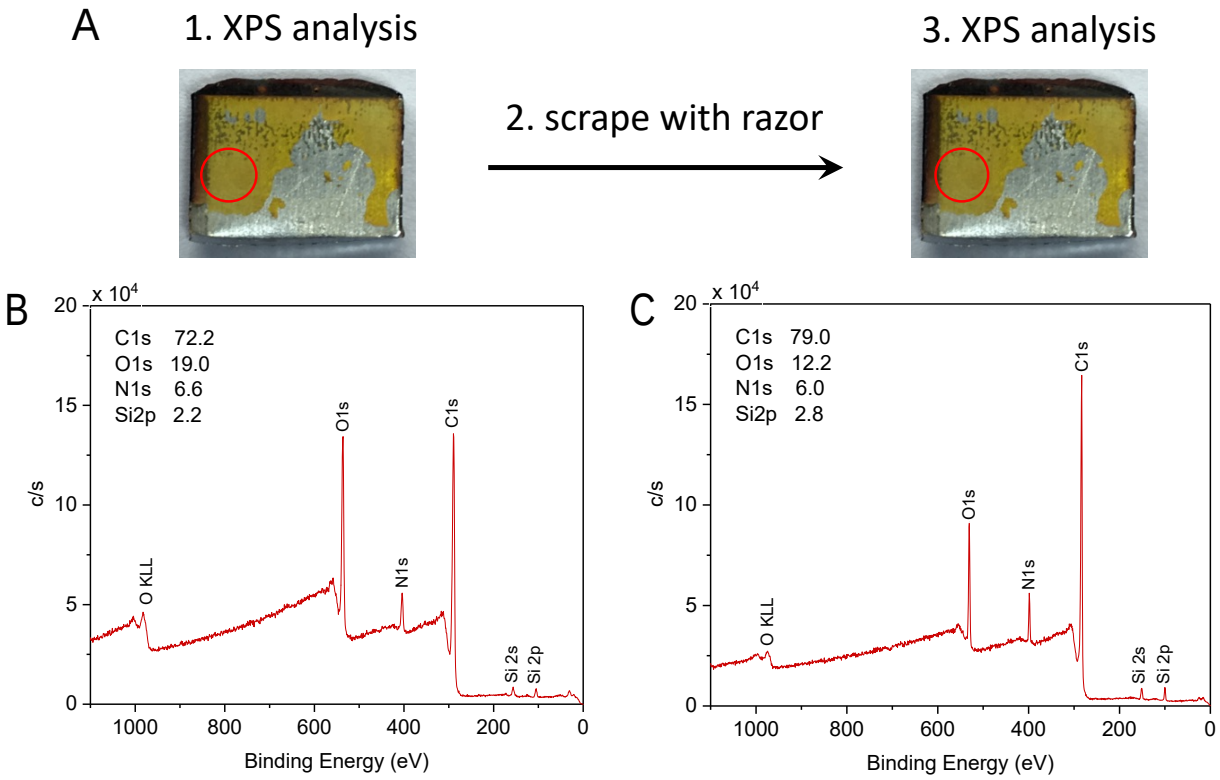

Figure S48. Low resolution XPS survey spectra of cured **1e** from a failed lap joint. (A) Procedure for analysis of cured **1e** at the bond interface and further from the interface after scraping the sample with a razor. (B) Survey spectrum of cured **1e** after adhesion testing. (C) Survey spectrum of cured **1e** sample after scraping some material away from the surface with a clean razor.

9. Thermal Gravimetric Analysis of Thermoset B-a, 1e, and 2e

Nitrogen atmosphere: Thermal gravimetric analysis was performed under nitrogen atmosphere on cured samples cut from fractured flexural testing specimens of **B-a**, **1e**, and **2e**. Decomposition traces were collected under a flow rate of 25 mL/min N_2 gas with a temperature ramp rate of 10 °C/min up to 600 °C. The remaining weight % at a given time was given by mass (mg)/initial mass(mg)*100 and was plotted vs temperature (**Figures S49**-**S51**). The temperatures at which 5% and 10% weight loss occurred ($T_{5\%}$ and $T_{10\%}$ respectively) were determined from this raw data and are summarized in **Table S2**. The first derivative curve was generated in Microsoft Excel by calculating the slope at a data point "i" by the following equation:

(weight % at "i+1" – weight % at "i-1")/(time at "i+1" – time at "i–1")

The slope was plotted against temperature with exponential smoothing with an alpha value of 0.01. The temperature of the maximum rate of weight loss, T_{peak}, was estimated at the absolute minimum of the first derivative curve, and the weight % remaining at this temperature was also noted (**Table S2**).

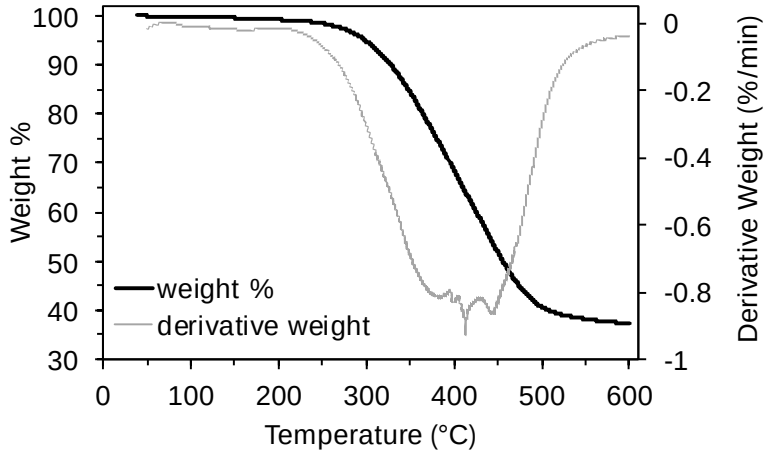

Figure S49. Thermal gravimetric analysis of **B-a** with overlaid 1st derivative curve in nitrogen atmosphere up to 600 °C.

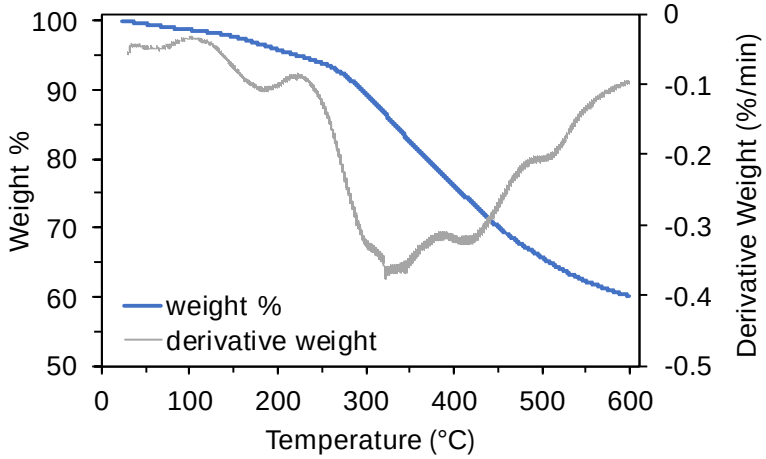

Figure S50. Thermal gravimetric analysis of **1e** with overlaid 1st derivative curve in nitrogen atmosphere up to 600 °C.

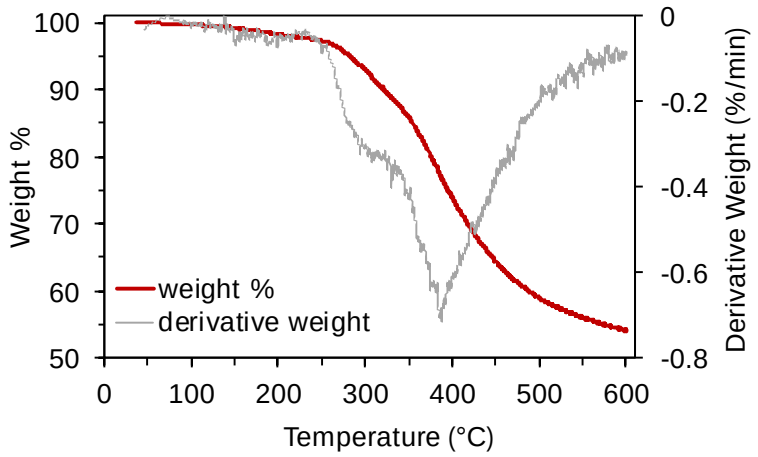

Figure S51. Thermal gravimetric analysis of **2e** with overlaid 1st derivative curve in nitrogen atmosphere up to 600 °C.

Table S2. Summarized thermal stability data for cured **B-a**, **2e**, and **1e** in N_2.

Sample	$T_{5\%\ mass\ loss}$	$T_{10\%\ mass\ loss}$	T_{peak}[a]	Weight % at T_{peak}[a]	Char Yield (600 °C)[b]
B-a	299 °C	328 °C	~413 °C	~64%	37%
2e	282 °C	322 °C	~388 °C	~77%	54%
1e	221 °C	295 °C	~321 °C	~86%	60%

(a) Determined from values at global minimum of first derivative curve. (b) Remaining weight % at 600 °C.

Air atmosphere: Thermal gravimetric analysis was performed on cured samples of **B-a** and **2e** under a flow rate of 25 mL/min of air as described above for nitrogen atmosphere. The remaining weight % at a given time was given by mass (mg)/initial mass(mg)*100 and was plotted vs temperature (**Figures S52-S54**). $T_{5\%}$ and $T_{10\%}$ values are summarized in **Table S3**. The first derivative curve was generated in Microsoft Excel by calculating the slope at a data point as described for N_2 atmosphere analyses. The temperature of the maximum rate of weight loss, T_{peak}, was estimated at the absolute minimum of the first derivative curve, and the weight % remaining at this temperature was noted.

Table S3. Summarized thermal stability data for cured **B-a** and **2e** in air.

Sample	$T_{5\%\ mass\ loss}$	$T_{10\%\ mass\ loss}$	T_{peak}[a]	Weight % at T_{peak}[a]	Residue (600 °C)[b]
B-a	326 °C	366 °C	~549 °C	~18%	0%
2e	280 °C	325 °C	~540 °C	~24%	0%

(a) Determined from values at global minimum of first derivative curve. (b) Remaining weight % at 600 °C.

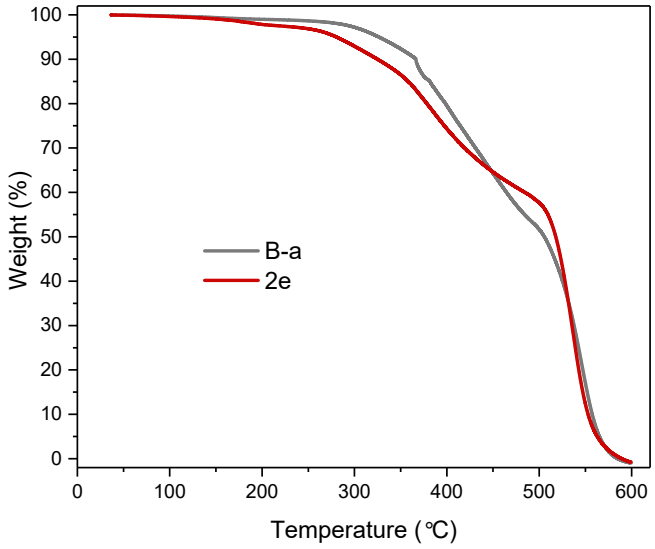

Figure S52. Thermal gravimetric analysis of cured **B-a** and **2e** in air up to 600 °C.

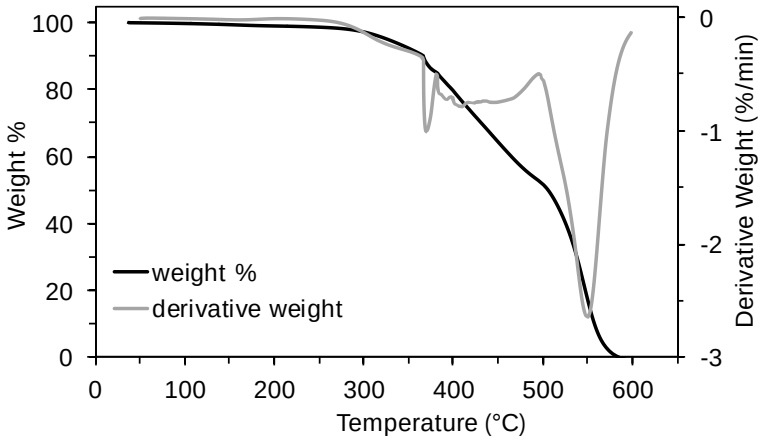

Figure S53. Thermal gravimetric analysis of **B-a** with overlaid 1st derivative curve in air up to 600 °C.

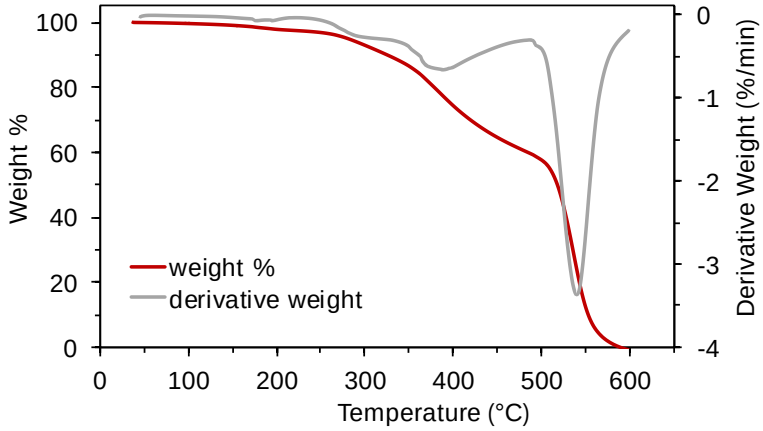

Figure S54. Thermal gravimetric analysis of **2e** with overlaid 1st derivative curve in air up to 600 °C.

10. Selected monomer curing behavior assessed by differential scanning calorimetry

Differential scanning calorimetry (DSC) measurements were performed with heating/cooling rates of 10 °C/minute in a vented aluminum pan to study the curing behavior, and in some cases the glass transition temperature of selected benzoxazine monomers. Typical curing programs of two cycles of heating and cooling from -20 °C to 295 °C were performed, except for main-chain derivatives for which the temperature range was extended to -90 °C. In some cases, a sharp endotherm was observed in the first heating cycle thermogram and was reported as the melting point (T_m). A curing exotherm typical for thermally accelerated ring-opening polymerization of benzoxazines was also observed in the first heating cycles, and the temperature of the peak apex was reported (T_{max}). When a glass transition was observed in the second heating cycle the midpoint temperature (T_g) of this transition was reported. Thermograms for selected benzoxazine monomers, and main-chain polybenzoxazines are presented in **Figures S55-S72**.

Supplementary Discussion:
Benzoxazine monomers and main-chain polybenzoxazines containing deprotected catechols exhibited complex curing behaviors characterized by broad curing exotherm peaks with multiple shoulders and local maxima. Furthermore, curing onset typically occurred at lower temperatures than for the corresponding TBS-protected derivatives, often coinciding or overlapping with monomer softening and melting. In contrast, TBS-protected derivatives exhibit well-separated melting (endothermic) and curing (exothermic) peaks. This complex curing behavior of catechol-modified monomers is likely a result of the catechol acting as both a catalyst (due to the presence of acidic protons) and a nucleophilic initiator (with unsubstituted *ortho* positions on the catechol ring).[12] Indeed, heating **B-a** with 1 equivalent of 4-methylcatechol **4** also results in a complex curing behavior beginning at a lower temperature compared to **B-a** alone.

Monomers **2b**, **2c**, and **2d** derived from 3,4-dihydroxybenzylamine exhibited particularly complex curing behaviors, and inspection of the samples after two heating cycles revealed that the samples had foamed during curing. This behavior is possibly the result of trapped solvent, or other degradation processes leading to the formation of volatiles. Attempts to dry **2b** at 70 °C under high vacuum resulted in partial degradation of the benzoxazine ring, assessed by ^{1}H-NMR (data not shown), and a darkening of the sample. We do not advise elevated temperature storage or drying of these derivatives. Furthermore, the curing behavior of these monomers may be further complicated by fragmentation reactions occurring by 1,6-elimination processes of the 4-hydroxybenzylamine moiety. Further studies beyond the scope of this report are required to fully understand the low curing onset temperature and complex curing mechanism of structurally related derivatives **2b**-**2d**.

Table S4. Summarized T_m, T_{max}, and T_g data for curing behavior assessed by DSC.

Sample	T_m (°C)	T_{max} (°C)	T_g (°C)
1a	83	276	85
1e	58	267	--
1e (hot pressed)	--	--	149
1e-Me	60	257	--
2a	--	164	172
2b	--	140	118
2c	--	~190 (complex)	--
2d	67	162	67
2e	181	196	208
2e (hot pressed)	--	--	183
2f	30 (softening)	197	193
2e-Me	59	225	-- (broad)
2e-Me$_2$	56	240	157
3a-TBS	--	224	35 (13 in first cycle)
3a	--	176	58 (30 in first cycle)
3b-TBS	--	261	-62 (-54 in first cycle)
3b	--	195	-62 (-54 first cycle)
B-a	47	215	141
B-a (hot pressed)	--	--	147
B-a+**2e** (1:1)	40 (B-a) and 162 (2e)	197	175
B-a+**4** (1:1)	66 (onset 36)	153	111

-- indicates not observed, or not determined due to peak complexity.

Curing thermograms for selected monomers and main-chain polybenzoxazine derivatives:

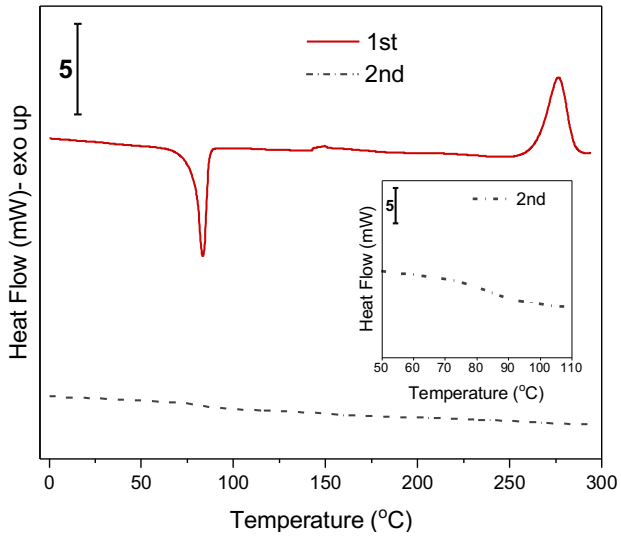

Figure S55. 1a heating cycles. T_m = 83 °C, T_{max} = 276 °C, broad T_g centered at 85 °C (inset) in second cycle.

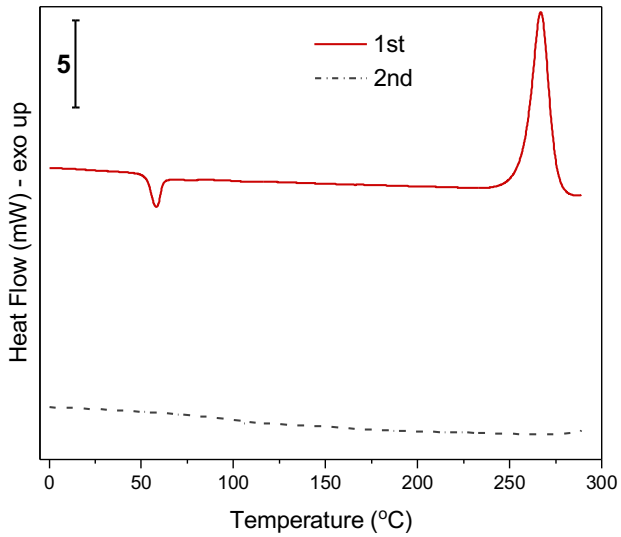

Figure S56. 1e heating cycles. T_m = 58 °C, T_{max} = 267 °C, T_g not apparent.

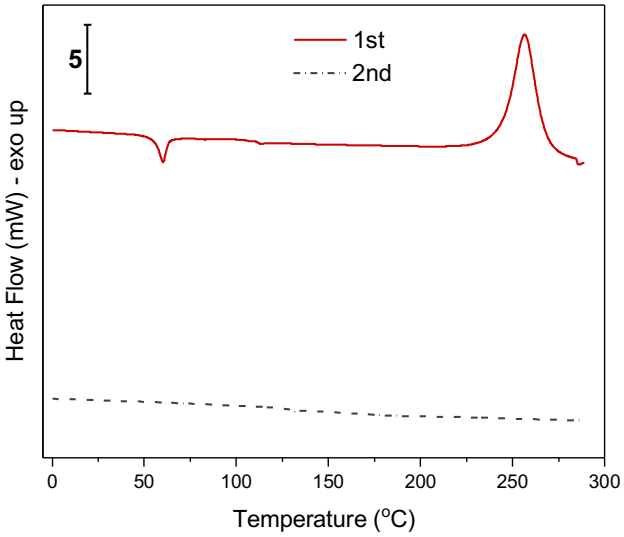

Figure S57. 1e–Me heating cycles. T_m = 60 °C, T_{max} = 257 °C, T_g not apparent.

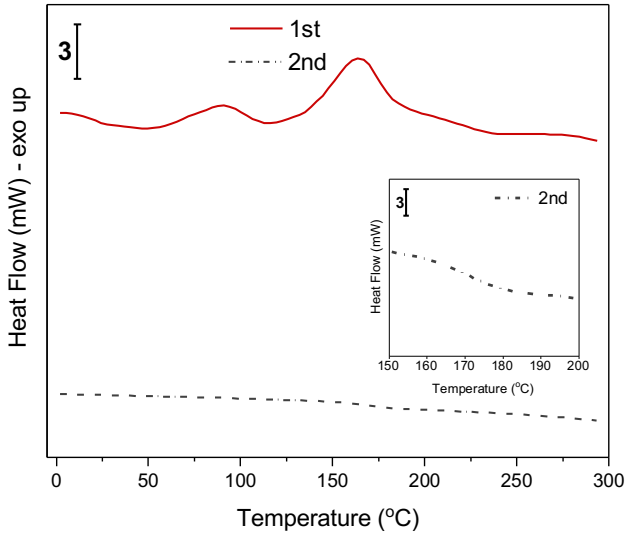

Figure S58. 2a heating cycles. T_{max} = 164 °C, an earlier exotherm is observed at 91 °C (onset 49 °C), T_g centered at 172 °C (inset) in second cycle.

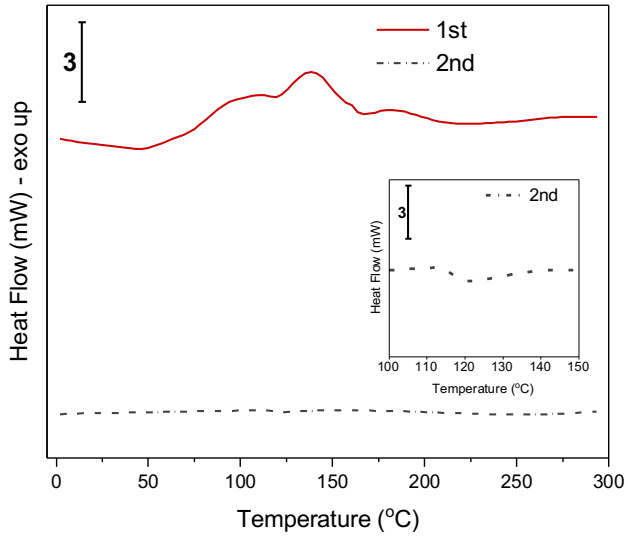

Figure S59. 2b heating cycles. T_{max} = 140 °C (onset 47 °C), weak T_g centered at 118 °C (inset) in second cycle.

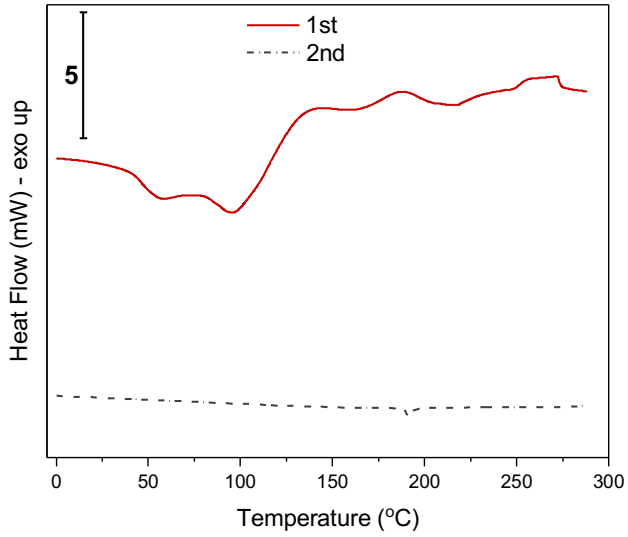

Figure S60. 2c heating cycles. This material foams extensively during curing, complicating thermogram analysis. No T_g is apparent in second cycle, minor endotherm at 190 °C.

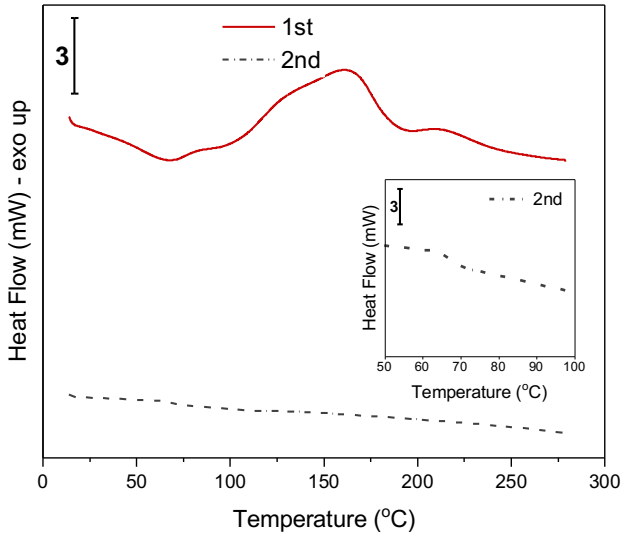

Figure S61. 2d heating cycles. Broad T_m = 67 °C, T_{max} = 162 °C, weak T_g centered at 67 °C (inset) in second cycle.

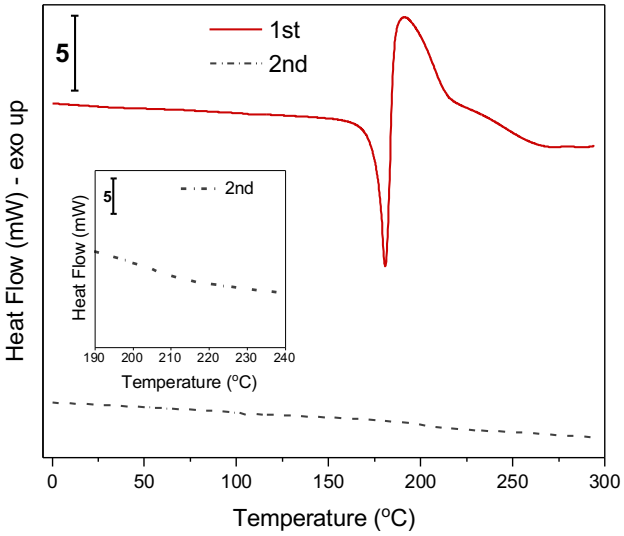

Figure S62. 2e heating cycles. T_m = 181 °C, T_{max} = 196 °C, weak T_g centered at 208 °C (inset) in second cycle.

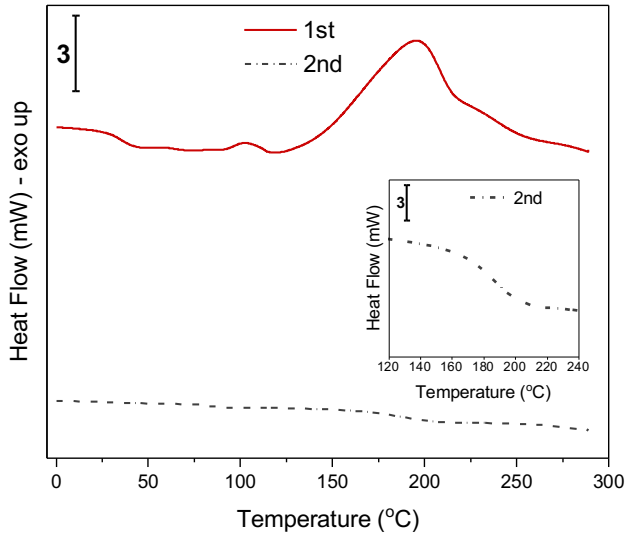

Figure S63. 2f heating cycles. Broad softening observed at 30 °C (onset), T_{max} = 197 °C, T_g centered at 193 °C (inset) in second cycle.

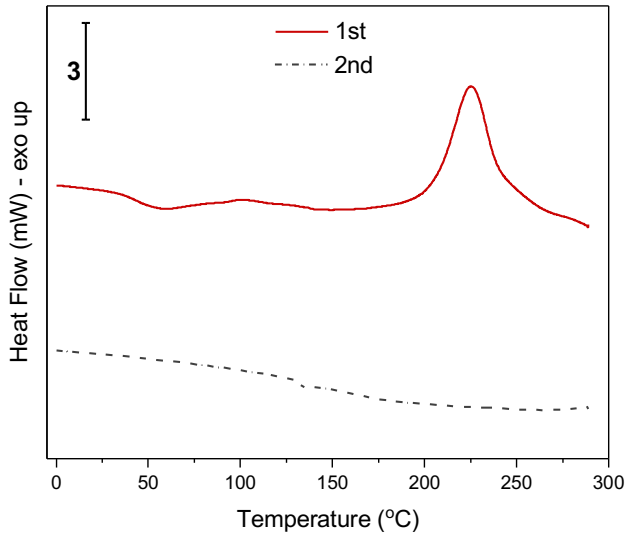

Figure S64. 2e-Me heating cycles. Broad softening/melting centered at 59 °C, T_{max} = 225 °C, Very broad, unclear T_g in second cycle.

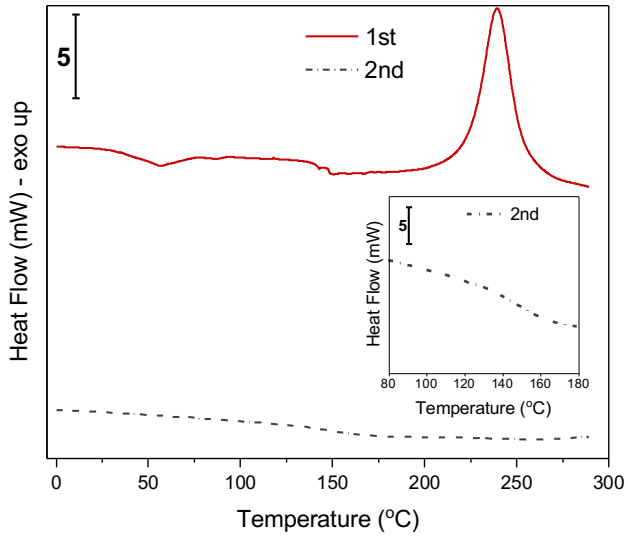

Figure S65. 2e-Me$_2$ heating cycles. Broad melting observed at 56 °C, T_{max} = 240 °C, broad T_g centered at 157 °C (inset) in second cycle.

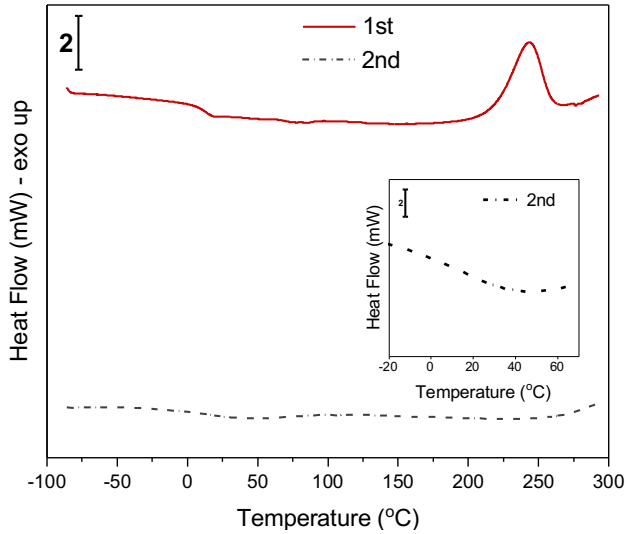

Figure S66. 3a-TBS heating cycles. $T_{g–1st\ cycle}$ = 13 °C, T_{max} = 244 °C, broad T_g centered at 35 °C (inset) in second cycle.

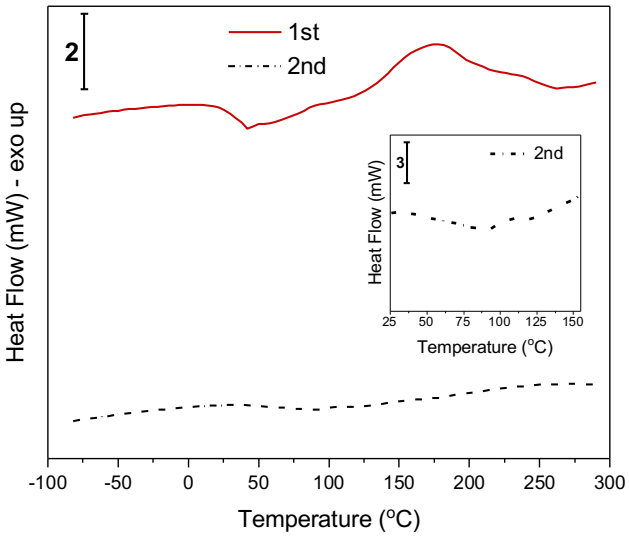

Figure S67. 3a heating cycles. $T_{g–1st\ cycle}$ centered at 30 °C, T_{max} = 176 °C, broad T_g centered at 58 °C (inset) in second cycle.

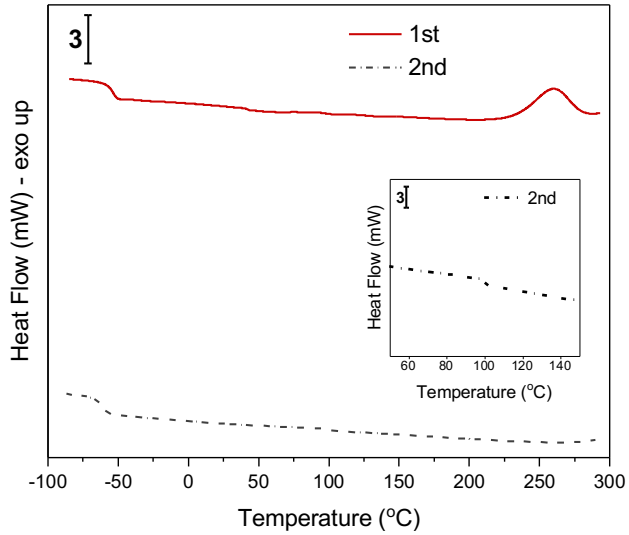

Figure S68. 3b-TBS heating cycles. $T_{g–1st\ cycle}$ centered at -54 °C, T_{max} = 261 °C, $T_{g–2nd\ cycle}$ centered at -62 °C and a second weak apparent T_g centered at 101 °C (inset) in second cycle.

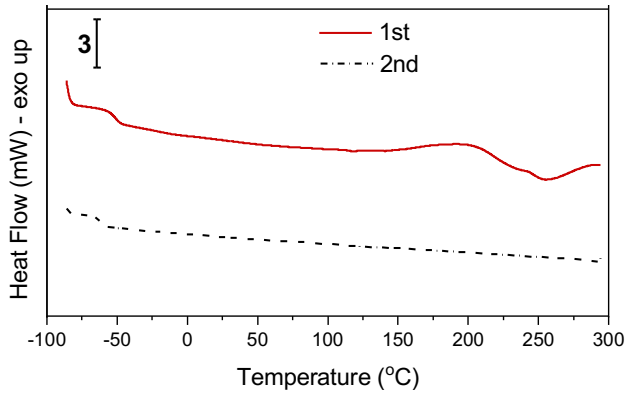

Figure S69. 3b heating cycles. $T_{g–1st\ cycle}$ centered at -54 °C, broad curing exotherm with T_{max} at 195 °C, $T_{g–2nd\ cycle}$ centered at -62 °C in second cycle.

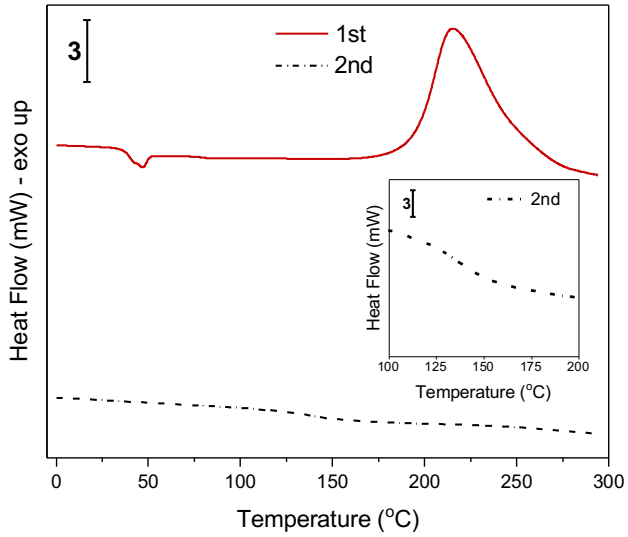

Figure S70. B-a (as received from Huntsman) heating cycles. T_m = 47 °C, T_{max} = 215 °C, T_g centered at 141 °C (inset) in second cycle.

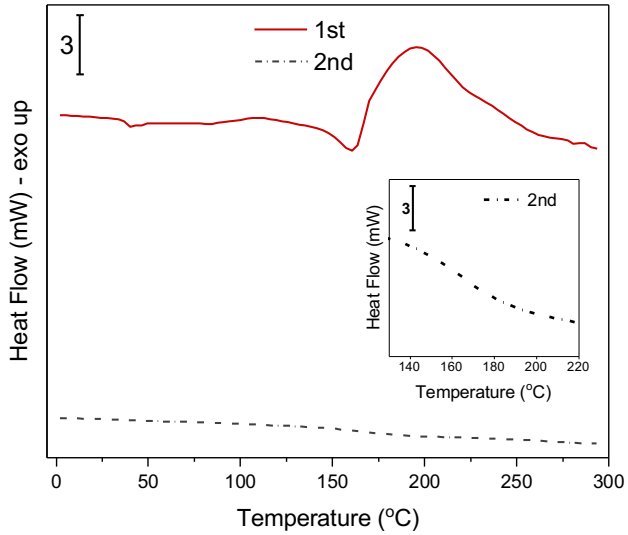

Figure S71. B-a+2e (1:1) heating cycles. Broad melting peaks observed for both components, T_{m1} = 40 °C, T_{m2} = 162 °C, T_{max} = 197 °C, broad T_g centered at 175 °C (inset) in second cycle.

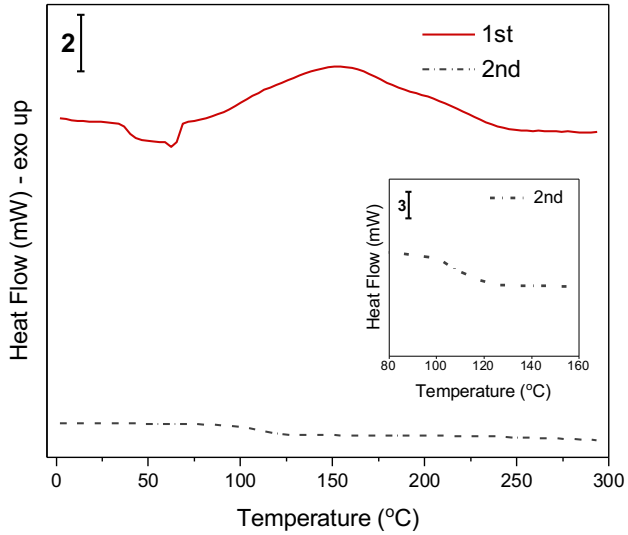

Figure S72. B-a+4 (1:1) heating cycles. Broad melting observed, T_m = 66 °C (onset 36 °C), broad curing exotherm with T_{max} = 153 °C (onset 82 °C), T_g centered at 111 °C (inset) in second cycle.

11. References

[1] G. Malik, A. Natangelo, J. Charris, L. Pouységu, S. Manfredini, D. Cavagnat, T. Buffeteau, D. Deffieux, S. Quideau, *Chemistry – A European Journal* **2012**, *18*, 9063.

[2] M. Ikeuchi, M. Ikeuchi, K. Inoue, S. Yamamoto, A. Yamauchi, M. Kihara, *Heterocycles* **2005**, *65*, 2925.

[3] C. Sawaryn, K. Landfester, A. Taden, *Polymer* **2011**, *52*, 3277.

[4] ASTM, D1002–10 Standard Test Method for Apparent Shear Strength of Single-Lap-Joint Adhesively Bonded Metal Specimens by Tension Loading (Metal-to-Metal), **2010**.

[5] N. Saleema, D. K. Sarkar, R. W. Paynter, D. Gallant, M. Eskandarian, *Applied Surface Science* **2012**, *261*, 742.

[6] A. D. Cort, *Synthetic Communications* **1990**, *20*, 757.

[7] ASTM, D790–17 Standard Test Method for Flexural Properties of Unreinforced and Reinforced Plastics and Electrical Insulating Materials by Four-Point Bending, **2017**.

[8] B. J. Briscoe, L. Fiori, E. Pelillo, *Journal of Physics D: Applied Physics* **1998**, *31*, 2395.

[9] G. M. Pharr, W. C. Oliver, F. R. Brotzen, *Journal of Materials Research* **1992**, *7*, 613.

[10] J. Zhou, K. Komvopoulos, *Journal of Applied Physics* **2006**, *100*, 114329.

[11] a) A. Sudo, R. Kudoh, H. Nakayama, K. Arima, T. Endo, *Macromolecules*, **2008**, *41*, 9030. b) L. Zhang, Z. Zhao, Z. Dai, L. Xu, F. Fu, T. Endo, X Liu *ACS Macro Letters*, **2019**, *8*, 506.

[12] a) G. Kaya, B. Kiskan, Y. Yagci, *Macromolecules* **2018**, *51*, 1688. b) I. Hamerton, L. T. McNamara, B. J. Howlin, P. A. Smith, P. Cross, S. Ward, *Macromolecules* **2013**, *46*, 5117.

12. NMR and ATR-FTIR Spectra

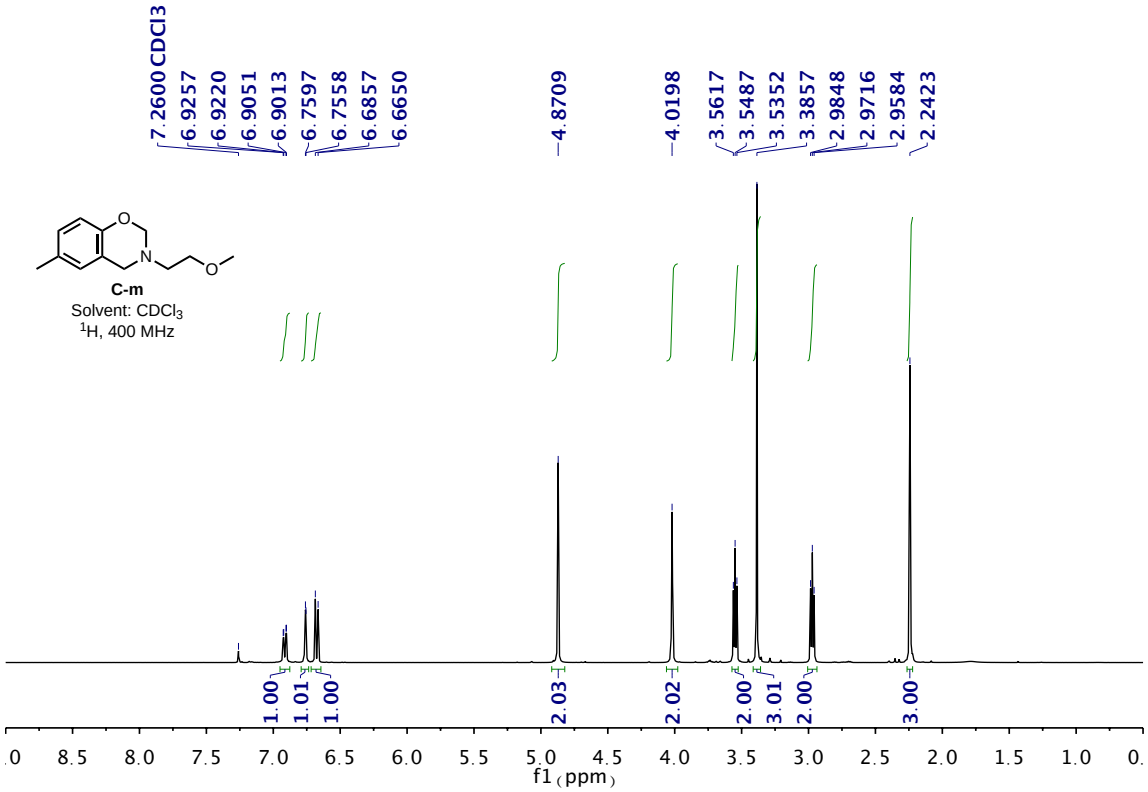

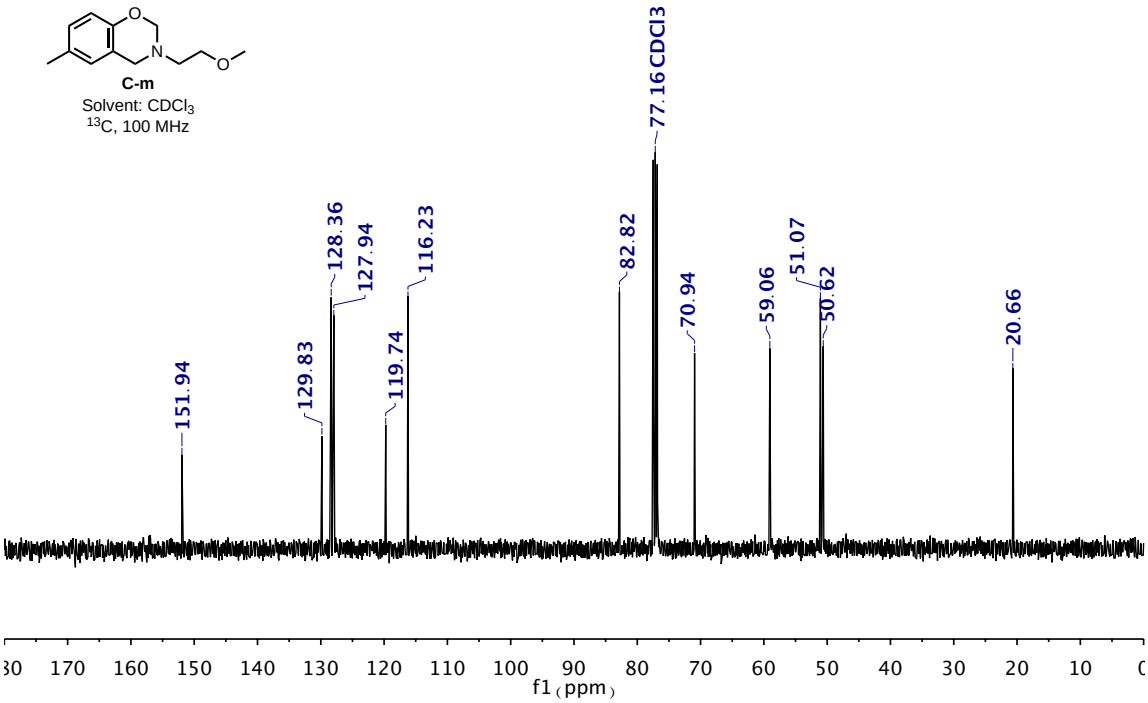

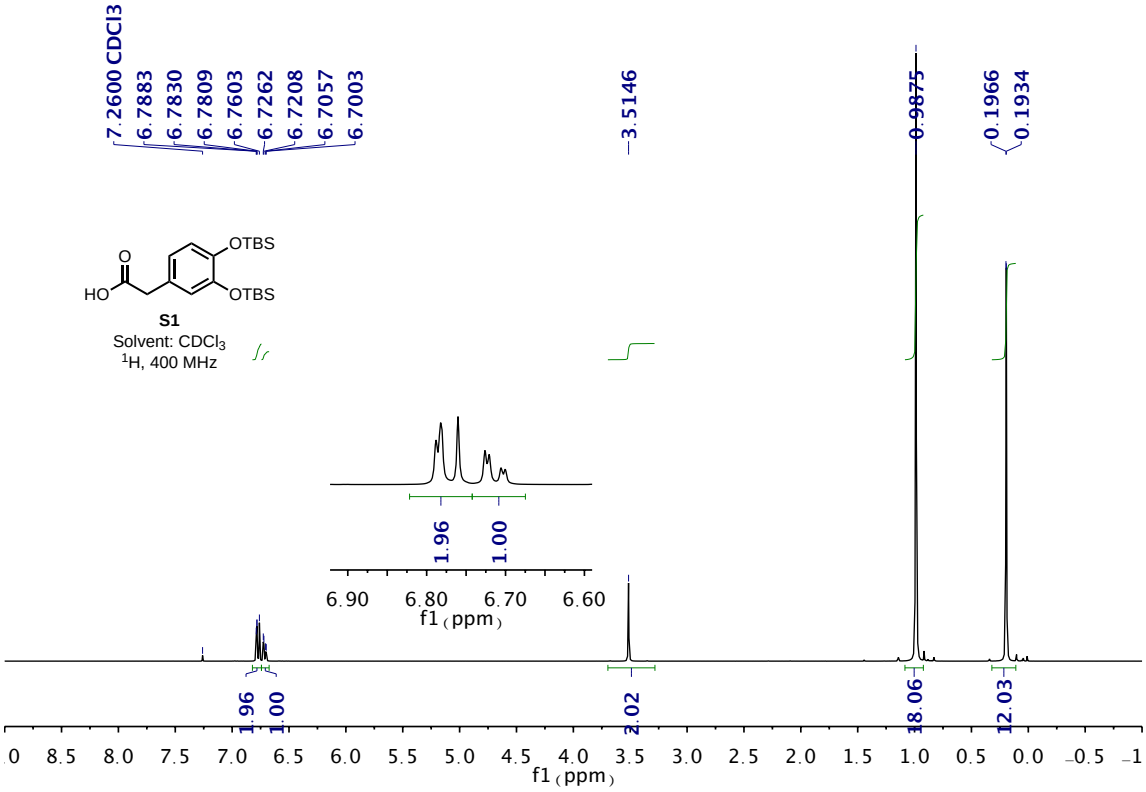
7.2600 CDCl3
6.7883
6.7830
6.7809
6.7603
6.7262
6.7208
6.7057
6.7003
3.5146
0.9875
0.1966
0.1934
OTBS
OTBS
HO
O
S1
Solvent: CDCl3
1H, 400 MHz
1.96
1.00
6.90
6.80
6.70
6.60
f1 (ppm)
1.96
1.00
2.02
18.06
12.03
f1 (ppm)

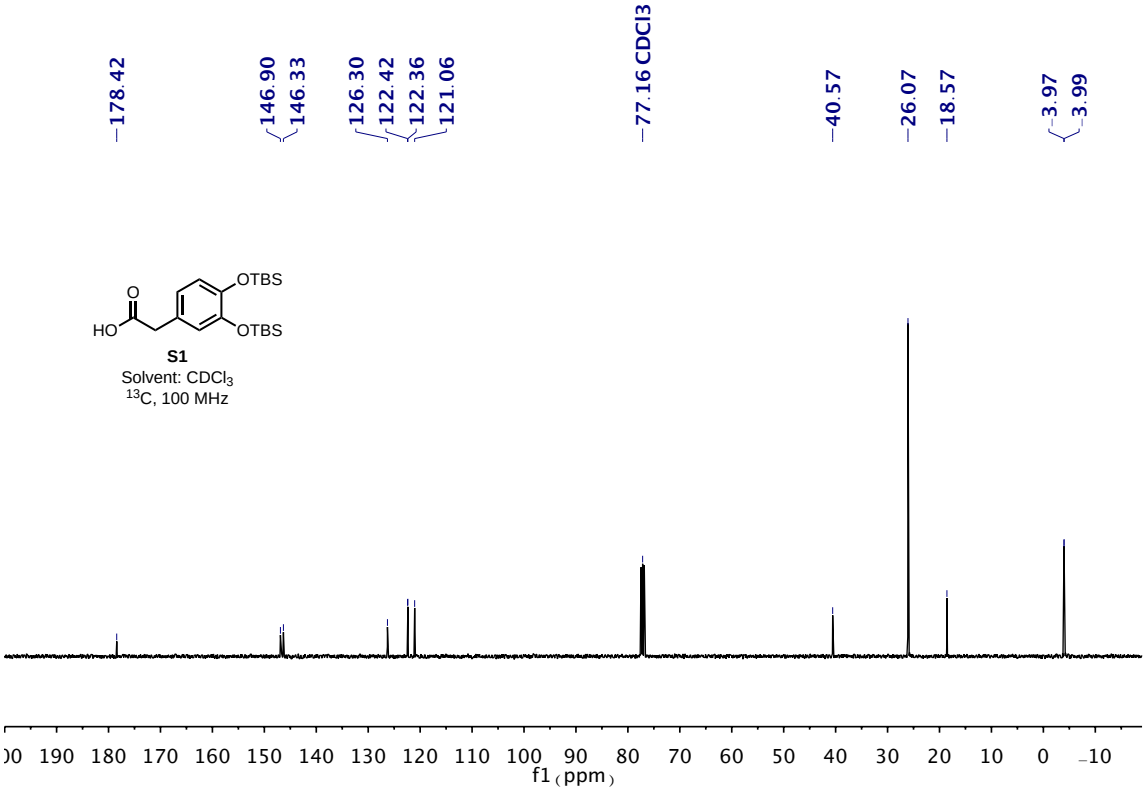
178.42
146.90
146.33
126.30
122.42
122.36
121.06
77.16 CDCl3
40.57
26.07
18.57
3.97
3.99
OTBS
OTBS
HO
O
S1
Solvent: CDCl3
13C, 100 MHz
f1 (ppm)

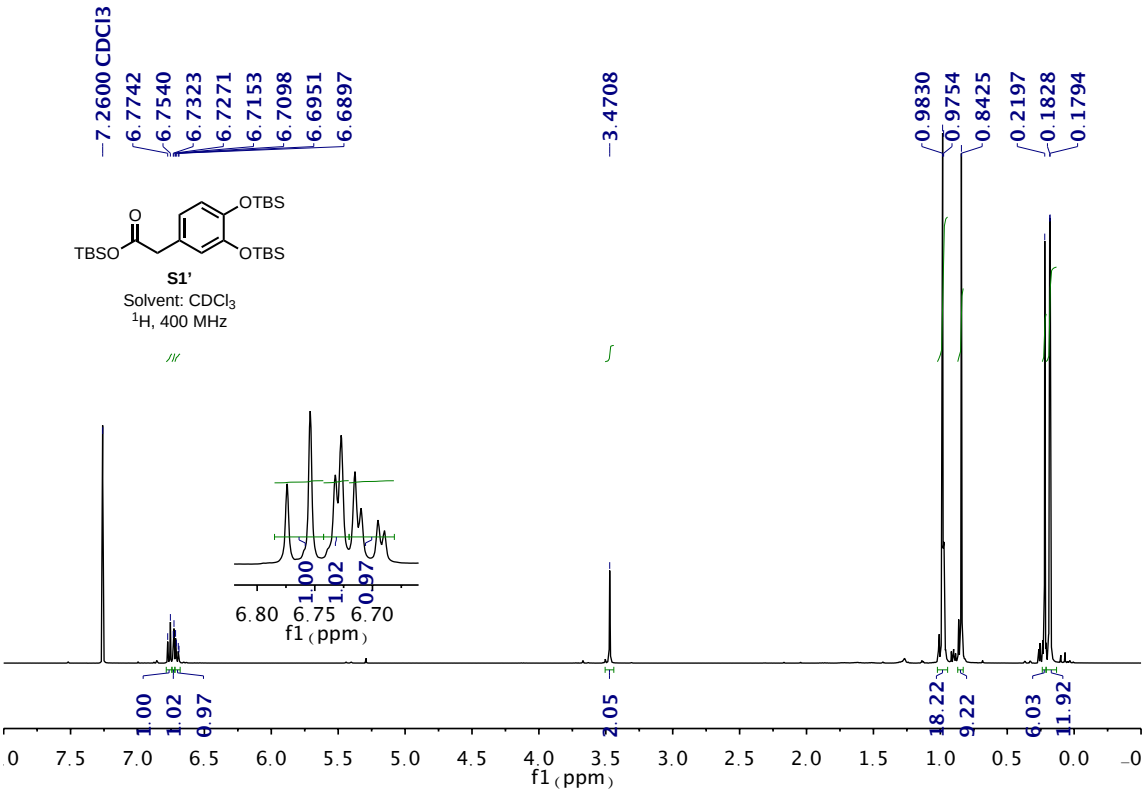
7.2600 CDCl3
6.7742
6.7540
6.7323
6.7271
6.7153
6.7098
6.6951
6.6897
3.4708
0.9830
0.9754
0.8425
0.2197
0.1828
0.1794
OTBS
TBSO
OTBS
S1'
Solvent: CDCl3
1H, 400 MHz
1.00
1.02
0.97
6.80 6.75 6.70
f1 (ppm)
1.00
1.02
0.97
2.05
18.22
9.22
6.03
11.92
f1 (ppm)

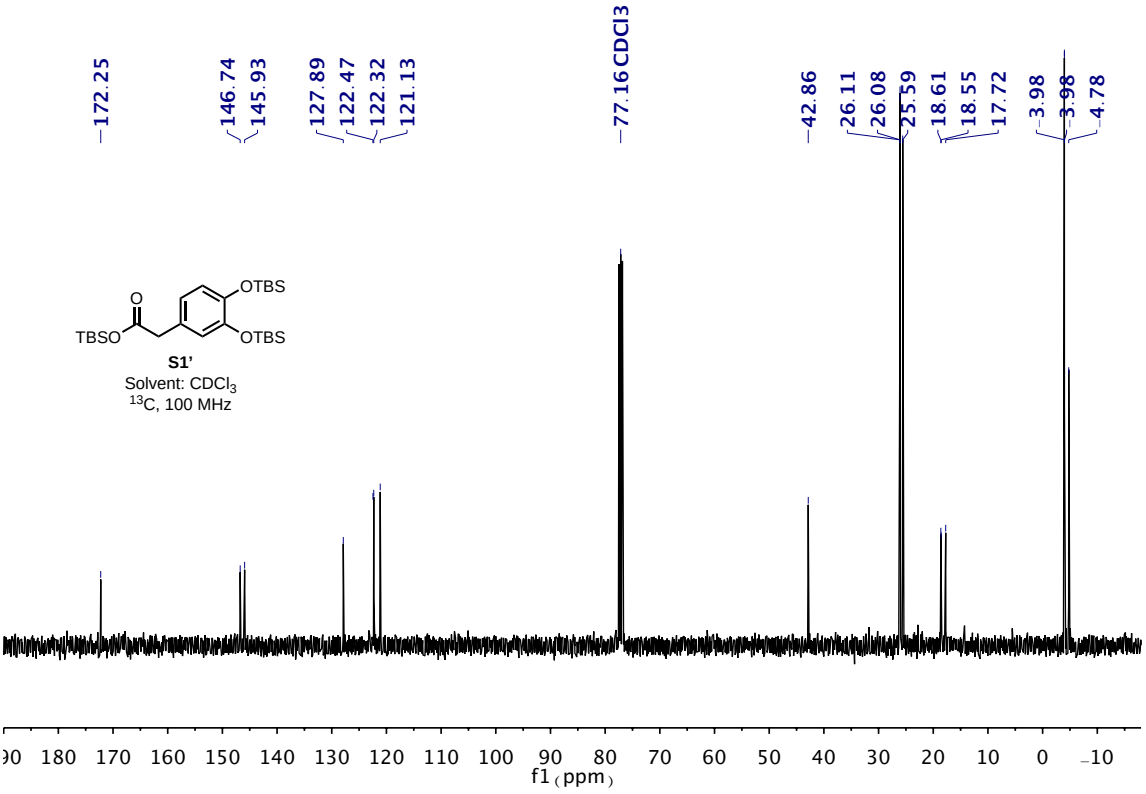
172.25
146.74
145.93
127.89
122.47
122.32
121.13
77.16 CDCl3
42.86
26.11
26.08
25.59
18.61
18.55
17.72
-3.98
-3.98
-4.78
OTBS
TBSO
OTBS
S1'
Solvent: CDCl3
13C, 100 MHz
f1 (ppm)

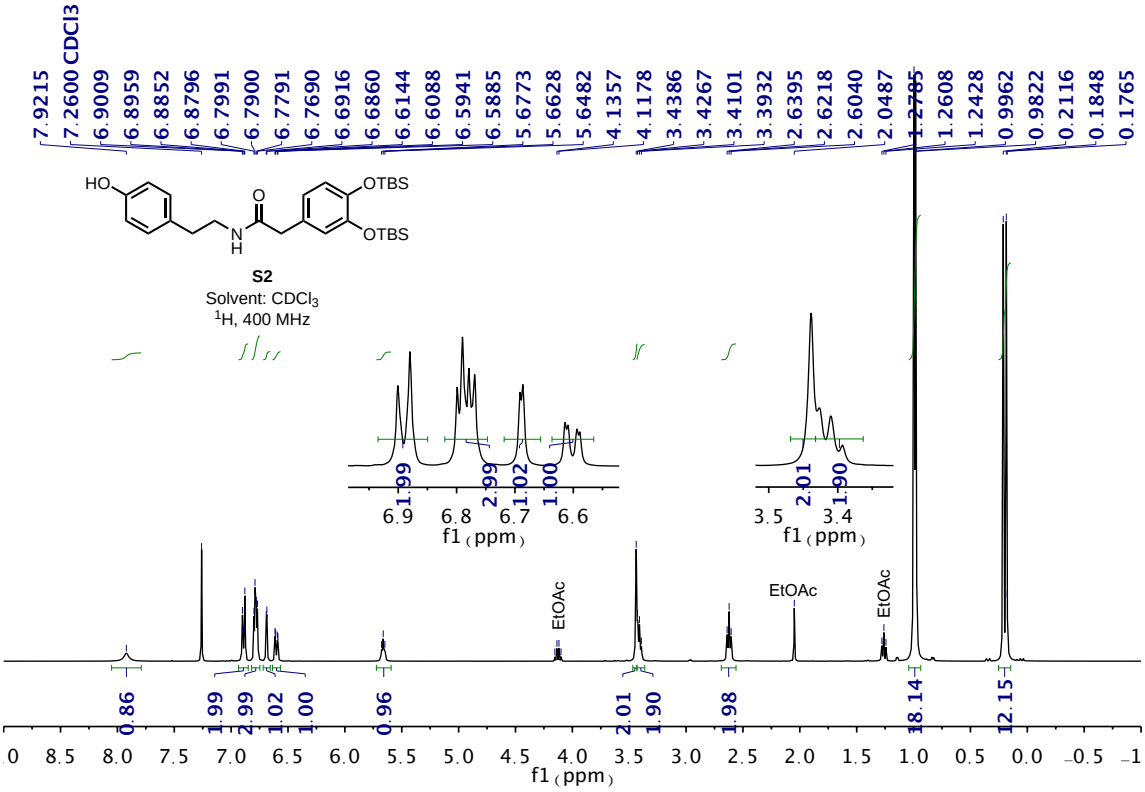
7.9215
7.2600 CDCl3
6.9009
6.8959
6.8852
6.8796
6.7991
6.7900
6.7791
6.7690
6.6916
6.6860
6.6144
6.6088
6.5941
6.5885
6.5773
6.5628
6.5482
4.1357
4.1178
3.4386
3.4267
3.4101
3.3932
2.6395
2.6218
2.6040
2.0487
1.2785
1.2608
1.2428
0.9962
0.9822
0.2116
0.1848
0.1765
HO
O
N
H
OTBS
OTBS
S2
Solvent: CDCl3
1H, 400 MHz
1.99
2.99
1.02
1.00
6.9
6.8
6.7
6.6
f1 (ppm)
2.01
1.90
3.5
3.4
f1 (ppm)
EtOAc
EtOAc
EtOAc
0.86
1.99
2.99
1.02
1.00
0.96
2.01
1.90
1.98
18.14
12.15
f1 (ppm)

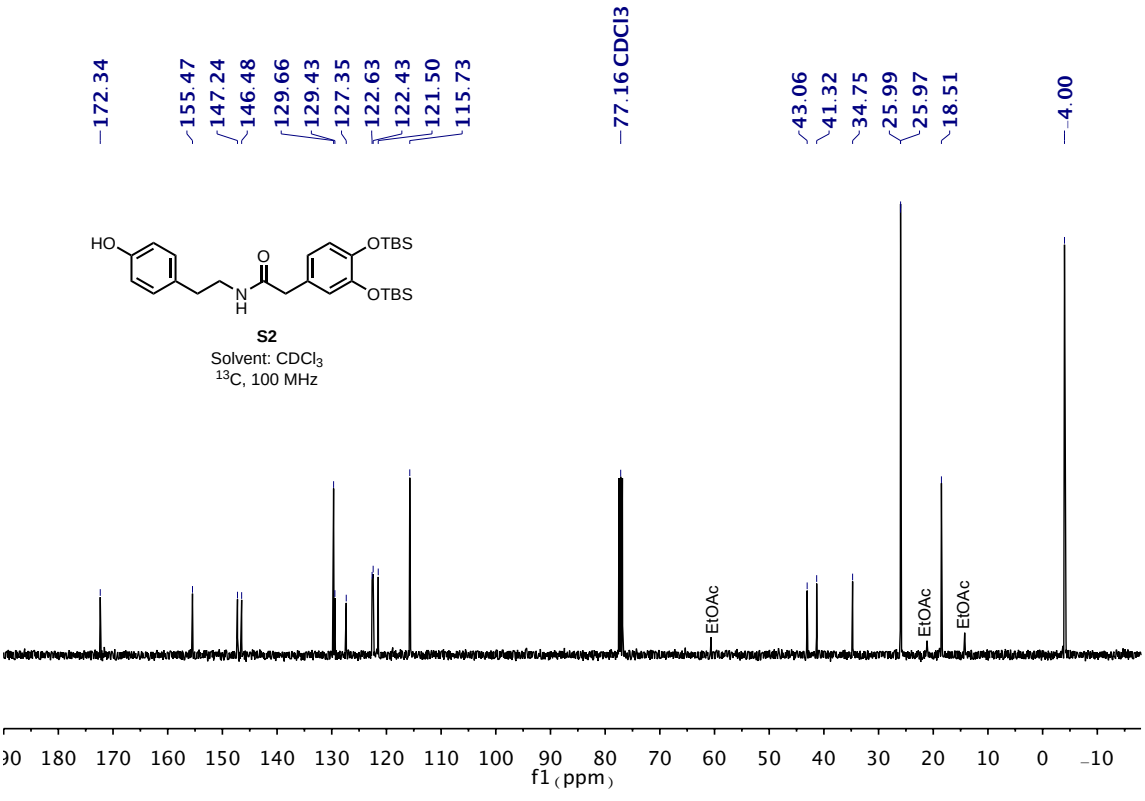
172.34
155.47
147.24
146.48
129.66
129.43
127.35
122.63
122.43
121.50
115.73
77.16 CDCl3
43.06
41.32
34.75
25.99
25.97
18.51
4.00
HO
O
N
H
OTBS
OTBS
S2
Solvent: CDCl3
13C, 100 MHz
EtOAc
EtOAc
EtOAc
f1 (ppm)

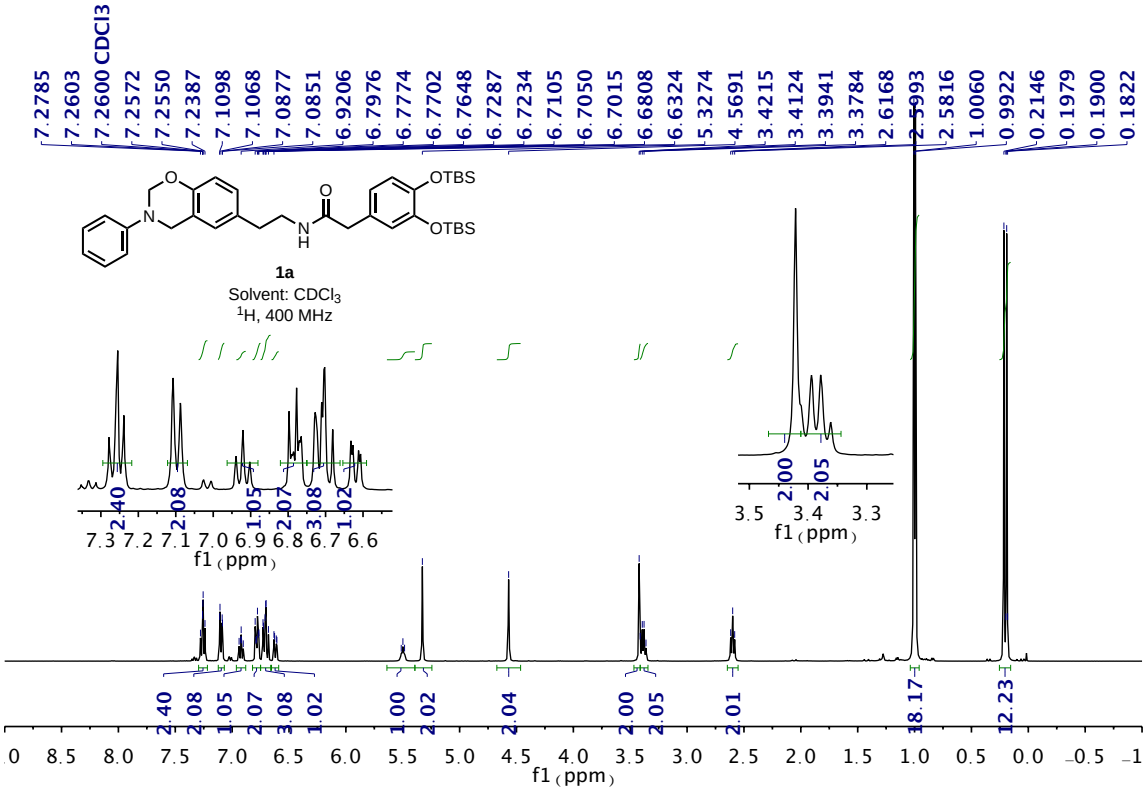
7.2785 7.2603 7.2600 CDCl3 7.2572 7.2550 7.2387 7.1098 7.1068 7.0877 7.0851 6.9206 6.7976 6.7774 6.7702 6.7648 6.7287 6.7234 6.7105 6.7050 6.7015 6.6808 6.6324 5.3274 4.5691 3.4215 3.4124 3.3941 3.3784 2.6168 2.5993 2.5816 1.0060 0.9922 0.2146 0.1979 0.1900 0.1822
OTBS
OTBS
1a
Solvent: CDCl3
1H, 400 MHz
2.40 2.08 1.05 2.07 3.08 1.02 1.00 2.02 2.04 2.00 2.05 2.01 18.17 12.23
f1 (ppm)

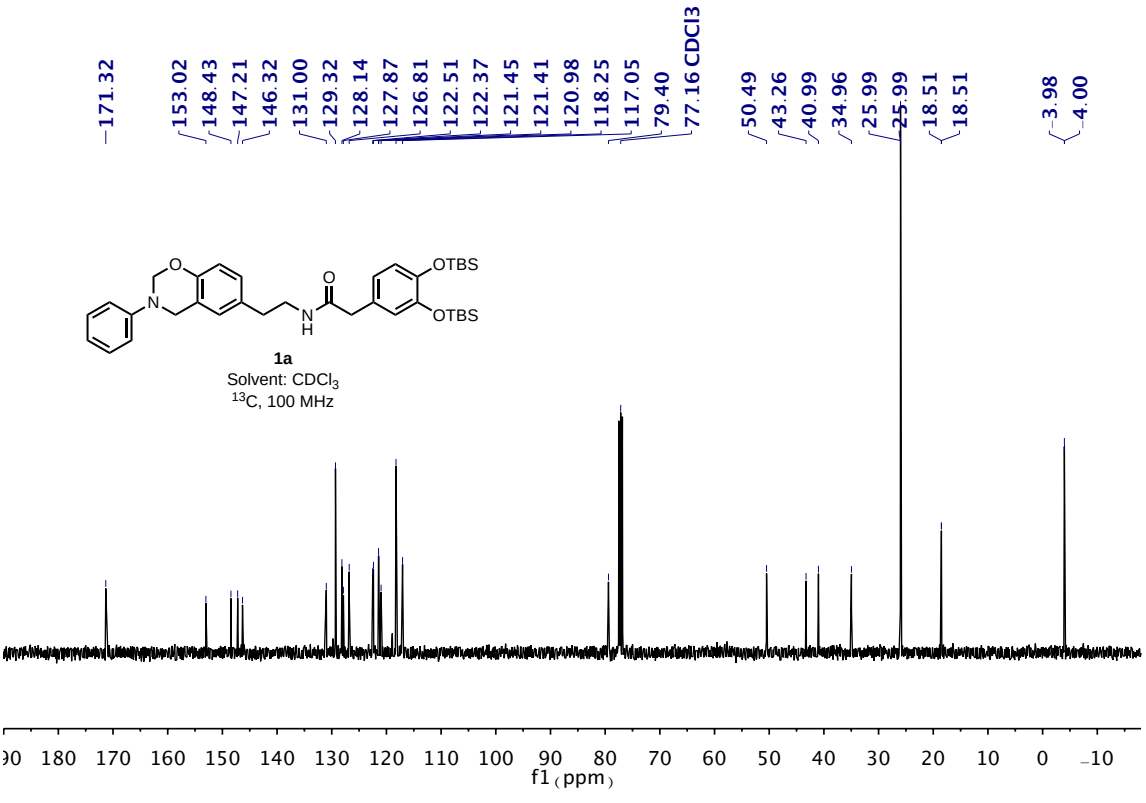
171.32 153.02 148.43 147.21 146.32 131.00 129.32 128.14 127.87 126.81 122.51 122.37 121.45 121.41 120.98 118.25 117.05 79.40 77.16 CDCl3 50.49 43.26 40.99 34.96 25.99 25.99 18.51 18.51 -3.98 -4.00
OTBS
OTBS
1a
Solvent: CDCl3
13C, 100 MHz
f1 (ppm)

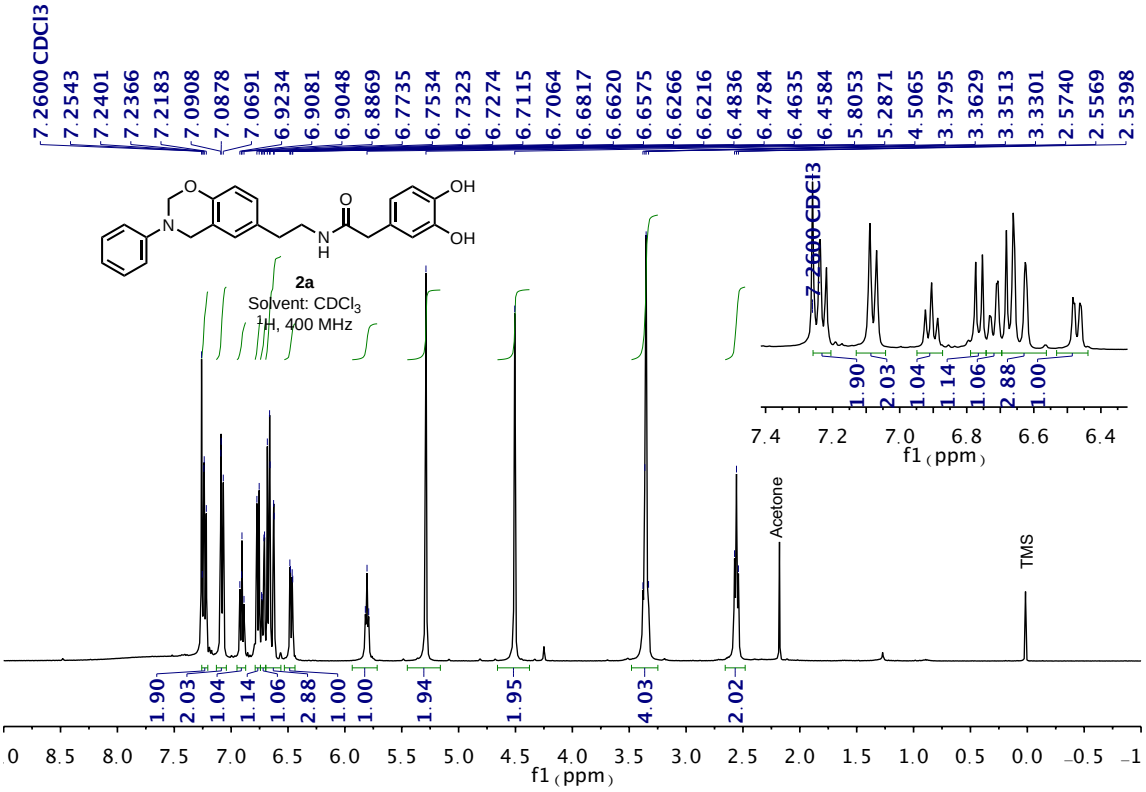
7.2600 CDCl3
7.2543
7.2401
7.2366
7.2183
7.0908
7.0878
7.0691
6.9234
6.9081
6.9048
6.8869
6.7735
6.7534
6.7323
6.7274
6.7115
6.7064
6.6817
6.6620
6.6575
6.6266
6.6216
6.4836
6.4784
6.4635
6.4584
5.8053
5.2871
4.5065
3.3795
3.3629
3.3513
3.3301
2.5740
2.5569
2.5398
OH
OH
O
N
H
2a
Solvent: CDCl3
1H, 400 MHz
Acetone
TMS
1.90
2.03
1.04
1.14
1.06
2.88
1.00
1.00
1.94
1.95
4.03
2.02
f1 (ppm)

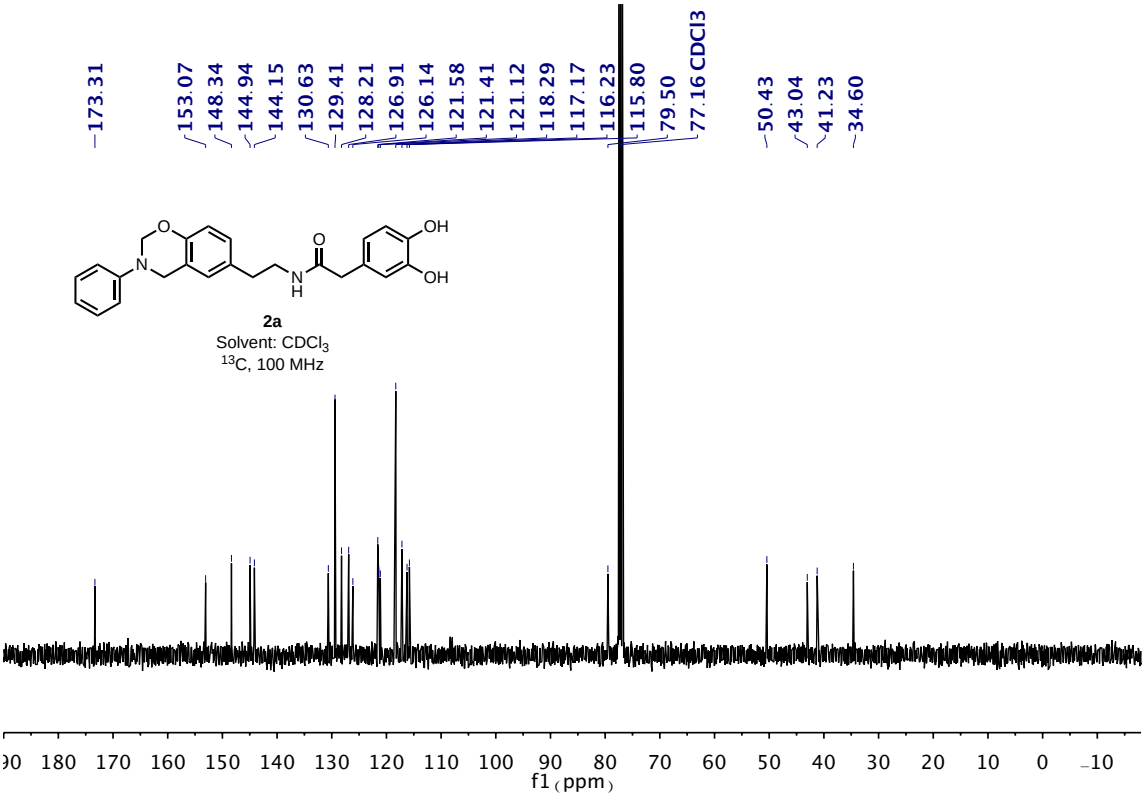
173.31
153.07
148.34
144.94
144.15
130.63
129.41
128.21
126.91
126.14
121.58
121.41
121.12
118.29
117.17
116.23
115.80
79.50
77.16 CDCl3
50.43
43.04
41.23
34.60
OH
OH
O
N
H
2a
Solvent: CDCl3
13C, 100 MHz
f1 (ppm)

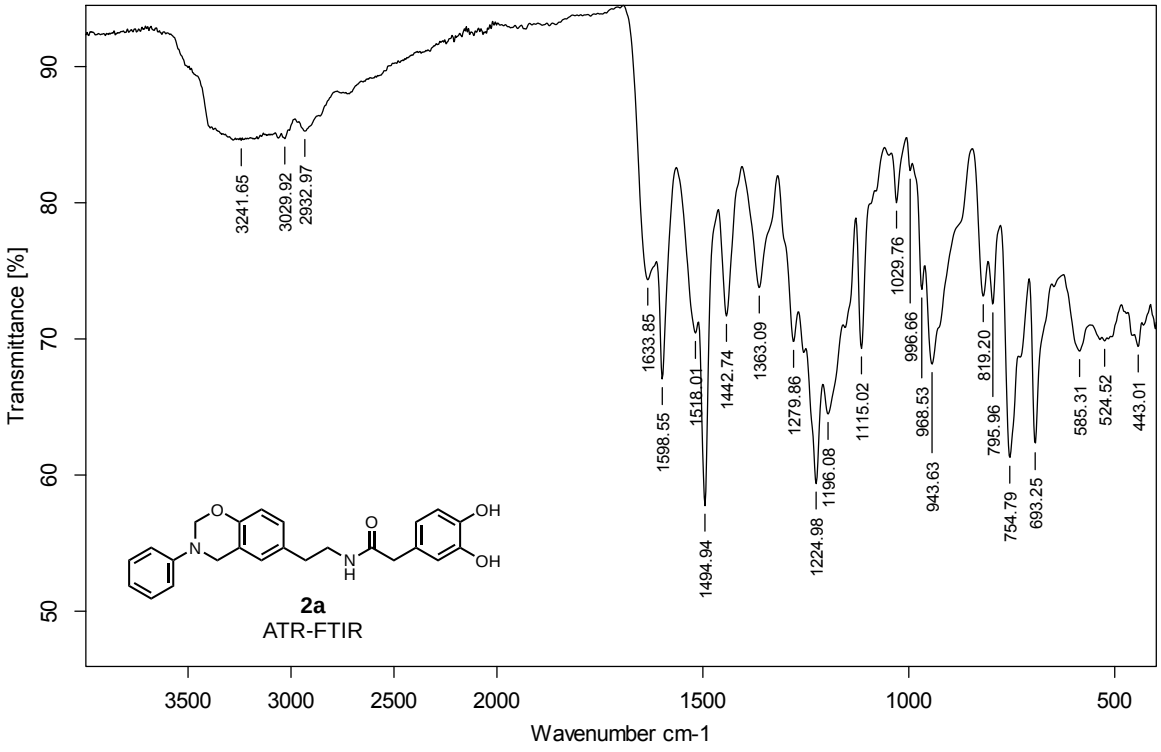
Transmittance [%]
Wavenumber cm-1
3241.65
3029.92
2932.97
1633.85
1598.55
1518.01
1494.94
1442.74
1363.09
1279.86
1224.98
1196.08
1115.02
1029.76
996.66
968.53
943.63
819.20
795.96
754.79
693.25
585.31
524.52
443.01
OH
OH
2a
ATR-FTIR

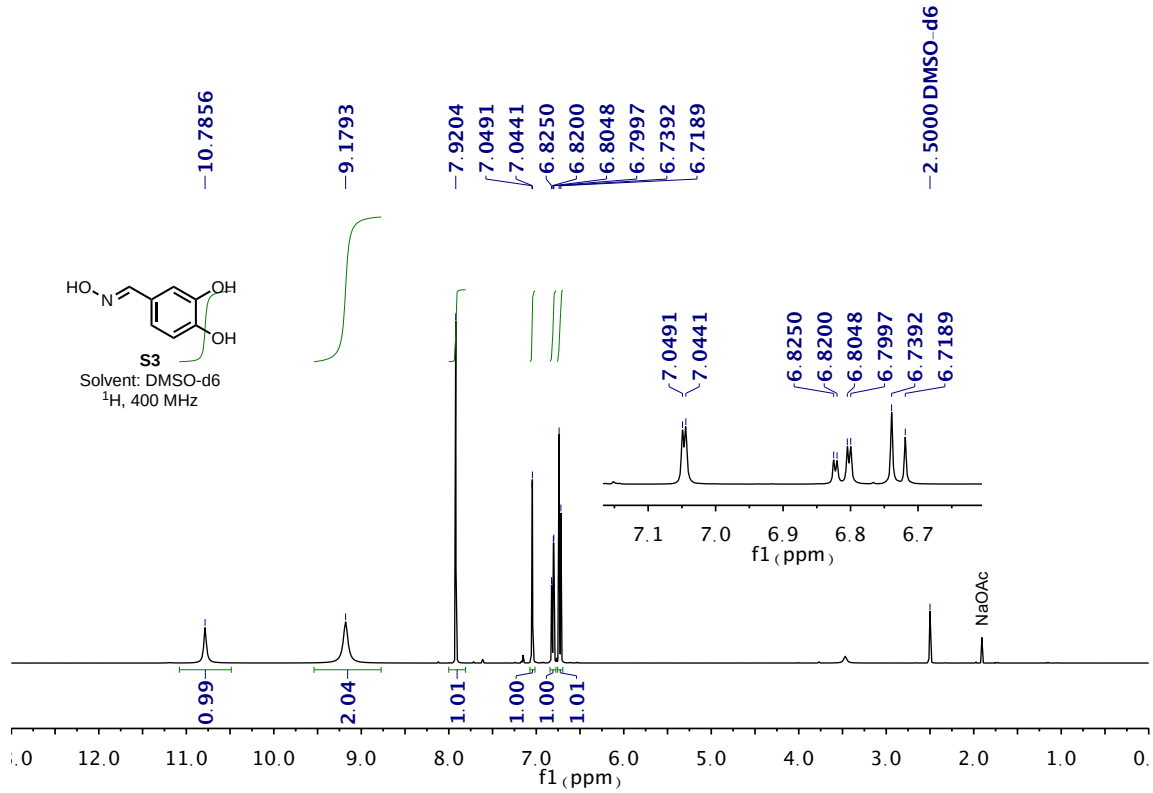
10.7856
9.1793
7.9204
7.0491
7.0441
6.8250
6.8200
6.8048
6.7997
6.7392
6.7189
2.5000 DMSO-d6
HO
OH
OH
S3
Solvent: DMSO-d6
1H, 400 MHz
NaOAc
0.99
2.04
1.01
1.00
1.00
1.01
f1 (ppm)

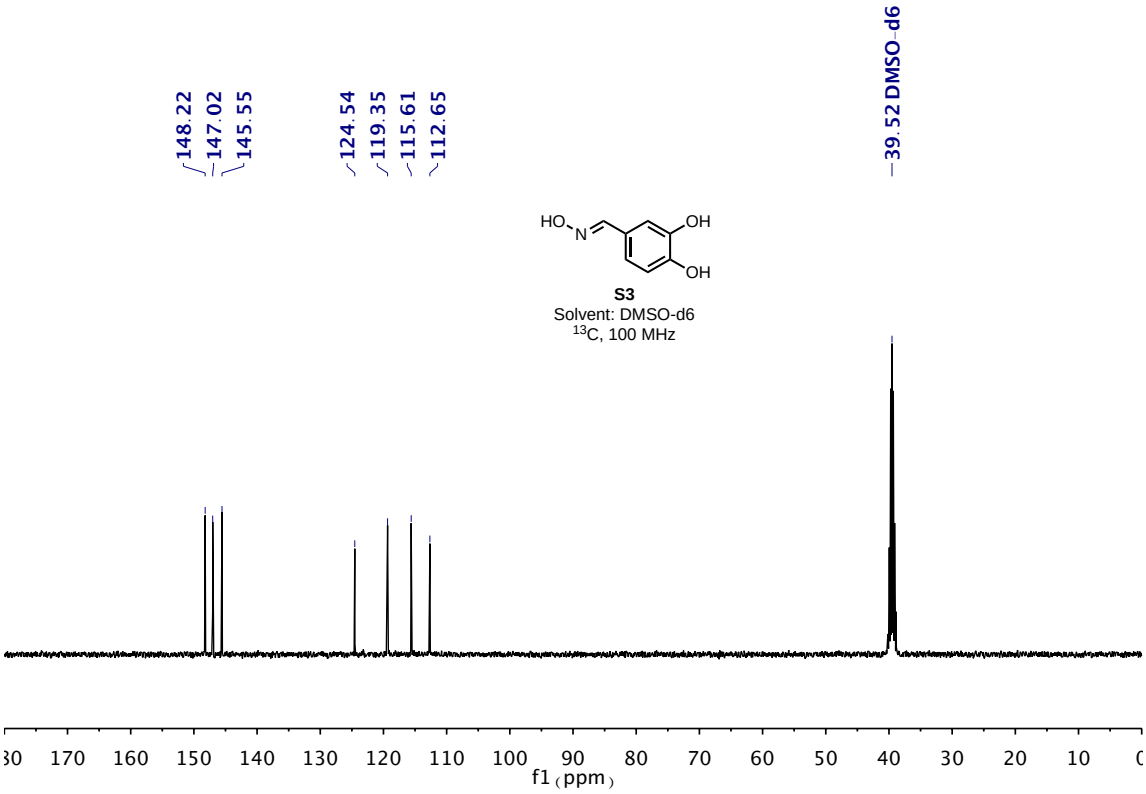
148.22
147.02
145.55
124.54
119.35
115.61
112.65
39.52 DMSO-d6
HO
N
OH
OH
S3
Solvent: DMSO-d6
13C, 100 MHz
f1 (ppm)

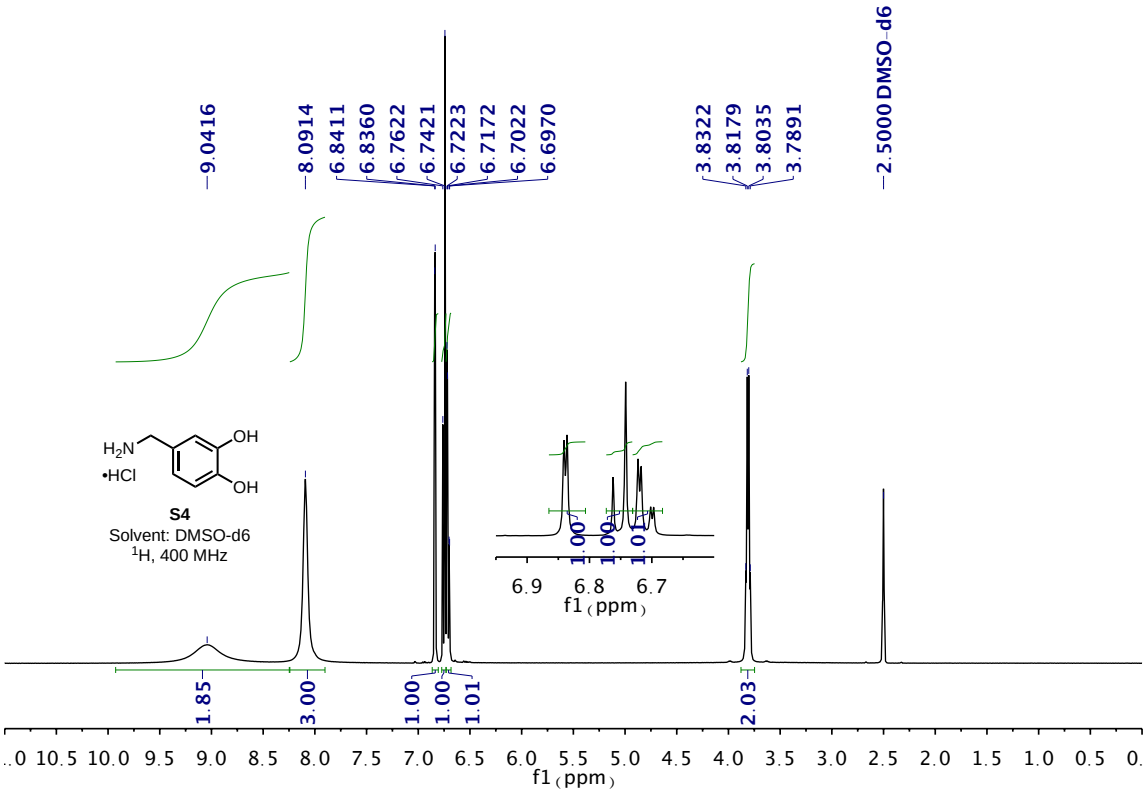
9.0416
8.0914
6.8411
6.8360
6.7622
6.7421
6.7223
6.7172
6.7022
6.6970
3.8322
3.8179
3.8035
3.7891
2.5000 DMSO-d6
H2N
•HCl
OH
OH
S4
Solvent: DMSO-d6
1H, 400 MHz
1.85
3.00
1.00
1.00
1.01
2.03
f1 (ppm)

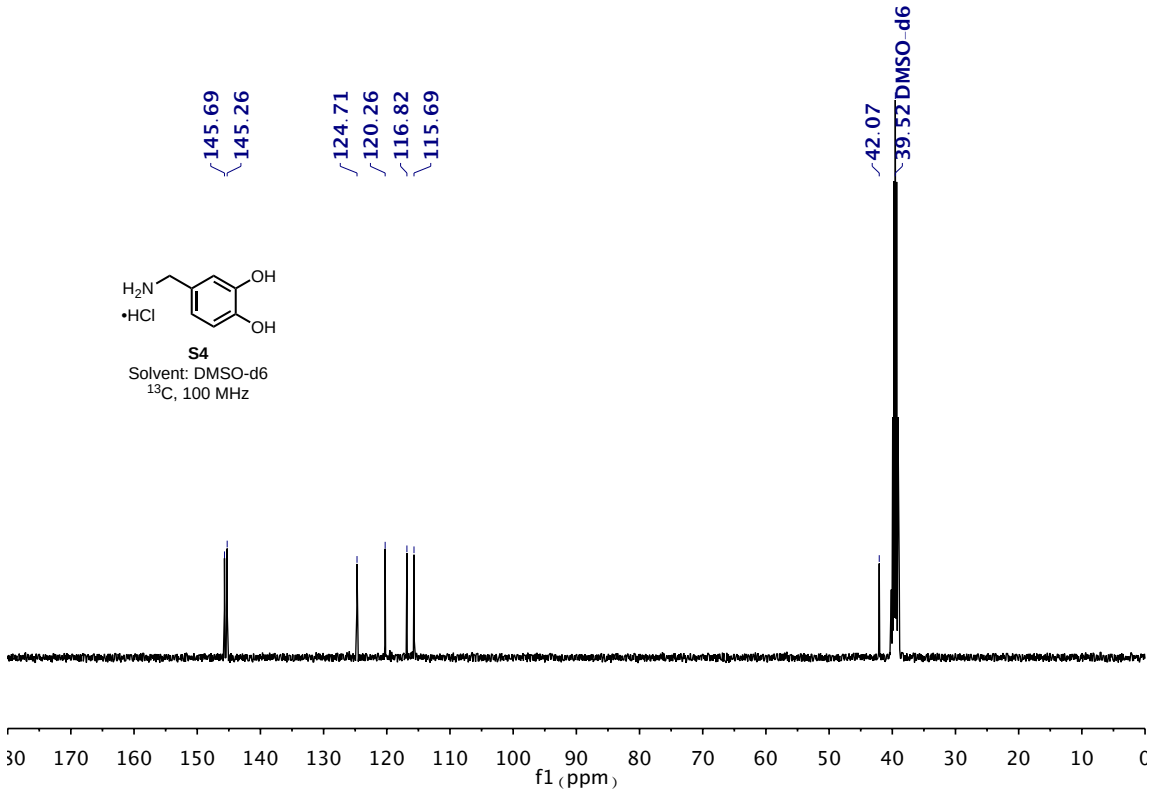
145.69
145.26
124.71
120.26
116.82
115.69
42.07
39.52 DMSO-d6
H2N
•HCl
OH
OH
S4
Solvent: DMSO-d6
13C, 100 MHz
f1 (ppm)

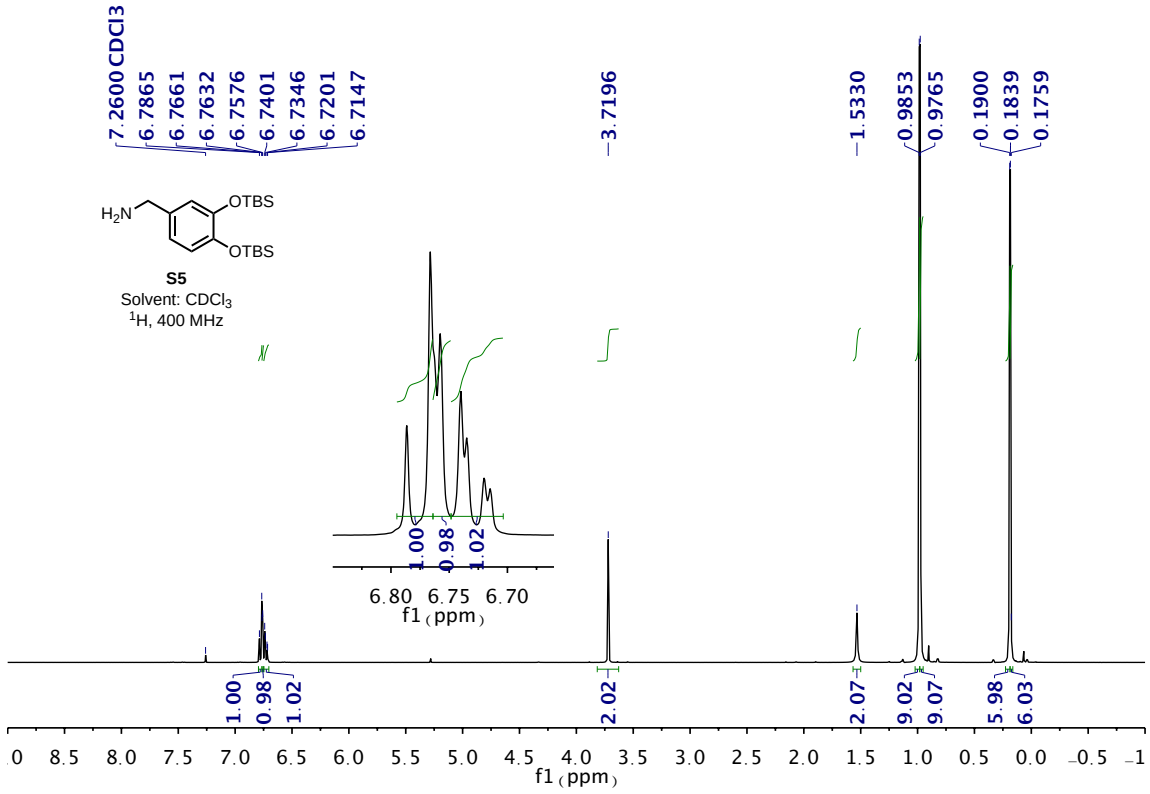
7.2600 CDCl3
6.7865
6.7661
6.7632
6.7576
6.7401
6.7346
6.7201
6.7147
3.7196
1.5330
0.9853
0.9765
0.1900
0.1839
0.1759
H2N
OTBS
OTBS
S5
Solvent: CDCl3
1H, 400 MHz
1.00
0.98
1.02
6.80 6.75 6.70
f1 (ppm)
1.00
0.98
1.02
2.02
2.07
9.02
9.07
5.98
6.03
f1 (ppm)

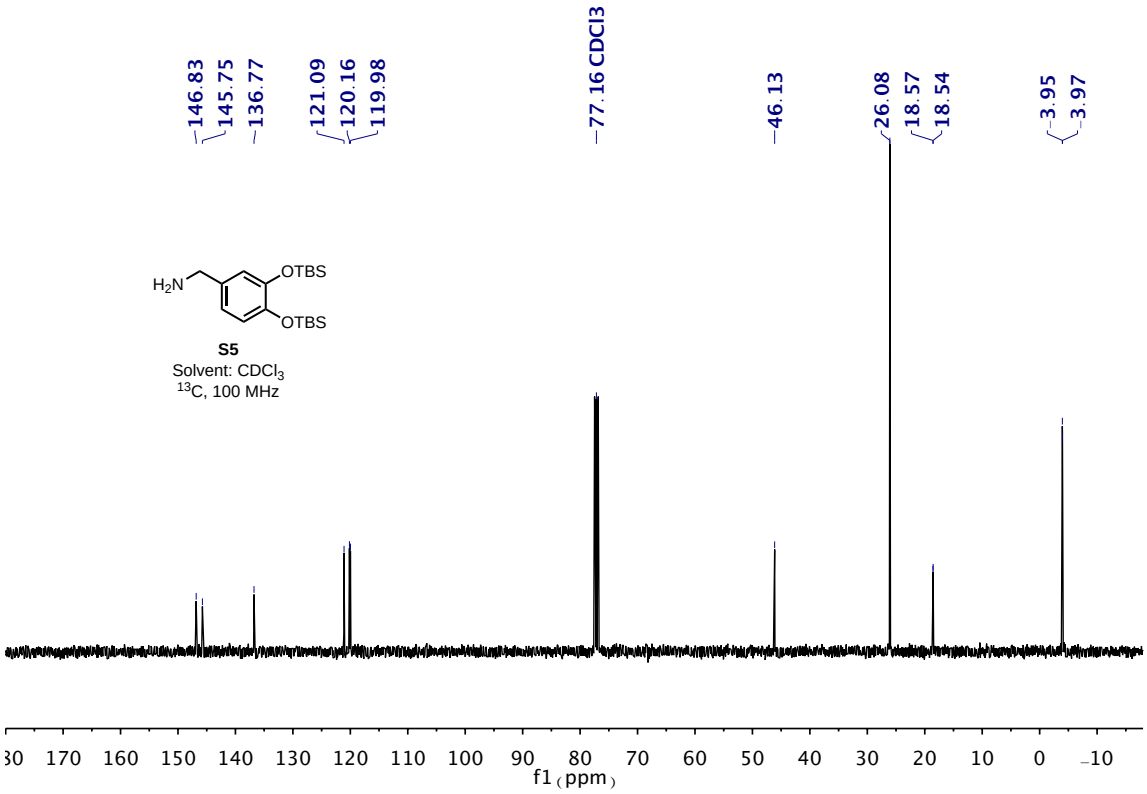
146.83
145.75
136.77
121.09
120.16
119.98
77.16 CDCl3
46.13
26.08
18.57
18.54
3.95
3.97
H2N
OTBS
OTBS
S5
Solvent: CDCl3
13C, 100 MHz
f1 (ppm)

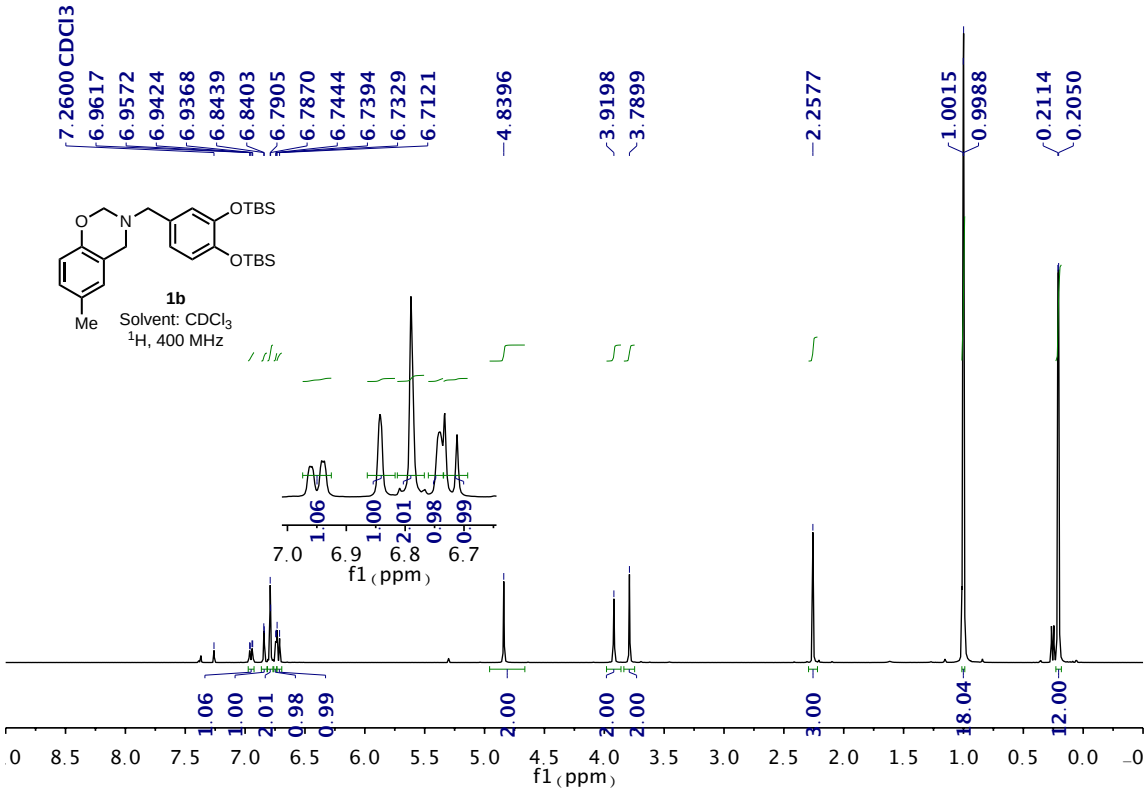
7.2600 CDCl3
6.9617
6.9572
6.9424
6.9368
6.8439
6.8403
6.7905
6.7870
6.7444
6.7394
6.7329
6.7121
4.8396
3.9198
3.7899
2.2577
1.0015
0.9988
0.2114
0.2050
OTBS
OTBS
Me
1b
Solvent: CDCl3
1H, 400 MHz
1.06
1.00
2.01
0.98
0.99
f1 (ppm)
2.00
2.00
2.00
3.00
18.04
12.00
f1 (ppm)

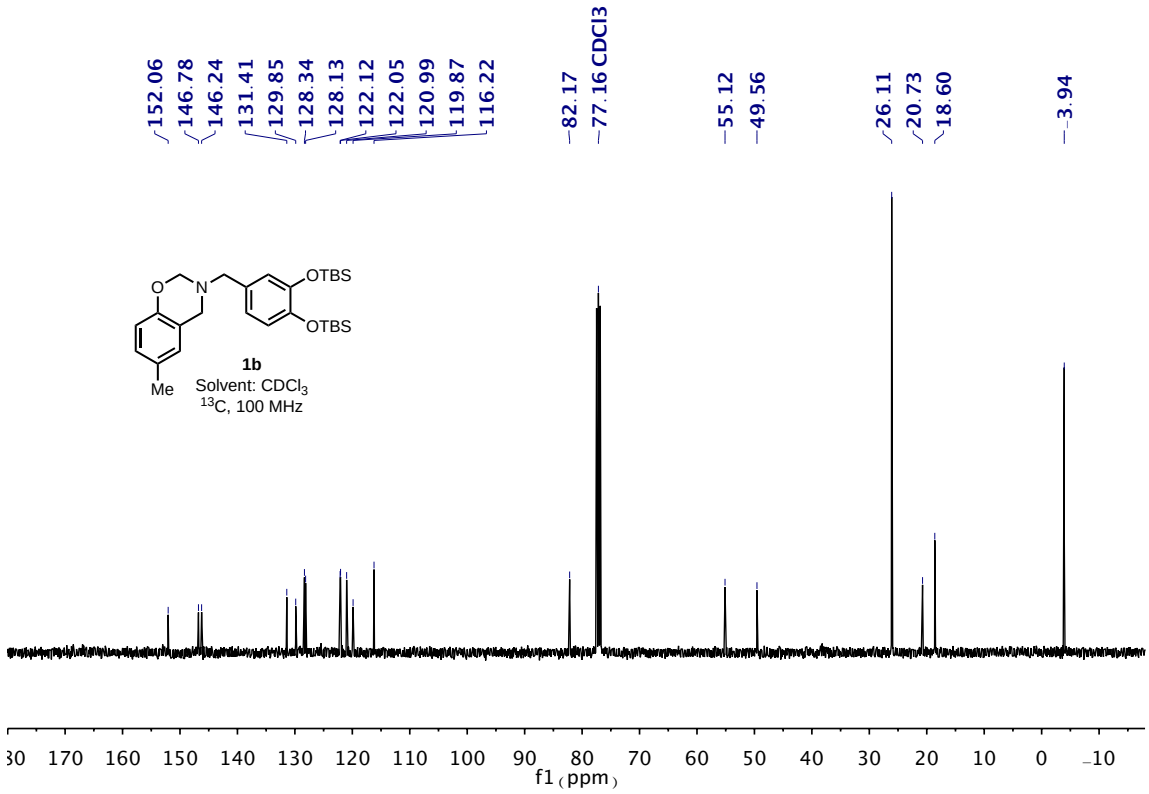
152.06
146.78
146.24
131.41
129.85
128.34
128.13
122.12
122.05
120.99
119.87
116.22
82.17
77.16 CDCl3
55.12
49.56
26.11
20.73
18.60
3.94
OTBS
OTBS
Me
1b
Solvent: CDCl3
13C, 100 MHz
f1 (ppm)

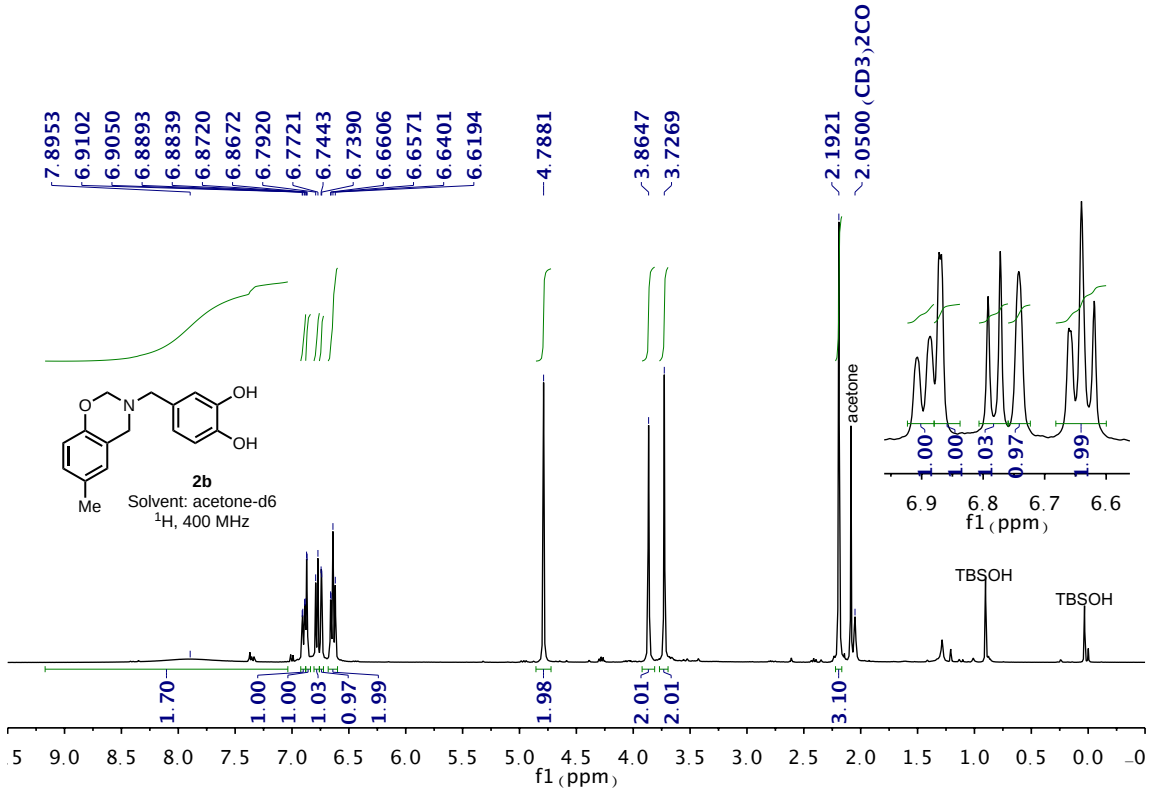
7.8953
6.9102
6.9050
6.8893
6.8839
6.8720
6.8672
6.7920
6.7721
6.7443
6.7390
6.6606
6.6571
6.6401
6.6194
4.7881
3.8647
3.7269
2.1921
2.0500 (CD3)2CO
acetone
TBSOH
TBSOH
OH
OH
Me
2b
Solvent: acetone-d6
1H, 400 MHz
1.70
1.00
1.00
1.03
0.97
1.99
1.98
2.01
2.01
3.10
f1 (ppm)

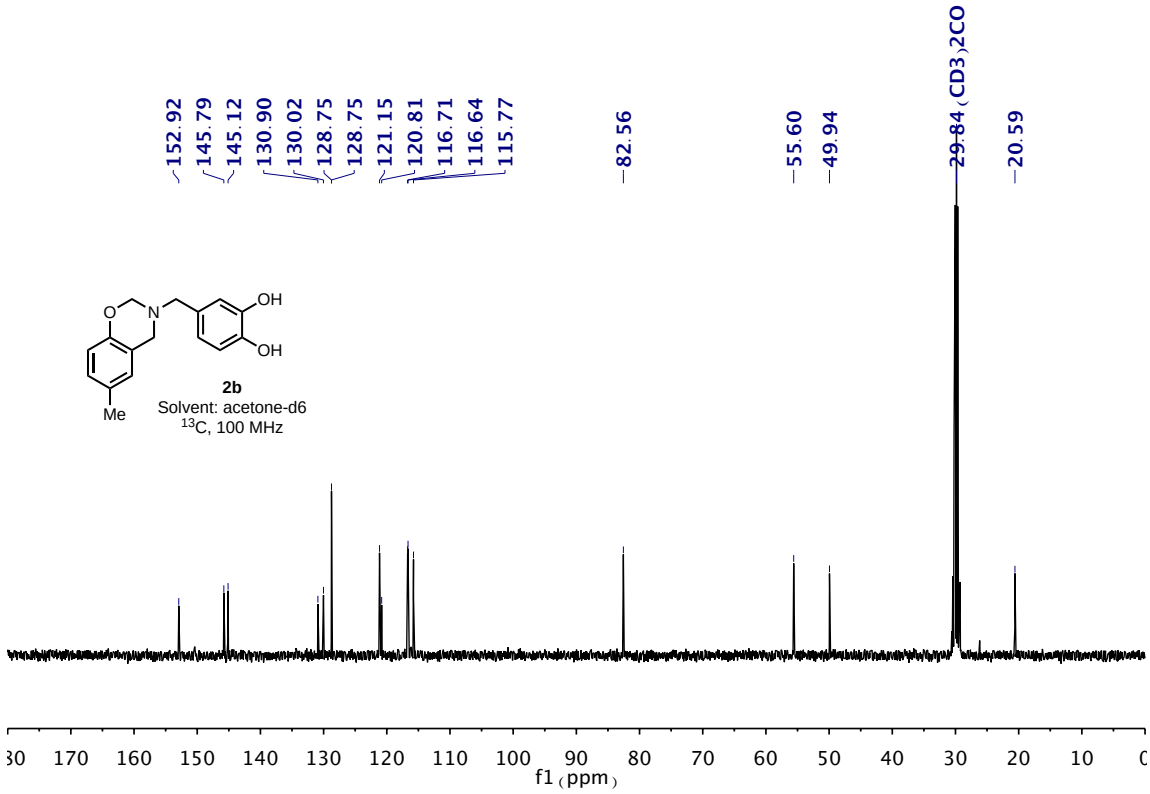
152.92
145.79
145.12
130.90
130.02
128.75
128.75
121.15
120.81
116.71
116.64
115.77
82.56
55.60
49.94
29.84 (CD3)2CO
20.59
OH
OH
Me
2b
Solvent: acetone-d6
13C, 100 MHz
f1 (ppm)

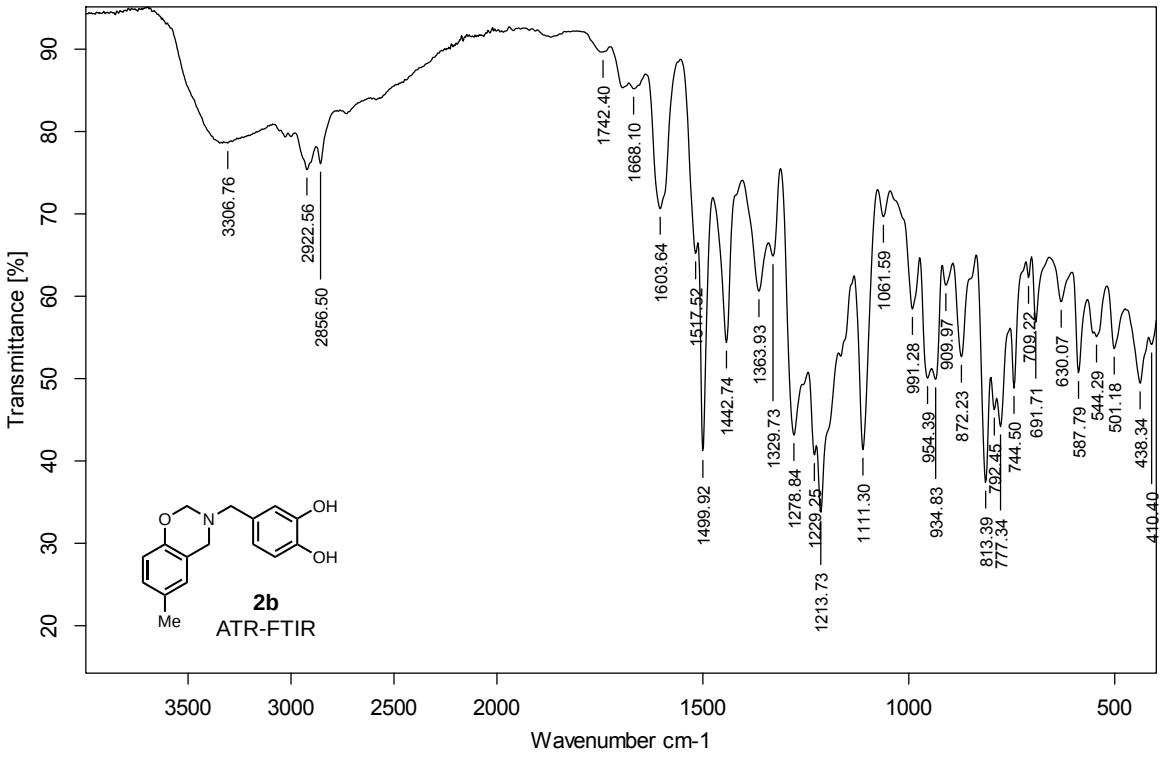
Transmittance [%]
3306.76
2922.56
2856.50
1742.40
1668.10
1603.64
1517.52
1499.92
1442.74
1363.93
1329.73
1278.84
1229.25
1213.73
1111.30
1061.59
991.28
954.39
934.83
909.97
872.23
813.39
777.34
792.45
744.50
709.22
691.71
630.07
587.79
544.29
501.18
438.34
410.40
OH
OH
Me
2b
ATR-FTIR
Wavenumber cm-1

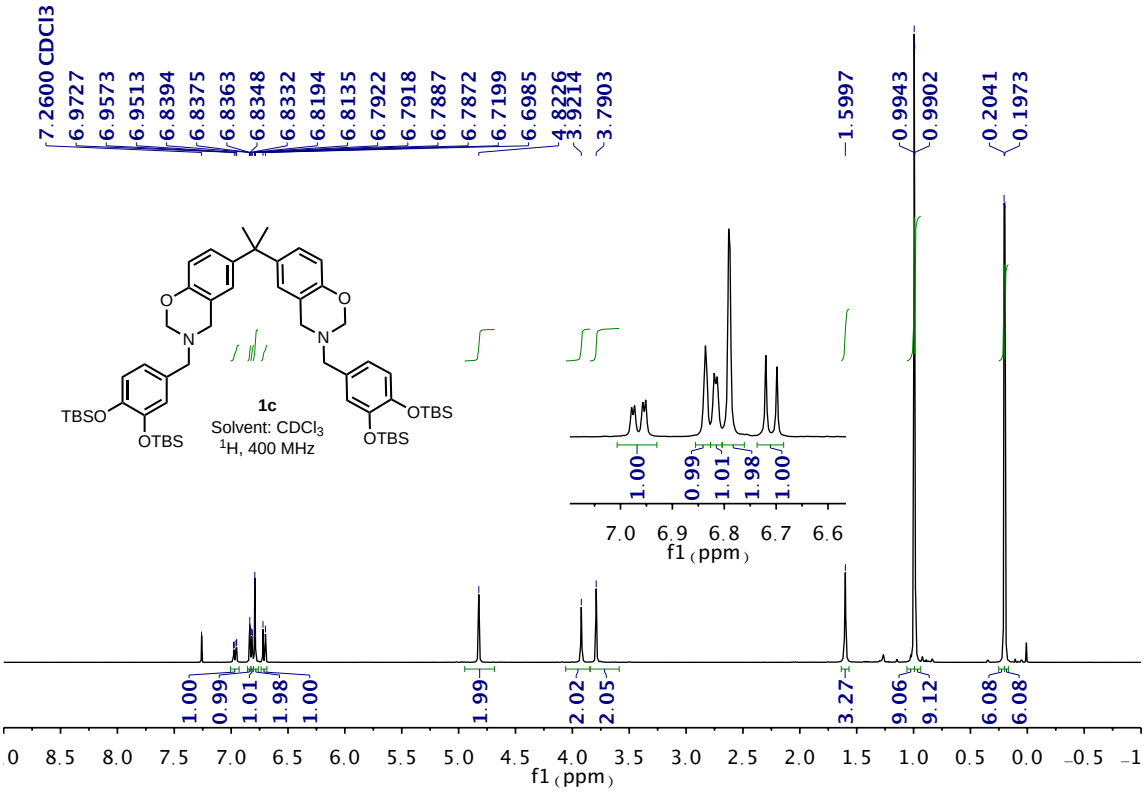
7.2600 CDCl3
6.9727
6.9573
6.9513
6.8394
6.8375
6.8363
6.8348
6.8332
6.8194
6.8135
6.7922
6.7918
6.7887
6.7872
6.7199
6.6985
4.8226
3.9214
3.7903
1.5997
0.9943
0.9902
0.2041
0.1973
1c
Solvent: CDCl3
1H, 400 MHz
TBSO
OTBS
OTBS
OTBS
OTBS
1.00
0.99
1.01
1.98
1.00
1.99
2.02
2.05
3.27
9.06
9.12
6.08
6.08
f1 (ppm)

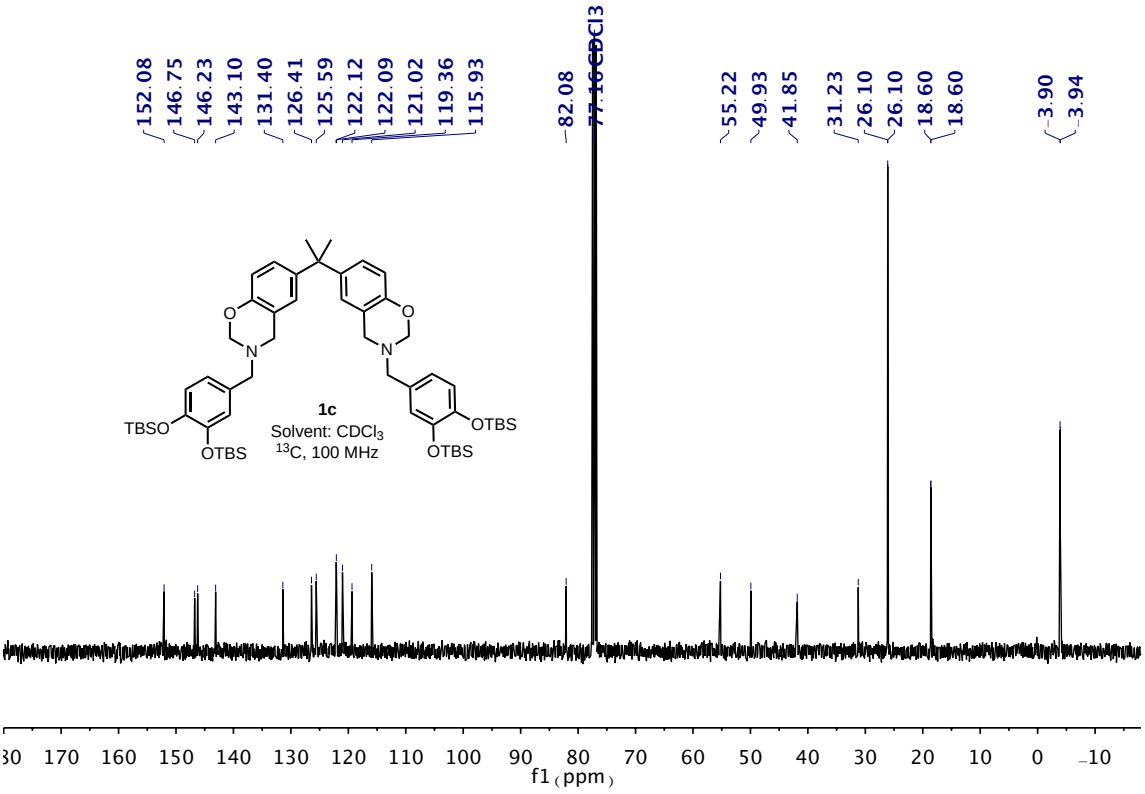
152.08
146.75
146.23
143.10
131.40
126.41
125.59
122.12
122.09
121.02
119.36
115.93
82.08
77.16 CDCl3
55.22
49.93
41.85
31.23
26.10
26.10
18.60
18.60
3.90
3.94
1c
Solvent: CDCl3
13C, 100 MHz
TBSO
OTBS
OTBS
OTBS
OTBS
f1 (ppm)

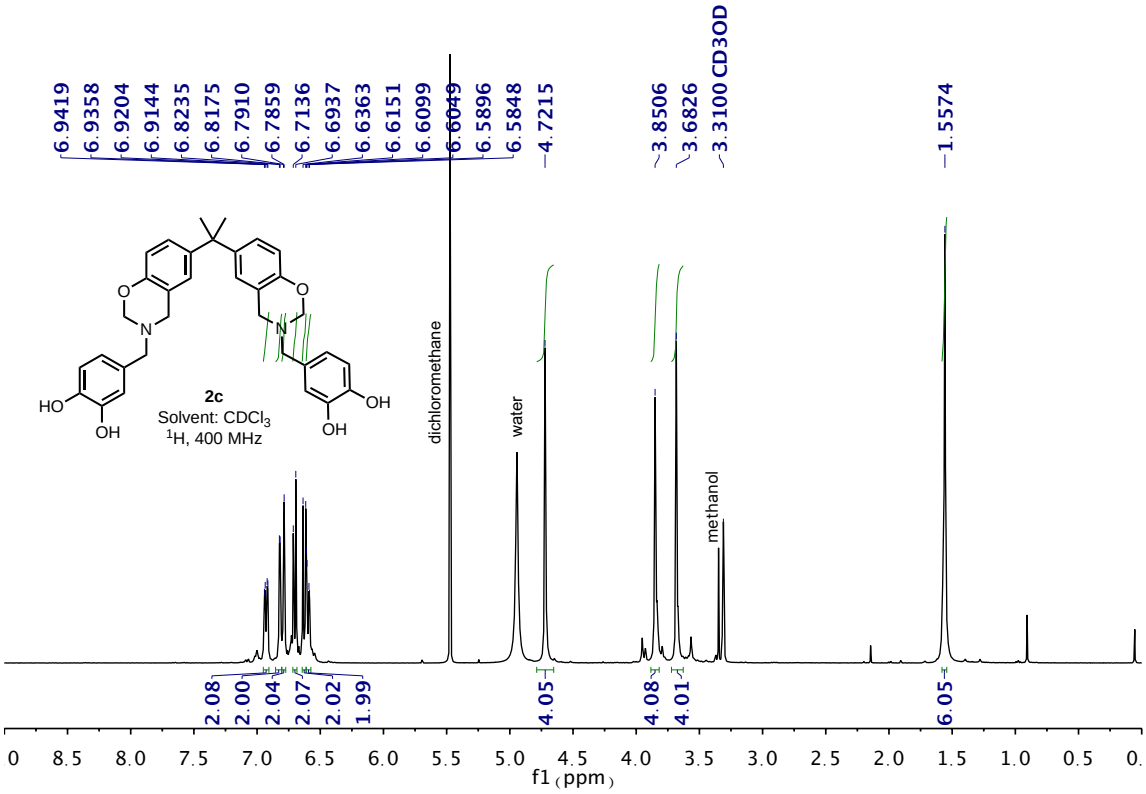
6.9419
6.9358
6.9204
6.9144
6.8235
6.8175
6.7910
6.7859
6.7136
6.6937
6.6363
6.6151
6.6099
6.6049
6.5896
6.5848
4.7215
3.8506
3.6826
3.3100 CD3OD
1.5574
dichloromethane
water
methanol
2c
Solvent: CDCl3
1H, 400 MHz
2.08
2.00
2.04
2.07
2.02
1.99
4.05
4.08
4.01
6.05
f1 (ppm)

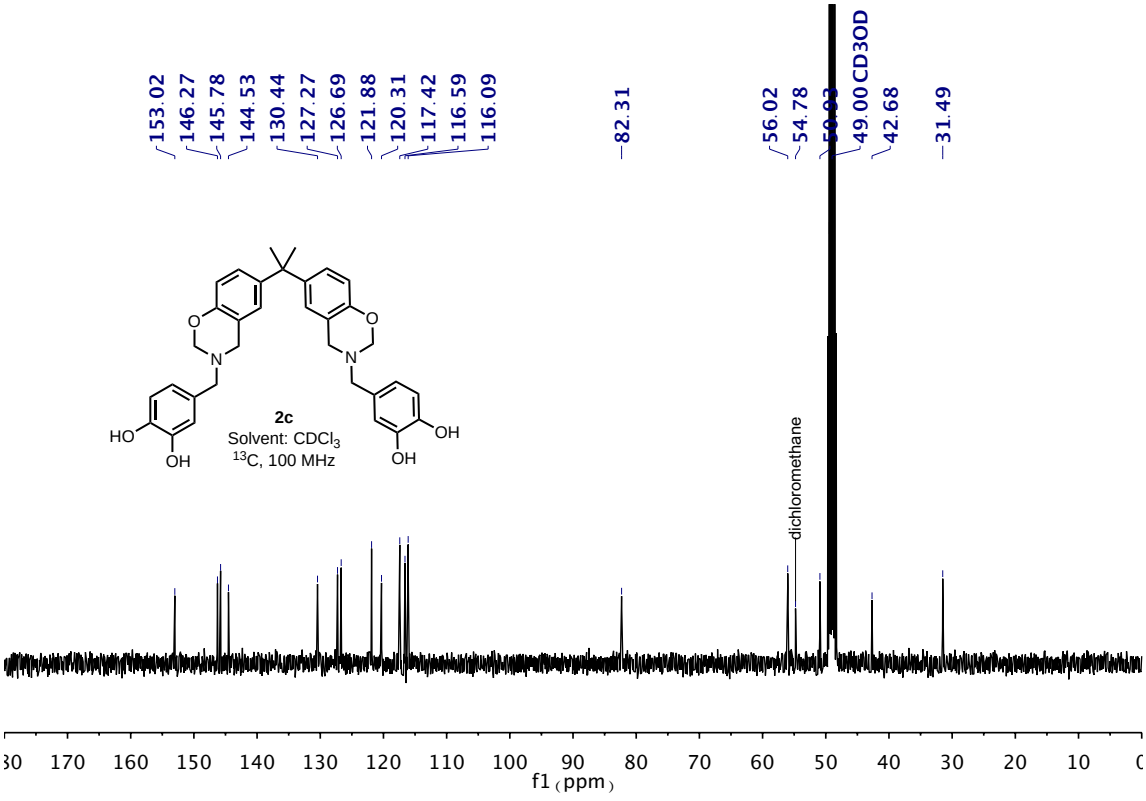
153.02
146.27
145.78
144.53
130.44
127.27
126.69
121.88
120.31
117.42
116.59
116.09
82.31
56.02
54.78
50.03
49.00 CD3OD
42.68
31.49
dichloromethane
2c
Solvent: CDCl3
13C, 100 MHz
f1 (ppm)

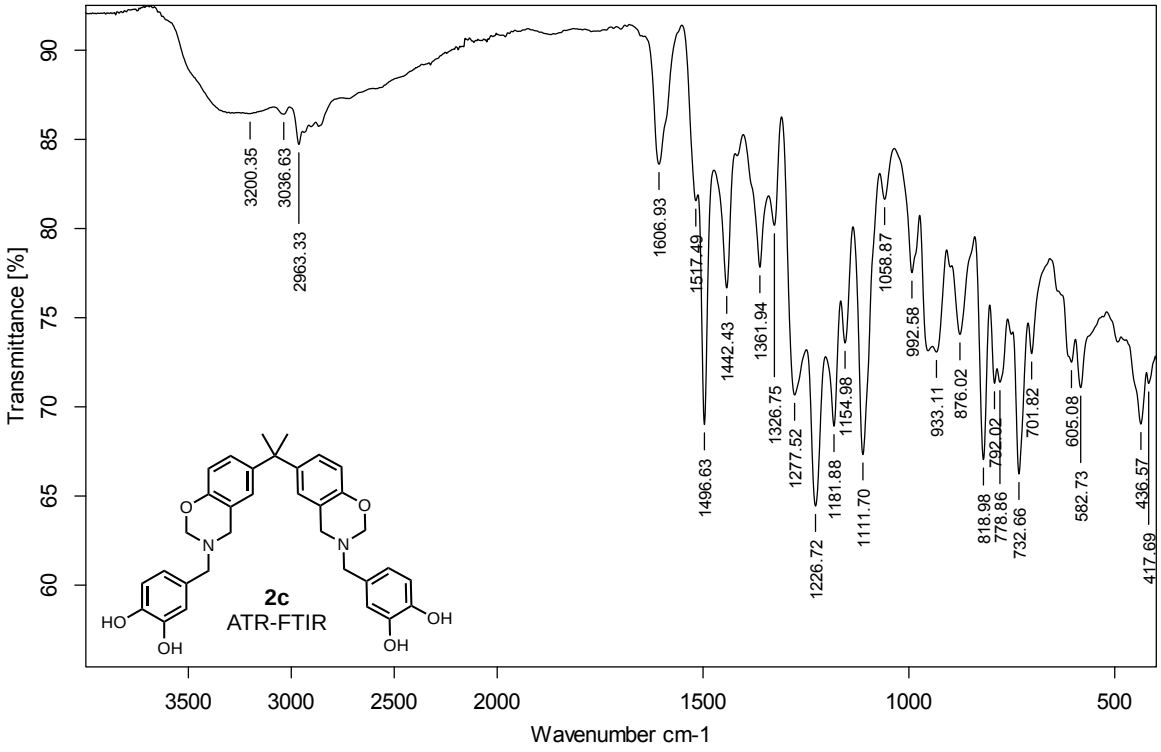
Transmittance [%]
Wavenumber cm-1
3200.35
3036.63
2963.33
1606.93
1517.49
1496.63
1442.43
1361.94
1326.75
1277.52
1226.72
1181.88
1154.98
1111.70
1058.87
992.58
933.11
876.02
818.98
792.02
778.86
732.66
701.82
605.08
582.73
436.57
417.69
2c
ATR-FTIR

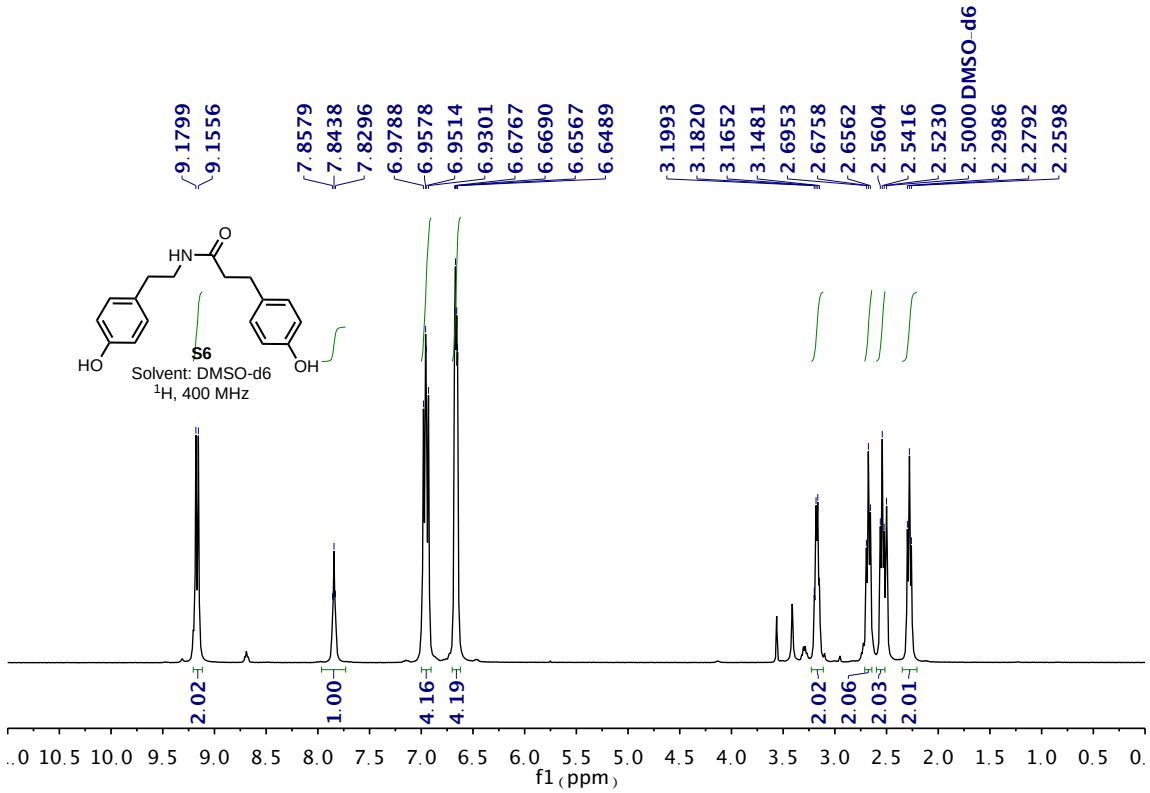
9.1799
9.1556
7.8579
7.8438
7.8296
6.9788
6.9578
6.9514
6.9301
6.6767
6.6690
6.6567
6.6489
3.1993
3.1820
3.1652
3.1481
2.6953
2.6758
2.6562
2.5604
2.5416
2.5230
2.5000 DMSO-d6
2.2986
2.2792
2.2598
S6
Solvent: DMSO-d6
1H, 400 MHz
2.02
1.00
4.16
4.19
2.02
2.06
2.03
2.01
f1 (ppm)

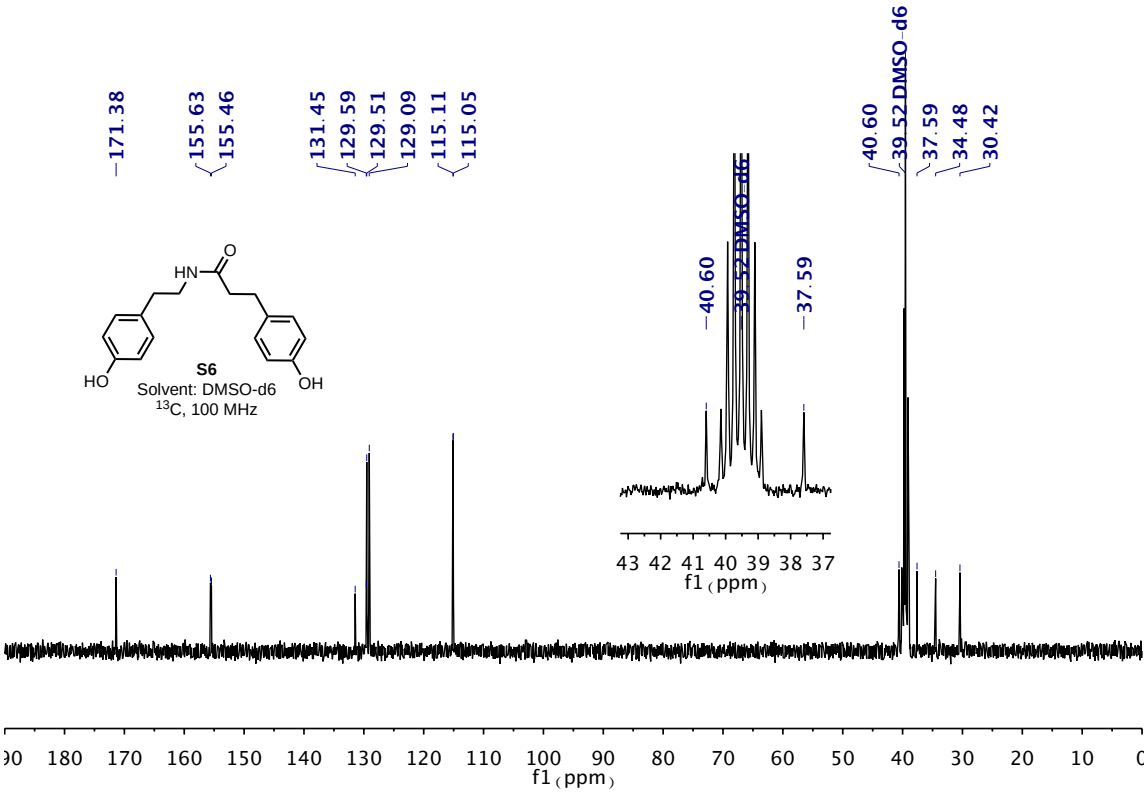
171.38
155.63
155.46
131.45
129.59
129.51
129.09
115.11
115.05
40.60
39.52 DMSO-d6
37.59
34.48
30.42
HN
O
HO
OH
S6
Solvent: DMSO-d6
13C, 100 MHz
f1 (ppm)

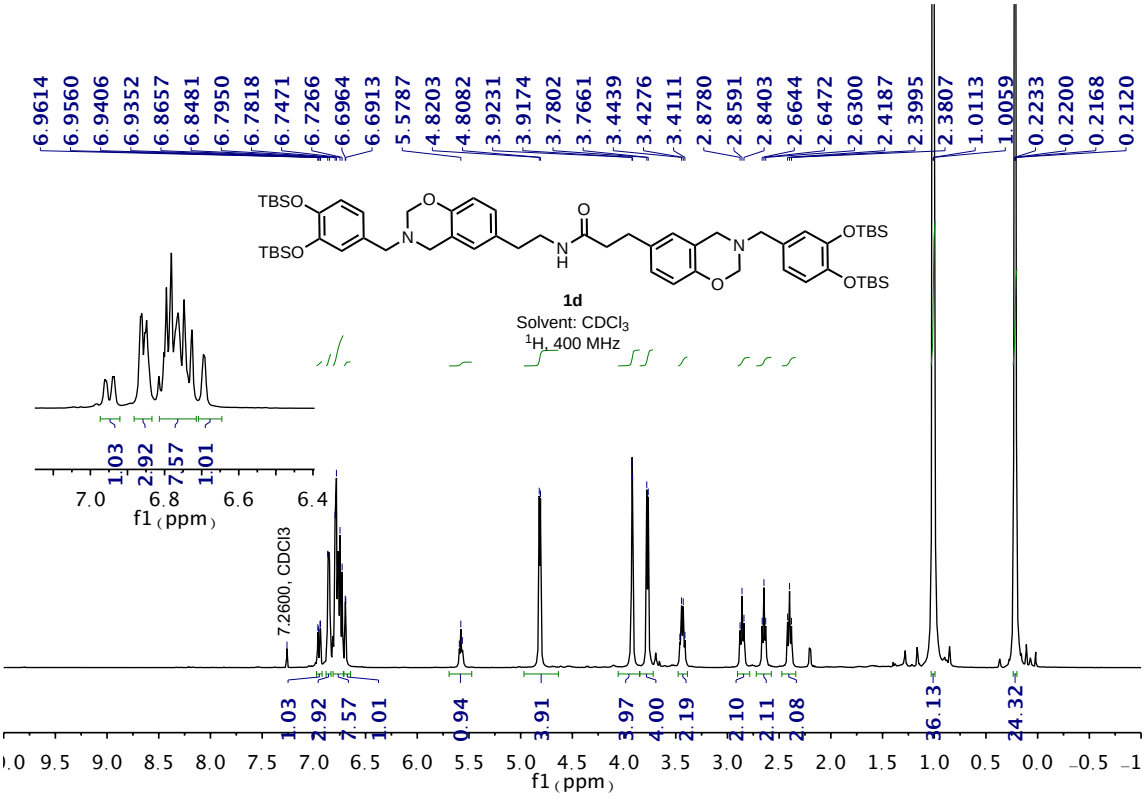
6.9614
6.9560
6.9406
6.9352
6.8657
6.8481
6.7950
6.7818
6.7471
6.7266
6.6964
6.6913
5.5787
4.8203
4.8082
3.9231
3.9174
3.7802
3.7661
3.4439
3.4276
3.4111
2.8780
2.8591
2.8403
2.6644
2.6472
2.6300
2.4187
2.3995
2.3807
1.0113
1.0059
0.2233
0.2200
0.2168
0.2120
TBSO
TBSO
OTBS
OTBS
1d
Solvent: CDCl3
1H, 400 MHz
7.2600, CDCl3
1.03
2.92
7.57
1.01
0.94
3.91
3.97
4.00
2.19
2.10
2.11
2.08
36.13
24.32
f1 (ppm)

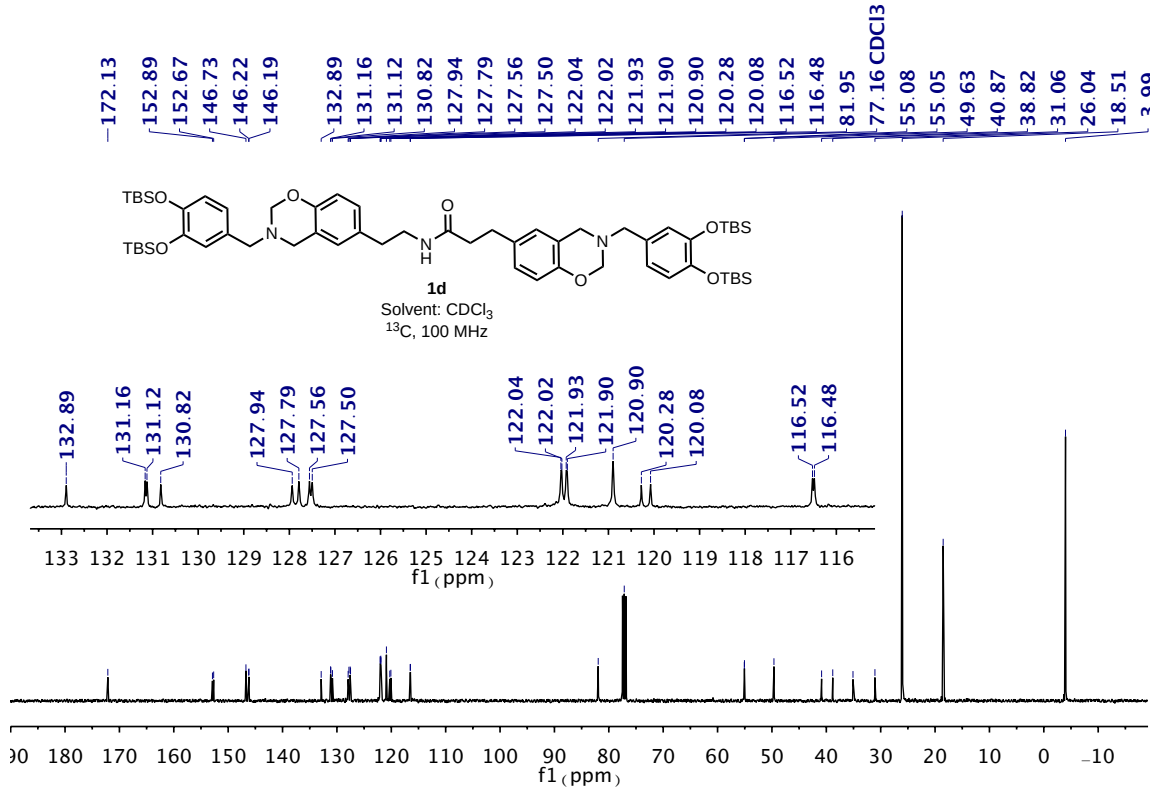
TBSO
TBSO
OTBS
OTBS
1d
Solvent: CDCl3
13C, 100 MHz
f1 (ppm)

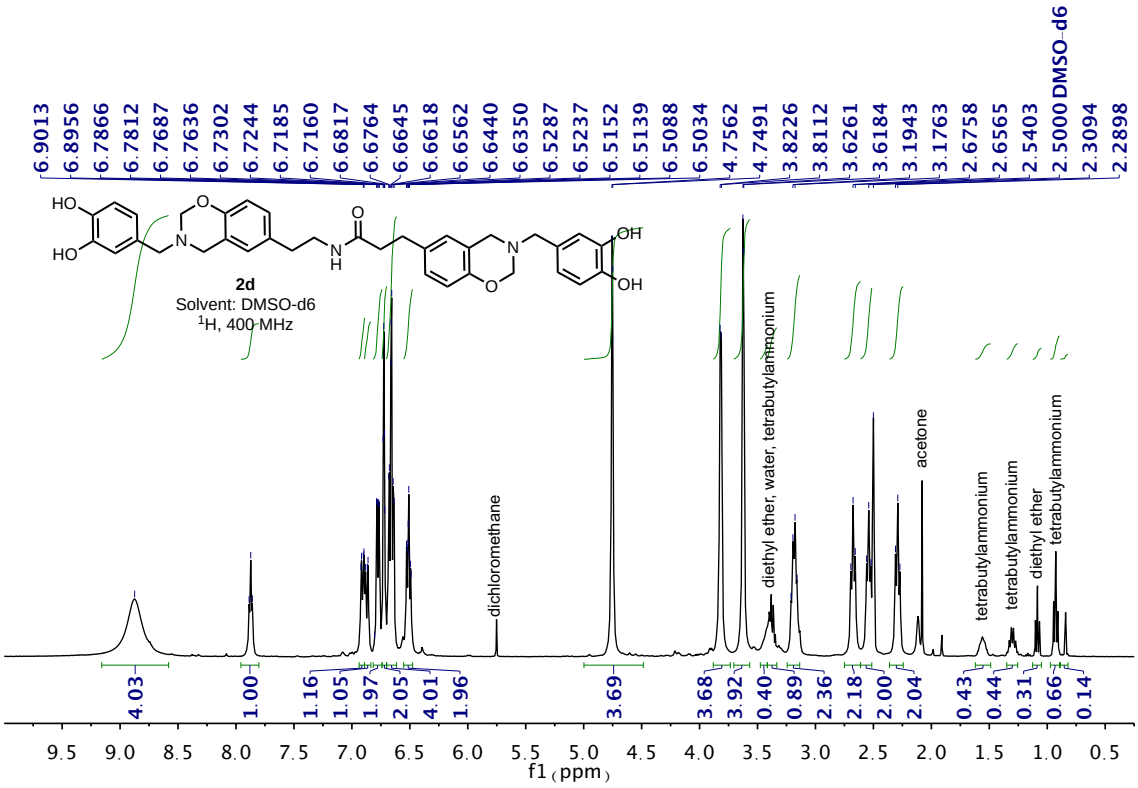
HO
HO
OH
OH
2d
Solvent: DMSO-d6
1H, 400 MHz
dichloromethane
diethyl ether, water, tetrabutylammonium
acetone
tetrabutylammonium
tetrabutylammonium
diethyl ether
tetrabutylammonium
f1 (ppm)

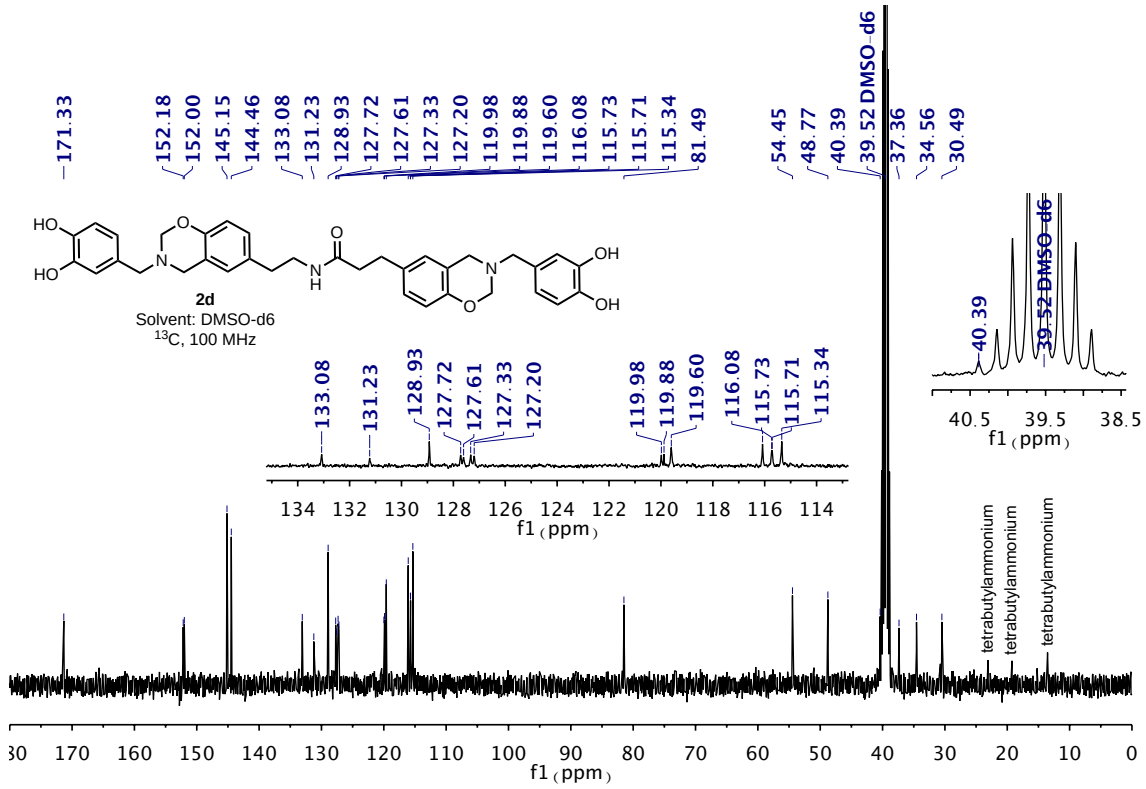
171.33
152.18
152.00
145.15
144.46
133.08
131.23
128.93
127.72
127.61
127.33
127.20
119.98
119.88
119.60
116.08
115.73
115.71
115.34
81.49
54.45
48.77
40.39
39.52 DMSO-d6
37.36
34.56
30.49
HO
HO
O
N
O
N
H
O
OH
OH
2d
Solvent: DMSO-d6
13C, 100 MHz
tetrabutylammonium
tetrabutylammonium
tetrabutylammonium
f1 (ppm)

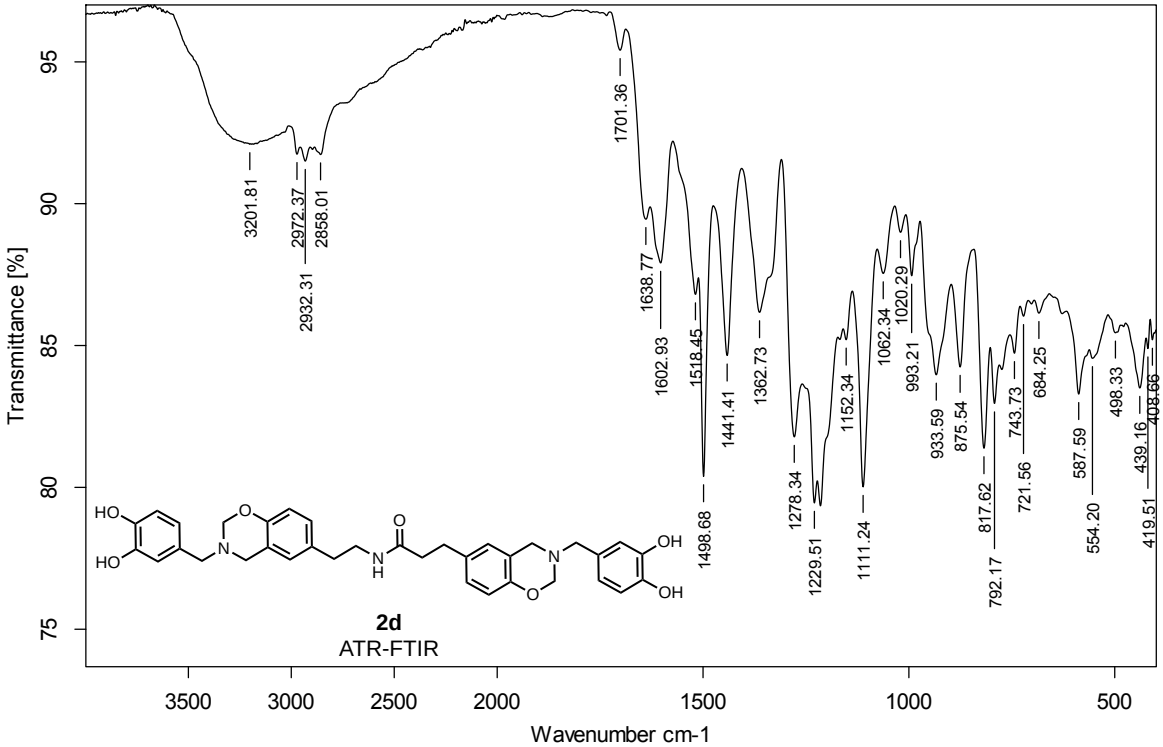
Transmittance [%]
3201.81
2972.37
2932.31
2858.01
1701.36
1638.77
1602.93
1518.45
1498.68
1441.41
1362.73
1278.34
1229.51
1152.34
1111.24
1062.34
1020.29
993.21
933.59
875.54
817.62
792.17
743.73
721.56
684.25
587.59
554.20
498.33
439.16
419.51
HO
HO
O
N
O
N
H
O
OH
OH
2d
ATR-FTIR
Wavenumber cm-1

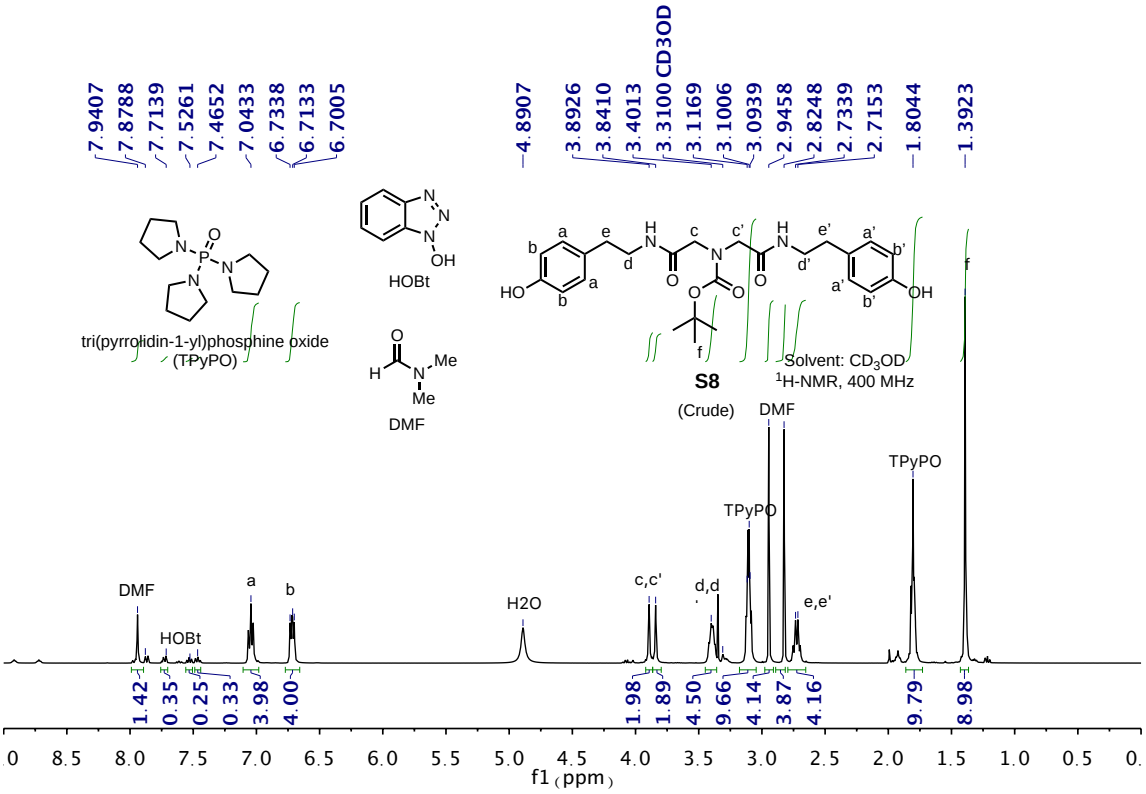
7.9407
7.8788
7.7139
7.5261
7.4652
7.0433
6.7338
6.7133
6.7005
4.8907
3.8926
3.8410
3.4013
3.3100 CD3OD
3.1169
3.1006
3.0939
2.9458
2.8248
2.7339
2.7153
1.8044
1.3923
tri(pyrrolidin-1-yl)phosphine oxide
(TPyPO)
HOBt
DMF
S8
(Crude)
Solvent: CD3OD
1H-NMR, 400 MHz
DMF
HOBt
a
b
H2O
c,c'
d,d
e,e'
TPyPO
TPyPO
DMF
TPyPO
1.42
0.35
0.25
0.33
3.98
4.00
1.98
1.89
4.50
9.66
4.14
3.87
4.16
9.79
8.98
f1 (ppm)

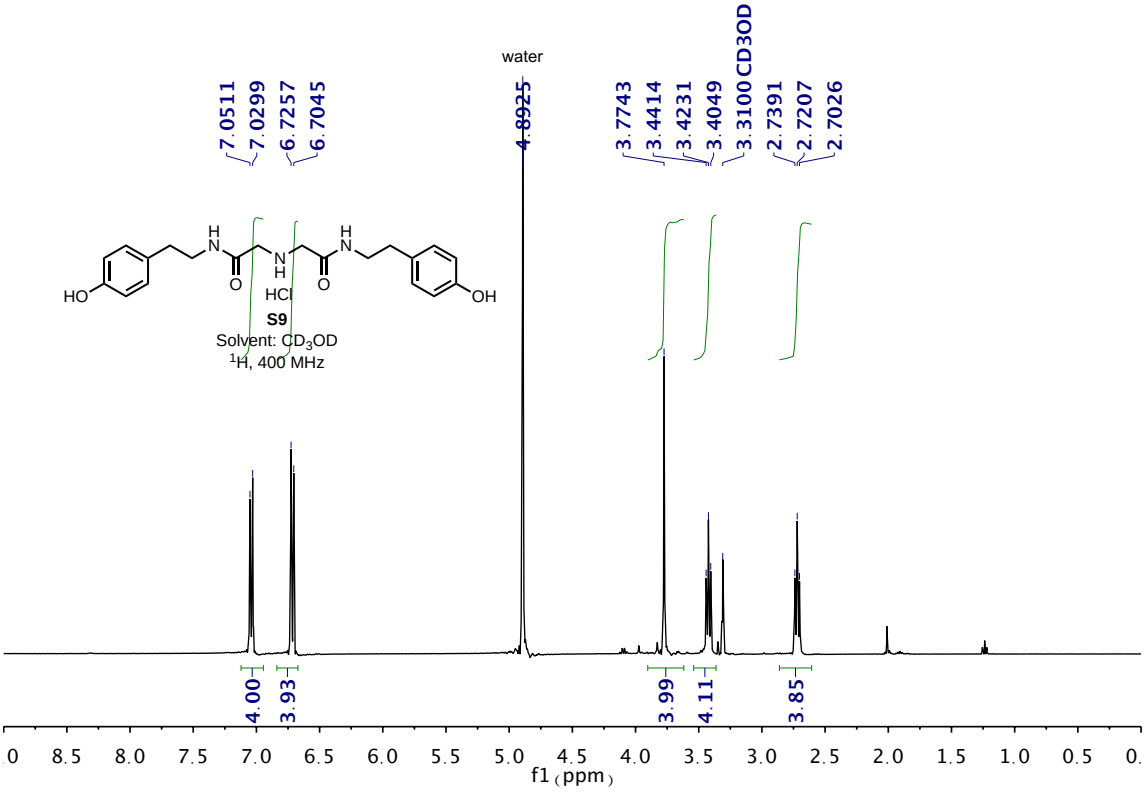
water
7.0511
7.0299
6.7257
6.7045
4.8925
3.7743
3.4414
3.4231
3.4049
3.3100 CD3OD
2.7391
2.7207
2.7026
HCl
S9
Solvent: CD3OD
1H, 400 MHz
4.00
3.93
3.99
4.11
3.85
f1 (ppm)

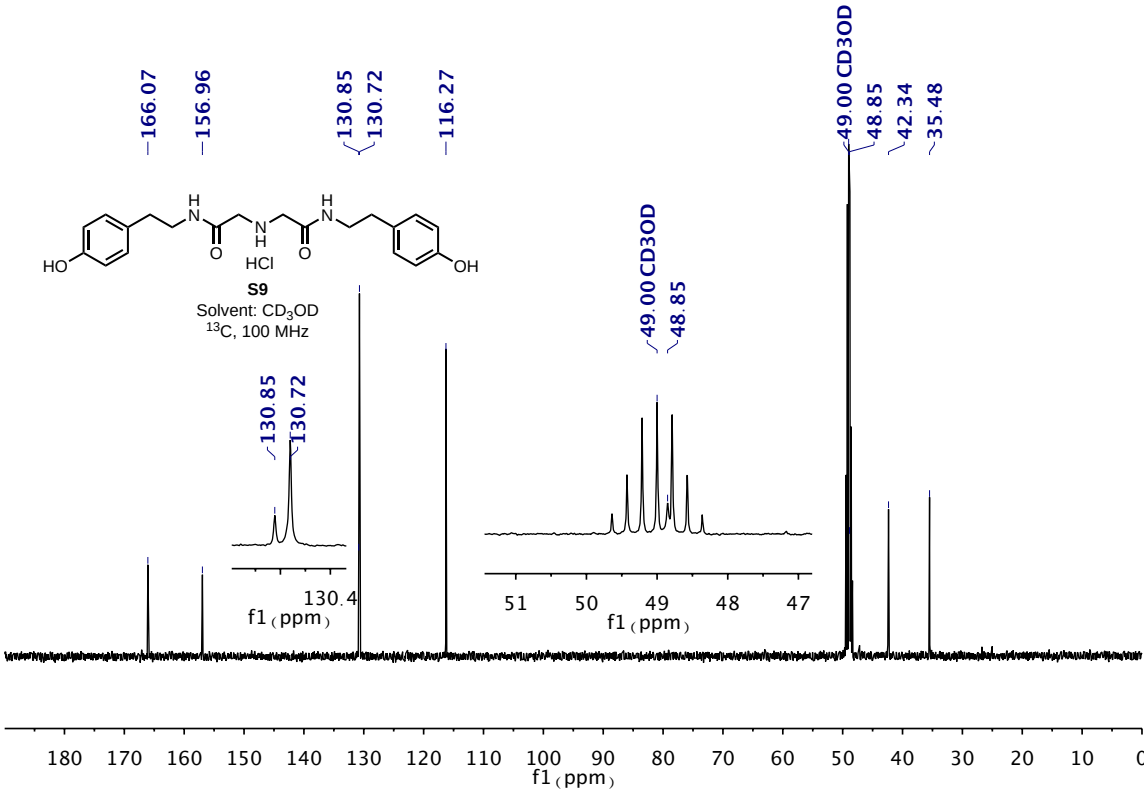
166.07
156.96
130.85
130.72
116.27
49.00 CD3OD
48.85
42.34
35.48
HO
HCl
OH
S9
Solvent: CD3OD
13C, 100 MHz
130.85
130.72
130.4
f1 (ppm)
49.00 CD3OD
48.85
51 50 49 48 47
f1 (ppm)
180 170 160 150 140 130 120 110 100 90 80 70 60 50 40 30 20 10
f1 (ppm)

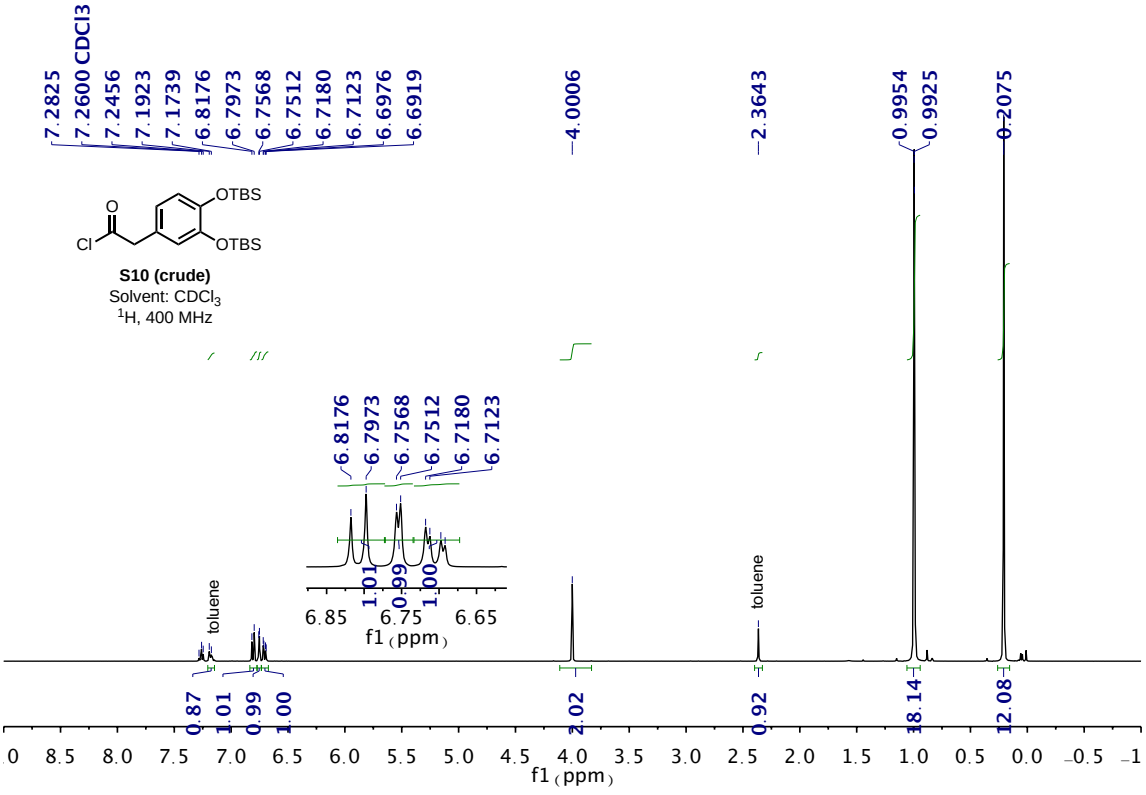
7.2825
7.2600 CDCl3
7.2456
7.1923
7.1739
6.8176
6.7973
6.7568
6.7512
6.7180
6.7123
6.6976
6.6919
4.0006
2.3643
0.9954
0.9925
0.2075
Cl
OTBS
OTBS
S10 (crude)
Solvent: CDCl3
1H, 400 MHz
6.8176
6.7973
6.7568
6.7512
6.7180
6.7123
1.01
0.99
1.00
6.85 6.75 6.65
f1 (ppm)
toluene
toluene
0.87
1.01
0.99
1.00
2.02
0.92
18.14
12.08
8.5 8.0 7.5 7.0 6.5 6.0 5.5 5.0 4.5 4.0 3.5 3.0 2.5 2.0 1.5 1.0 0.5 0.0 −0.5 −1
f1 (ppm)

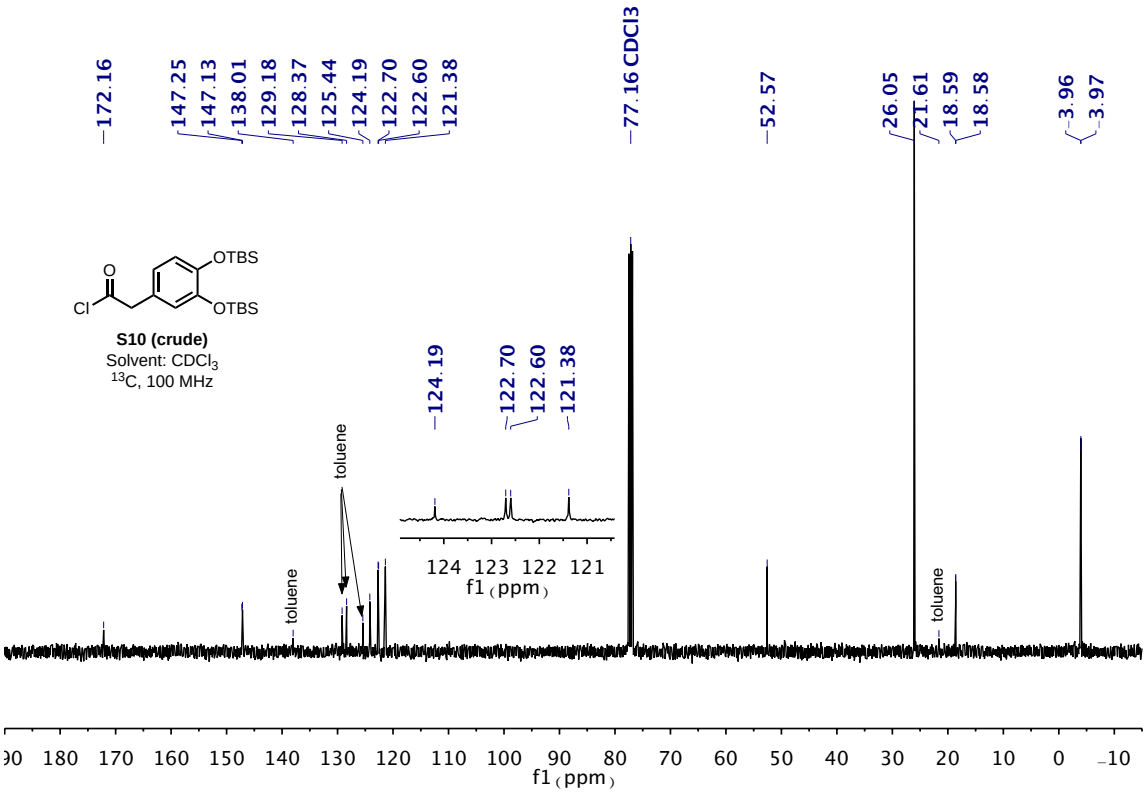
172.16
147.25
147.13
138.01
129.18
128.37
125.44
124.19
122.70
122.60
121.38
77.16 CDCl3
52.57
26.05
21.61
18.59
18.58
3.96
3.97
OTBS
OTBS
Cl
O
S10 (crude)
Solvent: CDCl3
13C, 100 MHz
toluene
toluene
toluene
124.19
122.70
122.60
121.38
124 123 122 121
f1 (ppm)
f1 (ppm)

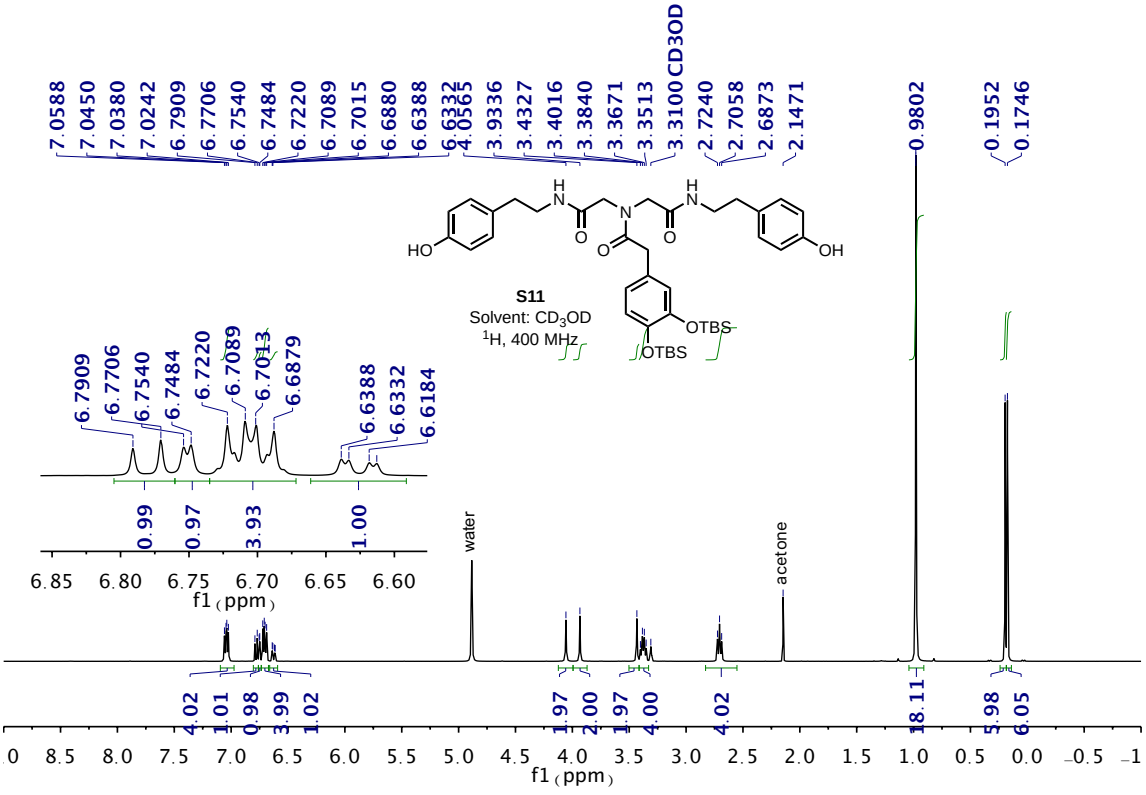
7.0588
7.0450
7.0380
7.0242
6.7909
6.7706
6.7540
6.7484
6.7220
6.7089
6.7015
6.6880
6.6388
6.6332
4.0565
3.9336
3.4327
3.4016
3.3840
3.3671
3.3513
3.3100 CD3OD
2.7240
2.7058
2.6873
2.1471
0.9802
0.1952
0.1746
HO
OH
OTBS
OTBS
S11
Solvent: CD3OD
1H, 400 MHz
6.7909
6.7706
6.7540
6.7484
6.7220
6.7089
6.7013
6.6879
6.6388
6.6332
6.6184
0.99
0.97
3.93
1.00
water
acetone
4.02
1.01
0.98
3.99
1.02
1.97
2.00
1.97
4.00
4.02
18.11
5.98
6.05
f1 (ppm)
f1 (ppm)

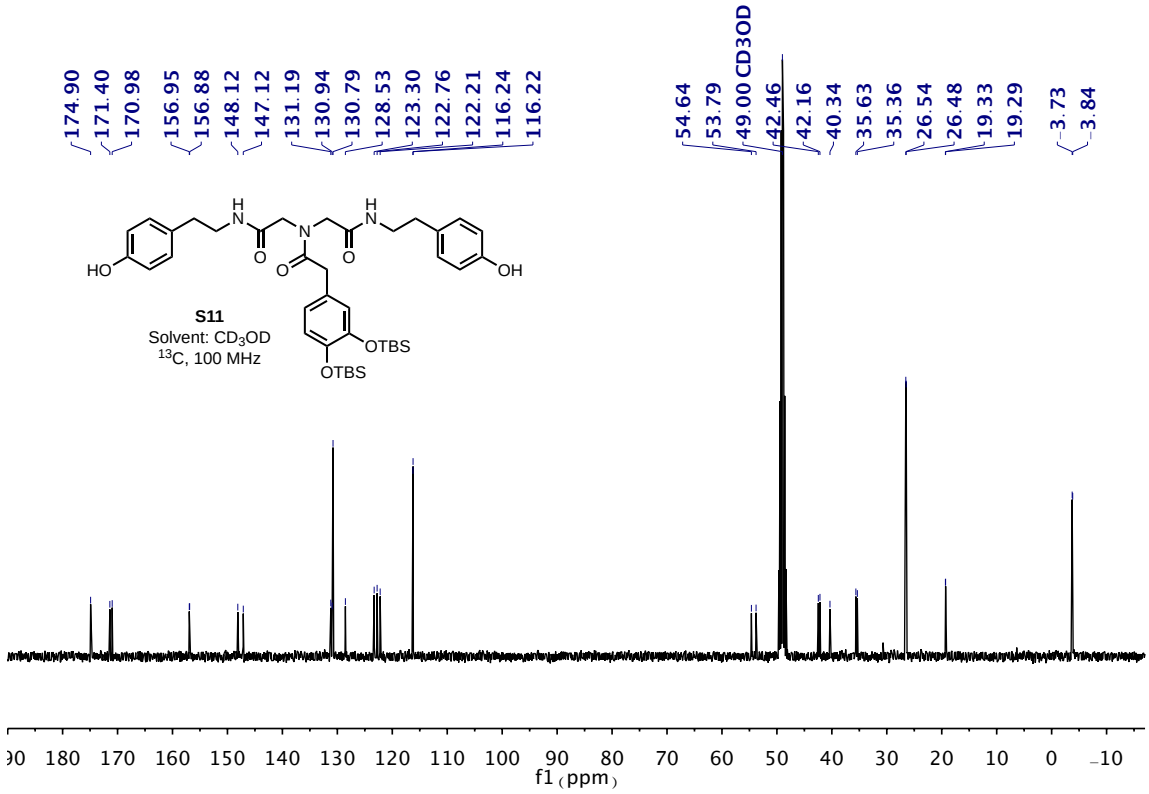
174.90
171.40
170.98
156.95
156.88
148.12
147.12
131.19
130.94
130.79
128.53
123.30
122.76
122.21
116.24
116.22
54.64
53.79
49.00 CD3OD
42.46
42.16
40.34
35.63
35.36
26.54
26.48
19.33
19.29
3.73
3.84
S11
Solvent: CD3OD
13C, 100 MHz
f1 (ppm)

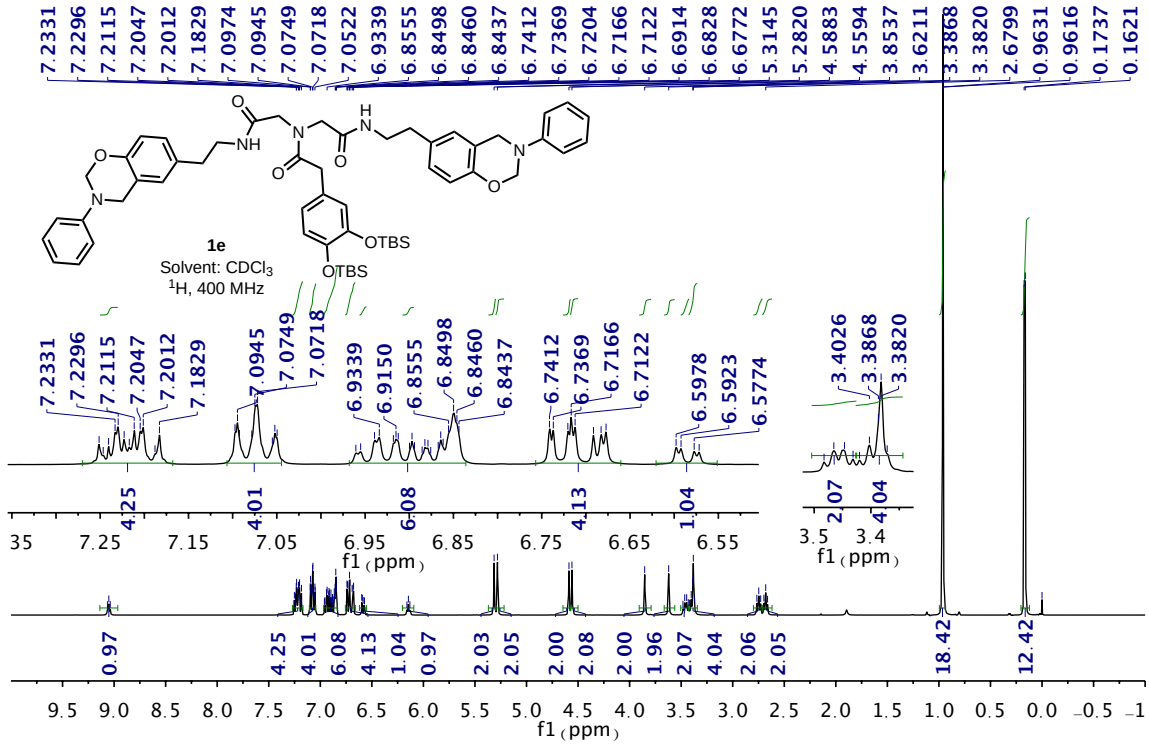
7.2331
7.2296
7.2115
7.2047
7.2012
7.1829
7.0974
7.0945
7.0749
7.0718
7.0522
6.9339
6.8555
6.8498
6.8460
6.8437
6.7412
6.7369
6.7204
6.7166
6.7122
6.6914
6.6828
6.6772
5.3145
5.2820
4.5883
4.5594
3.8537
3.6211
3.3868
3.3820
2.6799
0.9631
0.9616
0.1737
0.1621
1e
Solvent: CDCl3
1H, 400 MHz
f1 (ppm)

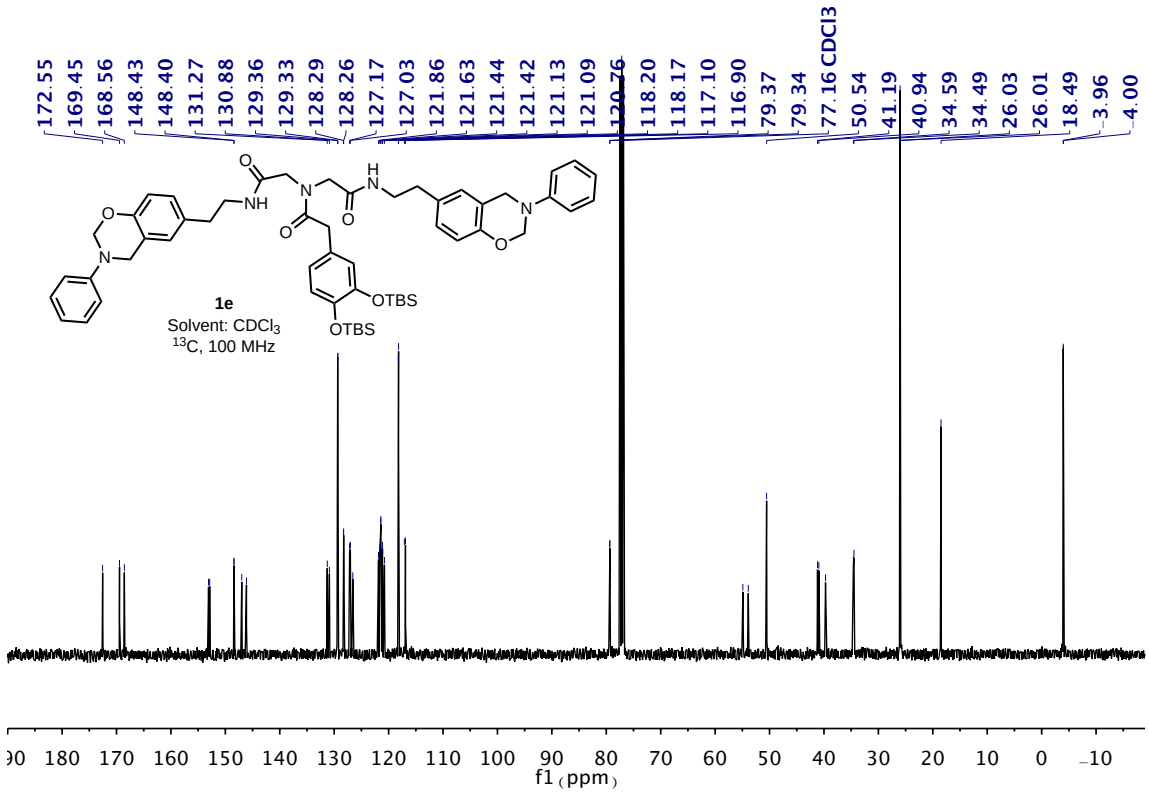
172.55
169.45
168.56
148.43
148.40
131.27
130.88
129.36
129.33
128.29
128.26
127.17
127.03
121.86
121.63
121.44
121.42
121.13
121.09
120.76
118.20
118.17
117.10
116.90
79.37
79.34
77.16 CDCl3
50.54
41.19
40.94
34.59
34.49
26.03
26.01
18.49
3.96
4.00
1e
Solvent: CDCl3
13C, 100 MHz
OTBS
OTBS
f1 (ppm)

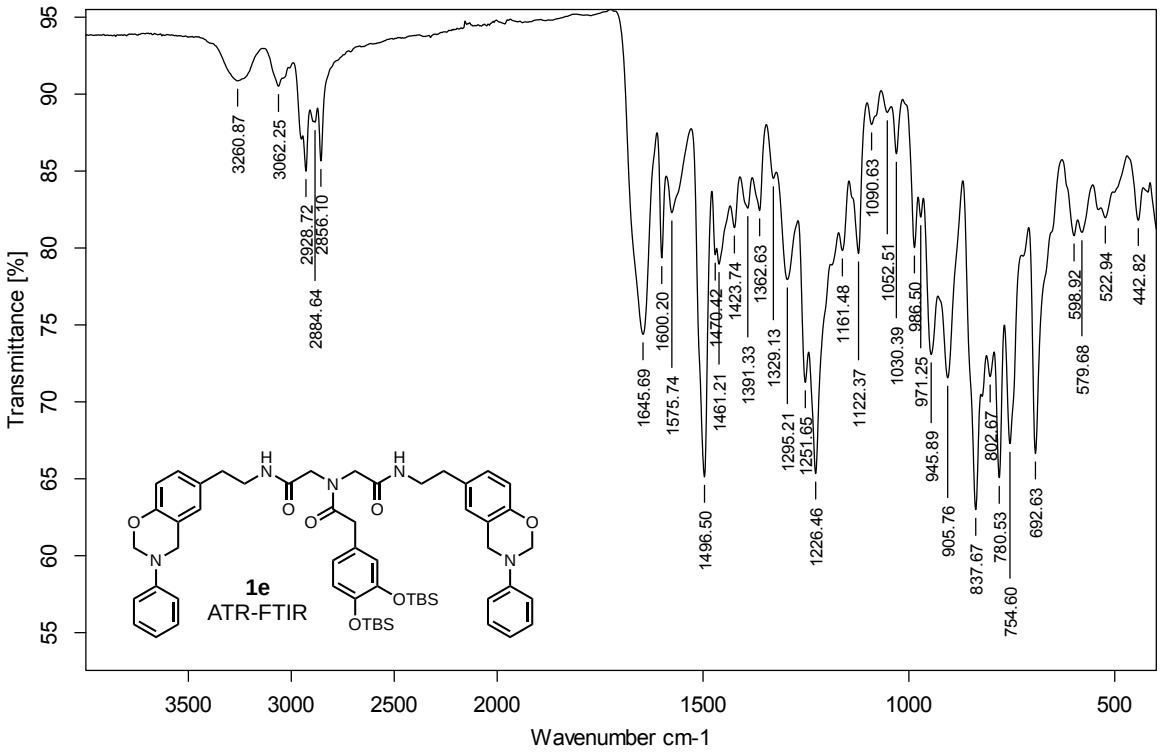
Transmittance [%]
3260.87
3062.25
2928.72
2856.10
2884.64
1645.69
1600.20
1575.74
1496.50
1461.21
1470.42
1423.74
1391.33
1362.63
1329.13
1295.21
1251.65
1226.46
1161.48
1122.37
1090.63
1052.51
1030.39
986.50
971.25
945.89
905.76
837.67
802.67
780.53
754.60
692.63
598.92
579.68
522.94
442.82
1e
ATR-FTIR
OTBS
OTBS
Wavenumber cm-1

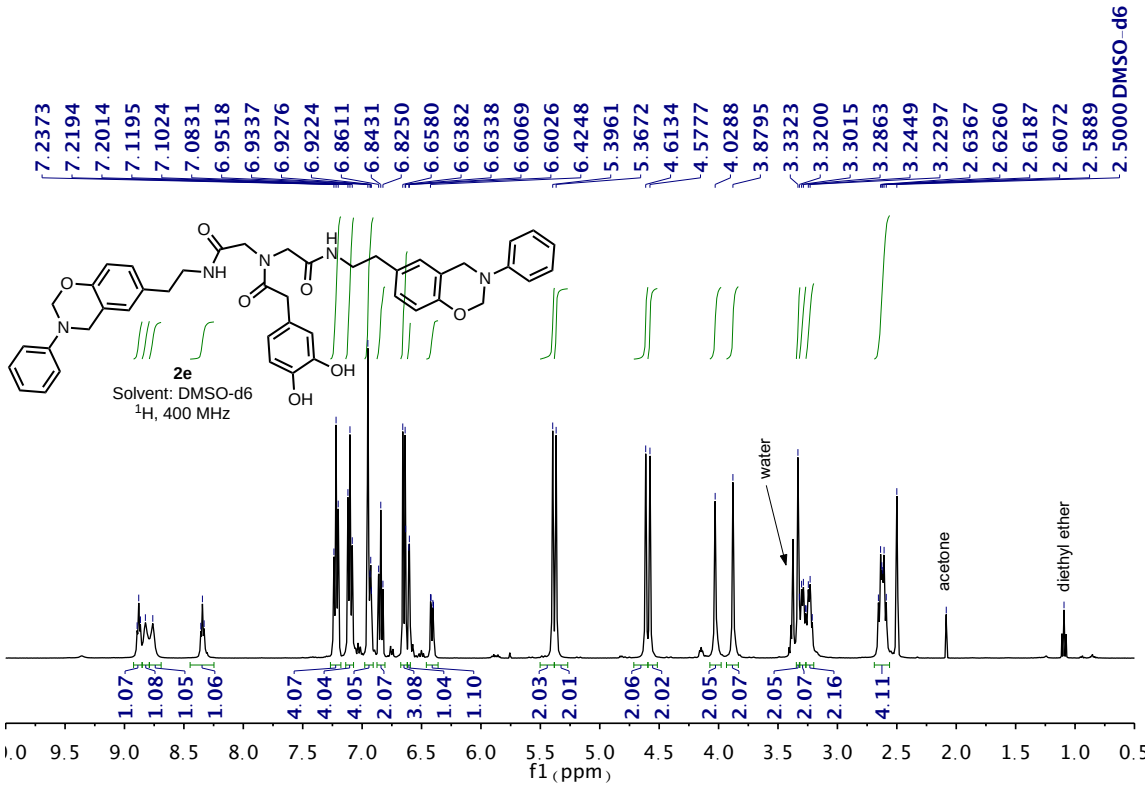
2e
Solvent: DMSO-d6
1H, 400 MHz
water
acetone
diethyl ether
f1 (ppm)

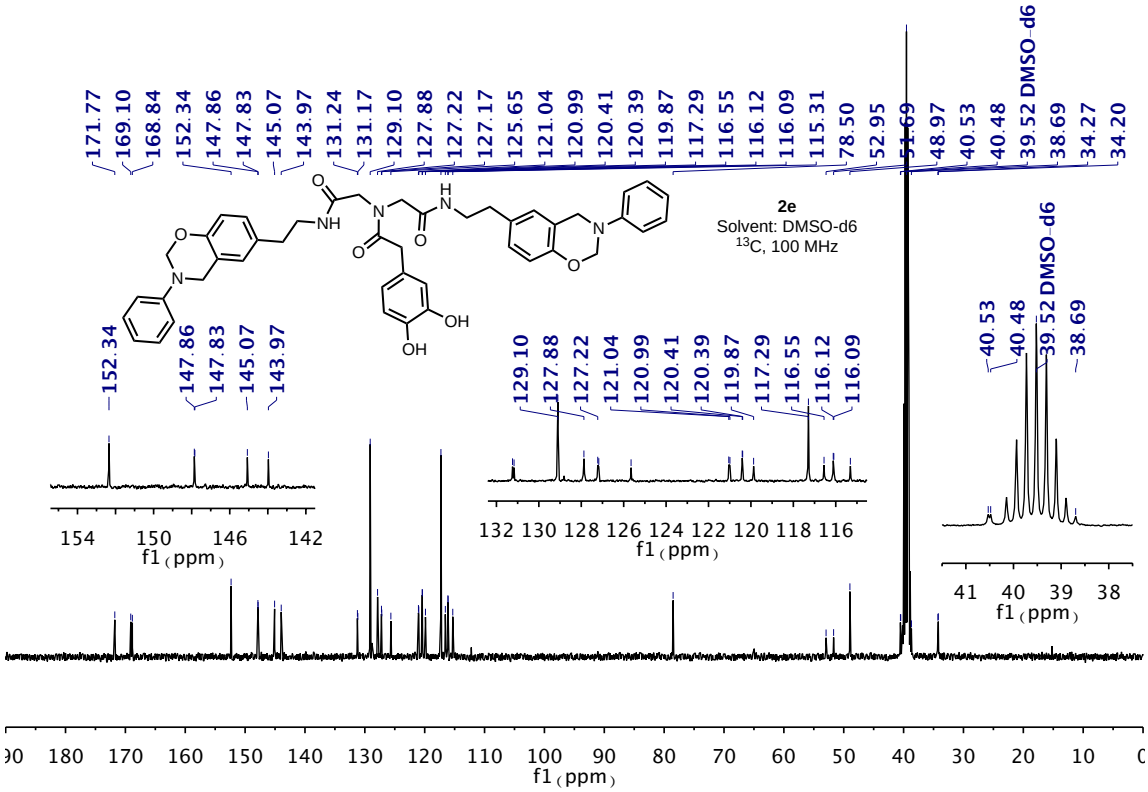
2e
Solvent: DMSO-d6
13C, 100 MHz
DMSO-d6
f1 (ppm)

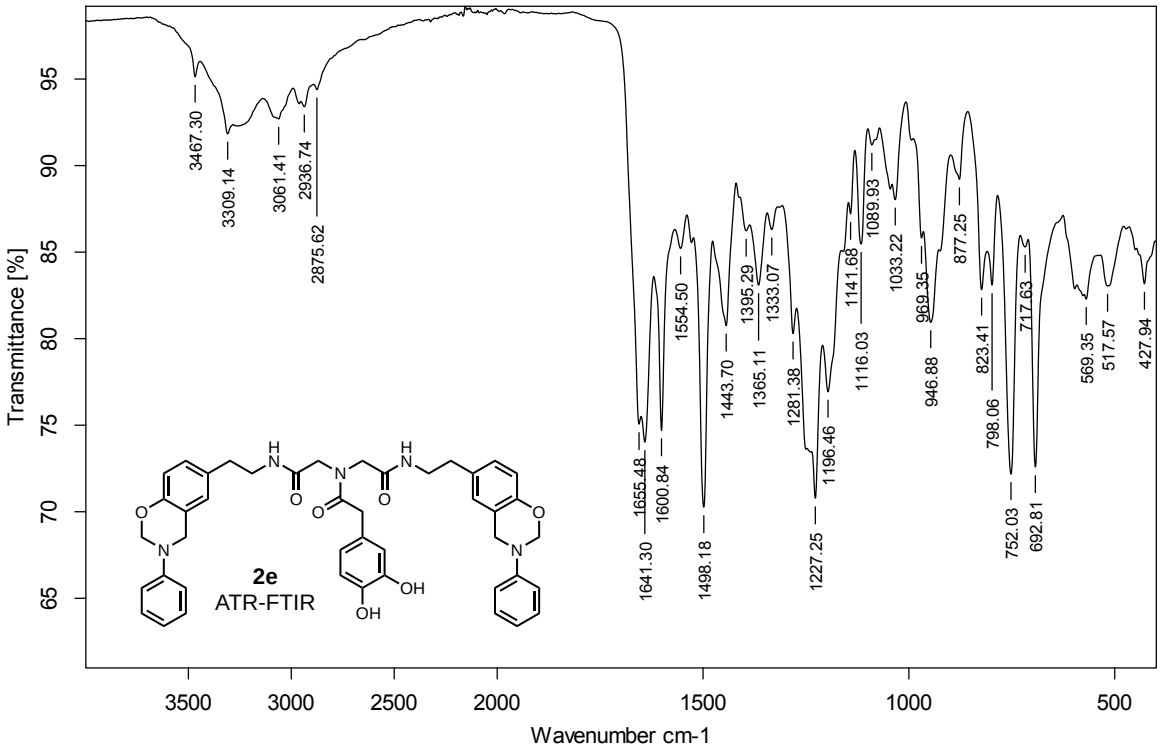
Transmittance [%]
Wavenumber cm-1
3467.30
3309.14
3061.41
2936.74
2875.62
1655.48
1641.30
1600.84
1554.50
1498.18
1443.70
1395.29
1365.11
1333.07
1281.38
1227.25
1196.46
1141.68
1116.03
1089.93
1033.22
969.35
946.88
877.25
823.41
798.06
752.03
717.63
692.81
569.35
517.57
427.94
2e
ATR-FTIR

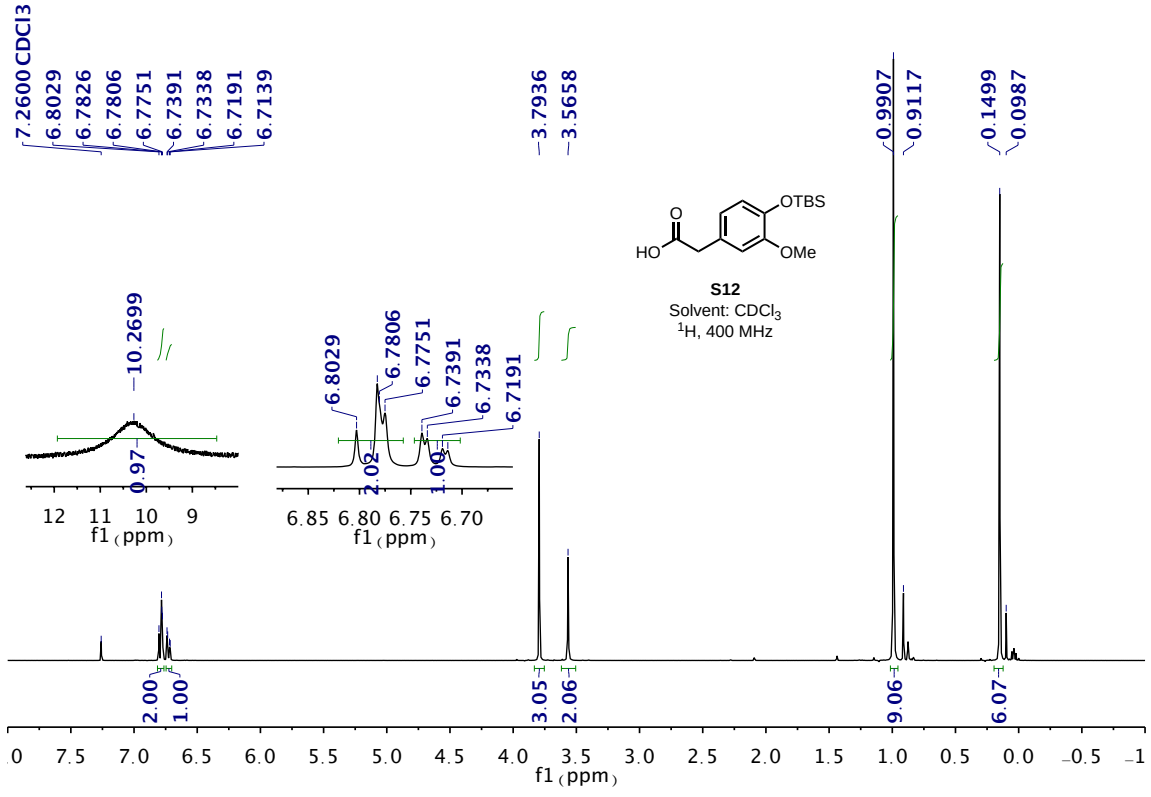
7.2600 CDCl3
6.8029
6.7826
6.7806
6.7751
6.7391
6.7338
6.7191
6.7139
3.7936
3.5658
0.9907
0.9117
0.1499
0.0987
10.2699
0.97
2.02
1.00
2.00
1.00
3.05
2.06
9.06
6.07
f1 (ppm)
S12
Solvent: CDCl3
1H, 400 MHz

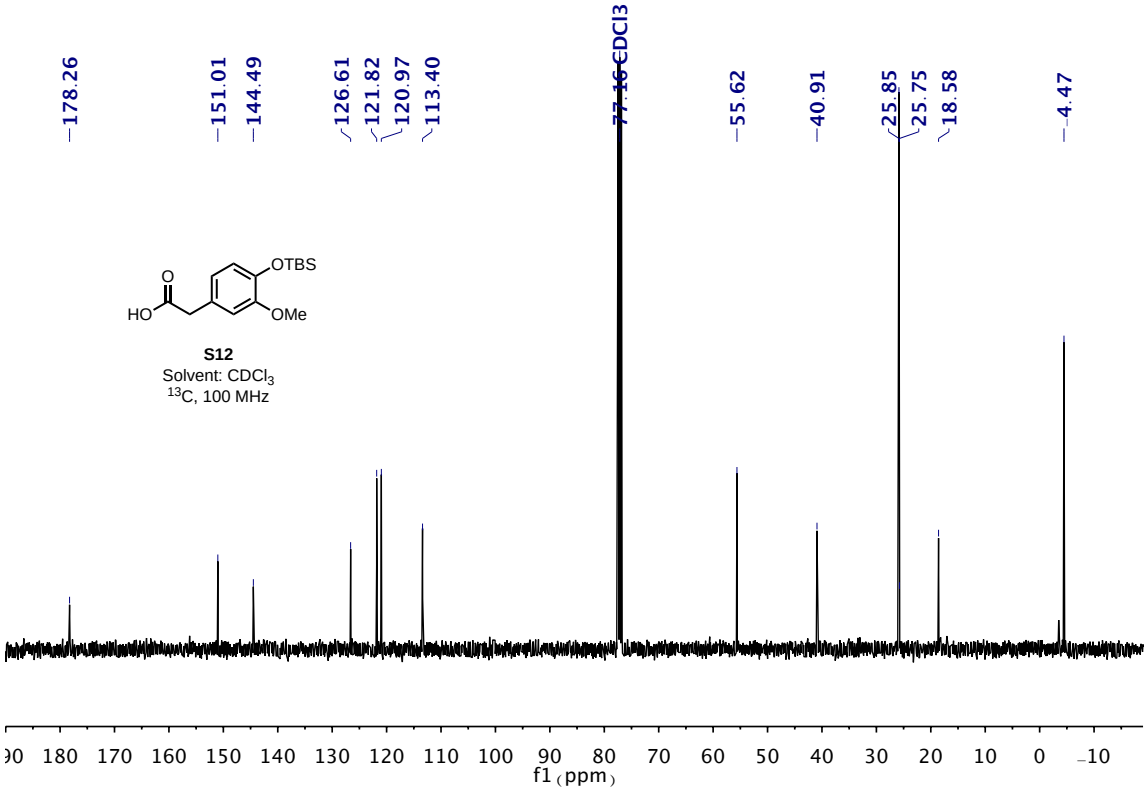

S12
Solvent: $CDCl_3$
^{13}C, 100 MHz

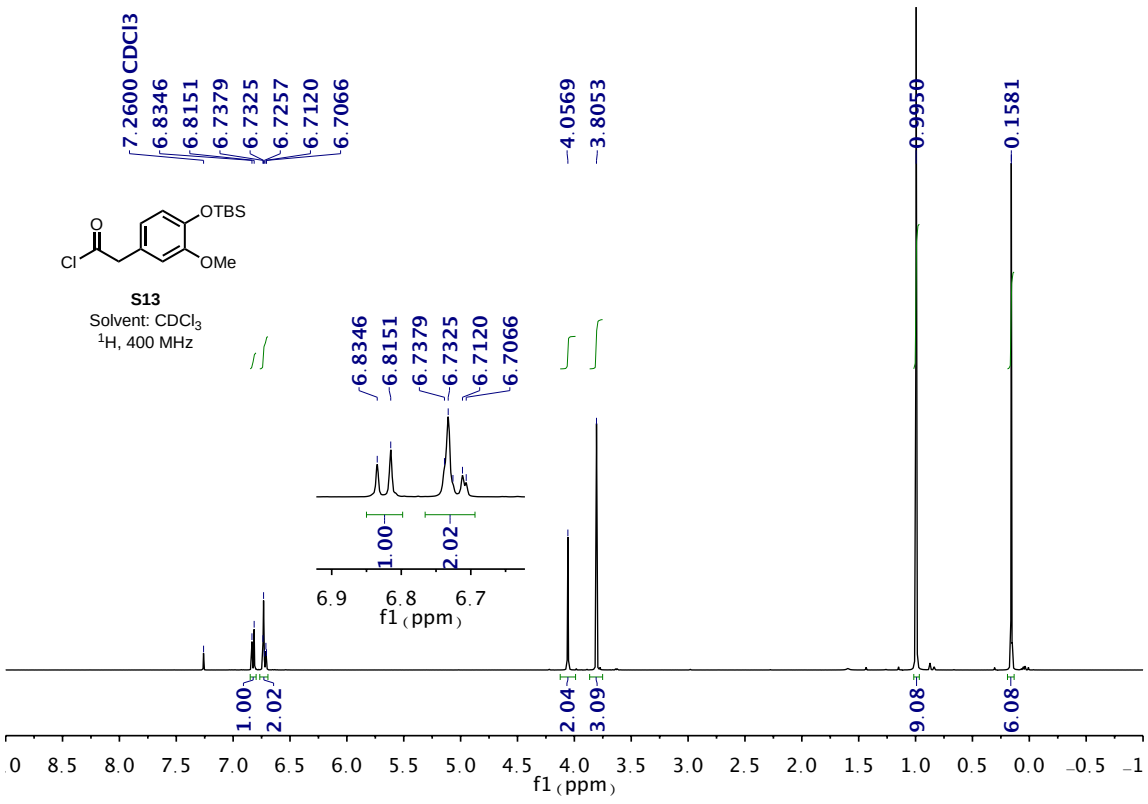

S13
Solvent: $CDCl_3$
^{1}H, 400 MHz

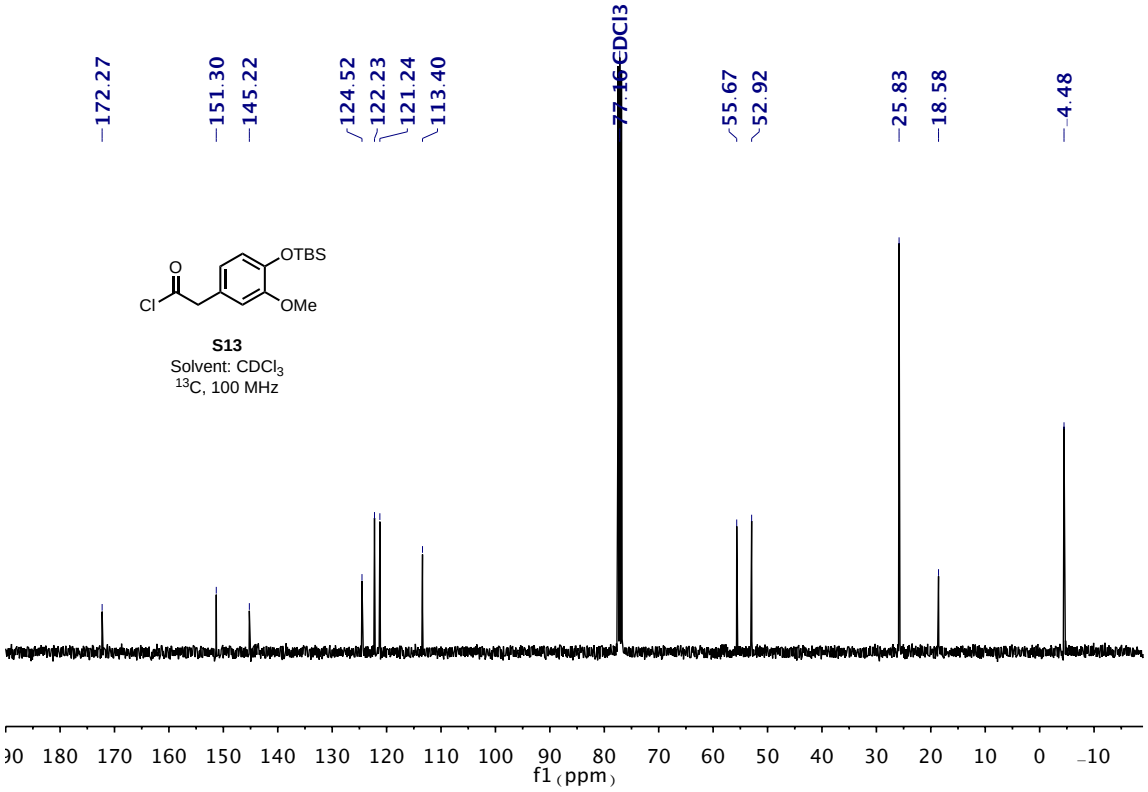
172.27
151.30
145.22
124.52
122.23
121.24
113.40
77.16 CDCl3
55.67
52.92
25.83
18.58
4.48
OTBS
OMe
Cl
O
S13
Solvent: CDCl3
13C, 100 MHz
f1 (ppm)

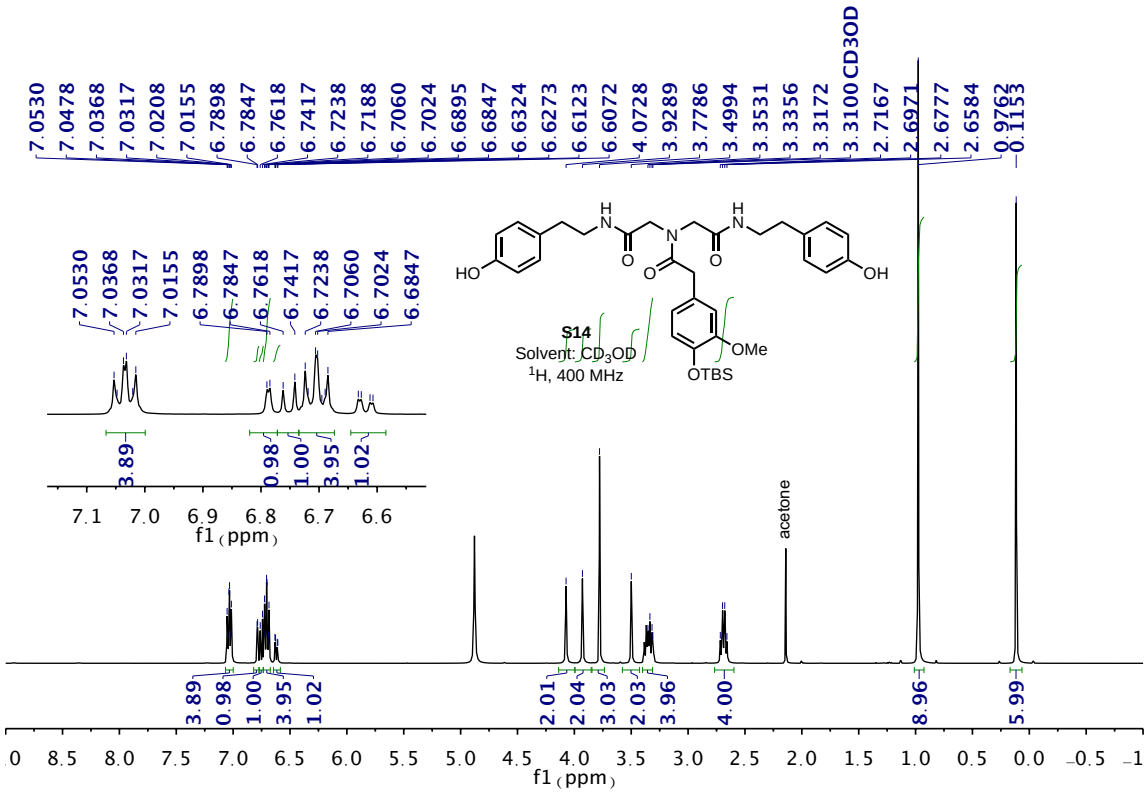
7.0530
7.0478
7.0368
7.0317
7.0208
7.0155
6.7898
6.7847
6.7618
6.7417
6.7238
6.7188
6.7060
6.7024
6.6895
6.6847
6.6324
6.6273
6.6123
6.6072
4.0728
3.9289
3.7786
3.4994
3.3531
3.3356
3.3172
3.3100 CD3OD
2.7167
2.6971
2.6777
2.6584
0.9762
0.1153
acetone
HO
OH
OMe
OTBS
S14
Solvent: CD3OD
1H, 400 MHz
3.89
0.98
1.00
3.95
1.02
2.01
2.04
3.03
2.03
3.96
4.00
8.96
5.99
f1 (ppm)

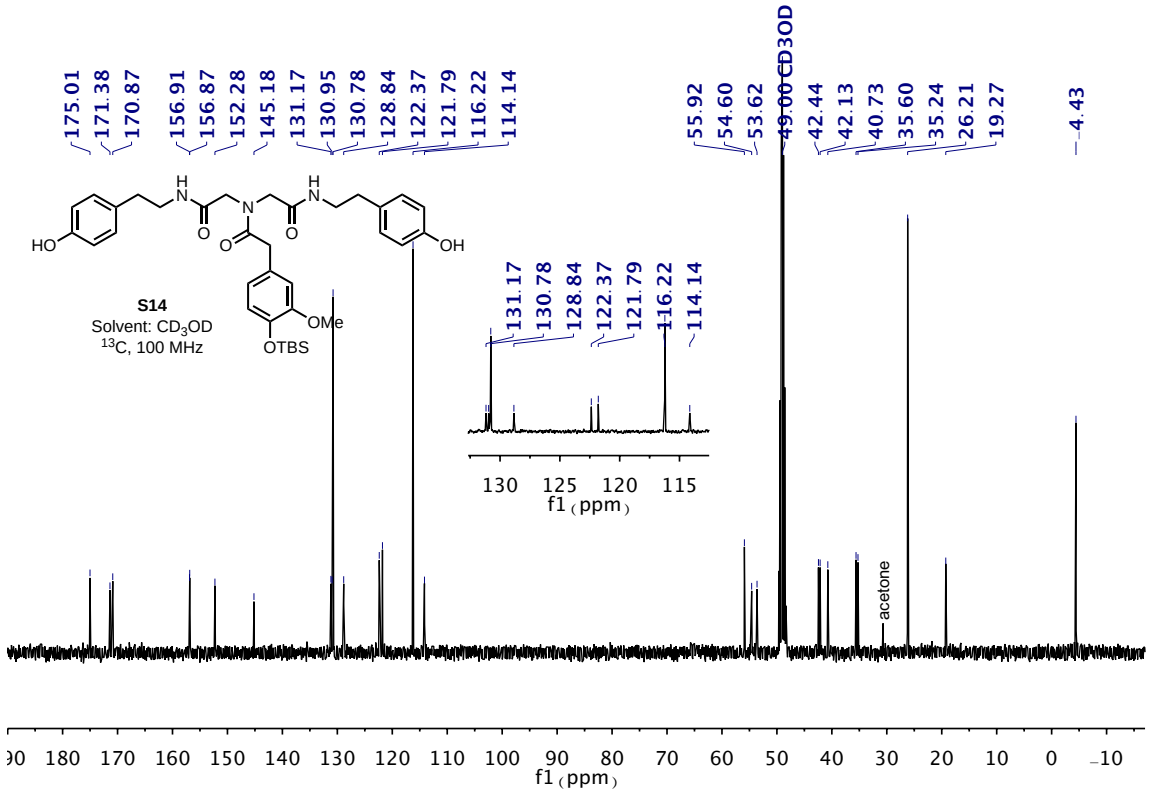
175.01
171.38
170.87
156.91
156.87
152.28
145.18
131.17
130.95
130.78
128.84
122.37
121.79
116.22
114.14
55.92
54.60
53.62
49.00 CD3OD
42.44
42.13
40.73
35.60
35.24
26.21
19.27
4.43
HO
OH
OMe
OTBS
S14
Solvent: CD3OD
13C, 100 MHz
acetone
f1 (ppm)

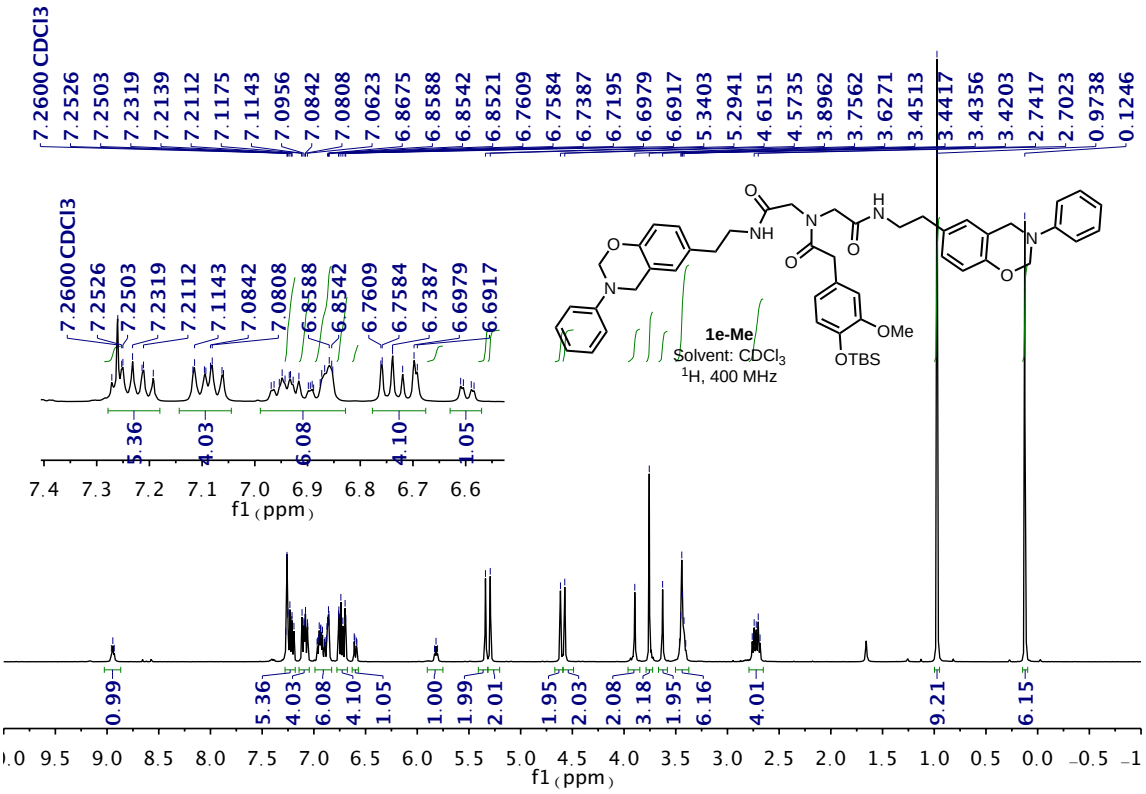
7.2600 CDCl3
7.2526
7.2503
7.2319
7.2139
7.2112
7.1175
7.1143
7.0956
7.0842
7.0808
7.0623
6.8675
6.8588
6.8542
6.8521
6.7609
6.7584
6.7387
6.7195
6.6979
6.6917
5.3403
5.2941
4.6151
4.5735
3.8962
3.7562
3.6271
3.4513
3.4417
3.4356
3.4203
2.7417
2.7023
0.9738
0.1246
1e-Me
Solvent: CDCl3
1H, 400 MHz
OMe
OTBS
0.99
5.36
4.03
6.08
4.10
1.05
1.00
1.99
2.01
1.95
2.03
2.08
3.18
1.95
6.16
4.01
9.21
6.15
f1 (ppm)

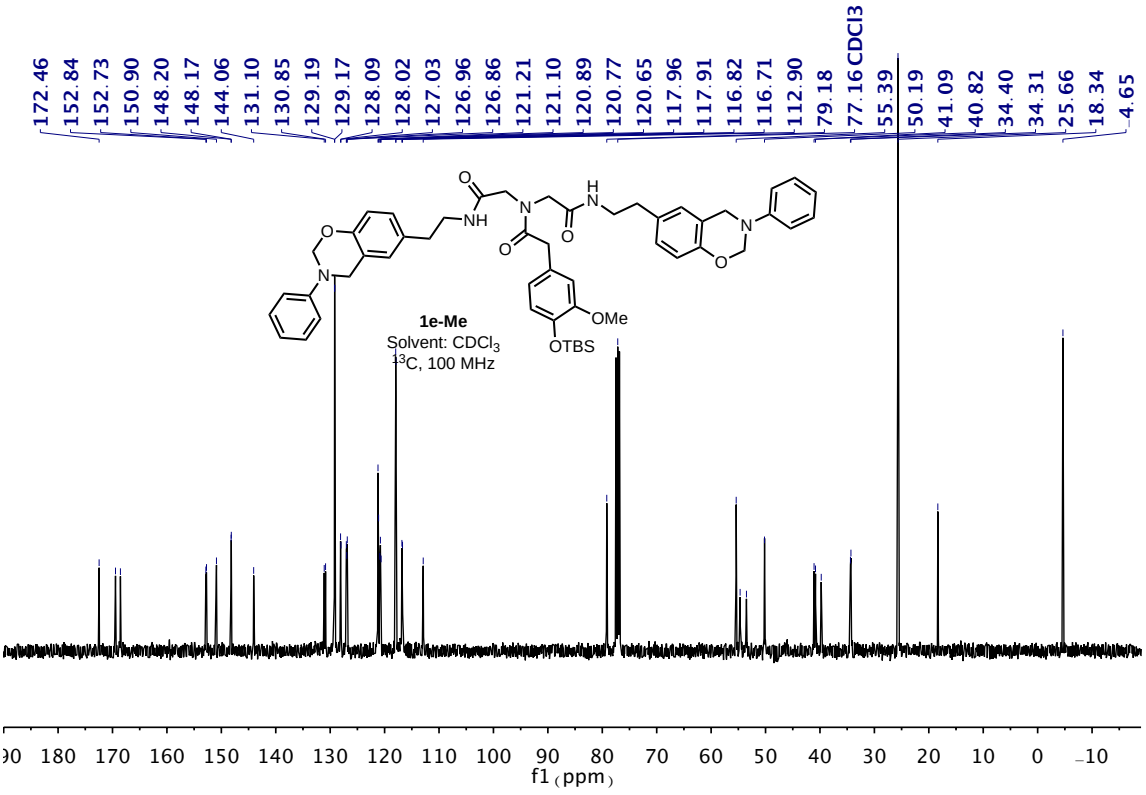
172.46
152.84
152.73
150.90
148.20
148.17
144.06
131.10
130.85
129.19
129.17
128.09
128.02
127.03
126.96
126.86
121.21
121.10
120.89
120.77
120.65
117.96
117.91
116.82
116.71
112.90
79.18
77.16 CDCl3
55.39
50.19
41.09
40.82
34.40
34.31
25.66
18.34
-4.65
1e-Me
Solvent: CDCl3
13C, 100 MHz
OMe
OTBS
f1 (ppm)

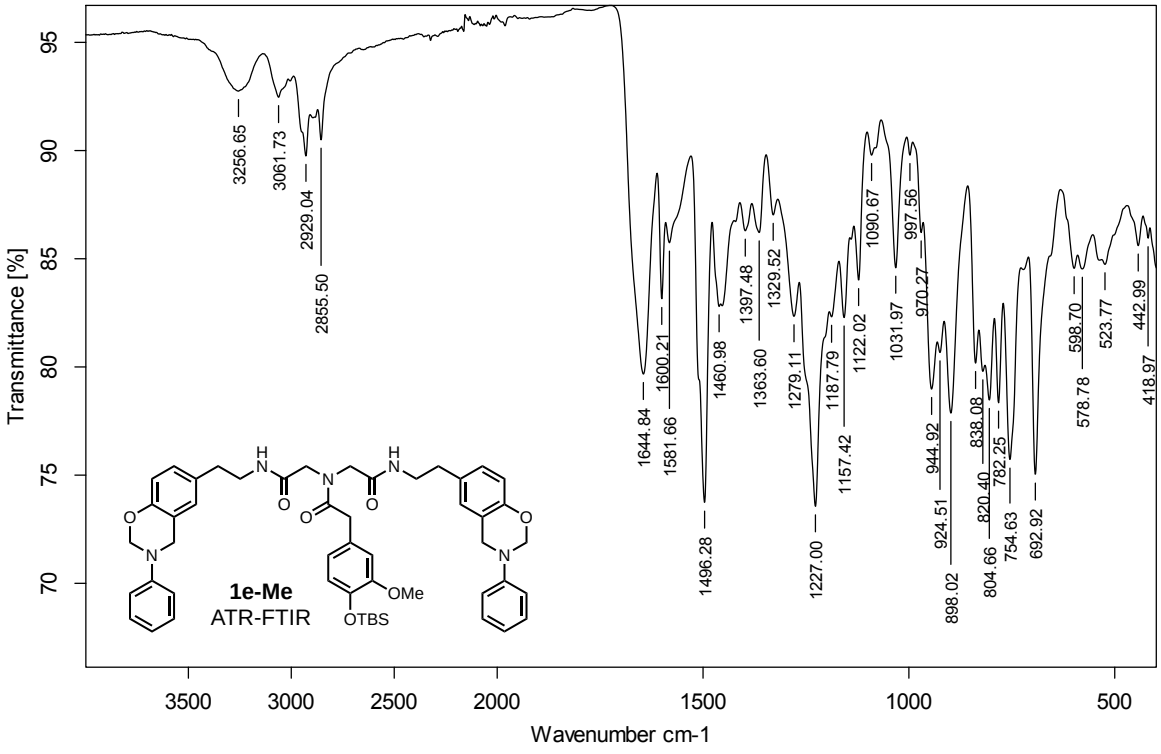
Transmittance [%]
Wavenumber cm-1
3256.65
3061.73
2929.04
2855.50
1644.84
1600.21
1581.66
1496.28
1460.98
1397.48
1363.60
1329.52
1279.11
1227.00
1187.79
1157.42
1122.02
1090.67
1031.97
997.56
970.27
944.92
924.51
898.02
838.08
820.40
804.66
782.25
754.63
692.92
598.70
578.78
523.77
442.99
418.97
1e-Me
ATR-FTIR
OMe
OTBS

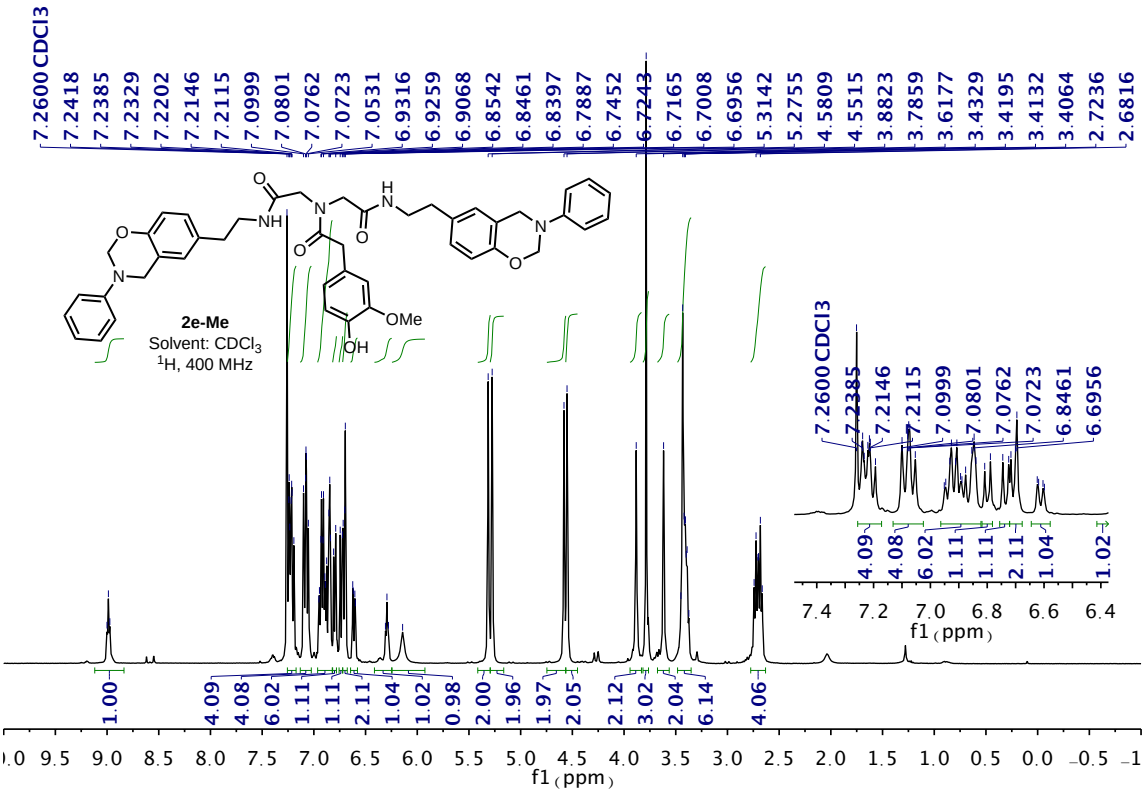
7.2600 CDCl3
2e-Me
Solvent: CDCl3
1H, 400 MHz
OMe
OH
f1 (ppm)

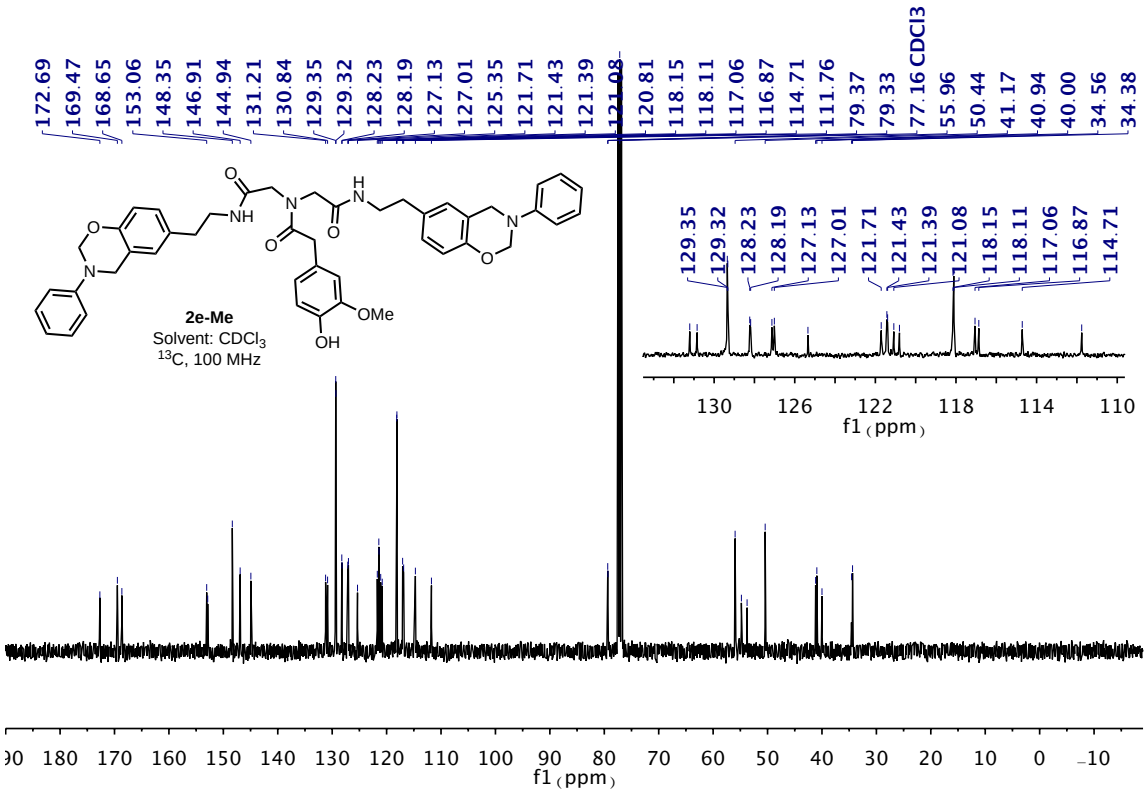
172.69
169.47
168.65
153.06
148.35
146.91
144.94
131.21
130.84
129.35
129.32
128.23
128.19
127.13
127.01
125.35
121.71
121.43
121.39
121.08
120.81
118.15
118.11
117.06
116.87
114.71
111.76
79.37
79.33
77.16 CDCl3
55.96
50.44
41.17
40.94
40.00
34.56
34.38
2e-Me
Solvent: CDCl3
13C, 100 MHz
OMe
OH
f1 (ppm)

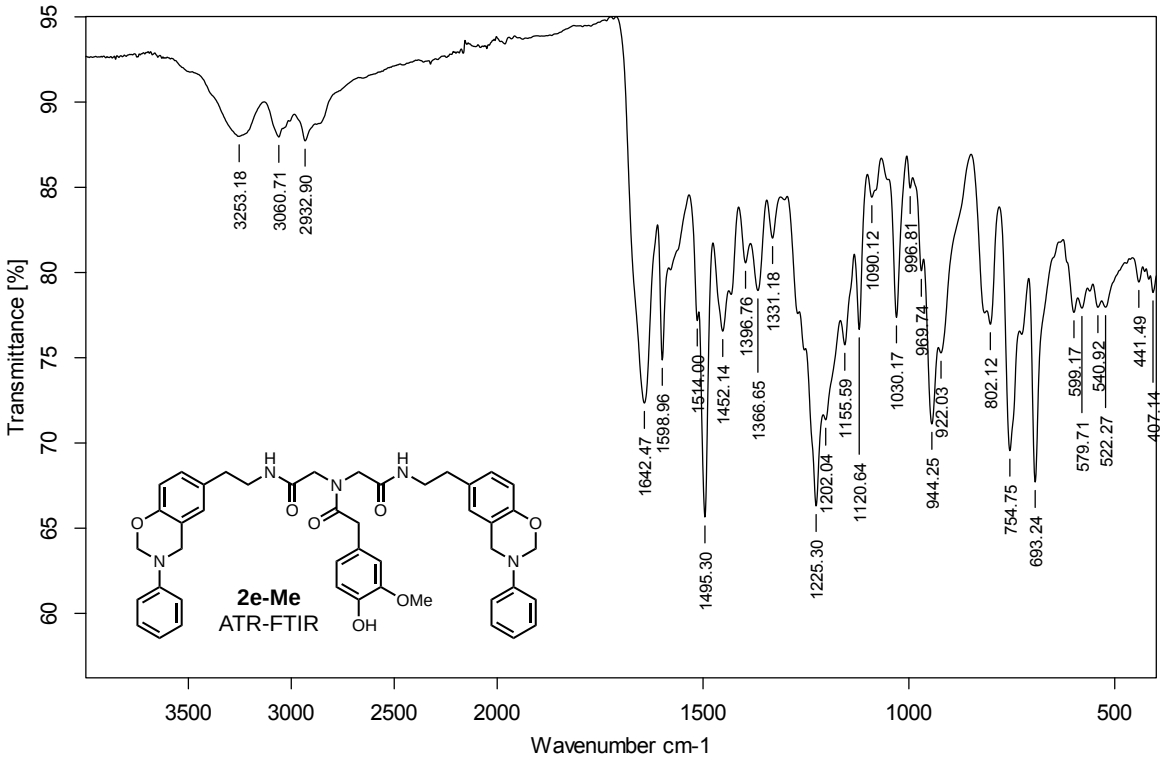
Transmittance [%]
3253.18
3060.71
2932.90
1642.47
1598.96
1514.00
1495.30
1452.14
1396.76
1366.65
1331.18
1225.30
1202.04
1155.59
1120.64
1090.12
1030.17
996.81
969.74
944.25
922.03
802.12
754.75
693.24
599.17
579.71
540.92
522.27
441.49
407.14
2e-Me
ATR-FTIR
OMe
OH
Wavenumber cm-1

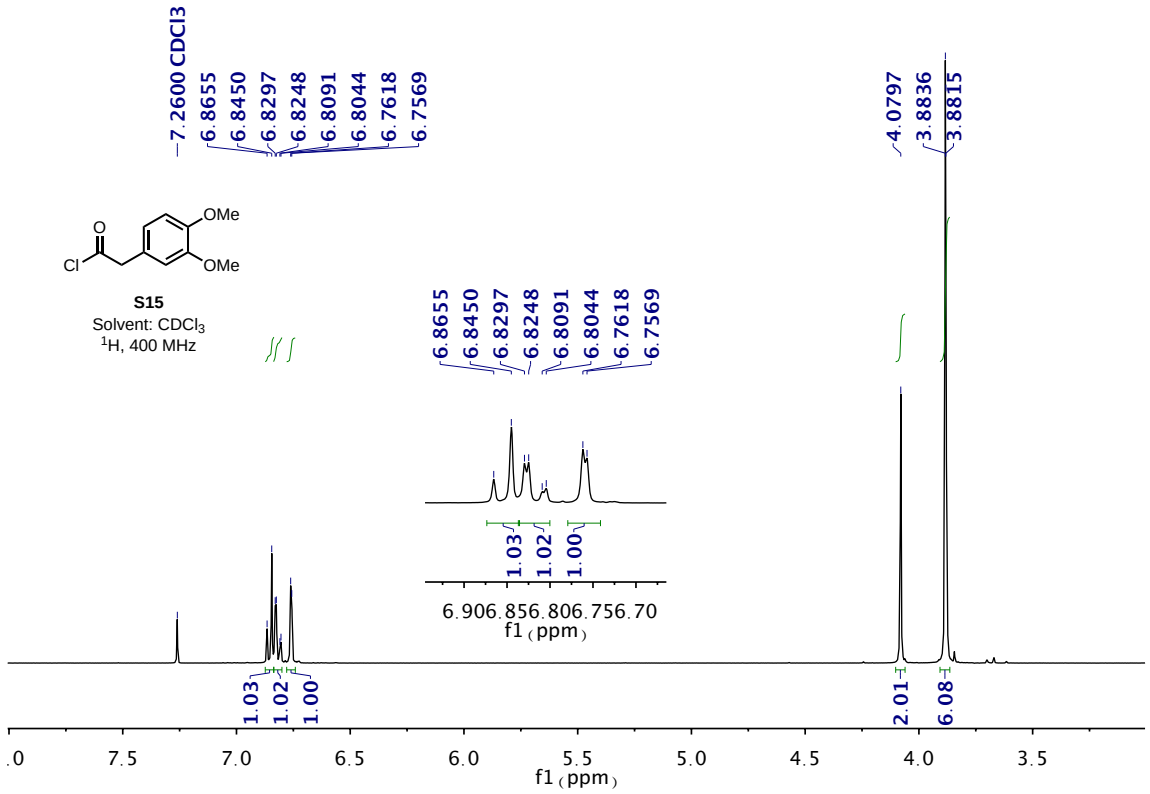
7.2600 CDCl3
6.8655
6.8450
6.8297
6.8248
6.8091
6.8044
6.7618
6.7569
4.0797
3.8836
3.8815
OMe
OMe
Cl
O
S15
Solvent: CDCl3
1H, 400 MHz
1.03
1.02
1.00
2.01
6.08
6.906.856.806.756.70
f1 (ppm)
7.5
7.0
6.5
6.0
5.5
5.0
4.5
4.0
3.5

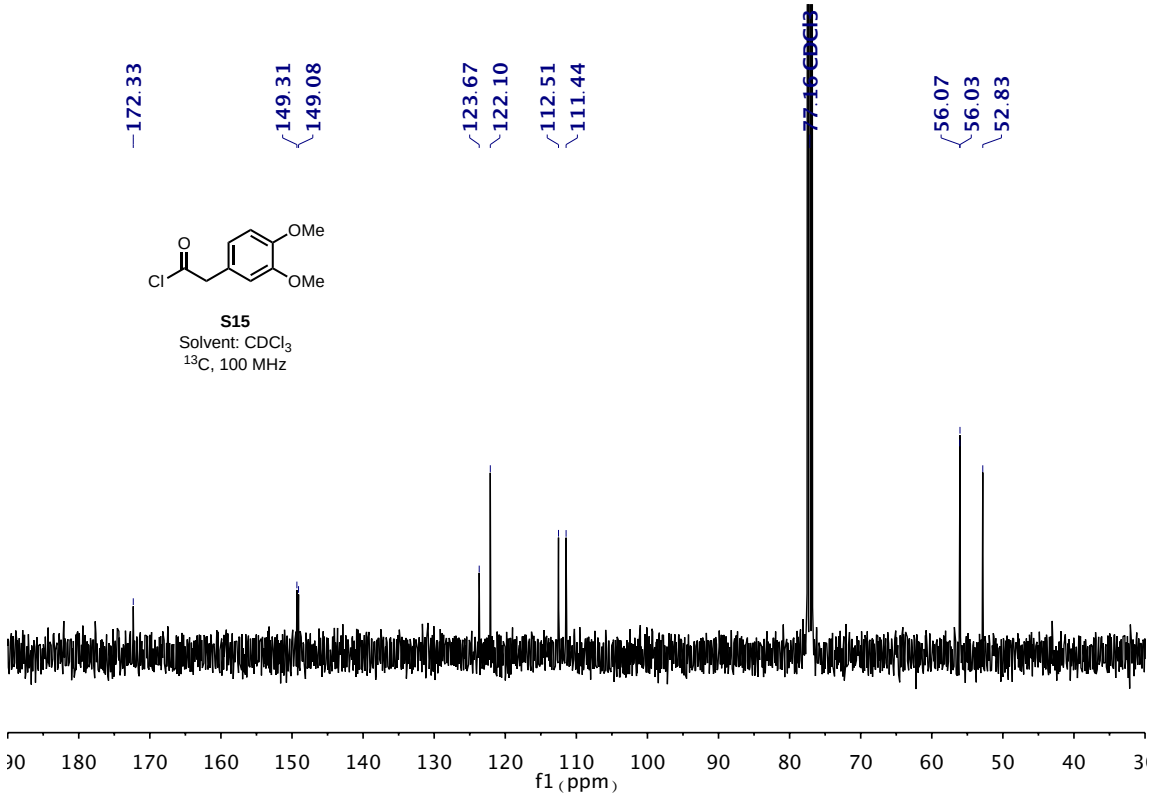
172.33
149.31
149.08
123.67
122.10
112.51
111.44
77.16 CDCl3
56.07
56.03
52.83
OMe
OMe
Cl
O
S15
Solvent: CDCl3
13C, 100 MHz
180
170
160
150
140
130
120
110
100
90
80
70
60
50
40
f1 (ppm)

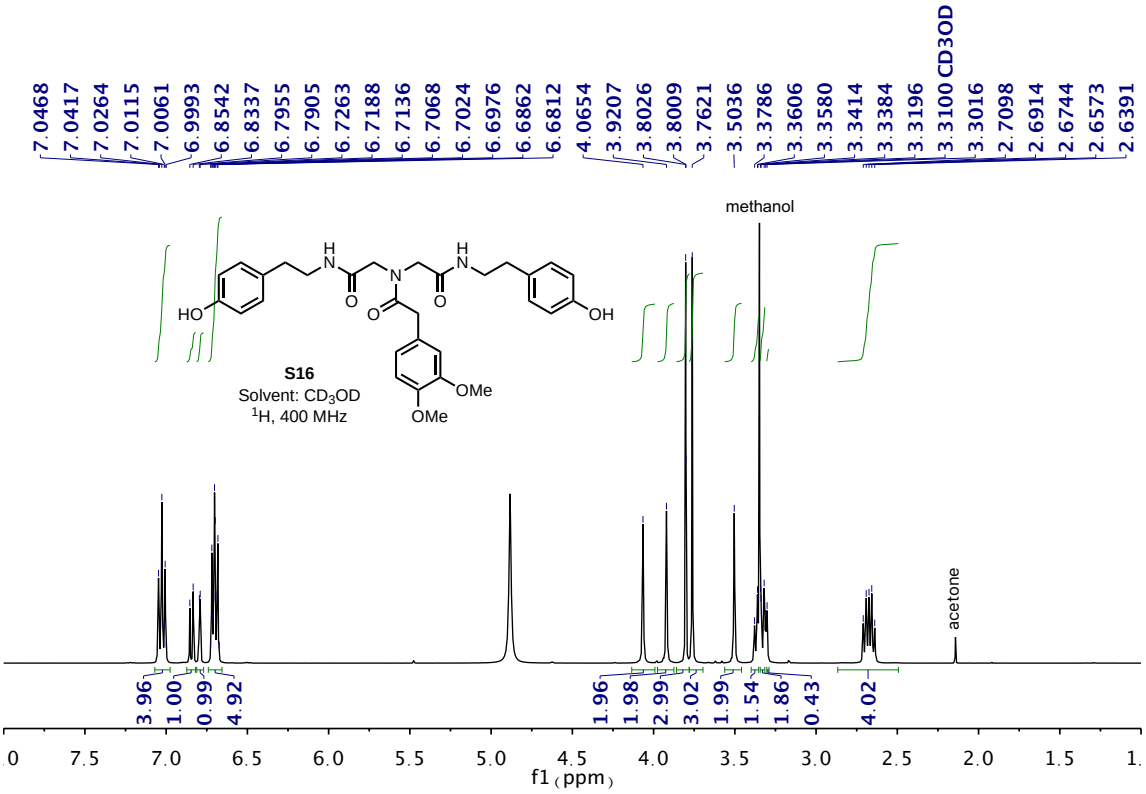
7.0468
7.0417
7.0264
7.0115
7.0061
6.9993
6.8542
6.8337
6.7955
6.7905
6.7263
6.7188
6.7136
6.7068
6.7024
6.6976
6.6862
6.6812
4.0654
3.9207
3.8026
3.8009
3.7621
3.5036
3.3786
3.3606
3.3580
3.3414
3.3384
3.3196
3.3100 CD3OD
3.3016
2.7098
2.6914
2.6744
2.6573
2.6391
methanol
acetone
S16
Solvent: CD3OD
1H, 400 MHz
3.96
1.00
0.99
4.92
1.96
1.98
2.99
3.02
1.99
1.54
1.86
0.43
4.02
f1 (ppm)

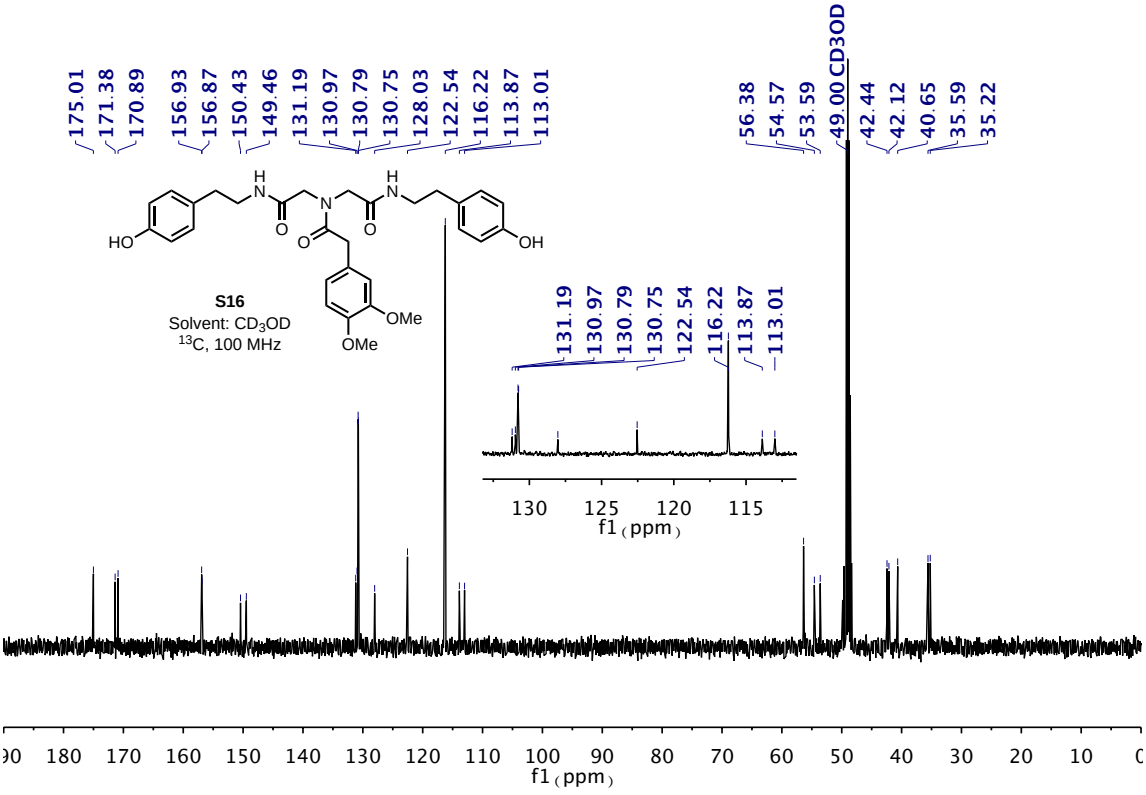
175.01
171.38
170.89
156.93
156.87
150.43
149.46
131.19
130.97
130.79
130.75
128.03
122.54
116.22
113.87
113.01
56.38
54.57
53.59
49.00 CD3OD
42.44
42.12
40.65
35.59
35.22
S16
Solvent: CD3OD
13C, 100 MHz
f1 (ppm)

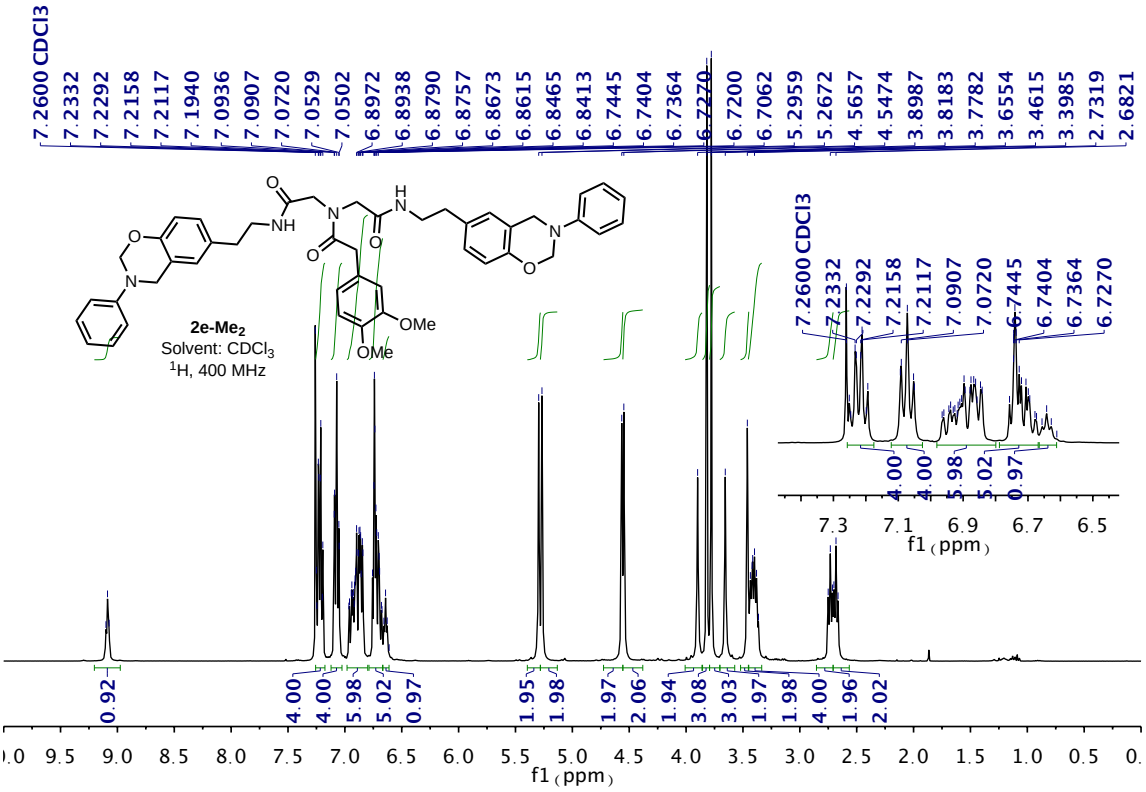
7.2600 CDCl3
7.2332
7.2292
7.2158
7.2117
7.1940
7.0936
7.0907
7.0720
7.0529
7.0502
6.8972
6.8938
6.8790
6.8757
6.8673
6.8615
6.8465
6.8413
6.7445
6.7404
6.7364
6.7270
6.7200
6.7062
5.2959
5.2672
4.5657
4.5474
3.8987
3.8183
3.7782
3.6554
3.4615
3.3985
2.7319
2.6821
2e-Me2
Solvent: CDCl3
1H, 400 MHz
OMe
OMe
0.92
4.00
4.00
5.98
5.02
0.97
1.95
1.98
1.97
2.06
1.94
3.08
3.03
1.97
1.98
4.00
1.96
2.02
f1 (ppm)

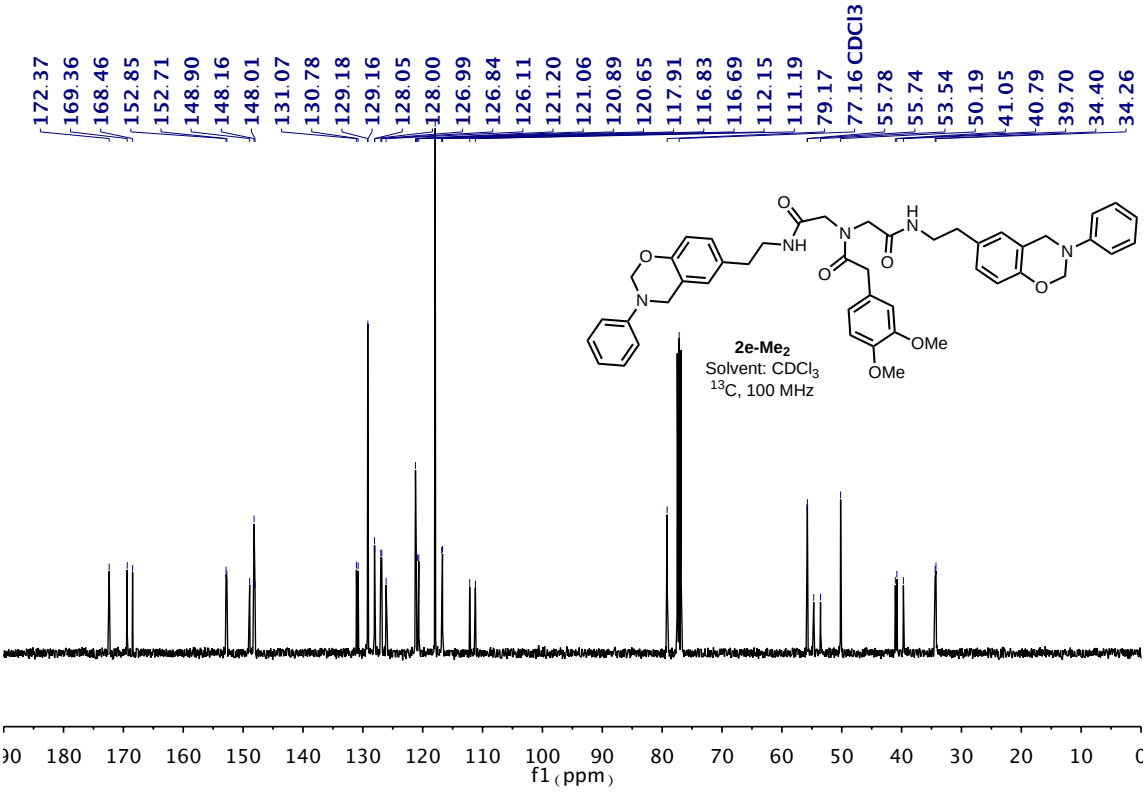
172.37
169.36
168.46
152.85
152.71
148.90
148.16
148.01
131.07
130.78
129.18
129.16
128.05
128.00
126.99
126.84
126.11
121.20
121.06
120.89
120.65
117.91
116.83
116.69
112.15
111.19
79.17
77.16 CDCl3
55.78
55.74
53.54
50.19
41.05
40.79
39.70
34.40
34.26
2e-Me2
Solvent: CDCl3
13C, 100 MHz
OMe
OMe
f1 (ppm)

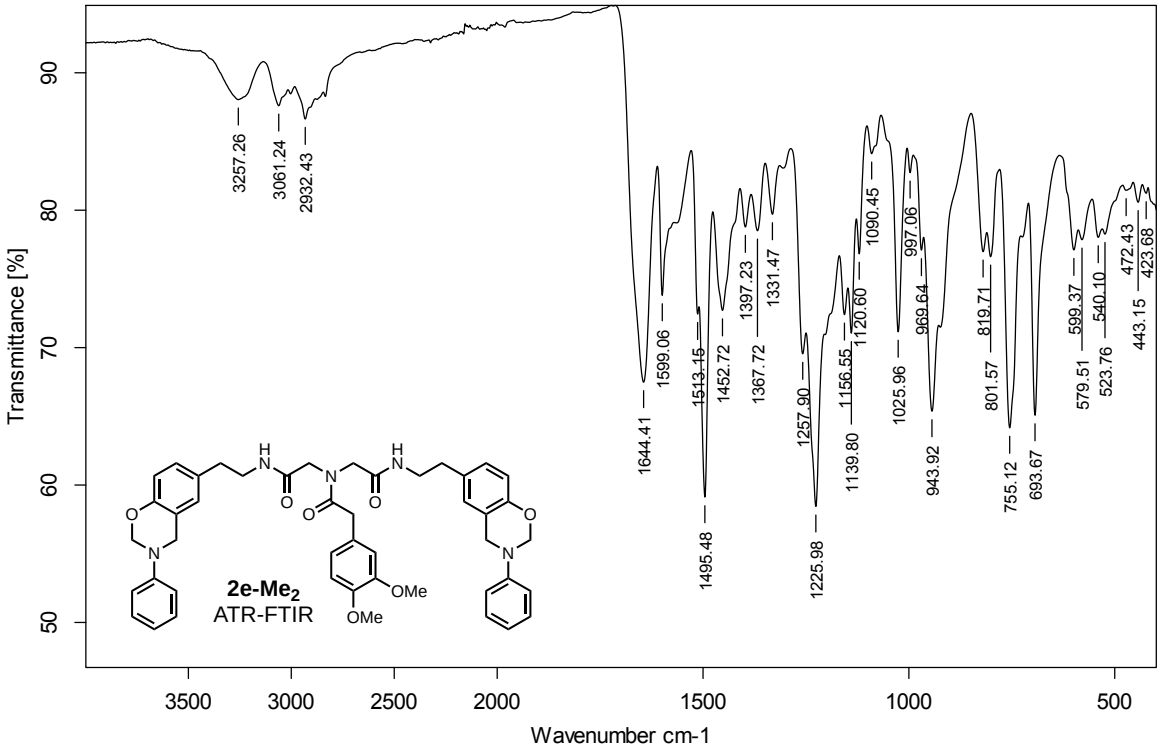
Transmittance [%]
Wavenumber cm-1
3257.26
3061.24
2932.43
1644.41
1599.06
1513.15
1495.48
1452.72
1397.23
1367.72
1331.47
1257.90
1225.98
1156.55
1139.80
1120.60
1090.45
1025.96
997.06
969.64
943.92
819.71
801.57
755.12
693.67
599.37
579.51
540.10
523.76
472.43
443.15
423.68
2e-Me2
ATR-FTIR
OMe
OMe

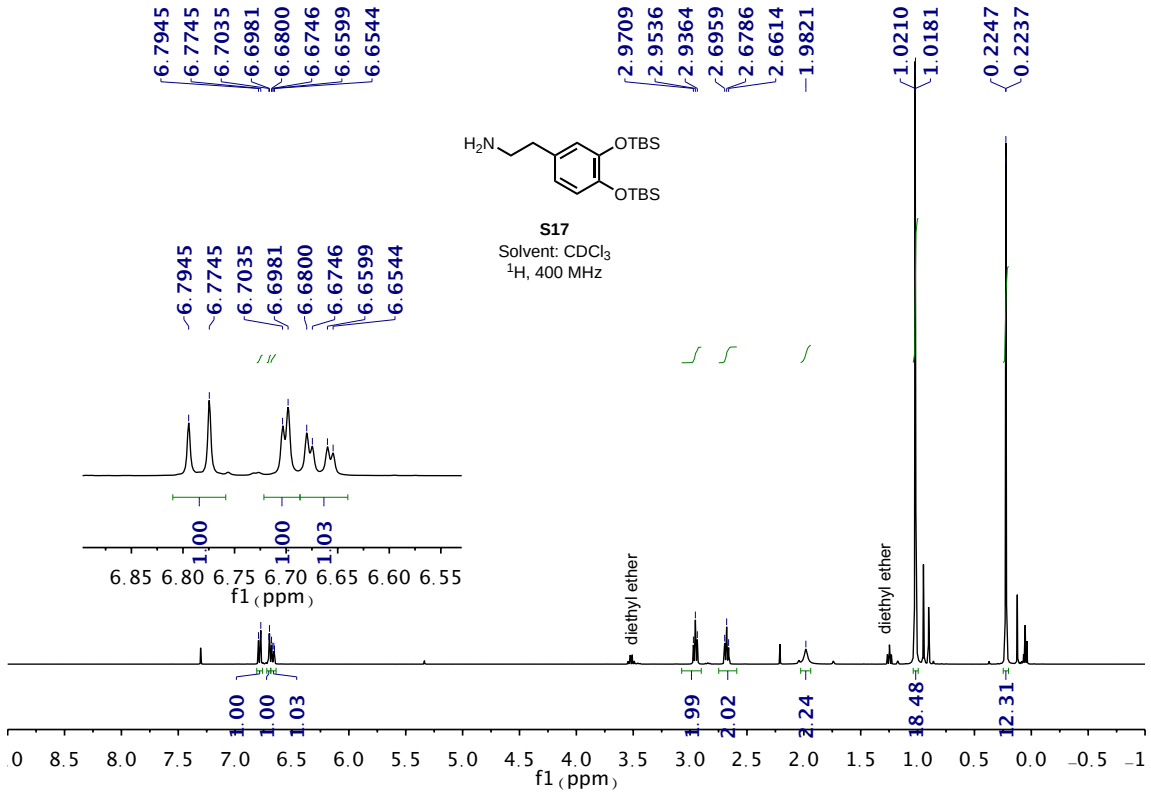
6.7945
6.7745
6.7035
6.6981
6.6800
6.6746
6.6599
6.6544
2.9709
2.9536
2.9364
2.6959
2.6786
2.6614
1.9821
1.0210
1.0181
0.2247
0.2237
H2N
OTBS
OTBS
S17
Solvent: CDCl3
1H, 400 MHz
diethyl ether
diethyl ether
1.00
1.00
1.03
1.99
2.02
2.24
18.48
12.31
f1 (ppm)

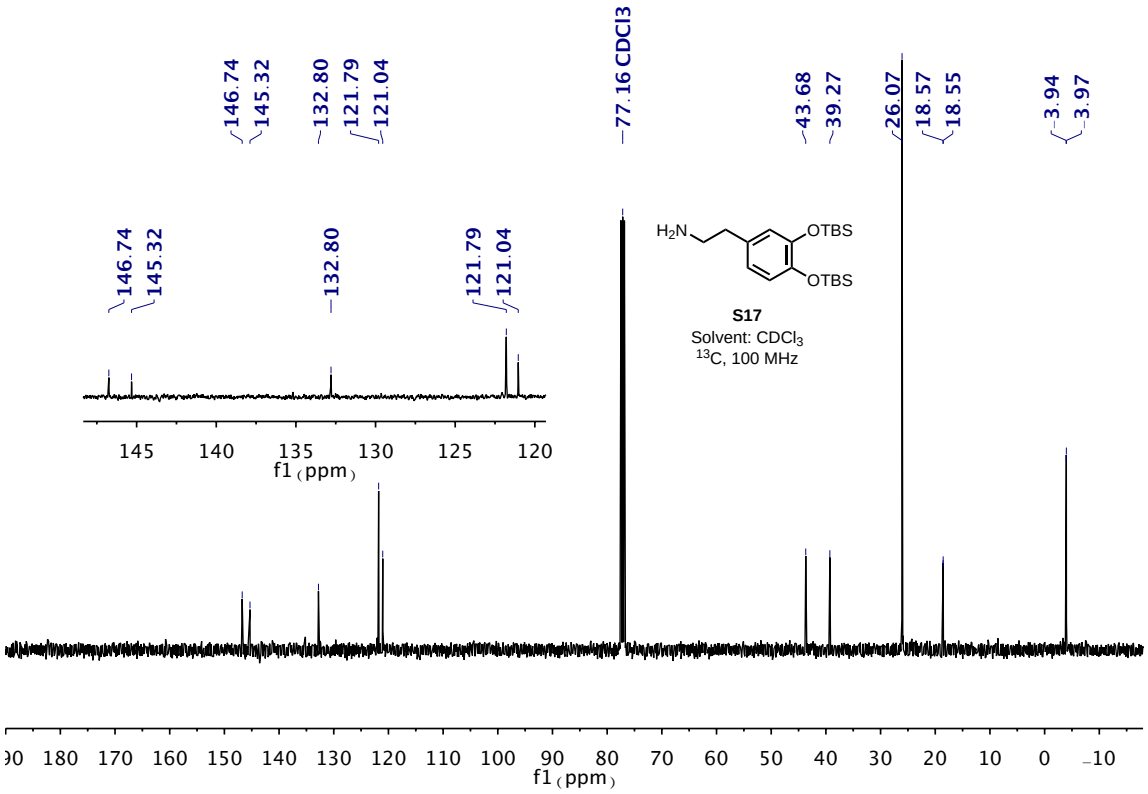
146.74
145.32
132.80
121.79
121.04
77.16 CDCl3
43.68
39.27
26.07
18.57
18.55
3.94
3.97
H2N
OTBS
OTBS
S17
Solvent: CDCl3
13C, 100 MHz
f1 (ppm)

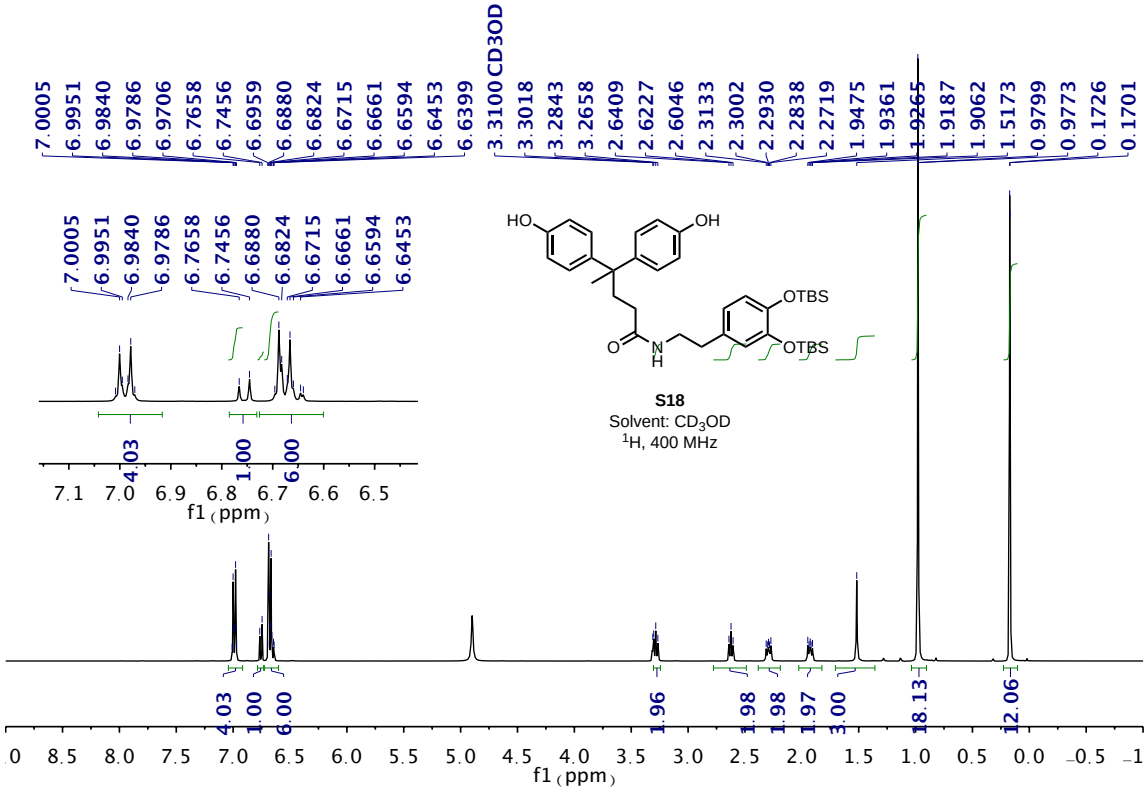
7.0005
6.9951
6.9840
6.9786
6.9706
6.7658
6.7456
6.6959
6.6880
6.6824
6.6715
6.6661
6.6594
6.6453
6.6399
3.3100 CD3OD
3.3018
3.2843
3.2658
2.6409
2.6227
2.6046
2.3133
2.3002
2.2930
2.2838
2.2719
1.9475
1.9361
1.9265
1.9187
1.9062
1.5173
0.9799
0.9773
0.1726
0.1701
HO
OH
OTBS
OTBS
O
N
H
S18
Solvent: CD3OD
1H, 400 MHz
4.03
1.00
6.00
1.96
1.98
1.98
1.97
3.00
18.13
12.06
f1 (ppm)

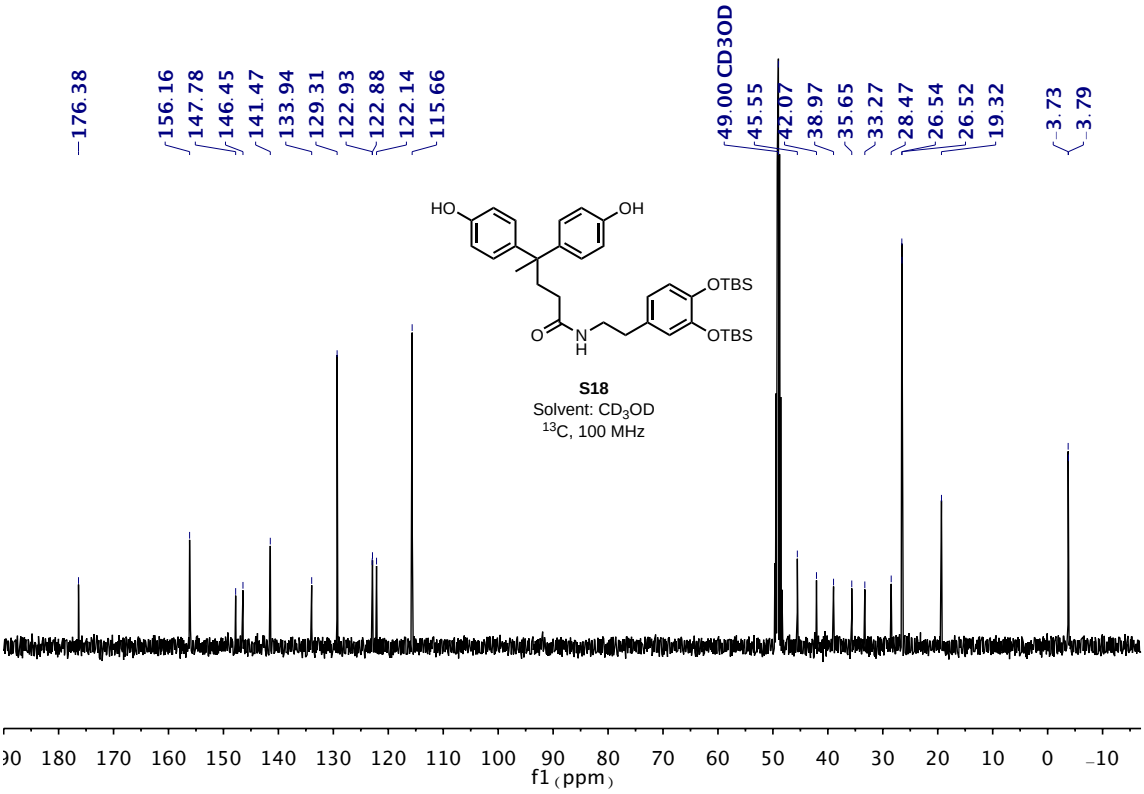
176.38
156.16
147.78
146.45
141.47
133.94
129.31
122.93
122.88
122.14
115.66
49.00 CD3OD
45.55
42.07
38.97
35.65
33.27
28.47
26.54
26.52
19.32
3.73
3.79
HO
OH
OTBS
OTBS
O
N
H
S18
Solvent: CD3OD
13C, 100 MHz
f1 (ppm)

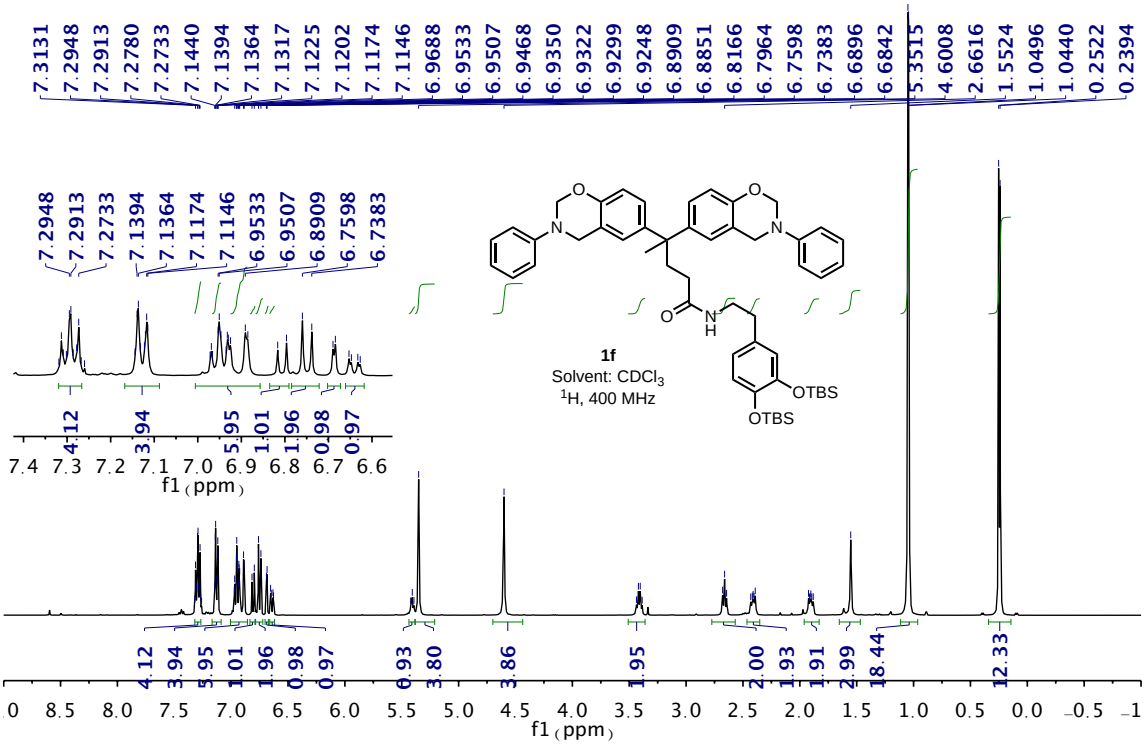
7.3131
7.2948
7.2913
7.2780
7.2733
7.1440
7.1394
7.1364
7.1317
7.1225
7.1202
7.1174
7.1146
6.9688
6.9533
6.9507
6.9468
6.9350
6.9322
6.9299
6.9248
6.8909
6.8851
6.8166
6.7964
6.7598
6.7383
6.6896
6.6842
5.3515
4.6008
2.6616
1.5524
1.0496
1.0440
0.2522
0.2394
4.12
3.94
5.95
1.01
1.96
0.98
0.97
6.93
3.80
3.86
1.95
2.00
1.93
1.91
2.99
18.44
12.33
1f
Solvent: CDCl3
1H, 400 MHz
OTBS
OTBS
f1 (ppm)

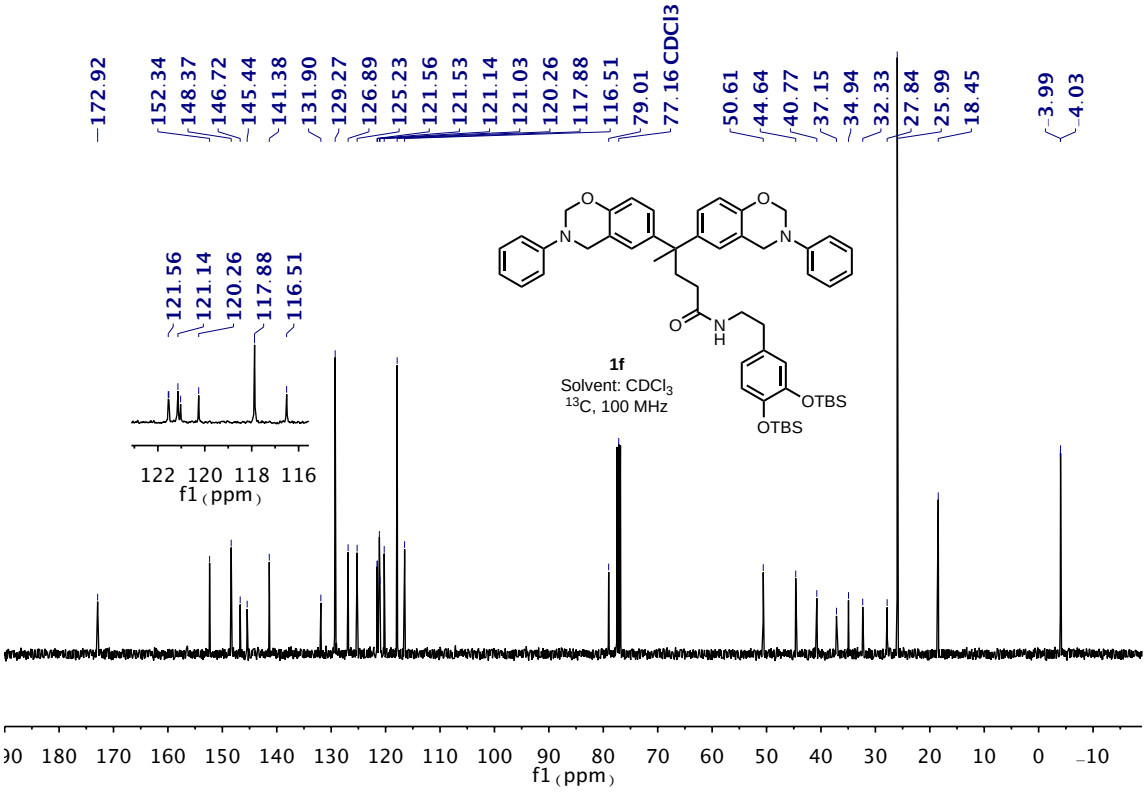
172.92
152.34
148.37
146.72
145.44
141.38
131.90
129.27
126.89
125.23
121.56
121.53
121.14
121.03
120.26
117.88
116.51
79.01
77.16 CDCl3
50.61
44.64
40.77
37.15
34.94
32.33
27.84
25.99
18.45
3.99
4.03
121.56
121.14
120.26
117.88
116.51
122 120 118 116
f1 (ppm)
1f
Solvent: CDCl3
13C, 100 MHz
OTBS
OTBS
f1 (ppm)

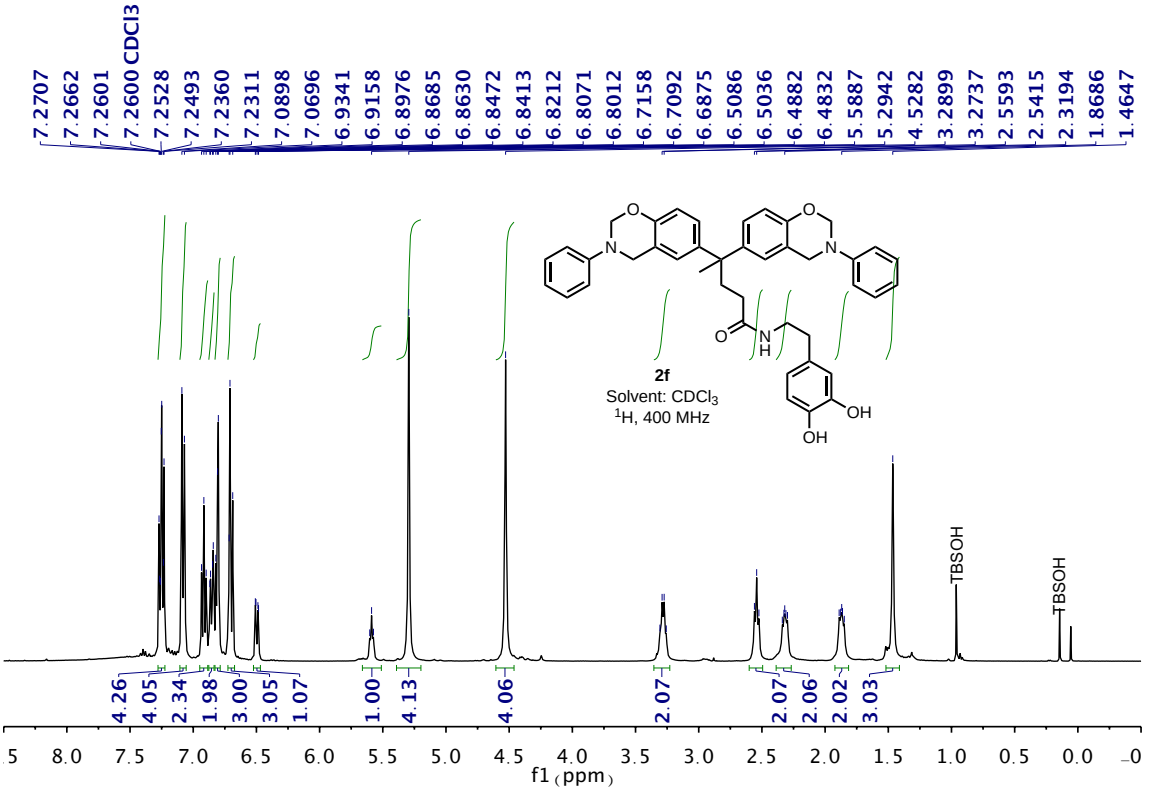
7.2707
7.2662
7.2601
7.2600 CDCl3
7.2528
7.2493
7.2360
7.2311
7.0898
7.0696
6.9341
6.9158
6.8976
6.8685
6.8630
6.8472
6.8413
6.8212
6.8071
6.8012
6.7158
6.7092
6.6875
6.5086
6.5036
6.4882
6.4832
5.5887
5.2942
4.5282
3.2899
3.2737
2.5593
2.5415
2.3194
1.8686
1.4647
2f
Solvent: CDCl3
1H, 400 MHz
OH
OH
TBSOH
TBSOH
4.26
4.05
2.34
1.98
3.00
3.05
1.07
1.00
4.13
4.06
2.07
2.07
2.06
2.02
3.03
f1 (ppm)

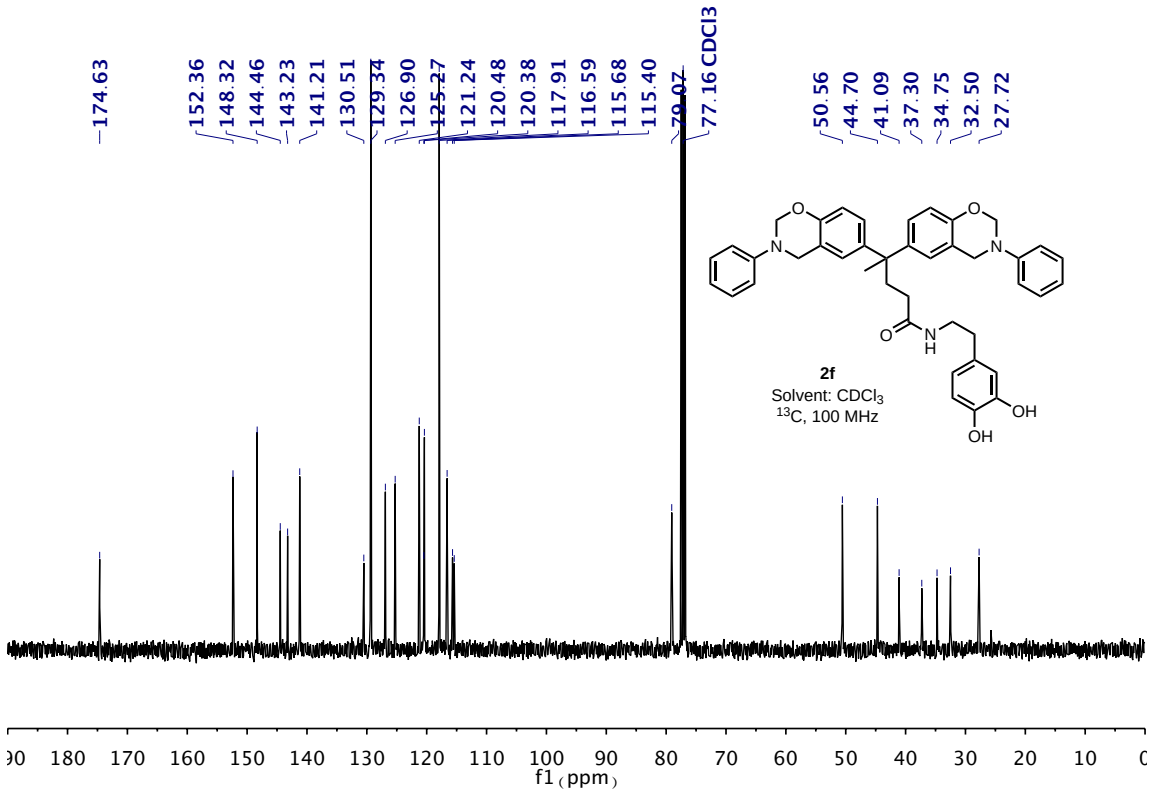
174.63
152.36
148.32
144.46
143.23
141.21
130.51
129.34
126.90
125.27
121.24
120.48
120.38
117.91
116.59
115.68
115.40
77.16 CDCl3
50.56
44.70
41.09
37.30
34.75
32.50
27.72
2f
Solvent: CDCl3
13C, 100 MHz
f1 (ppm)

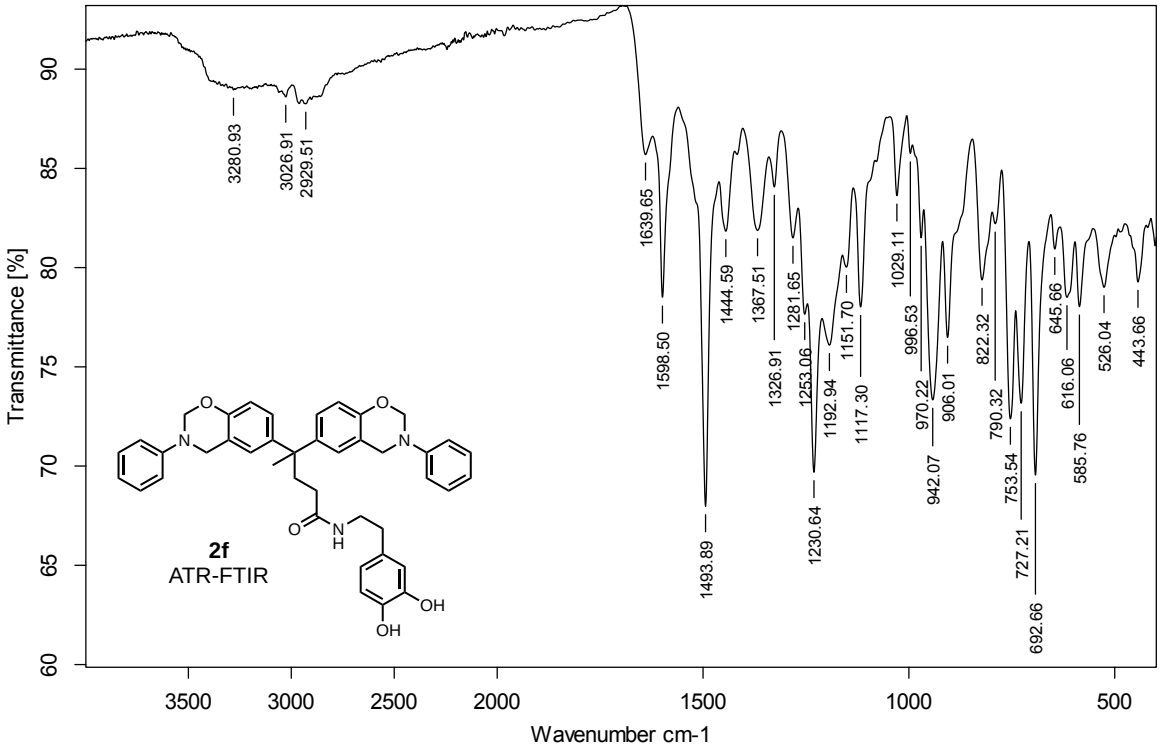
Transmittance [%]
3280.93
3026.91
2929.51
1639.65
1598.50
1493.89
1444.59
1367.51
1326.91
1281.65
1253.06
1230.64
1192.94
1151.70
1117.30
1029.11
996.53
970.22
942.07
906.01
822.32
790.32
753.54
727.21
692.66
645.66
616.06
585.76
526.04
443.66
2f
ATR-FTIR
Wavenumber cm-1

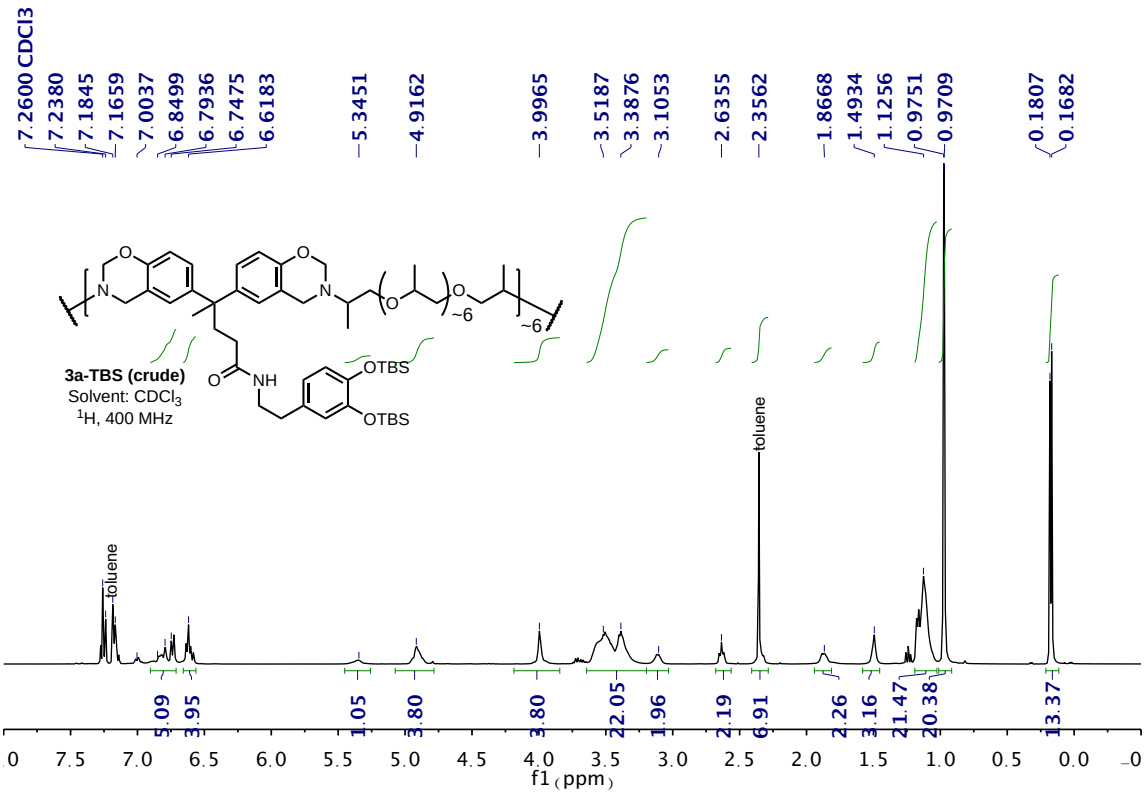
7.2600 CDCl3
7.2380
7.1845
7.1659
7.0037
6.8499
6.7936
6.7475
6.6183
5.3451
4.9162
3.9965
3.5187
3.3876
3.1053
2.6355
2.3562
1.8668
1.4934
1.1256
0.9751
0.9709
0.1807
0.1682
3a-TBS (crude)
Solvent: CDCl3
1H, 400 MHz
OTBS
OTBS
NH
~6
~6
toluene
toluene
5.09
3.95
1.05
3.80
3.80
22.05
1.96
2.19
6.91
2.26
3.16
21.47
20.38
13.37
f1 (ppm)

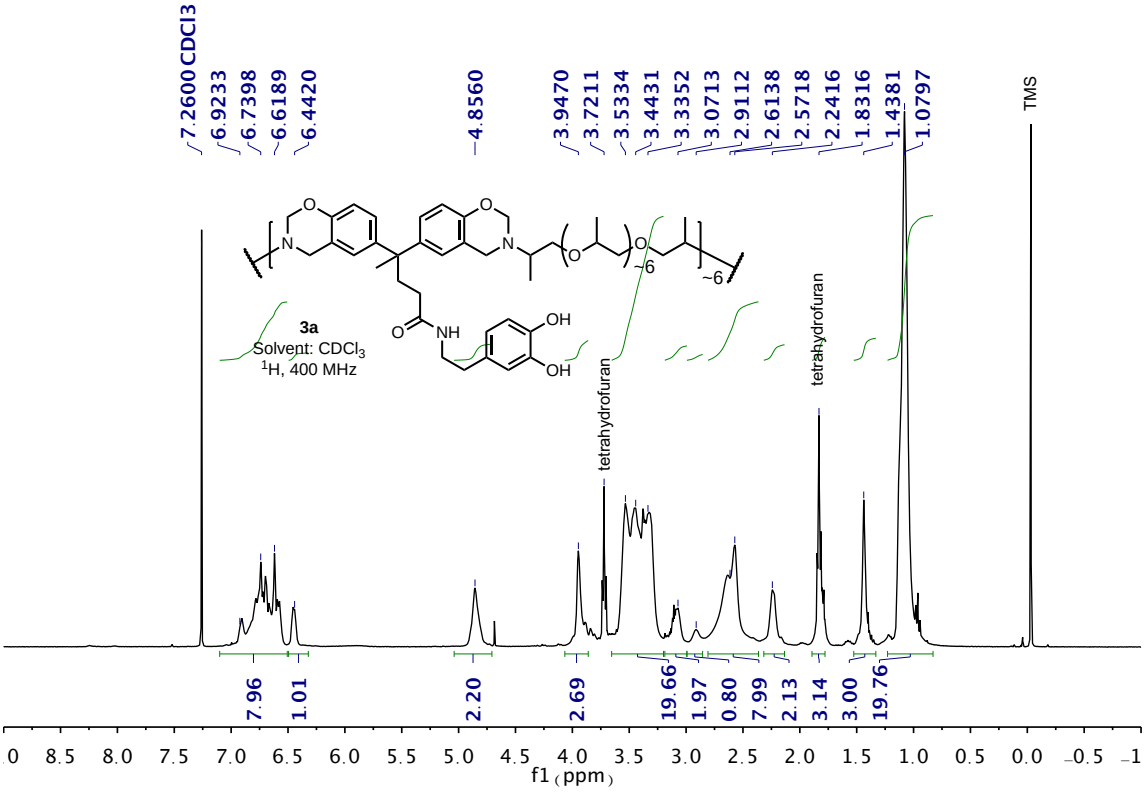
7.2600 CDCl3
6.9233
6.7398
6.6189
6.4420
4.8560
3.9470
3.7211
3.5334
3.4431
3.3352
3.0713
2.9112
2.6138
2.5718
2.2416
1.8316
1.4381
1.0797
TMS
3a
Solvent: CDCl3
1H, 400 MHz
OH
OH
NH
~6
~6
tetrahydrofuran
tetrahydrofuran
7.96
1.01
2.20
2.69
19.66
1.97
0.80
7.99
2.13
3.14
3.00
19.76
f1 (ppm)

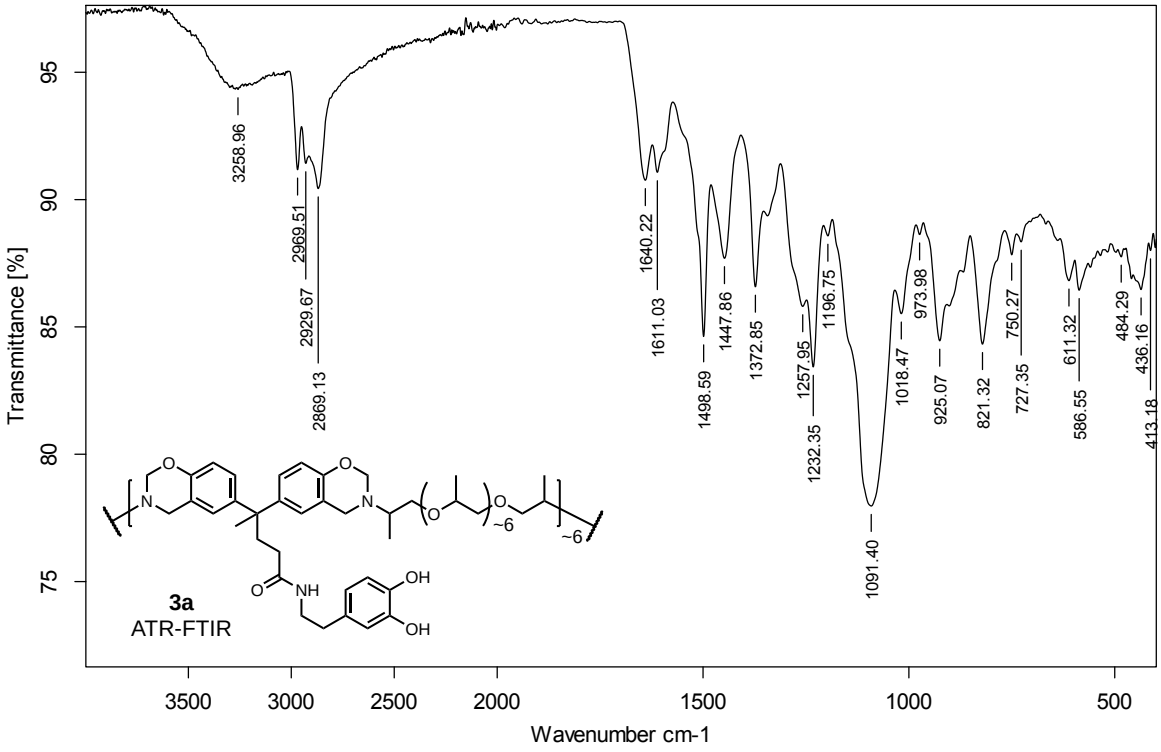
Transmittance [%]
95
90
85
80
75
3258.96
2969.51
2929.67
2869.13
1640.22
1611.03
1498.59
1447.86
1372.85
1257.95
1232.35
1196.75
1091.40
1018.47
973.98
925.07
821.32
750.27
727.35
611.32
586.55
484.29
436.16
413.18
3500
3000
2500
2000
1500
1000
500
Wavenumber cm-1
3a
ATR-FTIR

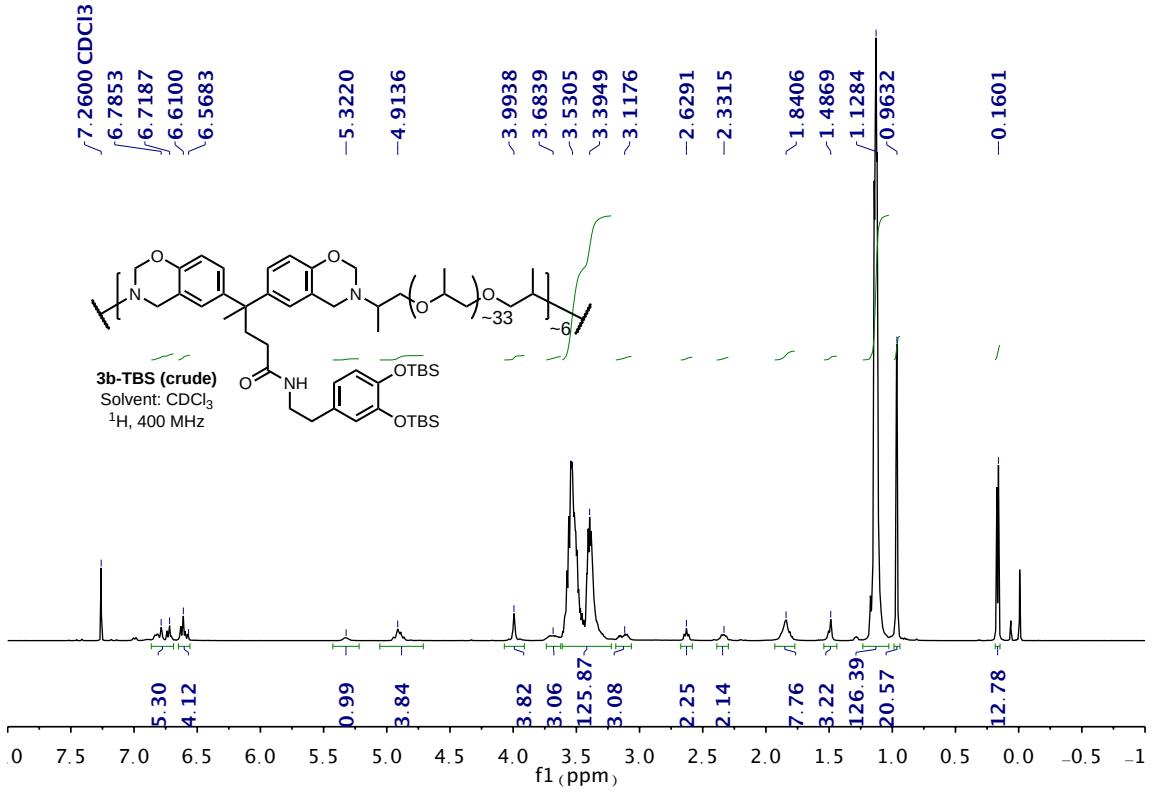
7.2600 CDCl3
6.7853
6.7187
6.6100
6.5683
5.3220
4.9136
3.9938
3.6839
3.5305
3.3949
3.1176
2.6291
2.3315
1.8406
1.4869
1.1284
0.9632
0.1601
3b-TBS (crude)
Solvent: CDCl3
1H, 400 MHz
5.30
4.12
0.99
3.84
3.82
3.06
125.87
3.08
2.25
2.14
7.76
3.22
126.39
20.57
12.78
f1 (ppm)

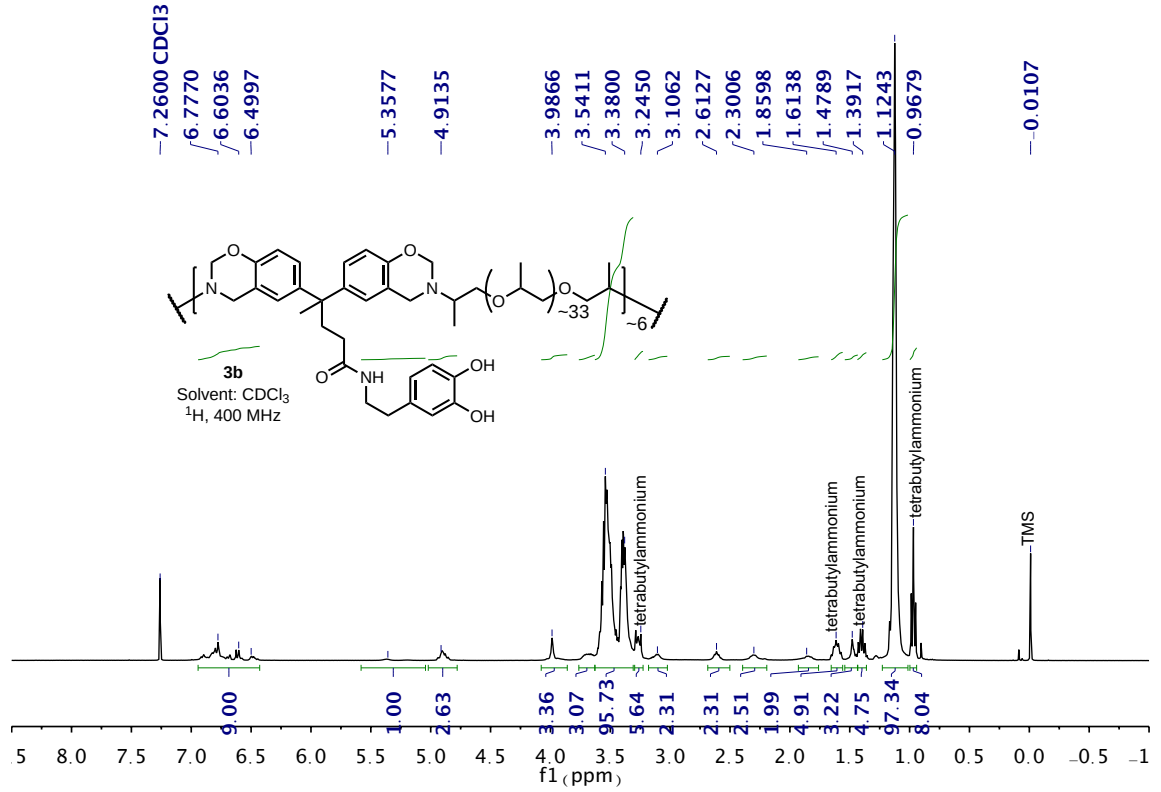
7.2600 CDCl3
6.7770
6.6036
6.4997
5.3577
4.9135
3.9866
3.5411
3.3800
3.2450
3.1062
2.6127
2.3006
1.8598
1.6138
1.4789
1.3917
1.1243
0.9679
0.0107
~33
~6
3b
Solvent: CDCl3
1H, 400 MHz
OH
NH
OH
tetrabutylammonium
tetrabutylammonium
tetrabutylammonium
tetrabutylammonium
TMS
9.00
1.00
2.63
3.36
3.07
5.73
5.64
2.31
2.31
2.51
1.99
4.91
3.22
4.75
37.34
8.04
f1 (ppm)

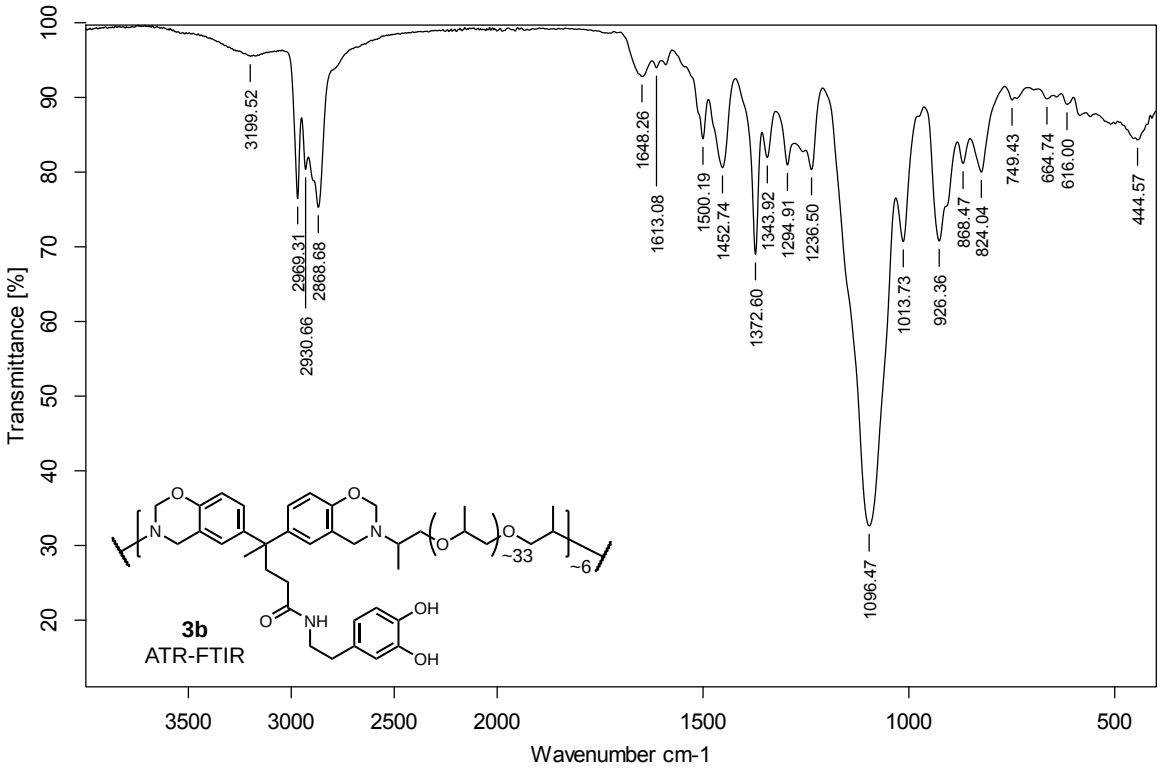
Transmittance [%]
3199.52
2969.31
2930.66
2868.68
1648.26
1613.08
1500.19
1452.74
1372.60
1343.92
1294.91
1236.50
1096.47
1013.73
926.36
868.47
824.04
749.43
664.74
616.00
444.57
~33
~6
3b
ATR-FTIR
OH
NH
OH
Wavenumber cm-1